UNIVERSITÀ DI PISA
FACOLTA di
INGEGNERIA

Universidade do Porto
FEUP Faculdade de Engenharia

Analysis of surface roughness and models of mechanical contacts

Sérgio Manuel Oliveira Tavares
(sergio.tavares@fe.up.pt)
ERASMUS Student in "Facoltà di Ingegneria – Università di Pisa"
from "Faculdade de Engenharia da Universidade do Porto" - Portugal

Tutors:

Prof. Enrico Ciulli
Eng. Giovanni Pugliese

Pisa - Italy
2004-2005

Acknowledgements

This dissertation was prepared through the ERASMUS program in "Facoltà di Ingegneria della Università di Pisa".

I would like to express my gratitude to my supervisor in this University, Professor Enrico Ciulli for all of his support given. I am also much indebted to the support of the PhD student Giovanni Pugliese.

Other persons who helped me include: Professor Marco Lorenzetti, PhD student Alessandro Pollaco, Sergio Martini, and all of the staff of the Mechanical Engineering Department.

Furthermore, I would like to thank the Portuguese professors: Professor Luís Andrade Ferreira; Professor André Teixeira Puga; Prof. Paulo Tavares de Castro; Prof. Lúcia Maria Dinis and Prof. Carlos da Conceição António.

Contents

Nomenclature ---- 1

Abstract ---- 3

1. Surface Texture Measurements ---- 4

1.1 Waviness and Roughness ---- 4

1.2 Measurement Methods ---- 4

1.3 Stylus method ---- 6

1.4 Optical interference method ---- 8

2. Roughness parameters and surface characterization ---- 11

2.1 Measure Parameters ---- 11

2.2 Filters to extract roughness profiles ---- 11

2.3 Main Parameters ---- 13

2.4 Waviness Parameters ---- 16

2.5 Spacing Parameters ---- 16

2.6 Hybrid Parameters ---- 18

2.7 Statistical parameters ---- 21

2.8 Three dimensional parameters ---- 25

3. Models of Contact Mechanics ---- 27

3.1 Hertz Theory ---- 27

3.2 Greenwood and Williamson Model ---- 31

3.3 Chang Model ---- 35

3.4 Zhao Model ---- 38

3.5 Jeng and Wang Model ---- 44

3.6 Analysis of the asperity contact in FEM ---- 50

4. Approximation of the roughness profiles by mathematical functions ---- 52

4.1 Parabola functions using the Aramaki formulation ---- 52

4.2 Parabola functions using the least mean squares ---- 54

4.3 Parabola functions with the same area ---- 57

4.4 Comparison of the approach profiles methods ---- 58

5. Experimental Results ---- 62

5.1 The measured specimens ---- 62

5.2 Roughness Measures with stylus method ---- 63

5.3 Analysis of the contact area in the specimens – theoretical values ---- 67

5.4 Analysis of the contact area in the specimens using a optical microscope --------- 72
Conclusions ---------- 82
References ---------- 83
Appendix 1 – Abbott-Firestone curve ---------- 87
Appendix 2 – Hertz formulas ---------- 89
Appendix 3 – FEM model of mechanical contact between an asperity and a smooth plane, in ANSYS® ---------- 91
Appendix 4 – Matlab® model for approach roughness profiles using the Aramaki formulation ---------- 94
Appendix 5 – Matlab® model for approach roughness profiles using the least mean squares ---------- 96
Appendix 6 – Matlab® model for approach roughness profiles using the same asperity area ---------- 100
Appendix 7 – Results of stylus device measures ---------- 103
Appendix 8 – Models in Matlab® for contacts mechanics analysis ---------- 127
Appendix 9 – Results from the mechanical contact apparatus ---------- 132

Nomenclature

a	=	Semiminor radius of contact area or the effective radius of a contact area
A_e	=	Elastic contact area
A_{ep}	=	Elastoplastic contact area
A_i	=	Total contact area for an asperity
a_i, b_i	=	Semiminor and semimajor radius of critical deformed elliptical contact area
A_n	=	Nominal contact area
A_p	=	Plastic contact area
A_t	=	Total real contact area
A_t^*	=	Dimensionless total contact area
a_u, b_u	=	Semininor and semimajor radius of undeformed elliptical contact
b	=	Semimajor radius of contact area
C	=	Plasticity factor
d	=	Separation based on asperity heights
d^*	=	Dimensionless mean separation, d/σ
e	=	Eccentricity of the ellipse
$E(e)$	=	Complete elliptic integrals of second kind
E^*	=	Effective elastic modulus
$E_{1,2}$	=	Elastic modulus of the surface 1 or 2
$F_m(D)$	=	Parabolic cylinder function
H	=	Hardness of the softer material
h	=	Separation based on surface heights
h^*	=	Dimensionless mean separation, h/σ
k	=	Mean contact pressure factor
$K(e)$	=	Complete elliptic integrals of the first kind
l	=	Height of asperity control volume
N	=	Total number of asperities
n	=	Number of asperity contacts
p_m	=	Mean contact pressure
p_n	=	Nominal contact pressure
p_o	=	Maximum contact pressure
p_t	=	Real contact pressure
R	=	Asperity radius of curvature
r	=	the contact radius of an circular asperity
R_m	=	Mean effective radius of the curvature of asperities
$R_{x,y}$	=	The effective radii of curvature in the principal x and y plane
V	=	Control volume of a plastically deformed asperity
W	=	Normal load applied
w_e	=	Elastic contact load of an asperity
w_{ep}	=	Elastoplastic contact load of an asperity
W_{ept}	=	Elastoplastic contact load of two rough surfaces
W_{et}	=	Elastic contact load of two rough surfaces
w_f	=	Critical contact load at the point of fully plastic flow
W_i	=	Total load for an asperity
w_p	=	Plastic contact load of an asperity
W_{pt}	=	Plastic contact load of two rough surfaces
W_t	=	Total contact load
w_y	=	Critical contact load at the point of initial yield
x	=	Coordinates of the roughness digitalized profile points

Y	=	Yield Stress
y_s	=	Distance between the mean of asperity and that of surfaces heights
y_s	=	Dimensionless distance between the mean of asperity and that of surface heights, y_s/σ
z	=	Asperity height measured from the mean of asperity heights, z(x)
z^*	=	Dimensionless asperity height, z/σ
α	=	Coefficient of autocorrelation length
β	=	$\eta R\sigma$
β^*	=	Correlation length
δ	=	Interference
δ^*	=	Dimensionless interference, δ/σ
δ_c	=	Critical interference at the inception of plastic deformation from elastic to plastic yield
δ_{c1}	=	Critical interference at the point of initial yield
δ_{c2}	=	Critical interference at the point of fully plastic yield
η	=	area density of asperities
σ	=	Standard deviation of surface heights
σ_p	=	Standard deviation of the equivalent rough surface
σ_r, σ_θ	=	Stress tension in direction radial and angular
σ_s	=	Standard deviation of asperity heights
σ_x, σ_y, σ_z	=	Stress tension in direction x,y,z
τ	=	Autocorrelation length
Φ	=	Distribution function of asperity heights
Φ^*	=	Dimensionless distribution function
Ψ	=	Plasticity index
$\upsilon_{1,2}$	=	Poisson's Ratios of the surface 1 and 2

Abstract

The study of contact between surfaces is fundamental to many engineering problems. Some these problems include thermal and electrical conductivity, scuffing, friction, sealing, performance and life of machine elements.

In this work some mechanical contact models are deeply analyses as well as their application to different engineering surfaces. The base of the chosen models is the Greenwood – Williamson model, that has been proved to produce an accurate approximation in certain conditions. Experimental investigation was performed to compare the theoretical results that gives some good preliminary qualitative results.

The first step in the mechanical contacts analysis is the surface characterization. The knowledge of some statistical surface parameters is sufficient to foresee the behaviour of the surface when in contact with another. The most common roughness parameters are presented in this dissertation.

Roughness measures have been carried with specimens, these results had been used in the contact models, the deformation values and real contact area percentage was estimated using contact mechanics models programmed in Matlab.

1. Surface Texture Measurements

1.1 Waviness and Roughness

All surfaces are composed by different types of imperfections and irregularities. These characteristics can be divided in to diverse categories (DIN 4760) which defines the effects macro geometrics and micro geometrics.

The measurement of the rough surface produces a primary profile, this profile has the designation 'profile P' and is divided in two forms of irregularities. The first form is waviness, that normally is the result of the guide-ways not being straight as well as machine tool vibration. The other form that can be obtained from the measured profile is the roughness profile, this profile has the micro geometric imperfections.

The waviness profile is designed as 'profile W' and the roughness profile is 'profile R'. In the figure 1.1.1 a schematic representation of measured profile extracted from one surface is reported.

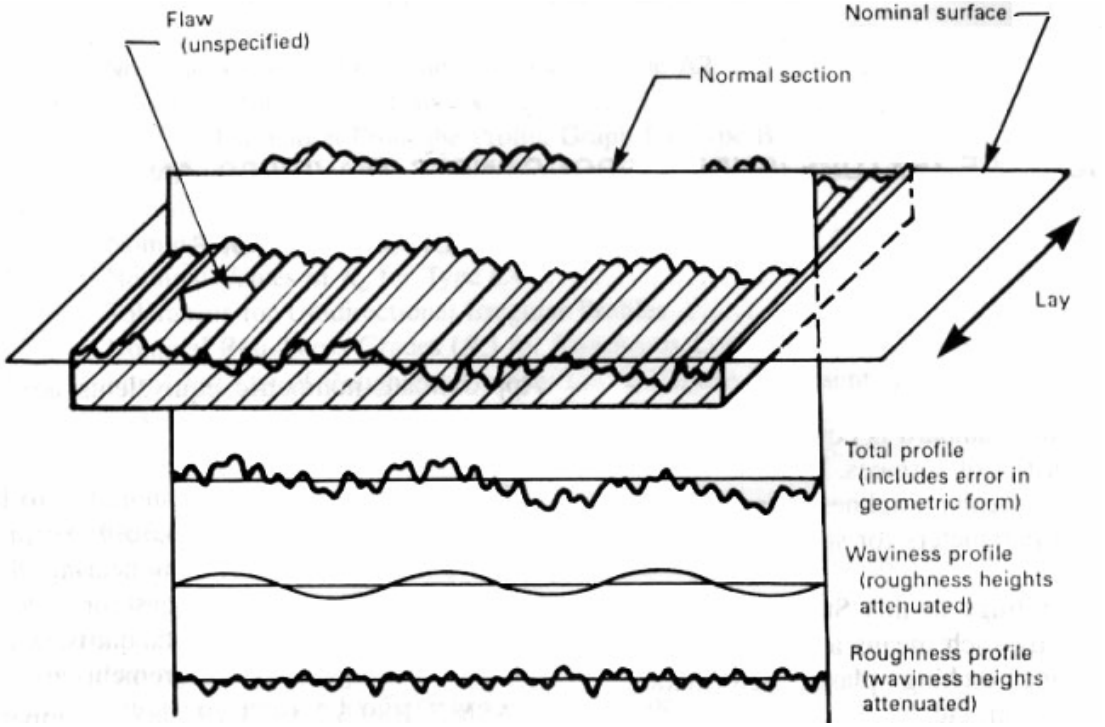

Fig. 1.1.1: Representation of a measured profile and the subdivision of this profile (from [1]).

The profile R and W are obtained from the 'profile P' with a digital or analog filter, as explained in the chapter 2.2 .

1.2 Measurement Methods

The measurement of the surface roughness is one of the most important steps for the analysis of the contact between two surfaces and is very important for the quality control of the surfaces. Various alternatives of the techniques for measure the roughness surface exist today. The adequate choice for the method that must be used is determined by the resolution and the limitations of the equipment.

In the table 1.2.1 is a summary of the present roughness measurements methods and the principal specifications.

Method	Quantitative Information	Three-dimensional data	Resolution (nm)		Limitations
			Spatial	Vertical	
Stylus instrument	Yes	Yes	15-100	0.1-1	Contact type can damage the surface
Optical Methods:					
Taper sectioning	Yes	No	500	25	Destructive, tedious specimen preparation
Light sectioning	Limited	Yes	500	0.1-1	Qualitative
Specular reflection	No	No	10^5-10^6	0.1-1	Semi quantitative
Diffuse reflection (scattering)	Limited	Yes	10^5-10^6	0.1-1	Smooth surface (< 100nm)
Speckle pattern	Limited	Yes			Smooth surface (< 100nm)
Optical interference	Yes	Yes	500-1000	0.1-1	
Scanning tunnelling microscopy	Yes	Yes	0.2	0.02	Require a conducting surface; scan small areas
Atomic force microscopy	Yes	Yes	0.2-1	0.02	Scan small areas
Fluid/Electrical	No	No			Semi quantitative
Electron Microscopy:					Expensive
Reflection/ replication	No	Yes	5	10-20	Instrumentation, tedious, limited data, requires a conducting surface, scans small areas
Integration of backscattered signal	Yes	Yes	5	10-20	
Stereo - microscopy	Yes	Yes	5	50	

Tab.1.2.1: Summary of the roughness measurement methods (from[2]).

In this dissertation the methods used for measuring the roughness is the stylus method and an optical microscope, that also allows an analysis of the roughness changes when one load is applied. Using an interferometer objective in the optical microscope it is possible to analyse the surface quantitatively. The following chapters a description of the stylus method and of the optical interference are reported.

1.3 Stylus method

The principle of this method is: while a diamond stylus which is traversed across the work-piece surface, the vertical displacement of this stylus is measured with a conversion into an electric signal. The signal is amplified and after converted into digital information; this information is then fed into a computer to analyse the measure profile and to calculate typical parameters.

The system used in this work is shown in figure 1.3.1.

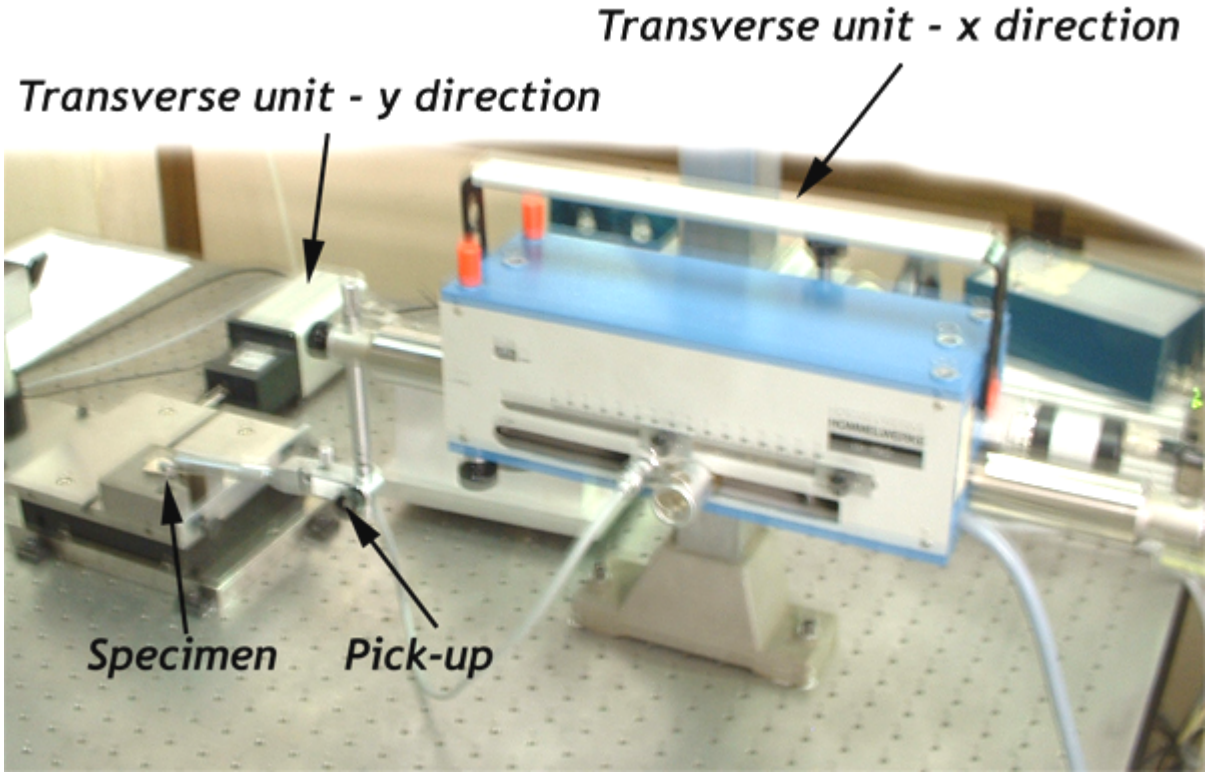

Fig.1.3.1: Image of the stylus surface analyser and the its components.

The pick-up is composed by three elements (Fig. 1.3.2):

The Stylus;
The Transducer;
The Skid.

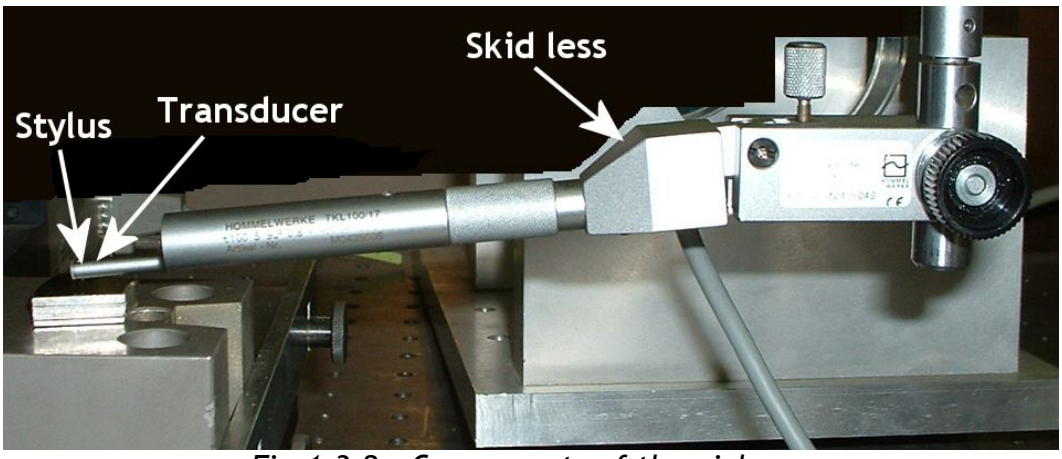

Fig.1.3.2 : Components of the pick-up.

The Stylus

The stylus is generally cone shaped in a diamond with 2-10 μm tip radius and a 60º-90º tip angle. The effect of the stylus geometry on the measurement is the first source of error in the system. This effect can be understood by the analysis of figure 1.3.3:

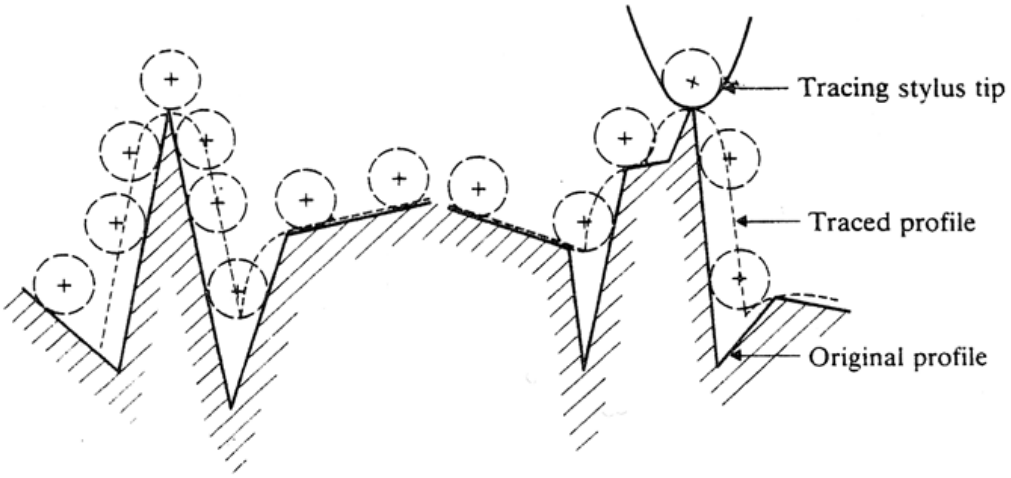

Fig.1.3.3: The stylus geometry error (from [2]).

The stylus with a smaller tip radius and a smaller angle will follow an angular profile closely, but the reduced contact area will mean higher contact pressure and will damage the surface.

The Transducer

The transducer will convert the vertical displacement in a electrical signal. There are different transducer types: inductive, piezoelectric, moving coil and laser interferometer. The schematic of a moving coil transducer is shown in figure 1.3.4:

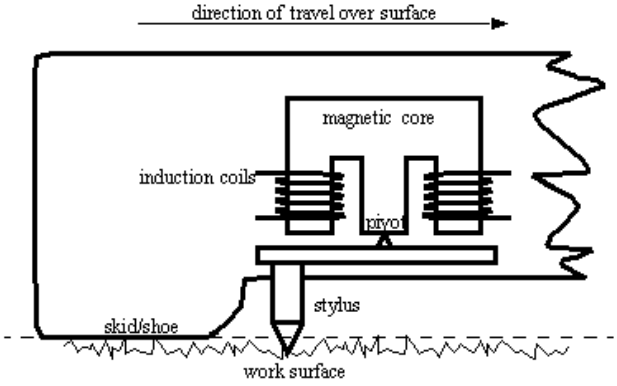

Fig.1.3.4: Schematic of a moving coil transducer [3].

The Skid

The skid can give the possibility to measure the macro profile features (skid less) or to refuse the macro profile features (skid type). Today is usual to use the skid less and remove the macro profiles features with a appropriate software.

The linear traverse unit is used in order to moving the pick-up or the work-piece. Normally two units are used, one for the transversal movement (direction x) and an other for the perpendicular direction (direction y), alternatively it is possible to use one for angular motion. All these mechanisms are controlled by a computer.

An other important component is the Analog to Digital Converter (ADC), which converts the amplified signal from the pick-up to a digital signal. The principal characteristic of the ADC is the resolution in bits, for example, 16 bits ADC can divide the transversal length in 2^{16}=65536 steps. This signal is captured and saved in a computer and it is possible to analyse the surface profile with specific software.

1.4 Optical interference method

The main principle of the interference is when a transparent wedge of small angle, surrounded by air, is illuminated with monochromatic light, an interference pattern is created. This principle can be used for measuring the surface roughness, using a reference flat fitted at the interference microscopy. When there is a small angle between the reference flat and the surface in examination, lines with equal thickness are generated. The local changes in this otherwise regular fringe pattern are a measure of the surface roughness. For measuring the surface roughness there are a two techniques that can extend the range of measurement of surface roughness where the surface slopes are large. One of these techniques is measuring the surface heights at two or more visible wavelengths, which increases the dynamic range of the measurement by the ratio of the synthetic wavelength to the visible wavelength. Another, more powerful technique is using the a white-light scanning interferometer, which involves measuring the degree of fringe modulation, instead of the phase of the interference fringes. In this case the surface heights are measured by changing the path length of the sample arm of the interferometer to determine the location of the sample for which the white-light fringe with the best contrast is obtained, then the vertical position at each location gives the surface map. The date of these images with fringes are converted in digital data after, with the analysis of the fringes is possible to reconstruct a 3d map of the measured surface.

The actual available instruments are based on these two techniques, in the figure 1.4.1 there is a schematic of the digital optical interferometer.

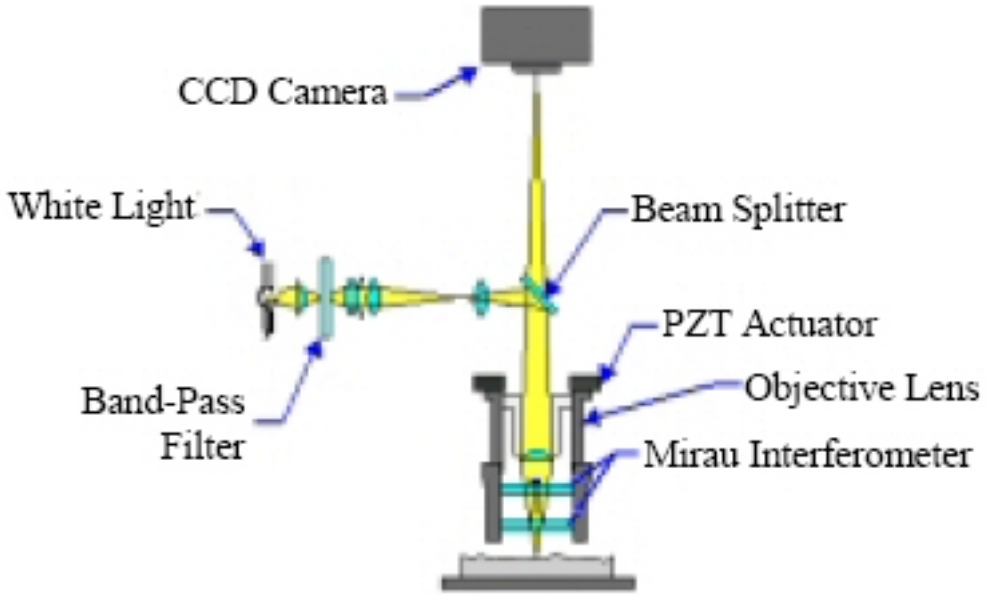

Fig.1.4.1: Schematic of the three dimensional interferometer with Mirau interference objective (from [4]).

In the figure 1.4.2 there is detailed of a Mirau interference objective.

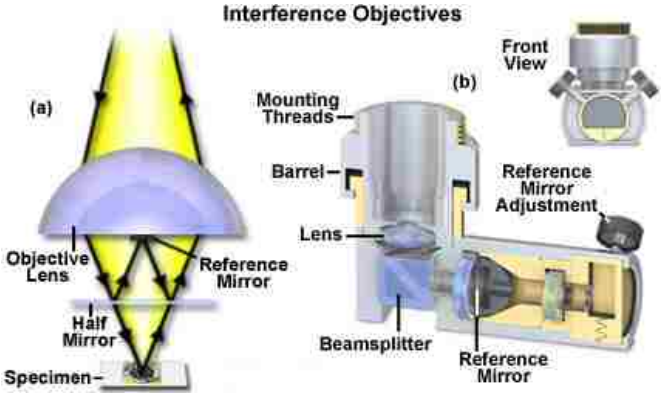

Fig.1.4.2: Principle of the two-beam interferometer (a) and Mirau interference objective (b) (from [5]).

The figure 1.4.3 is an image from one surface with the represented profile shape.

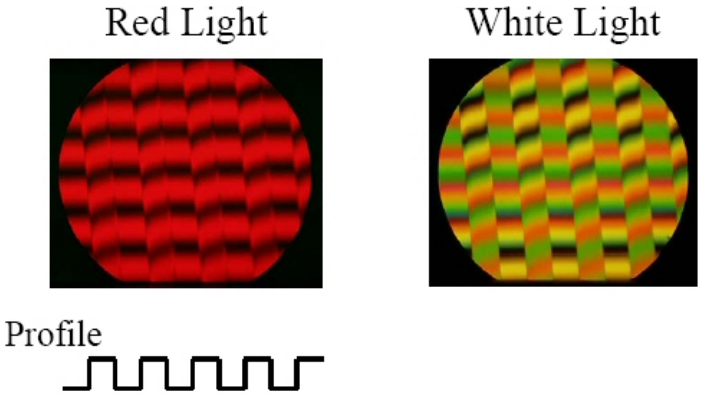

Fig.1.4.3: Interferometer images of the represented profile and using the red light and white light (from [6]).

From the figure 1.4.3, are can conclude that using white light it is possible to connect the fringes orders across a step even if the step height is greater than one fourth of the wavelength. But with white light there are more reflections that give spurious interference fringes.

2. Roughness parameters and surface characterization

2.1 Measure Parameters

When the profile is measured the height of the individual profile features is measured relative to a reference and normally the profile is not aligned and has a different form of 'noise'. In order to prepare the measured profile and remove the different forms this profile needs two stages: levelling the profile and applying one filter.

Levelling the profile is used to determine the reference of the profile. Normally when the work-piece is level, the profile measure has one inclination and the function of the levelling is to remove this inclination, the process used most is the least squares method with all measured points used in order to determine the levelling line. If the work-piece has another form (circular or elliptical) a reference line must be used that has the same form a the nominal profile.

2.2 Filters to extract roughness profiles

The function of the filter is to separate the roughness profile (profile R) and the waviness profile (profile W) from the profile measured. The parameter that determines what is roughness and what is waviness is the cut-off length. The cut-off length should be at least 2.5 times the peak-to-peak spacing of the profile roughness, but if the surface is anisotropic a recognizable pattern does not exist. In this case the standard DIN 4768/1 or more recent ISO 4288:1996 gives the reference value of cut-off for profiles with different characteristics.

Cut-off λ_c (mm)	Periodic Profiles	Non-periodic Profiles		Sampling Length/ Evaluation Length λ_c/L (mm)
	Peak spacing S_m (mm)	Ra (µm)	R_z (µm)	
0.08	0.013-0.04	(0.006)-0.02	(0.025)-0.1	0.08/0.4
0.25	0.04-0.13	0.02-0.1	0.1-0.5	0.25/1.25
0.8	0.13-0.4	0.1-2	0.5 – 10	0.8/4
2.5	0.4-1.3	2 – 10	10 – 50	2.5/12.5
8	1.3-4	10-80	50-200	8/40

Table 2.2.1: Selection of the cut-off length λ_c according to ISO 4288:1996.

It is possible to use a analog filter or digital filter, the analog filter is a commonly 2RC filter. Today, digital filter is used more because it is more simple and does not use electronic components and we can apply different filters or cut-offs for the same profile measured.

The digital filters can be phase correct filter (ISO 11562:1996) and valley suppression filter (ISO 13565-1). The phase correct filter (or Gaussian filter) is used for determining the mean line in surface metrology, and the procedure to obtain the roughness filtered profile is:

Gaussian filtered mean line: $m(z) = x(z) * W(z)$, where x(z) is the unfiltered profile, (*) is the convolution of the two functions and W(z) is:

Weighting function: $W(z)=\frac{1}{\alpha\lambda_c}e^{-\pi\left(\frac{z}{\alpha\lambda_c}\right)^2}$, with α=0.4697 and λ_c is cut-off length;

Then the roughness profile is: $R(z)=x(z)-m(z)$.

In the next image have a representation of the profile P, R e W from the an surface measure:

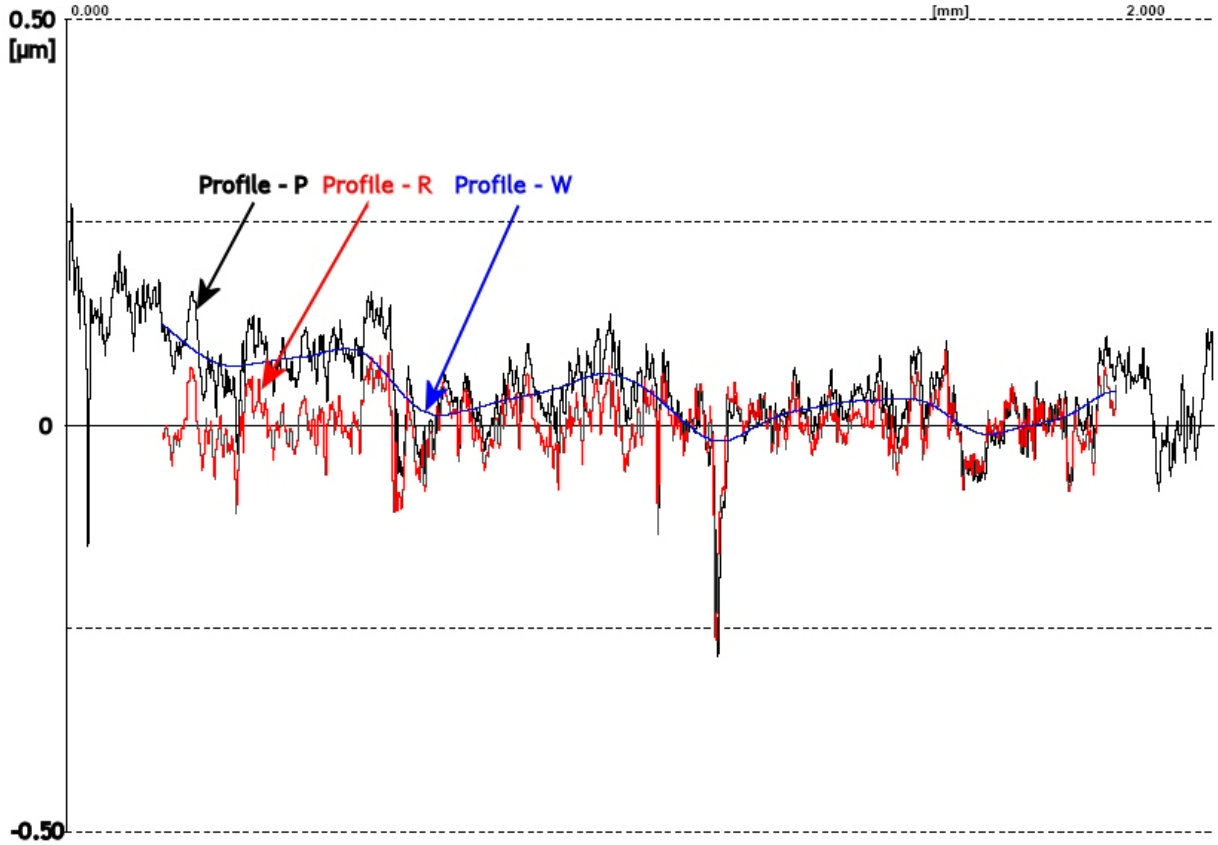

Fig. 2.2.1: Representation of the profiles-P, R and W from the measured surface.

The valley suppression filter is used for calculation of the R_k parameters. The surface is filtered with a phase correct filter, after all valleys beneath the mean line are removed and the profile is filtered again with a phase correct filter. The mean line obtained with these filter is superimposed in the original and mean line is straightened out to obtain the roughness profile.

2.3 Main Parameters

- Average roughness (Ra or AA):

$$R_a = \frac{1}{l}\int_0^l |z(x)|\,dx \tag{2.3.1}$$

The average roughness is the area between the roughness profile and its mean line, or the integral of the absolute value of the roughness profile height over the evaluation length.

When we have digital data the integral is normally approximated by a trapezoidal rule:

$$R_a = \frac{1}{N}\sum_{i=1}^{N} |r_i| \tag{2.3.2}$$

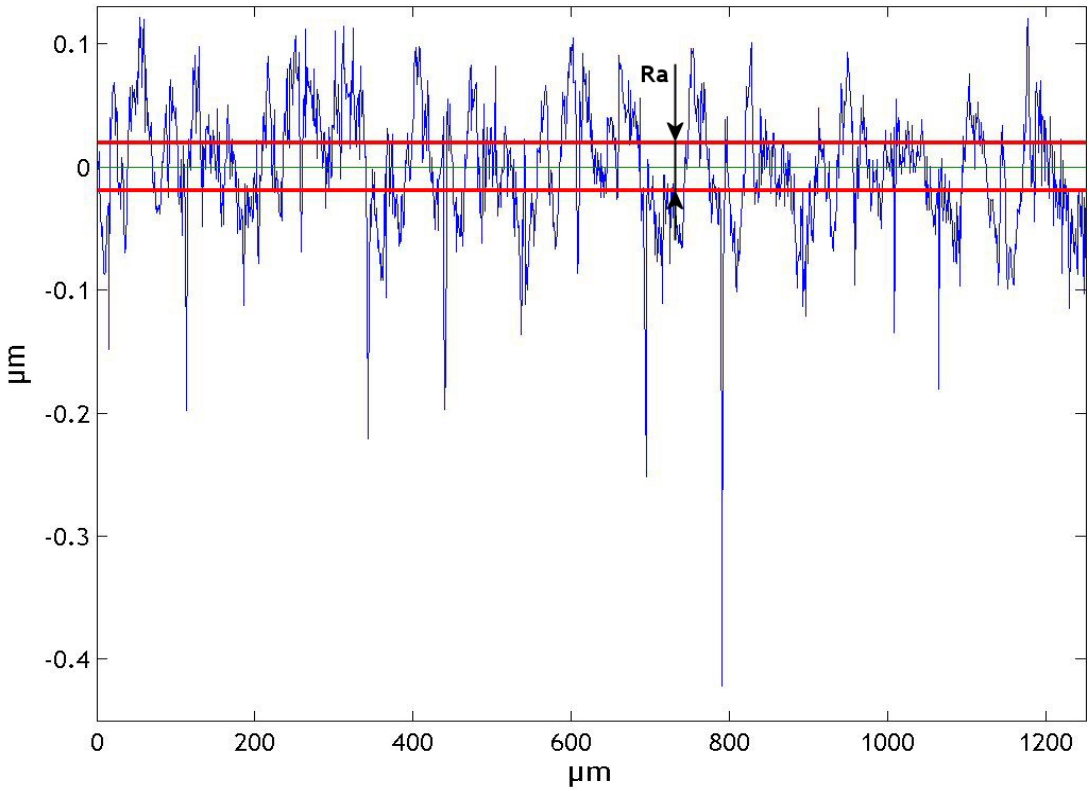

Fig.2.3.1: Schematic of the value Ra from an measured profile.

- Root mean square (RMS or R_q):

$$R_q = \sqrt{\frac{1}{l}\int_0^l z^2(x)dx} \tag{2.3.3}$$

The root mean square is the square root of the average of the square of the deviation of the profile from the mean line. This parameter is more sensitive to the peaks and valleys than R_a.

The digital equivalent formula normally used is:

$$R_q = \sqrt{\frac{1}{N}\sum_{i=1}^{N} r_i^2} \tag{2.3.4}$$

If the roughness profile follows a Gaussian distribution R_a and R_q are interchangeable:

$$R_q \sim \sqrt{\frac{\pi}{2}} R_a \sim 1.25 \times R_a \tag{2.3.5}$$

- The height of the highest peak (R_p) and the depth of the deepest valley (R_v):

The peak roughness Rp is the height of the highest peak in the roughness profile over the evaluation length. Similarly, Rv is the depth of the deepest valley in the roughness profile over the evaluation length.

$$R_p = \left|\min\left[r(x)\right]\right|, 0 \le x \le L \tag{2.3.6}$$

$$R_v = \left|\max\left[r(x)\right]\right|, 0 \le x \le L \tag{2.3.7}$$

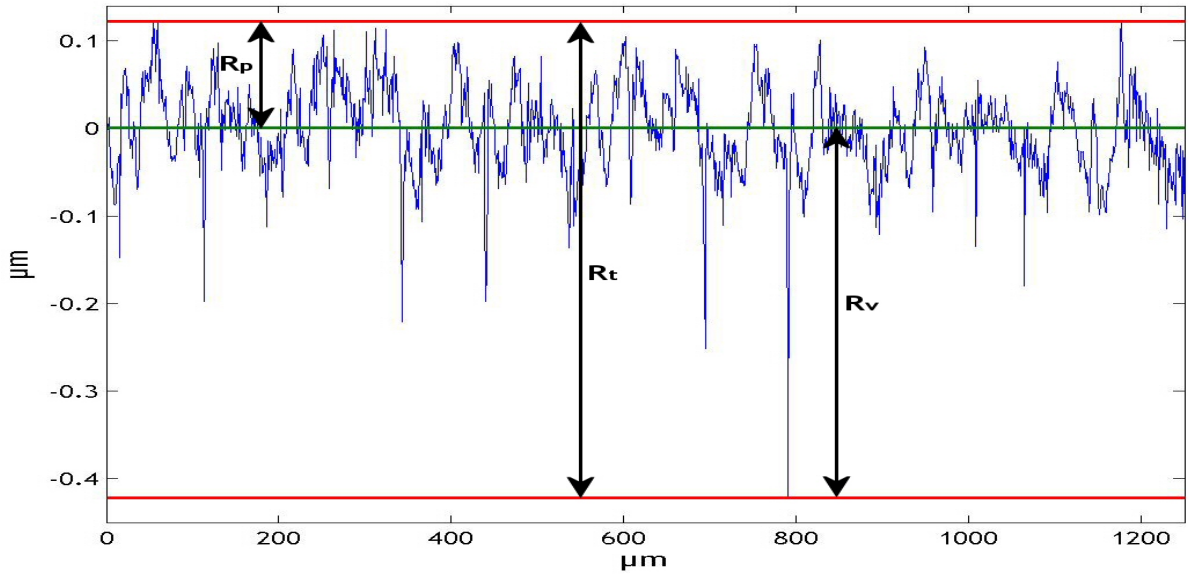

Fig.2.3.2: Representation schematic of the parameters Rp, Rv and Rt.

- The total roughness (Rt):

The total roughness, Rt, is the sum of these two, or the vertical distance from the deepest valley to the highest peak, for a digital profile:

$$R_t = R_p + R_v \tag{2.3.8}$$

- Average maximum peak height (Rpm), Average maximum valley depth (Rvm) and Average maximum height (Rtm):

$$R_{pm} = \frac{1}{k}\sum_{i=1}^{k} R_{pi} \tag{2.3.9}$$

$$R_{vm} = \frac{1}{k}\sum_{i=1}^{k} \left|R_{vi}\right| \tag{2.3.10}$$

where Rpi and Rvi is maximum peak or valley height, respectively, in an cut-off length, k is the number of cut-off lengths that divide the profile length. This parameter is represented in the figure 2.3.3 .

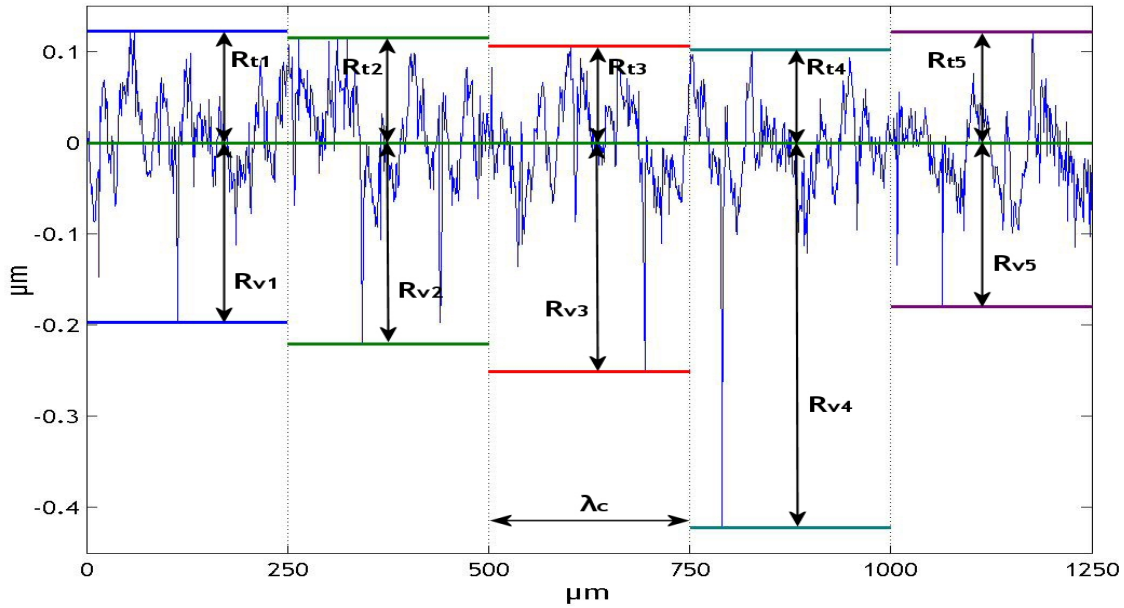

Fig. 2.3.3: Representation of the parameters Rvm and Rpm

The average maximum height is the average of the successive values of the maximum heights values in an cut-off length:

$$R_{tm} = \frac{1}{k}\sum_{i=1}^{k} R_{ti} \qquad (2.3.11)$$

The graphical representation of this parameter:

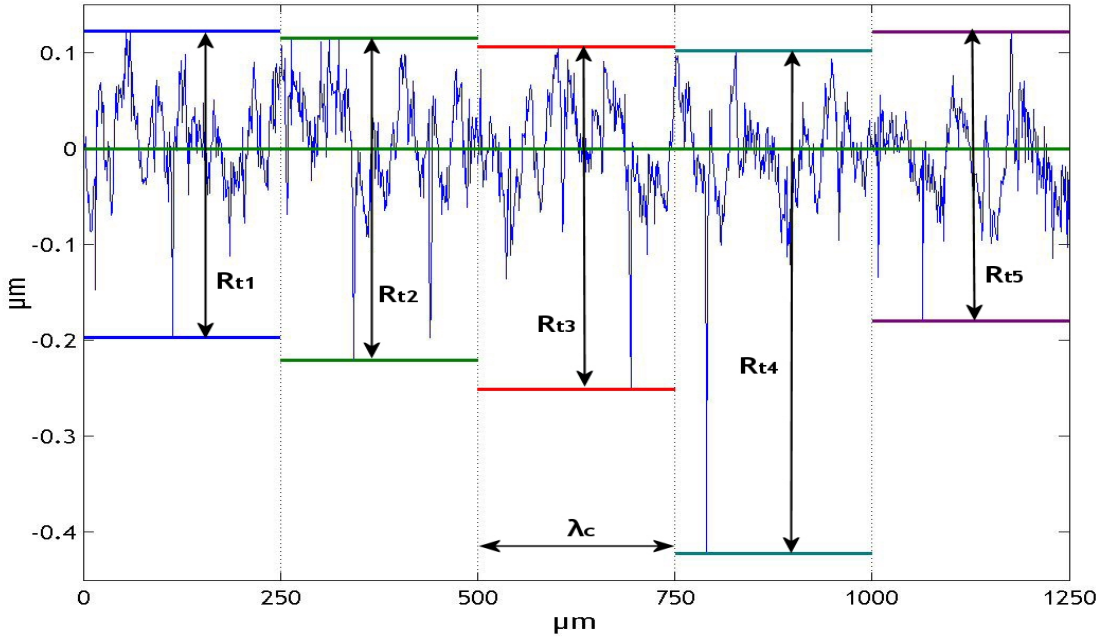

Fig. 2.3.4: Graphical representation of the parameter Rtm

The other parameter R_z(ISO) is the sum of the height of the highest peak plus the lowest valley depth but within a sampling length.

But R_z (DIN) is the mean peak to valley height in 5 equal lengths (normally this length is equal of the one cut-off length), is determined by the following formula:

$$R_{z(DIN)} = \frac{1}{5}\sum_{i=1}^{5} z_i \qquad (2.3.12)$$

This parameter is generally more sensitive to changes in surface finish than R_a.

- Maximum peak-to-valley height (R_{max} or R_y):

The R_{max} is the maximum peak to valley height within one cut-off length.

- Mean peak height (R_{pm}) and mean valley depth(R_{Vm}):

$$R_{pm} = \frac{1}{5}\sum_{i=1}^{5} p_i \quad \text{and}$$

$$R_{vm} = \frac{1}{5}\sum_{i=1}^{5} v_i \qquad (2.3.13)$$

2.4 Waviness Parameters

- Total waviness height - W_t:

Total waviness height is the maximum peak to valley height of the levelled and filtered waviness profile, is show in the next figure:

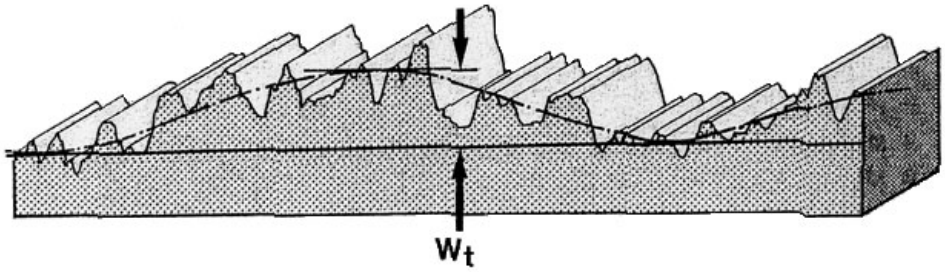

Fig.2.4.1: Total waviness height representation.(from [8]).

The others waviness parameters (W_p, W_v, W_z, etc.) have the same meaning that the roughness parameters, but relatively to the waviness profile.

2.5 Spacing Parameters

- Peak count or peak density (RP_c or P_c or N_r):

Peak count is a number giving the number of peaks per length of trace in a profile. In order to calculate RPc a peak is defined relative to an upper and lower threshold. Usually this is a single number, the "peak count threshold", the distance from a lower threshold up to an upper threshold, centred on the mean line. In order to count the peaks we need the definition of a peak, in a profile we need to identify the major peaks and exclude the minor peaks from the calculation of the peak count, these

conditions are called *cutting depths*. These cutting depths are both selected by the operator to suit the profile being analyzed.

$$RP_c = \frac{N^{\circ}.\,of\ \ counts}{Assessment\ lenght\ (cm)} = Peaks/cm \qquad (2.5.1)$$

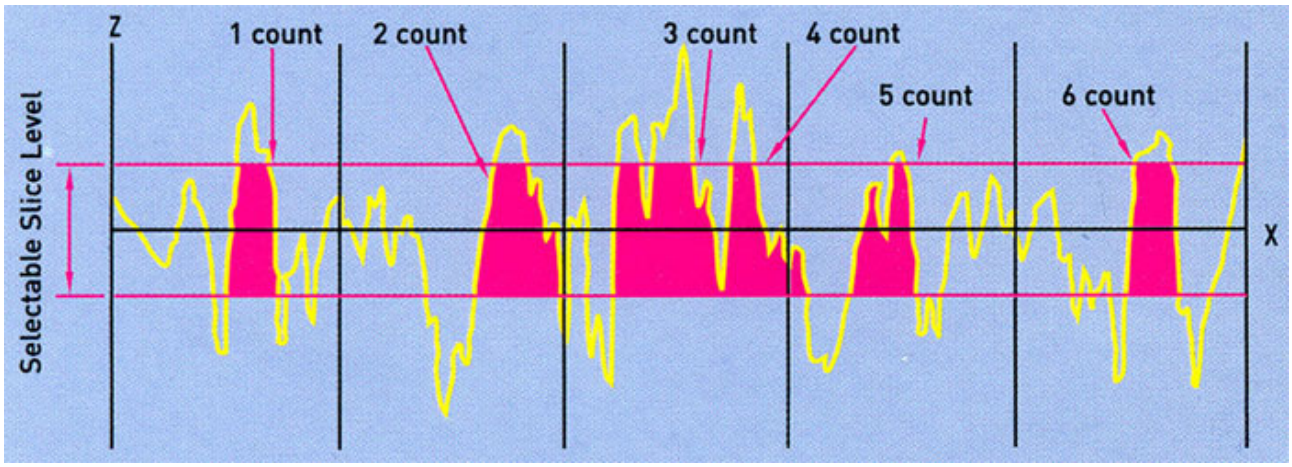

Fig.2.5.1: Schematic of peak density - RP_c or P_c or N_r (from [8]).

- Profile peak count (RHSC or D):

Profile peak count is the number of the profile peaks that exceed a pre-selected threshold, and is calculated over the entire assessment length, and is not normalized to a standard length.

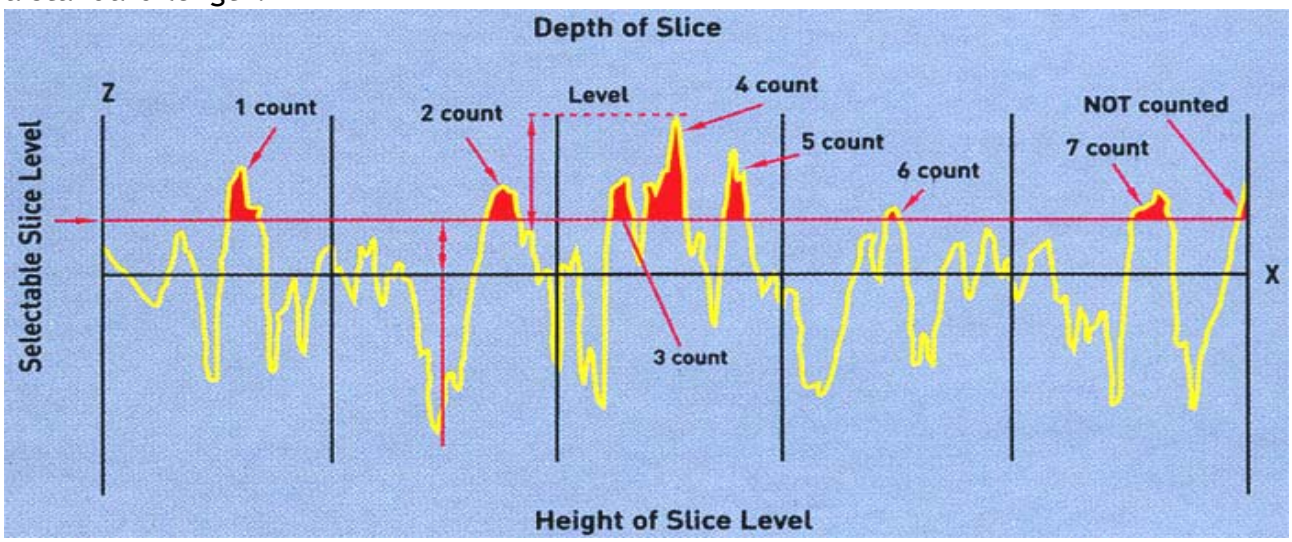

Fig.2.5.2: Profile peak count - RHSC or D (from [9]).

- Mean peak spacing (RS_m or S_m):

Mean peak spacing is the mean spacing between profile peaks at the mean line, measured within the sampling length.

$$RS_m = \frac{1}{N}\sum_{i=1}^{N} S_i \qquad (2.5.2)$$

where N is the number of peak spacings.

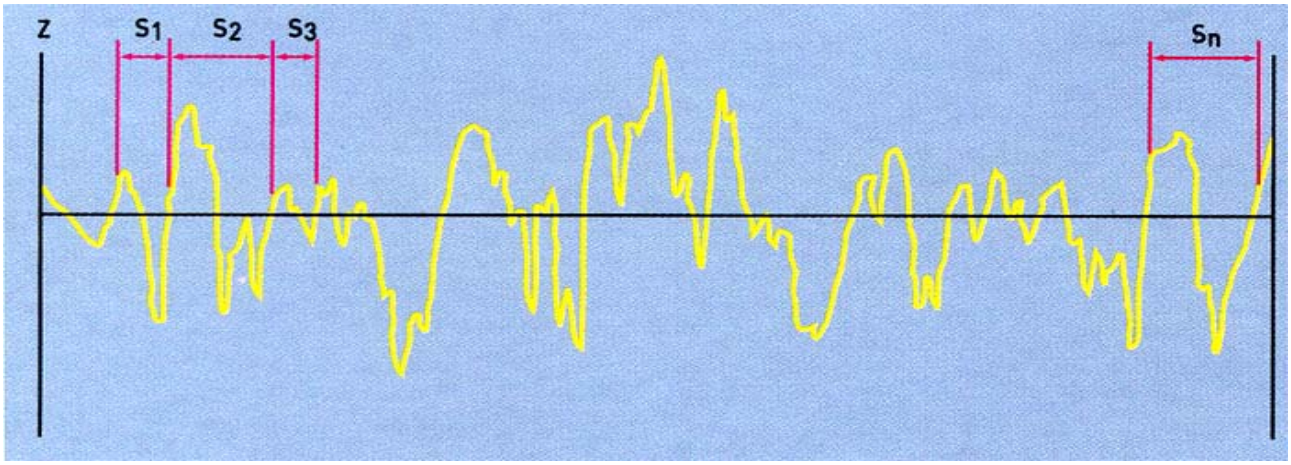

Fig. 2.5.3: Mean peak spacing - RS_m or S_m (from [9]).

2.6 Hybrid Parameters

- Abbot-Firestone Curve

This curve is also called the Bearing Area Curve or Material Ratio and it gives the ratio of air to material ratio at any level, starting at the highest peak. In order to produce this curve from a surface profile, some distance from a reference line a parallel line is drawn, the length of each material intercept along the line is calculated and these lengths are added together. The proportion of this sum to the total length, the bearing length (t_p) is calculated. If we repeat this along all of the surface profile, starting at the highest peak to the lowest valley, the fractional land length as a function of the height of each slice from the highest peak is plotted:

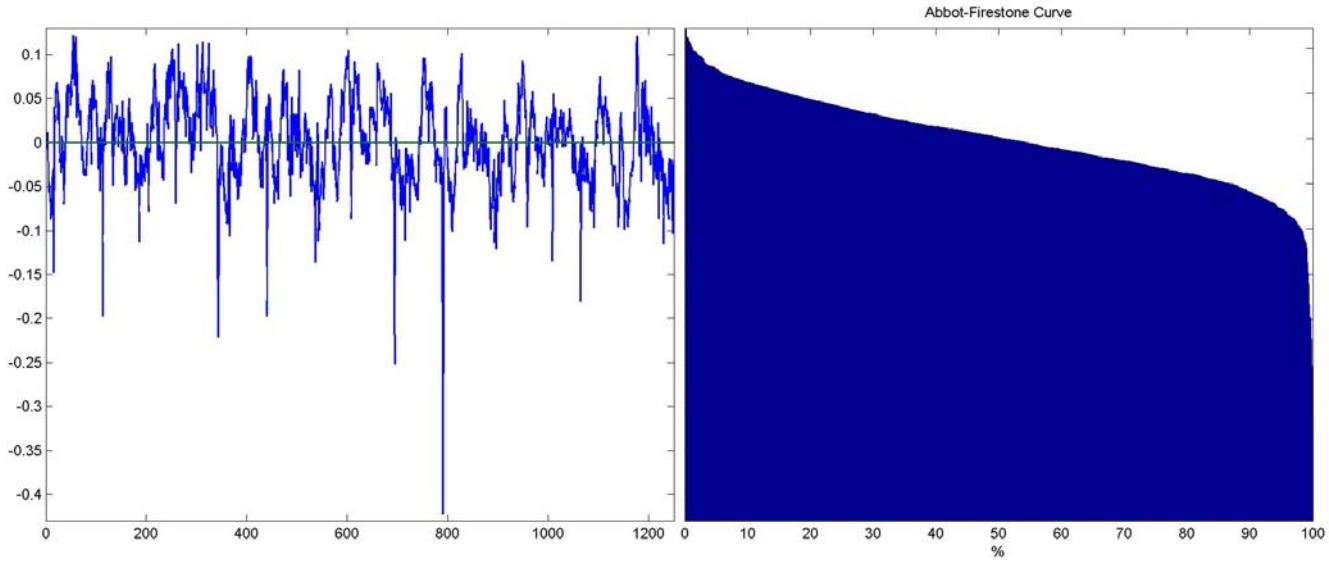

Fig. 2.6.1: Example of the an Abbot-Firestone Curve

In appendix 1, a logarithm for Matlab to draw this curve and probability curve.

- R_k Parameters (kernel roughness depth)

The Abbot-Firestone curve has significant information about the measured profile. The R_k parameters are a simple approach where the Abbot-Firestone curve is approximated by a set of straight lines.

In order to calculate the R_k parameters the straight lines are divided in to three parts: one part describe the peaks, an other part describes the valleys and the other describes the core roughness. The first step is to find the point of minimum secant slope ('turning point'). Two points, A and B are arbitrarily separated by 40% on the horizontal axis, the turning point is located by shifting these points along the curve until the vertical distance between them is at a minimum. Next draw a line through these two points to find the intercepts at 0% and 100%, points C and D, the vertical height between C and D is the first parameter – R_k, this parameter is designated the core roughness, because this part of the profile has the greatest increase an the material ratio. In order to calculate the parameters M_{r1} and M_{r2}: draw a horizontal line across from C to the Abbot-Firestone curve this fraction of surface is M_{r1}, and draw an other horizontal line across from D to the Abbot-Firestone curve this fraction is M_{r2}. Can see the graphical representation of this parameters in the next diagram.

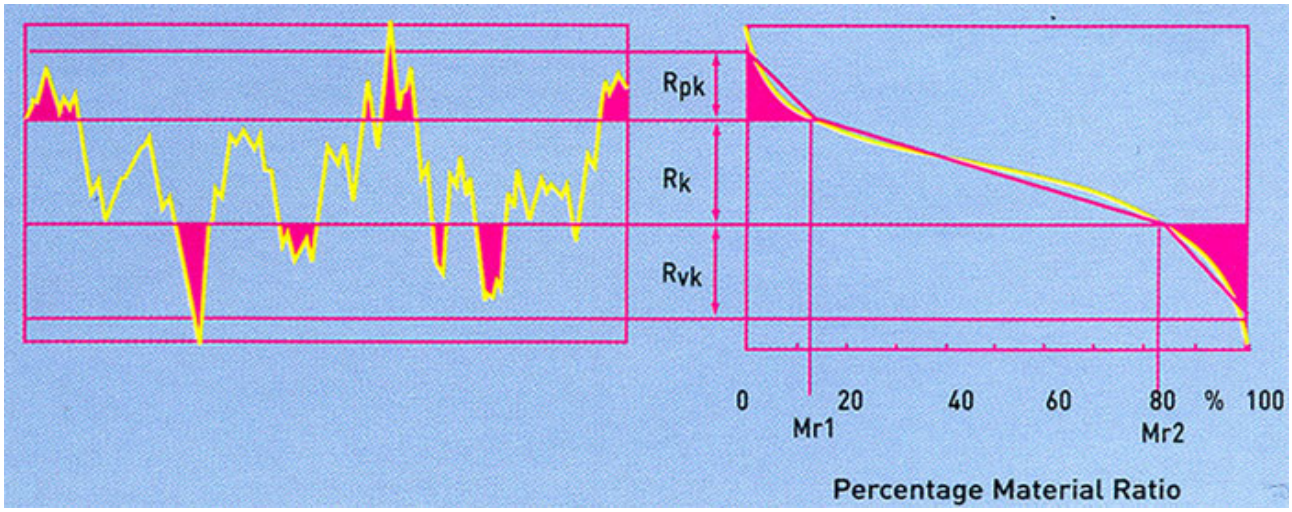

Fig. 2.6.2: Representation of the kernel roughness depth (R_k), reduced peak height (R_{pk}), trough depth (R_{vk}), material ratio corresponding to upper limit (M_{r1}) and material ratio corresponding to the lower limit (M_{r2}) (from [9]).

The Reduced Peak Height (R_{pk}) is the height of triangle that have the same area that the area below the Abbot-Firestone curve and above the line CE. The Trough Depth (R_{vk}) is the height of a triangle that have the same area below the Abbot-Firestone curve and above the line FD.

The other parameter is oil retention volume (V_o), is an indication of the oil retained by a cylinder bore surface after it has been scraped by a piston ring for example. It is calculated as follows:

$$V_o = \frac{R_{vk}(100 - M_{r2})}{200} \tag{2.6.1}$$

- Average profile slope ($R\Delta_a$):

This parameter is the average of the absolute value of the slope of the roughness profile over the evaluation length:

$$R\Delta_a = \frac{1}{L}\int_0^L \left|\frac{dr(x)}{dx}\right| dx \tag{2.6.2}$$

With a digital data this parameter can be approached by the equation:

$$R\Delta_a = \frac{1}{N-1}\sum_{i=1}^{N-1}\frac{\left|r_{i+1}-r_i\right|}{\Delta x} \tag{2.6.3}$$

- RMS profile slope ($R\Delta_q$):

The root mean square of the profile slope is useful because this value is its increased sensitivity to extreme values unlike the numerical value of the average of the profile slopes which tends to minimize their influence.

$$R\Delta_q = \sqrt{\frac{1}{L}\int_0^L \left(\frac{dr(x)}{dx}\right)^2 dx} \tag{2.6.4}$$

And if have digitalized data:

$$R\Delta_q = \sqrt{\frac{1}{N-1}\sum_{i=1}^{N-1}\frac{\left(r_{i+1}-r_i\right)^2}{\Delta x}} \tag{2.6.5}$$

- Average Wavelength ($R\lambda_a$):

$$R\lambda_a = 2\pi\frac{R_a}{R\Delta_a} \tag{2.6.6}$$

Average Wavelength is a measure of the spacings of the spacing between local peaks and local valleys, taking into account their relative amplitudes and individual spatial frequencies.

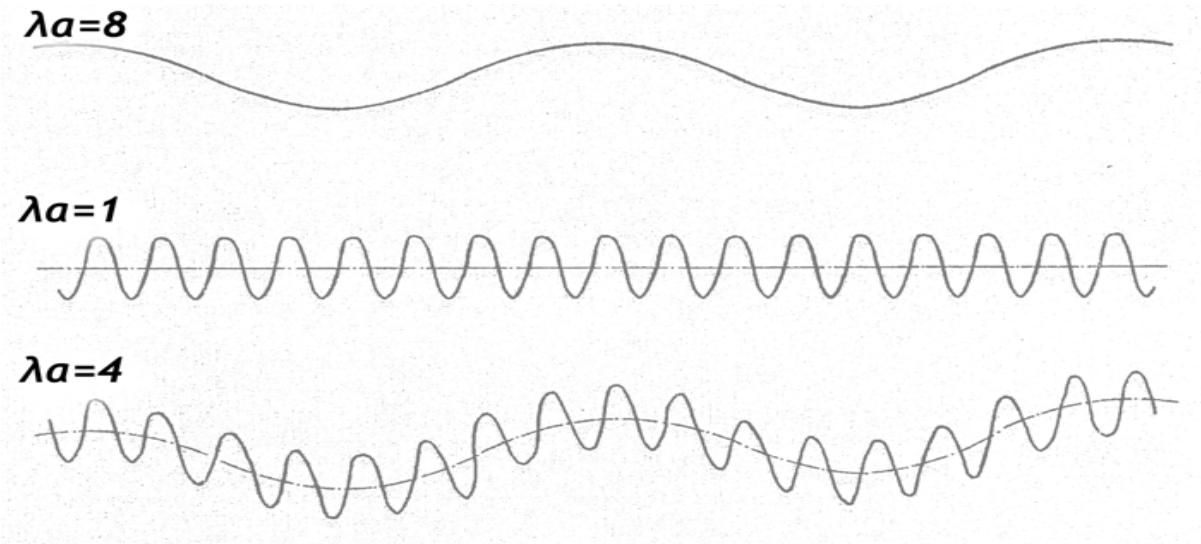

Fig. 2.6.3 : Graphic representation of average wavelength (from [8]).

- RMS Profile Wavelength ($R\lambda_q$):

$$R\lambda_q = 2\pi\frac{R_q}{R\Delta_q} \tag{2.6.7}$$

The RMS value is an average more sensitive to the extreme values than the $R\lambda_a$.

2.7 Statistical parameters

- The amplitude distribution function (ADF) or $\phi(z)$

This is a probability function that gives the probability that a roughness profile has a certain height at a position.

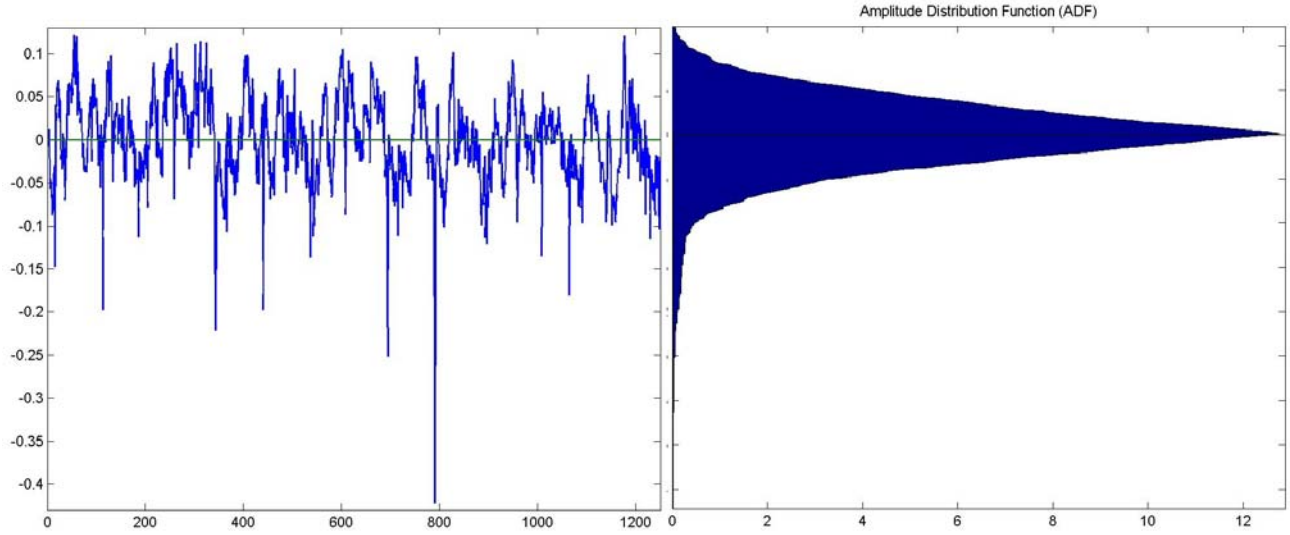

Fig. 2.7.1: Representation of the amplitude distribution function.

This function can be described mathematically by so-called moments:

First moment:

$$m_1 = \overline{z} = \frac{1}{N}\sum_{i=1}^{N} z_i \tag{2.7.1}$$

The first moment gives the arithmetic average of the roughness profile.

Second moment – Variance:

$$m_2 = Rq^2 = \sigma^2 = \frac{1}{N}\sum_{i=1}^{N}\left(z_i\right)^2 \tag{2.7.2}$$

The second moment gives the variance of the roughness profile and is an indication of the range of profile heights.

Third moment – Skewness (R_{Sk} or S_k):

$$m_3 = Sk = \frac{1}{\left(Rq\right)^3}\frac{1}{N}\sum_{i=1}^{N}\left(z_i\right)^3 \tag{2.7.3}$$

Skewness indicated by the one profile shows the asymmetry of the amplitude distribution function. Positive Skewness indicates a concentration of the material near the base of the profile or negative Skewness indicates a concentration of the material near the top.

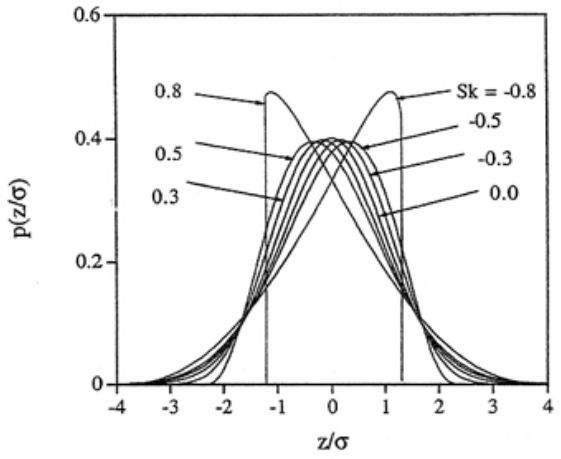

Fig . 2.7.2: Skewness variation with the form of the amplitude distribution function (from [2], pag. 117).

Fourth moment – Kurtosis (R_{ku} or K_u):

$$m_4 = Ku = \frac{1}{(Rq)^4}\frac{1}{N}\sum_{i=1}^{N}(z_i)^4 \qquad (2.7.4)$$

Kurtosis is a parameter that measures the sharpness of the amplitude distribution function. A flat amplitude distribution function indicates many small, rounded peaks and valleys in the roughness profile.

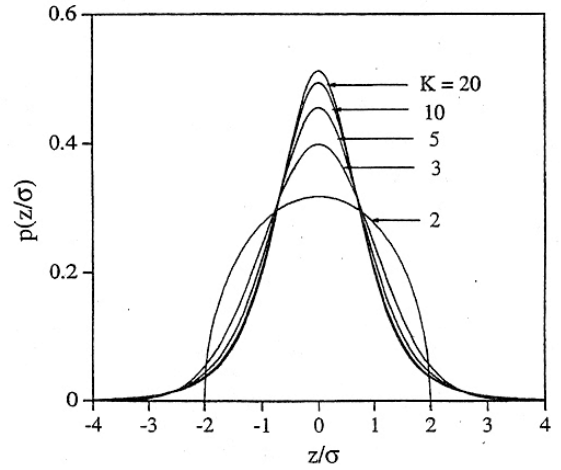

Fig. 2.7.3: Kurtosis variation with the form of the amplitude distribution function (from [2], pag. 117).

If the amplitude distribution function (ADF) is a symmetric Gaussian distribution the R_{Sk}=1 and the R_{Ku}=3. Many engineering surfaces have a symmetrical Gaussian height distribution and a experience with most engineering surfaces shows that the height distribution is Gaussian at the high end, but at the lower end, the bottom of the distribution is generally found to be non-Gaussian. But many common machining processes produce surfaces with non-Gaussian distributions.

- Mean slope and mean curvature:

The mean slope is the same that $R\Delta_a$. Mean curvature is not normalized parameter, but is very used for contact analysis with statistical roughness parameters. The profile curvature are given as: $-\frac{\partial^2 z}{\partial x^2}$, for a digitized profile are approximately as:

$$\frac{1}{N-2}\sum_{i=2}^{N-1}\frac{2z_i - z_{i-1} - z_{i+1}}{\Delta x^2} \tag{2.7.5}$$

- The cumulative sum of the amplitude distribution curve or Gaussian probability distribution function:

This function is the same shape as that of the Abbot-Firestone curve, but this function is normalized for statistics analysis and gives the cumulative probability of the roughness surface.

- Autocovariance function (ACVF) and autocorrelation function (ACF):

The covariance measure of how much the deviations of the two or more variables match and the correlation of two variables provides a measure of how the two variables affect one another. The autocovariance function (ACVF) can be calculated duplicating the profile, with these two profiles multiplying the two ordinate series. The average of the ordinate products is the ACVF value. The next ACVF value of the ACVF series ACVF(τ) is found by shifting the duplicate profile by a distance, τ, and calculating the average sum of the products of these two ordinate series. These ACVF values will be lower, and duplicated profile is continuously shifted and the multiplication of the ordinates is repeated. The curve ACVF can be generated plotting ACVF values on a graph versus the shift distance.

Mathematically:

$$ACVF(\tau) = \lim_{L\to\infty}\frac{1}{L}\int_0^L z(x)\times z(x+\tau)dx \tag{2.7.6}$$

The normalized form of the ACVF is called autocorrelation function (ACF), in mathematical form is:

$$ACF(\tau) = \frac{ACVF(\tau)}{(R_q)^2} \tag{2.7.7}$$

The autocorrelation does not include information about the profile amplitude, and the range values are from negative one (correlation of the inverted shifted profile) to one (perfect correlation).

The correlation length is a parameter that measures how quickly ACF decays, the threshold value for the correlation length is not defined, but commonly is used ACF(τ)=0.1. In some cases the correlation length is defined as the distance at which value of ACF=1/e, that is 0.368. The correlation length can be taken as that at which two points on a function at a distance τ apart are strongly interdependent.

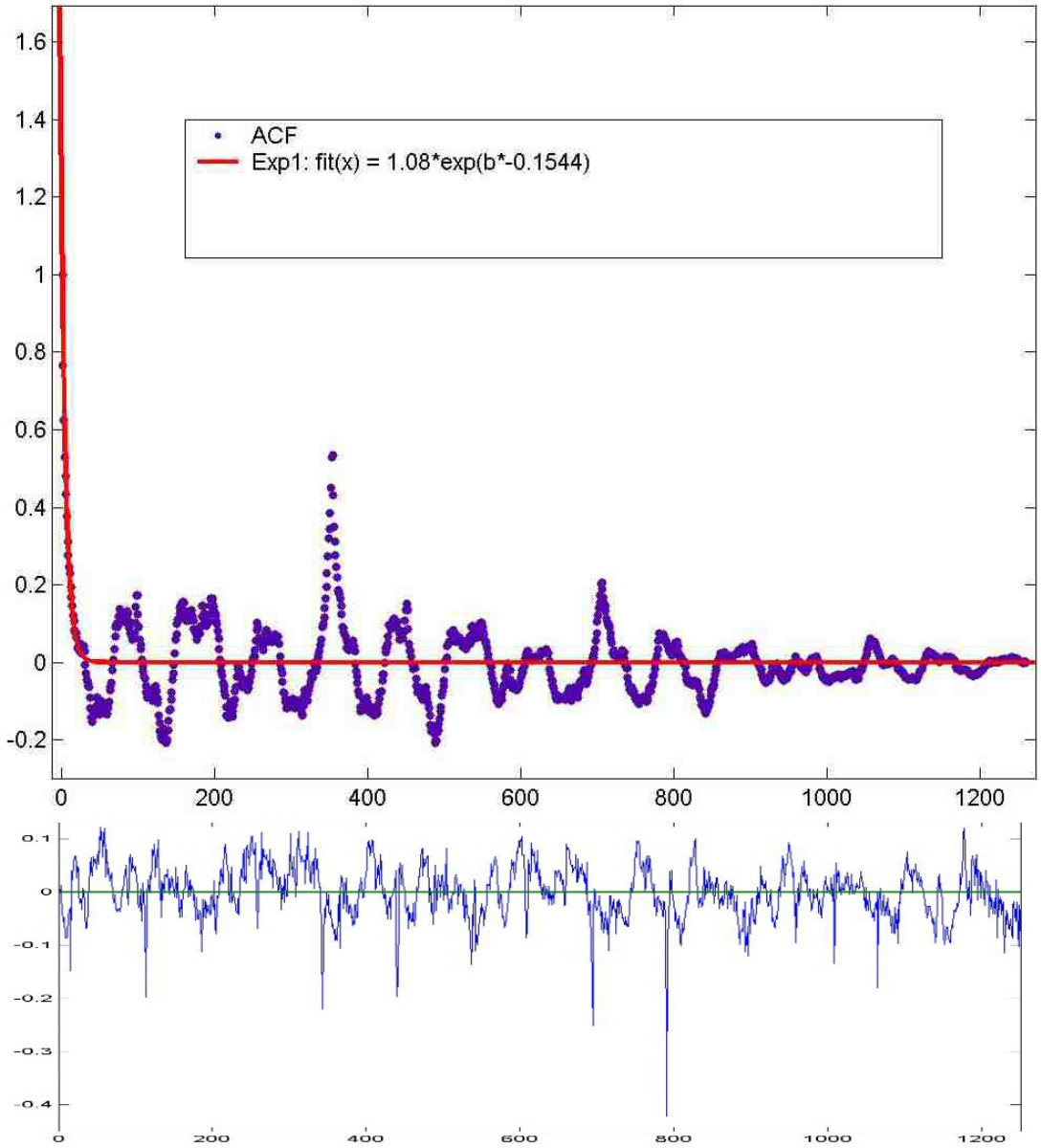

Fig.2.7.4: Representation of the ACF function and the fitting with a exponential function, of the profile represent in down. .

- Structure Function (SF) or Variance Function (VF):

$$SF(\tau) = 2\sigma^2 \left[1 - ACF(\tau)\right] \tag{2.7.8}$$

This function represents the mean square of the difference in height expected over any spatial distance τ.

- Fourier Analysis

Fourier Analysis is a method that is based on the concept that real roughness surfaces can be approximated by a sum of sinusoidal functions, each at a different frequency.

The Fast Fourier Analysis (FFT) is a algorithm developed by Tukey and Cooley in 1965 to convert the Fourier transform function in discrete data.

The information contained in a Fourier analysis is identical to the information presented by the autocorrelation function, but in a different form.

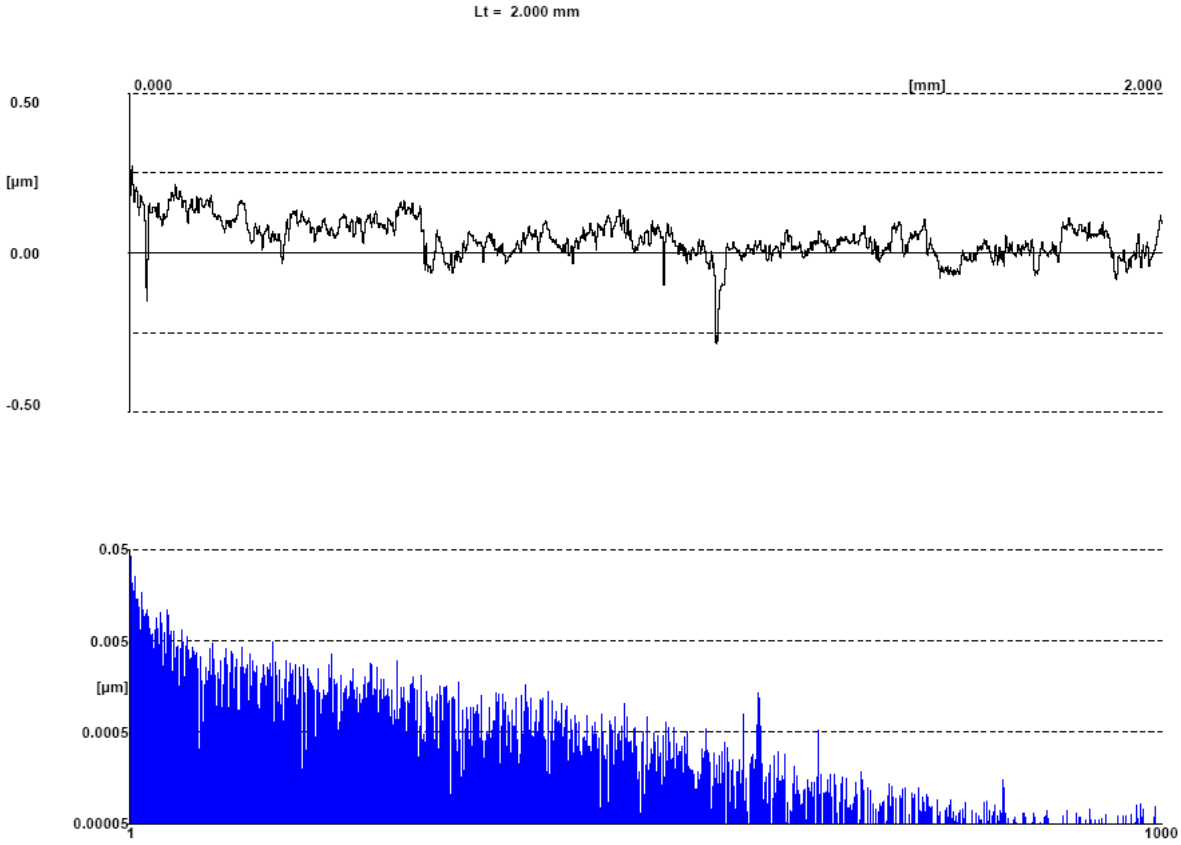

Fig. 2.7.5: Represation of the FFT, of the profile represented in up.

- Power Spectral Density Function (PSDF):

These function is the Fourier transform of the Autocovariance Function:

$$P(w) = \int_{-\infty}^{\infty} ACVF(\tau)\exp(-iw\tau)d\tau = \int_{-\infty}^{\infty} \sigma^2 ACF(\tau)\exp(-iw\tau)d\tau \qquad (2.7.9)$$

Since the ACVF is an even function of τ, the power spectral density function is given by the real part:

$$PSDF(w) = \frac{2}{\pi}\int_{0}^{\infty} \sigma^2 ACF(\tau)\cos(w\tau)d\tau \qquad (2.7.10)$$

2.8 Three dimensional parameters

The three dimensional parameters do not yet have a standard, but is these parameters commonly used:
Amplitude parameters:

- Spatial Average roughness:

$$S_a = \frac{1}{M \times N}\sum_{i=1}^{M}\sum_{j=1}^{N}\left|z_{ij}\right| \qquad (2.8.1)$$

- Spatial root mean square (Sq):

$$S_q = \sqrt{\frac{1}{M \times N} \sum_{i=1}^{M} \sum_{j=1}^{N} z_{ij}^2} \tag{2.8.2}$$

- Spatial maximum height (St):

$$S_t = Max(z_{ij}) - Min(z_{ij}) \tag{2.8.3}$$

- Spatial maximum peak height (S_p):

$$S_p = Max\left(x_{ij}\right) \tag{2.8.4}$$

- Spatial maximum valley height (S_v):

$$S_v = Min\left(x_{ij}\right) \tag{2.8.5}$$

- Spatial average maximum height (DIN):

$$S_z = \frac{1}{5} \sum_{i=1}^{5} z_i - \frac{1}{5} \sum_{j=1}^{5} z_j \tag{2.8.6}$$

where z_i is five maximums, and z_j is five minimums of the all profile.

- Spatial Skewness

$$S_{sk} = \frac{1}{S_q^3} \frac{1}{M \times N} \sum_{i=1}^{M} \sum_{j=1}^{N} z_{ij}^3 \tag{2.8.7}$$

- Spatial Kurtosis

$$S_{Ku} = \frac{1}{S_q^4} \frac{1}{M \times N} \sum_{i=1}^{M} \sum_{j=1}^{N} z_{ij}^4 \tag{2.8.8}$$

- Material volume per unit area at 10% on BAC (S_m or S_{mmr}):

The material volume is defined as the material portion enclosed in the 10% bearing area and normalised to unity.

- Core Void Volume of the Surface (Sc):

A core void volume is enclosed from 10% to 80% of surface bearing area and normalised to the unit sampling area.

- Valley void volume per unit area at 80% - 100% on BAC (S_v or S_{mvr})

The valley void volume of the unit sampling area is defined as a void volume at the valley zone from 80% to 100% surface bearing area. The void volumes is proposed here to provide a direct inspection of lubrication and fluid retention of surfaces. It represents the fluid retention ability of a highly wear surface. For a flat topped surface, such as a honed surface, the core void volume may decrease quickly with the truncation level, whereas for a spiked surface, such as a bored surface, the function shows a slow decrease. Thus functionally, the void volumes reflect the fluid retention property [10].

3. Models of Contact Mechanics

In this part the models to analyse the contacts of two surfaces are introduced. The first model was established by Heinrick Hertz in 1882, but this model only considers the elastic contact and disdains the effects of the roughness and the effects of the plasticity, and the real contact area is unvalued.

Nowadays there exist numerical and analytical models that consider the effect of the roughness and the plastic/elastic-plastic deformations, most of them using the statistical analysis of the roughness in order to estimate the real contact area. In this dissertation the most important models are introduced.

In the following chapter, an introduction to the Hertz Theory is presented, this theory is important for estimated the apparent area of the contact and the interaction between two asperities in elastic yield.

3.1 Hertz Theory

The Hertz theory analysis the contact between two bodies whereby at least one have a circular form, the contact is beginning in one point (contact between one sphere and other sphere or smooth surface) or beginning in one line (two cylinders or one cylinder and one smooth surface).

The analysis of the Hertz is based on four assumptions:

- The surfaces are continuous, smooth and nonconforming;
- The strains are small;
- Each solid can be considered as an elastic half-space in the proximity of the contact region;
- The surfaces are frictionless.

In the figure 3.1.1 has the schematic of the simple case of contact between two solids of revolution with radius R_1 and R_2, the contact area is circular and have radius *a*:

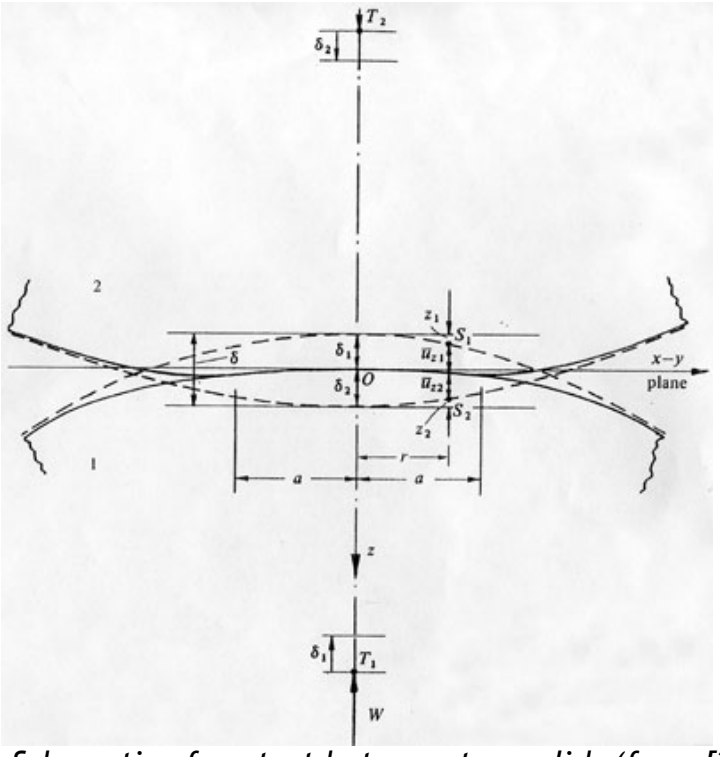

Fig. 3.1.1: Schematic of contact between two solids (from [2]).

Defining the composite radius as:

$$\frac{1}{R}=\frac{1}{R_1}+\frac{1}{R_2} \tag{3.1.1}$$

If the $\bar{u}_{z1}$ and $\bar{u}_{z2}$ is the normal displacements, can be written:

$$\bar{u}_{z1}+\bar{u}_{z2}=\delta-\left(\frac{1}{2}R\right)r^2, \quad \delta=\delta_1+\delta_2 \tag{3.1.2}$$

The pressure distribution proposed by Hertz:

$$p=p_0\left(1-\left(\frac{r}{a}\right)^2\right)^{1/2} \tag{3.1.3}$$

The normal displacements can be given by:

$$\bar{u}_z=\frac{1-\upsilon^2}{E}\frac{\pi p_0}{4a}\left(2a^2-r^2\right), \quad r\le a \tag{3.1.4}$$

The pressure in the second body is the same on the first, so that are can define the composite of effective modulus by:

$$\frac{1}{E^*}=\frac{1-\upsilon_1^2}{E_1}+\frac{1-\upsilon_2^2}{E_2} \tag{3.1.5}$$

Substituting the expressions for $\bar{u}_{z1}$ and $\bar{u}_{z2}$ -(3.1.4) in equation (3.1.2), are obtains:

$$\frac{\pi p_0}{4aE^*}\left(2a^2-r^2\right)=\delta-\left(\frac{1}{2}R\right)r^2 \tag{3.1.6}$$

The nominal contact area:

$$A_n=\pi a^2=\pi R\delta \tag{3.1.7}$$

The radius of the contact is given by:

$$a=\frac{\pi p_0 R}{2E^*} \tag{3.1.8}$$

and

$$\delta=\frac{\pi a p_0}{2E^*} \tag{3.1.9}$$

The pressure is related to the normal load applied (W) by:

$$W=\int_0^a p(r)2\pi r dr=\frac{2}{3}p_0\pi a^2 \tag{3.1.10}$$

Then the maximum pressure p_0 is 3/2 times the mean pressure p_m.

Expressing the radius of the contact in function of W:

$$a=\left(\frac{3WR}{4E^*}\right)^{\frac{1}{3}} \tag{3.1.11}$$

and

$$p_0 = \frac{3W}{2\pi a^2} = \left(\frac{6WE^{*2}}{\pi^3 R^2} \right)^{\frac{1}{3}} \tag{3.1.12}$$

The stress distributions in polar coordinates in the surface z=0, inside the loaded circle r≤a (from Johnson [17] page 62):

$$\frac{\sigma_r}{p_0} = \frac{1-2\upsilon}{3}\left(\frac{a^2}{r^2}\right)\left[1-\left(1-\frac{r^2}{a^2}\right)^{\frac{3}{2}}\right]-\left(1-\frac{r^2}{a^2}\right)^{\frac{1}{2}} \tag{3.1.13}$$

$$\frac{\sigma_\theta}{p_0} = \frac{1-2\upsilon}{3}\left(\frac{a^2}{r^2}\right)\left[1-\left(1-\frac{r^2}{a^2}\right)^{\frac{3}{2}}\right]-2\upsilon\left(1-\frac{r^2}{a^2}\right)^{\frac{1}{2}} \tag{3.1.14}$$

$$\frac{\sigma_z}{p_0} = -\left(1-\frac{r^2}{a^2}\right)^{\frac{1}{2}} \tag{3.1.15}$$

and outside of the circle:

$$\frac{\sigma_r}{p_0} = -\frac{\sigma_\theta}{p_0} = \frac{(1-2\upsilon)}{3r^2}a^2 \tag{3.1.16}$$

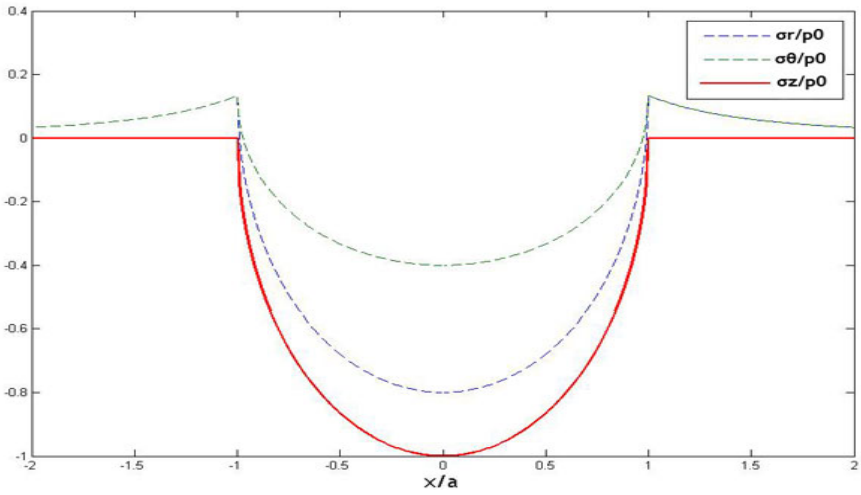

Fig.3.1.2: Variation of the σ_z/p_0, σ_r/p_0, σ_θ/p_0 in plane z=0.

The stresses on the z axis may be calculated by considering a ring of concentrated force at radius *r*:

$$\frac{\sigma_r}{p_0} = \frac{\sigma_\theta}{p_0} = -(1-\upsilon)\left[1-\left(\frac{z}{a}\right)\tan^{-1}\left(\frac{a}{z}\right)\right]+\frac{1}{2}\left(1+\frac{z^2}{a^2}\right)^{-1} \tag{3.1.17}$$

$$\frac{\sigma_z}{p_0} = -\left(1+\frac{z^2}{a^2}\right)^{-1} \tag{3.1.18}$$

$$\tau_1 = \frac{1}{2}\left|\sigma_z - \sigma_r\right| \tag{3.1.19}$$

Fig.3.1.3: Variation of the σ_z/p_0, σ_r/p_0, σ_θ/p_0 and τ_1 in plane x=0.

The limit of the elastic yielding in the Hertz theory is for approximately $0.31p_0$ at a depth of 0.48a, hence plastic yielding would be expected to initiate beneath the surface. In order to estimate the limit of elastic deformation, are can use two criteria: Tresca maximum shear stress criterion and the Von Mises shear strain energy criterion.

By the Tresca criterion, the value of p_0 for yield is given by:

$$(p_0)_y = \frac{3}{2}(p_m)_y = 3.2k = 1.6Y \tag{3.1.20}$$

and the Von Mises criterion:

$$(p_0)_y = 2.8k = 1.4Y \tag{3.1.21}$$

where:

$$k = \max\left\{\tfrac{1}{2}|\sigma_1 - \sigma_2|; \tfrac{1}{2}|\sigma_1 - \sigma_3|; \tfrac{1}{2}|\sigma_2 - \sigma_3|\right\} \tag{3.1.22}$$

and Y is the yield stress.

3.2 Greenwood and Williamson Model

All surfaces are rough on a microscopic scale, and when the two rough surfaces are in contact the real area is very small compared to the apparent area of the contact.

When loading presses two rough surfaces together, only some peaks of the surfaces will be in contact, thus, these peaks often carry very high loads. This effect was analysed by Greenwood and Williamson in 1966 [28].

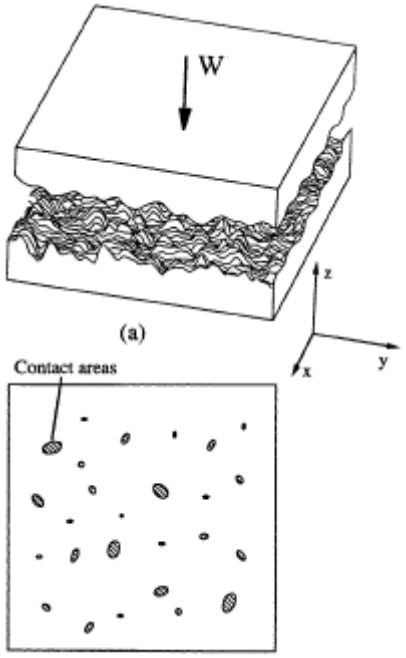

Fig.3.2.1: Schematic of the real area of contact (from [2]).

The Greenwood and Williamson [18] model is one of the earliest models of elastic asperity contact.

This is a statistical model that assumes the next simplifications:

- The rough surface is covered with a large number of asperities, which, at least near their summit, are spherical;
- Asperity summits have a constant radius on each surface;
- Asperity heights vary randomly;
- Most engineering surfaces have a Gaussian distribution of peak heights.

The analysis of the contact between two rough surfaces can be simplified by a contact between one smooth surface and one rough surface. The rough surface has a equivalent roughness of the two surfaces. This equivalent rough surface has the asperity curvature equal of the sum of the curvatures of the two rough surfaces:

$$\frac{1}{R_p} = \frac{1}{R_{p1}} + \frac{1}{R_{p2}} \tag{3.2.1}$$

and the standard deviation of the equivalent rough surface is given by:

$$\sigma_p = \sqrt{\left(\sigma_{p1}^2 + \sigma_{p2}^2\right)} \tag{3.2.2}$$

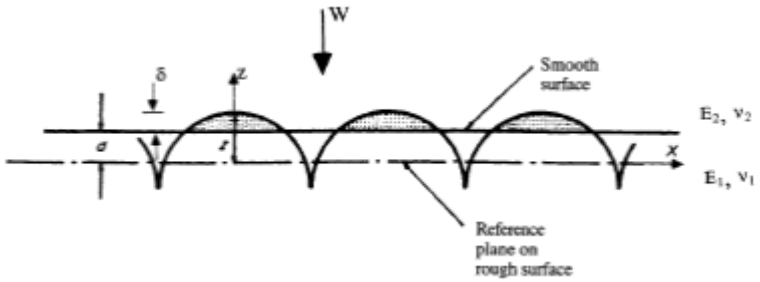

Fig.3.2.2: Schematic of the contact between one smooth plane and one rough surface with equal asperities - (from [2])

The behaviour of an individual asperity is known from the Hertzian equations, the load W_i and the area of contact A_i for each asperity is:

$$W_i = \frac{4E^*}{3} R^{1/2} \delta^{3/2} \tag{3.2.3}$$

and

$$A_i = \pi R \delta \tag{3.2.4}$$

For N asperities the total load W_t will be equal to NW_i, and the total real area

$$A_t = NA_i \tag{3.2.5}$$

then:

$$W_t = \frac{4E^* A_t^{3/2}}{3\pi^{1/2} N^{1/2} R} \tag{3.2.6}$$

The critical load beyond which the plastic deformation occurs can be estimated calculating the mean (p_m) or maximum contact pressure (p_0):

$$p_m = \frac{2}{3} p_0 = \frac{W_i}{A_i} = \frac{4E^* \delta^{1/2}}{3\pi R^{1/2}} = \left(\frac{16WE^*}{9\pi^3 NR^2} \right)^{1/3} \tag{3.2.7}$$

Using the Von Mises shear stress energy criterion, the initial yielding is initiated for: $p_m \approx 0.9Y \approx H/3$, then the critical load which the plasticity occurs is :

$$\frac{W_{crit}}{N} \approx \frac{\pi^3 R^2 H^3}{48 E^{*2}} \tag{3.2.8}$$

For a contact between one rough surface and a smooth plane, Greenwood and Williamson proposed to analyse this contact with amplitude distribution function:

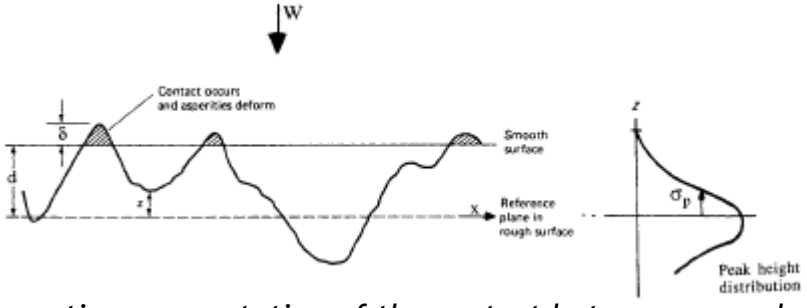

Fig.3.2.3: Schematic representation of the contact between a rough surface and a smooth surface, and representation of the amplitude distribution function.

If the two surfaces are separated by a distance d, the probability of making contact at any given asperity of height z is:

$$P(z > d) = \int_d^\infty \phi(z)dz \tag{3.2.9}$$

and if there are N asperities in the surface, the probability of the number of contacts is:

$$n = N\int_d^\infty \phi(z)dz \tag{3.2.10}$$

also, $\delta=z-d$ and $A_i=\pi\delta R_p$ the expected total area of contact will be given by:

$$A_t = \pi N R_p \int_d^\infty (z-d)p(z)dz \tag{3.2.11}$$

and the total load is:

$$W_t = p_t A_t = p_n A_n = \frac{4}{3} N E^* R_p^{1/2} \int_d^\infty (z-d)^{3/2}\, p(z)dz \tag{3.2.12}$$

where p_t is real pressure, p_n is apparent pressure, A_t is the real area of the contact and A_n is the apparent area.

Using standardized variables, and describe heights in terms of the standard deviation σ of the height distribution. Also, introducing the surface of asperity summits per unit area: $N=\eta A_n$, where η is the density of asperities, gives:

Number of contact spots:

$$n = \eta A_n F_0(D) \tag{3.2.13}$$

Total contact area:

$$A_t = \pi\eta A_n R_p \sigma_p F_1(D) \tag{3.2.14}$$

Load:

$$W = \frac{4}{3}\eta A_a E^* R_p^{1/2} \sigma_p^{3/2} F_{3/2}(D) \tag{3.2.15}$$

Where D is the dimensionless separation: $D = d/\sigma_p$ and $F_m(D)$ is a parabolic cylinder function and is given by:

$$F_m(D) = \int_D^\infty (s-D)^m\, p^*(s)ds \tag{3.2.16}$$

for the case that the amplitude distribution function is a Gaussian distribution:

$$p^*(s) = \frac{1}{(2\pi)^{1/2}} \exp\left(-\frac{s^2}{2}\right) \tag{3.2.17}$$

$$F_m = \left[\frac{1}{(2\pi)^{1/2}}\right]\int_D^\infty (s-D)^m \exp\left(-\frac{s^2}{2}\right)ds = \left[\frac{m!}{(2\pi)^{1/2}}\right]\left[\exp\left(-\frac{D^2}{4}\right)\right]U\left(m+\frac{1}{2}D\right) \tag{3.2.18}$$

for the case $m\geq 0$.

The values of U are listed in Abramowitz and Stegun (1965) page 702-706, or can calculate numerically the function $F_m(D)$.

This contact model is defined by three parameters of the rough surfaces: σ_p, R_p and η. It is possible to use this model with the standard deviation of surface heights (σ) and the correlation length (β^*) at which autocorrelation function ACF(τ)=0.1. This

possibility is presented by Onions and Archard in the paper “The contact of surfaces having a random structure”.

In the contact have asperities that plasticize, the probability of a plastic contact is:

$$prob\left(z > d + \delta_p\right) = \int_{d+\delta_p}^{\infty} \phi(z) dz \tag{3.2.19}$$

where w_p is the limit for don’t have plastic deformation.

The total area of the contacts which become plastic (A_{pt}) is given by:

$$A_{pt} = \pi \eta R_p A_n \int_{d+\delta_p}^{\infty} (s-d) \phi(z)\, dz = \pi \eta R_p A_n \int_{d+\delta_p^*}^{\infty} (s-d) \phi^*(z)\, dz \tag{3.2.20}$$

where:

$$\delta_p^* = \frac{\delta_p}{\sigma_p} = \left(\frac{R_p}{\sigma_p}\right)\left(\frac{H}{E^*}\right)^2 \tag{3.2.21}$$

The factor w_p is slightly inadequate for a generalized surface roughness parameter because when the roughness increase the w_p decrease. Therefore it is substituted by:

$$\psi = \left(\delta_p^*\right)^{-\frac{1}{2}} = \left(\frac{E^*}{H}\right)\sqrt{\left(\frac{\sigma_p}{R_p}\right)} \tag{3.2.22}$$

This factor is called the plasticity index and indicates the degree of plasticity in the contact. The critical value of the plasticity index varies with A_{pt}/A_n but this variation is not significant. If assume A_{pt}/A_n=0.02, if ψ<0.6, the deformation is largely elastic and if ψ>1, asperities deformation is largely plastic. One important conclusion of the index is if>1, the plastic flow occurs even at trivial normal loads. The probability of plastic flow is independent of the load and solely a function of the plasticity index as long as the asperities continue to deform independently.

In a plastic contact the mean contact pressure will be equal to the hardness and virtually independent of the load and of the geometry, the real area of plastic contact is given by:

$$A_{pt} = \frac{p_n A_n}{H} \tag{3.2.23}$$

where H is the hardness of the softer material.

3.3 Chang Model

The Chang or CEB model is an elastic-plastic asperities model for the contact between rough surfaces accomplished by Chang, Etsion, and Bogy in the article: “An Elastic-Plastic Model for the Contact of Rough Surfaces” in 1987 [20].

The main characteristic of this model is the volume conservation of an asperity control volume during the plastic deformation.

This model is similar to the Greenwood and Williamson model but it includes the consideration of the volume conservation. In the Greenwood-Williamson model the contact area is underestimated if a substantial percent of the contacts are plastic.

It is assumed that asperity deformation is localized mainly in the vicinity of the contact, therefore, beyond a certain depth l under the contact the asperity remains undeformed as shown in next figure:

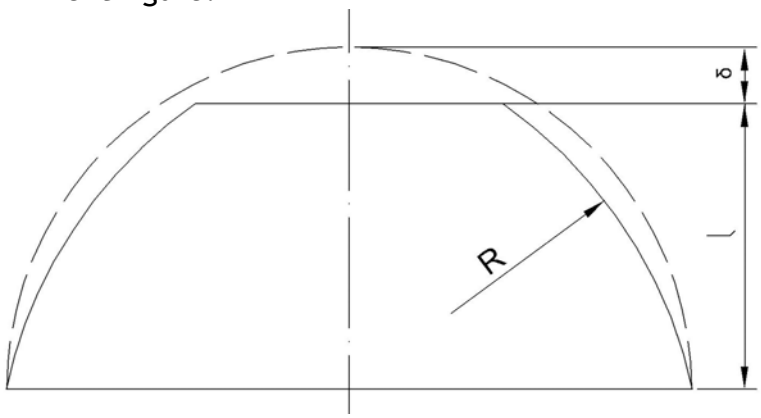

Fig. 3.3.1: Schematic of the plastically deformed asperity.

For interference δ/R<<1 (which is the normal case of contacting rough surfaces) the radius R is very close to that of the undeformed asperity shown by the dashed line.

It is further assumed that the initial depth l_i at $\delta=\delta_c$ which defines the control volume to be preserved at any interference $\delta=\delta_c+\delta_p$ is proportional to the total interference δ. Hence, the effect of a larger interference is felt deeper under the contact than that of a smaller interference:

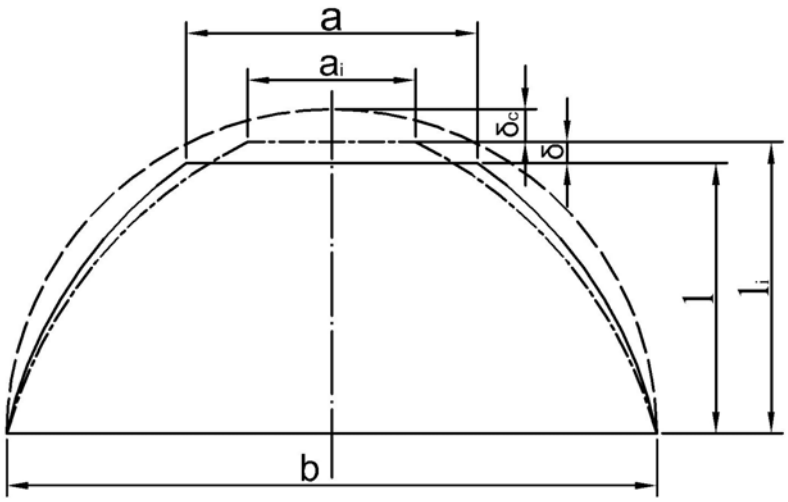

Fig.3.3.2: Schematic of the volume conservation.

The contact area of plastically deformed asperity at interference $\delta>\delta_c$ can be found from the initial depth l_i at the inception of plastic deformation $\delta=\delta_c$ and the additional plastic interference $\delta_p=\delta-\delta_c$.

Defining:

$$l_i = K_i\delta \tag{3.3.1}$$

where K_i is a constant of proportionality that will be determined later.

The diameter a_i of the to area of this model is obtained from Hertz theory and is:

$$a_i = 2\left(R\delta_c\right)^{1/2} \tag{3.3.2}$$

And the diameter of the lower boundary of the control region, located at a distance $l_i+\delta_c$ below the peak of the original undeformed asperity, is:

$$b = 2\left[2R\left(l_i+\delta_c\right)\right]^{1/2} \tag{3.3.3}$$

Therefore the control volume is:

$$V = \frac{\pi l_i}{6}\left(\frac{3}{4}a_i^2+\frac{3}{4}b^2+l_i^2\right) \tag{3.3.4}$$

This volume has to be preserved as plastic deformation proceeds for $\delta>\delta_c$, and the final height l of the deformed portion of the asperity is: $l = l_i-\delta_p = l_i-\left(\delta-\delta_c\right)$. The final diameter of its top contact surface is a and its volume can be expressed as:

$$V = \frac{\pi l}{6}\left(\frac{3}{4}a^2+\frac{3}{4}b^2+l^2\right) \tag{3.3.5}$$

Using the equation of the control volume and the equations (3.3.1), (3.3.2), (3.3.3), it is possible to obtain the diameter of the contact area for interferences $\delta\geq\delta_c$ in the form:

$$a^2 = 4R\delta C \tag{3.3.6}$$

where:

$$C = \frac{K_1\left(2-\frac{\delta_c}{\delta}\right)+2\frac{\delta_c}{\delta}\left(1-\frac{\delta_c}{\delta}\right)}{K_1-1+\frac{\delta_c}{\delta}} \tag{3.3.7}$$

From this equation it can be seen that when $\delta=\delta_c$, C=1 regardless of K_1 and for this condition the equation 3.5 gives the diameter of the Hertz theory. For $\delta>\delta_c$ and provided K>1, have C>1 assuring that the contact area of a plastically deformed asperity is always larger than that obtained from the Hertz solution for the same interference δ. Assuming that the upper limit of the contact area is the one obtained from the surface micro geometry model of purely plastic contacts, then it is required for an interference δ that:

$$\frac{a}{2} < \left(2R\delta\right)^{1/2} \tag{3.3.8}$$

which yields the result: C<2 or:

$$K_1 > 2\left[1-\left(\frac{\delta_c}{\delta}\right)^2\right]\frac{\delta_c}{\delta} \tag{3.3.9}$$

With this equation, concluding that for larger interferences δ, so that δ_c/δ approaches zero, K_1 becomes larger. Hence, by selecting a sufficiently large value for K_1 the requirement in equation (3.3.8) is maintained over the whole range of δ_c/δ. From the equation (3.3.7) it is observed that as K_1 increases the value of C approaches to:

$$C = 2-\frac{\delta_c}{\delta} \tag{3.3.10}$$

Substituting the equation (3.3.10) in the equation (3.3.2) the contact area of a plastically deformed asperity is obtained in the form:

$$\bar{A}_p = \frac{\pi a^2}{4} = \pi R\delta\left(2-\frac{\delta_c}{\delta}\right) \tag{3.3.11}$$

In the Greenwood model and Williamson the contact area at an interference δ is: $\pi R\delta$ whereas the purely plastic surface microgeometry model gives $2\pi R\delta$ for the contact area. Hence, from the equation (3.3.11) we can concluded that these two models have a different results. The contact area of an elastic-plastic asperity depends not only on the total interference δ but also on the ratio δ_c/δ representing the intensity of plastic deformation.

They assume that for all plastically deformed asperities the average pressure over the contact area is equal to kH, i.e., the pressure p_m. The contact load for such an asperity is:

$$\bar{W} = \pi R\delta\left(2-\frac{\delta_c}{\delta}\right)kH \tag{3.3.12}$$

This assumption is reasonable since asperities in the early stages of plastic deformation have average contact pressures less than kH while those with relatively large plastic interferences will have average contact pressure approaching H.

Now it is possible to obtain the contact area for an elastic-plastic contact, if have the amplitude distribution function of the profile. The total contact area is:

$$A_t(d) = A_e(d) + A_p(d) \tag{3.3.13}$$

Where:

$$A_e(d) = \eta A_n \pi R\int_d^{d+\delta_c}(z-d)\phi(z)dz \tag{3.3.14}$$

$$A_p(d) = \eta A_n \pi R\int_{d+\delta_c}^{\infty}\left[2(z-d)-\delta_c\right]\phi(z)dz \tag{3.3.15}$$

And the contact load is given by:

$$P(d) = \eta A_a E^*\left(\frac{4}{3}R^{1/2}\int_d^{d+\delta_c}(z-d)^{3/2}\phi(z)dz + \pi Rk\frac{H}{E^*}\int_{d+\delta_c}^{\infty}\left[2(z-d)-\delta_c\right]\phi(z)dz\right) \tag{3.3.16}$$

This model is more efficient than the Greenwood and Williamson model because is applied to the entire deformation range, from fully elastic to fully plastic. The results of

GW model deviate greatly from the experimental results for loads that exceeds about half of the yield point load (Powierza et al. 1992), however, this model has a several shortcomings: the discontinuity in the contact load at the critical point of the initial yielding (the average contact pressure is allowed to jump from 2/3*KH* in the elastic regime to *KH* in the plastic regime) and the other shortcoming is that this model allows only two possible states of deformation for a contacting asperity, either fully plastic or fully elastic, the transition from fully elastic to fully plastic is not modelled.

3.4 Zhao Model

This model is an other elastic-plastic asperity microcontact model for contact between two nominally flat surfaces with the transition between fully elastic deformation to fully plastic deformation, accomplish by Zhao, Maietta and Chang in the article: "An Asperity Microcontact Model Incorporating the Transition from Elastic Deformation to Fully Plastic Flow" in 2000 [21]. The transition from fully elastic deformation to fully plastic flow of the contacting asperity is modelled based on contact mechanics theories in conjunction with the continuity and smoothness of variables across different modes of deformation.

The assumptions following in this model are the same as those made in the GW model and CEB model:

- The asperity distributions is isotropic;
- Asperities are, at least near their summits, spherical;
- Asperity summits have a uniform radius R, but their heights vary randomly;
- The interactions among contacting asperities are neglected;
- Only the asperities deform during contact and no bulk deformation occurs.

The Elastic Contact:

From the Hertz theory the interference (δ), the contact load (w_e), and the mean contact pressure (p_m) are given by:

$$\delta = \left(\frac{3\pi p_a}{4E^*} \right)^2 R \tag{3.4.1}$$

$$w_e = \left(\frac{4}{3} \right) E^* R^{1/2} \omega^{3/2} \tag{3.4.2}$$

$$p_m = \frac{2}{3} p_0 = \frac{4E^*}{3\pi} \left(\frac{\omega}{R} \right)^{1/2} \tag{3.4.3}$$

the critical interference is for p_0=kH:

$$\delta_{c1} = \left(\frac{3\pi kH}{4E^*} \right)^2 R \tag{3.4.4}$$

when $\delta < \delta_{c1}$, the contact is elastic, and when $\delta \geq \delta_{c1}$, the contact is either elastoplastic or fully plastic.

Fully Plastic:

When δ increases to another critical value δ_{c2} at which the mean contact pressure p_a of the asperity reaches the value of H, fully plastic deformation occurs. For this stage ($\delta > \delta_{c2}$), the mean contact pressure p_m remains constant at H:

$$p_m = H \tag{3.4.5}$$

The contact area in this stage is equal to the geometrical intersection of the flat with the original undeformed profile of the asperity:

$$A_p = 2\pi R\delta \tag{3.4.6}$$

The contact load w_p is equal to the contact area multiplied by the mean contact pressure:

$$w_p = 2\pi R\delta H \tag{3.4.7}$$

The minimum value of this critical value (δ_{c2}) may be estimated based on a simple analysis, at $\delta=\delta_{c2}$ the load carried by the contact is equal to $2\pi R\delta_{c2}H$, by equation (3.4.7), and the load carried by the contact at $\delta=\delta_{c2}$ had it been elastic, would have been equal $\left(\frac{4}{3}\right)E^{*1/2}\delta_{c2}^{3/2}$, by the equation (3.4.2). Therefore:

$$2\pi R\delta_{c2}H < \left(\frac{4}{3}\right)E^* R^{1/2}\delta_{c2}^{3/2} \tag{3.4.8}$$

or

$$\delta_{c2} > \left(\frac{3\pi H}{2E^*}\right)^2 R = \frac{4}{k^2}\left(\frac{3\pi kH}{4E^*}\right)^2 R \tag{3.4.9}$$

Using the equation (3.4.4) into the above expression yields:

$$\delta_{c2} > 25\delta_{c1} \tag{3.4.10}$$

The minimum value of δ_{c2} may also be further estimated using experimental results from Johnson (1985), fully plastic deformation occurs when the contact force at fully plastic deformation, w_f, is about equal to 400 times that at initial yielding, w_y:

$$\frac{w_f}{w_y} = 400 \tag{3.4.11}$$

Using the equation (3.4.2), the following expressions are obtained for w_f and w_y:

$$w_y = \left(\frac{4}{3}\right)E^* R^{1/2}\delta_{c1}^{3/2} \tag{3.4.12}$$

$$w_f \le \left(\frac{4}{3}\right)E^* R^{1/2}\delta_{c2}^{3/2} \tag{3.4.13}$$

and dividing the equation (3.4.13) by equation (3.4.12):

$$\left(\frac{\delta_{c2}}{\delta_{c1}}\right)^{3/2} \ge \frac{w_f}{w_y} = 400 \tag{3.4.14}$$

or

$$\delta_{c2} \geq 54\delta_{c1} \tag{3.4.15}$$

This expression shows that the contact interference at the onset of fully plastic deformation would be at least 54 times that the initial yielding.

Elastoplastic Contact:

When the interference is between δ_{c1} and δ_{c2}, the asperity deforms elastoplastically. Since the total deformation is composed of a mixture of the elastic and plastic deformations in this stage, the relations for the contact area (A_{ep}) and the mean contact pressure (p_m) as functions of the interference δ become complex.

The relationship between P_m and δ can be derived from the one equation presented by H. A. Francis (1976) based on a statistical analysis of spherical indentations:

$$\frac{p_m}{Y_R} = C_1 + C_2 \ln\left(\frac{h/b}{Y_R/E}\right) \tag{3.4.16}$$

where, Y_R is the unaxial flow stress of the material, h the displacement of the contact center, b the radius of the contact area, C_1 and C_2 are the regression constants.
Therefore, the dependence of P_a and δ in the regime of the elastoplastic deformation of the asperity may analogously be characterized by the following logarithmic function:

$$p_m = a_1 + a_2 \ln\left(\frac{\delta}{a}\right) \tag{3.4.17}$$

where a_1 and a_2 are two constants to be determined and a is the contact radius of the asperity.

The relation between a and δ within the transitional regime may be established from the a - δ relations for the two extremes of elastic and fully plastic deformations. These two relations are:

$$a = (\delta R)^{1/2} \quad (\delta \leq \delta_{c1}) \tag{3.4.18}$$

$$a = (2\delta R)^{1/2} \quad (\delta \geq \delta_{c2}) \tag{3.4.19}$$

When the asperity deforms elastoplastically, the following relation is expected:

$$a = (C\delta R)^{1/2} \tag{3.4.20}$$

where C is a variable coefficient having a value between: $1 \leq C \leq 2$. Substituting this equation in (4.17) we have:

$$p_m = a_3 + a_4 \ln(\delta) \tag{3.4.21}$$

where:

$$a_3 = a_1 + a_2 \ln(C) - 0.5 a_2 \ln(R) \tag{3.4.22}$$

and

$$a_4 = 0.5 a_2 \tag{3.4.23}$$

are the functional parameters to be determined.

The continuity between p_a and δ requires that the mean contact pressure p_a in the elastoplastic transitional regime be equal to that in the elastic regime at $\delta=\delta_{c1}$. It also requires P_m to be equal to the fully plastic contact pressure at $\delta=\delta_{c2}$. Then for elastic regime we have:

$$a_3 + a_4 \ln(\delta_1) = p_m = kH \tag{3.4.24}$$

and for plastic regime we have:

$$a_3 + a_4 \ln(\delta_2) = H \tag{3.4.25}$$

Solving these two equations:

$$a_3 = H - H(1-k)\frac{\ln(\delta_2)}{\ln(\delta_2) - \ln(\delta_1)} \tag{3.4.26}$$

and

$$a_4 = \frac{H(1-k)}{\ln(\delta_2) - \ln(\delta_1)} \tag{3.4.27}$$

Therefore, the mean contact pressure in the regime of the elastoplastic deformation is given by:

$$P_m = H - H(1-k)\frac{\ln(\delta_2) - \ln(\delta)}{\ln(\delta_2) - \ln(\delta_1)} \tag{3.4.28}$$

The relation between contact area A_{ep} and the contact interference δ can be modelled by a polynomial smoothly joining the expressions for A_e and A_p as functions of δ. The domain of this polynomial is from δ_{c1} to δ_{c2} and it should monotonically increase and satisfy four boundary conditions:

$$A_{ep}(\delta_{c1}) = A_e(\delta_{c1}) \tag{3.4.29}$$

$$\frac{dA_{ep}(\delta_{c1})}{d\delta} = \frac{dA_e(\delta_{c1})}{d\delta} \tag{3.4.30}$$

$$A_{ep}(\delta_{c2}) = A_p(\delta_{c2}) \tag{3.4.31}$$

$$\frac{dA_{ep}(\delta_{c2})}{d\delta} = \frac{dA_p(\delta_{c2})}{d\delta} \tag{3.4.32}$$

Using a polynomial of the third degree, the template of these curve is:

$$y = -2x^3 + 3x^2,\ 0 \le x \le 1 \tag{3.4.33}$$

This curve passes through the lower left and upper right corners of its bounding box (x=0, x=1, y=0 and y=1) and is tangential to the lower and upper edges. For this curve to satisfy the four stated boundary conditions will need to be transformed which involves translating and scaling δ so that $\delta=\delta_{c1}$ and $\delta=\delta_{c2}$ corresponded to x=0 and x=1 respectively:

$$x = \frac{\delta - \delta_{c1}}{\delta_{c2} - \delta_{c1}} \tag{3.4.34}$$

The function output must then be scaled by the distance between the top and bottom of the quadrilateral on the A_{ep}-δ plane, which represents the asperity contact areas at the fully plastic and fully elastic states. The scaled function is translated by adding it to the fully elastic A_e- δ function. The function simplified for A_{ep} are:

$$A_{ep} = \pi R\delta\left[1 - 2\left(\frac{\delta - \delta_{c1}}{\delta_{c2} - \delta_{c1}}\right)^3 + 3\left(\frac{\delta - \delta_{c1}}{\delta_{c2} - \delta_{c1}}\right)^2\right] \tag{3.4.35}$$

In the figure 3.4.1 the plot with relation between the real area of contact and the interference is shown.

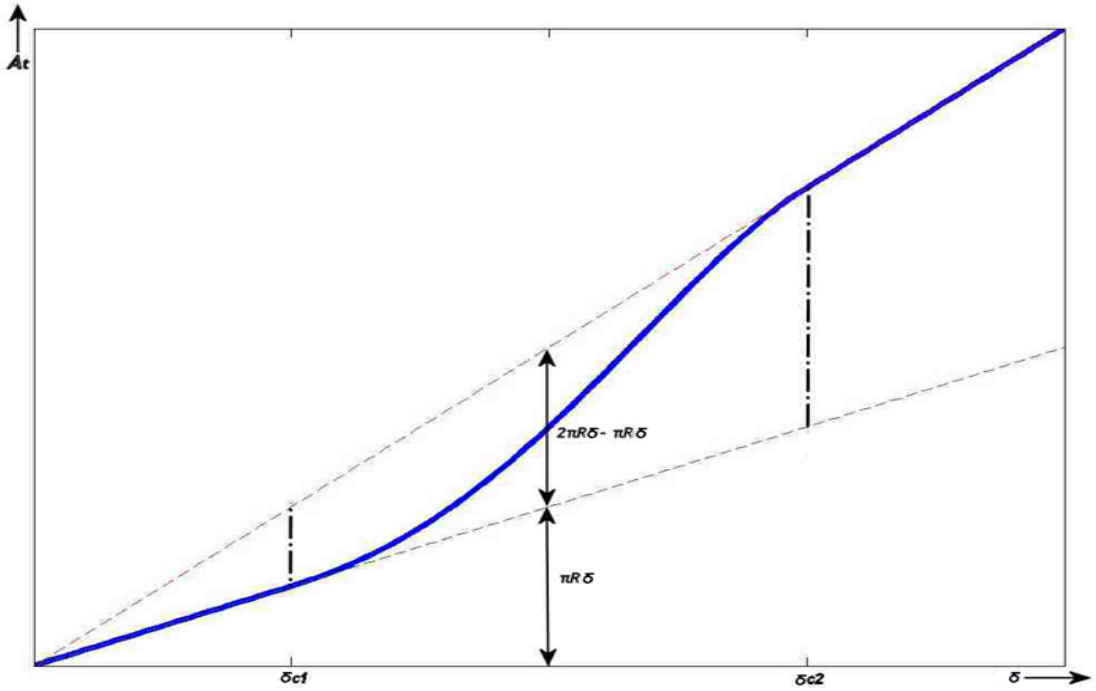

Fig. 3.4.1: Relation between the real area of contact (A) and interference (δ)

Using the equations (4.26) and (4.29) it is possible determine the contact load (w_{ep}) of the asperity in the regime of elastoplastic deformation:

$$w_{ep} = p_a A_{ep} = \left[H - H(1-k)\frac{\ln(\delta_{c2}) - \ln(\delta)}{\ln(\delta_{c2}) - \ln(\delta_{c1})}\right] \times \left[1 - 2\left(\frac{\delta - \delta_{c1}}{\delta_{c2} - \delta_{c1}}\right)^3 + 3\left(\frac{\delta - \delta_{c1}}{\delta_{c2} - \delta_{c1}}\right)^2\right]\pi R\delta \tag{3.4.36}$$

Now the expressions in order to calculate the total real area (A_t) and the total load (W_t) in the contact between two rough surfaces can be given with the amplitude distribution function ($\Phi(z)$):

$$A_t(d) = A_{et}(d) + A_{ept}(d) + A_{pt}$$

$$= N\int_d^{d+\delta_{c1}} A_e\phi(z)\,dz + N\int_{d+\delta_{c1}}^{d+\delta_{c2}} A_{ep}\phi(z)dz + N\int_{d+\delta_{c2}}^{\infty} A_p\phi(z)\,dz$$

$$= \eta A_a \pi R \int_d^{d+\delta_{c1}} \delta\phi(z)dz + \eta A_a \pi R \int_{d+\delta_{c1}}^{d+\delta_{c2}} \delta\left[1-2\left(\frac{\delta-\delta_{c1}}{\delta_{c2}-\delta_{c1}}\right)^3+3\left(\frac{\delta-\delta_{c1}}{\delta_{c2}-\delta_{c1}}\right)^2\right]\phi(z)\,dz + \tag{3.4.37}$$
$$+2\eta A_a \pi R \int_{d+\delta_{c2}}^{\infty} \delta\phi(z)dz$$

and

$$W_t(d) = W_{et}(d) + W_{ept}(d) + W_{pt}(d) =$$
$$= N\int_d^{d+\delta_{c1}} w_e\phi(z)dz + N\int_{d+\delta_{c1}}^{d+\delta_{c2}} w_{ep}\phi(z)\,dz + N\int_{d+\delta_{c2}}^{\infty} w_p\phi(z)dz$$
$$= \frac{4}{3}\eta A_a E R^{1/2}\int_d^{d+\delta_{c1}} \delta^{3/2}\phi(z)\,dz +$$
$$+\eta A_a \pi R\int_{d+\delta_{c1}}^{d+\delta_{c2}}\left[H - H(1-k)\frac{\ln\delta_{c2}-\ln\delta}{\ln\delta_{c2}-\ln\delta_{c1}}\right]\times\left[1-2\left(\frac{\delta-\delta_{c1}}{\delta_{c2}-\delta_{c1}}\right)^3+3\left(\frac{\delta-\delta_{c1}}{\delta_{c2}-\delta_{c1}}\right)^2\right]\delta\phi(z)\,dz + \tag{3.4.38}$$
$$+2\pi\eta A_a HR\int_{d+\delta_{c2}}^{\infty}\delta\phi(z)\,dz$$

The normalization of these equations can be done diving by A_a and A_aE respectively, and the all length parameters in these equations are normalized by σ:

$$A^*_t = \frac{A_t}{A_a} = \pi\beta\int_{h^*-y_s^*}^{h^*-y_s^*+\omega_{c1}} \omega^*\phi^*(z^*)\,dz^* +$$
$$+\pi\beta\int_{h^*-y_s^*+\omega_{c1}}^{h^*-y_s^*+\omega_{c1}}\left[1-2\left(\frac{\omega^*-\omega_{c1}^*}{\omega_{c2}^*-\omega_{c1}^*}\right)^3+3\left(\frac{\omega^*-\omega_{c1}^*}{\omega_{c2}^*-\omega_{c1}^*}\right)^2\right]\omega^*\phi^*(z^*)\,dz^* + \tag{3.4.39}$$
$$+2\pi\beta\int_{h^*-y_s^*+\omega_{c2}}^{\infty}\omega^*\phi^*(z^*)\,dz^*$$

and

$$W_t^* = \frac{W_t}{A_a E} = \frac{4}{3}\beta\left(\frac{\sigma}{R}\right)^{1/2}\int_{h^*-y_s^*}^{h^*-y_s^*+\delta_{c1}^*}\delta^{*3/2}\phi^*(z^*)\,dz^* +$$
$$+\frac{\pi H\beta}{E}\int_{h^*-y_s^*+\delta_{c1}^*}^{h^*-y_s^*+\delta_{c2}^*}\left[1-(1-k)\frac{\ln\delta_{c2}^*-\ln\delta^*}{\ln\delta_{c2}^*-\ln\delta_{c1}^*}\right]\times\left[1-2\left(\frac{\delta^*-\delta_{c1}^*}{\delta_{c2}^*-\delta_{c1}^*}\right)^3+3\left(\frac{\delta^*-\delta_{c1}^*}{\delta_{c2}^*-\delta_{c1}^*}\right)^2\right]+ \tag{3.4.40}$$
$$+\frac{2\pi H\beta}{E}\int_{h^*-y_s^*+\delta_{c2}^*}^{\infty}\delta^*\phi^*(z^*)\,dz^*$$

where in this case:

$$\beta = \eta\sigma R \tag{3.4.41}$$

$$\delta^* = z^* - h^* + y_s^* \tag{3.4.42}$$

3.5 Jeng and Wang Model

Jeng and Wang model is another elastic-plastic microcontact model taking into account the elastic, elasto-plastic and fully plastic deformation, but the difference is that this model consider that the contact area between the two rough surfaces is elliptic. This model is accomplish by Jeng and Wang in the article "An Elliptical Microcontact Model Considering Elastic, Elastoplastic, and Plastic Deformation" in 2003 [23].

The Elastic Contact

In the contact of the one elliptic asperity and a smooth plane the contact area is an ellipse with semiminor radius *a* and semimajor radius *b* . The eccentricity of the one ellipse (*e*) is:

$$e^2 = 1 - \left(\frac{a}{b}\right)^2 \tag{3.5.1}$$

and the mean effective radius of curvature (R_m) is:

$$\frac{1}{R_m} = \frac{1}{2}\left(\frac{1}{R_x} + \frac{1}{R_y}\right) \tag{3.5.2}$$

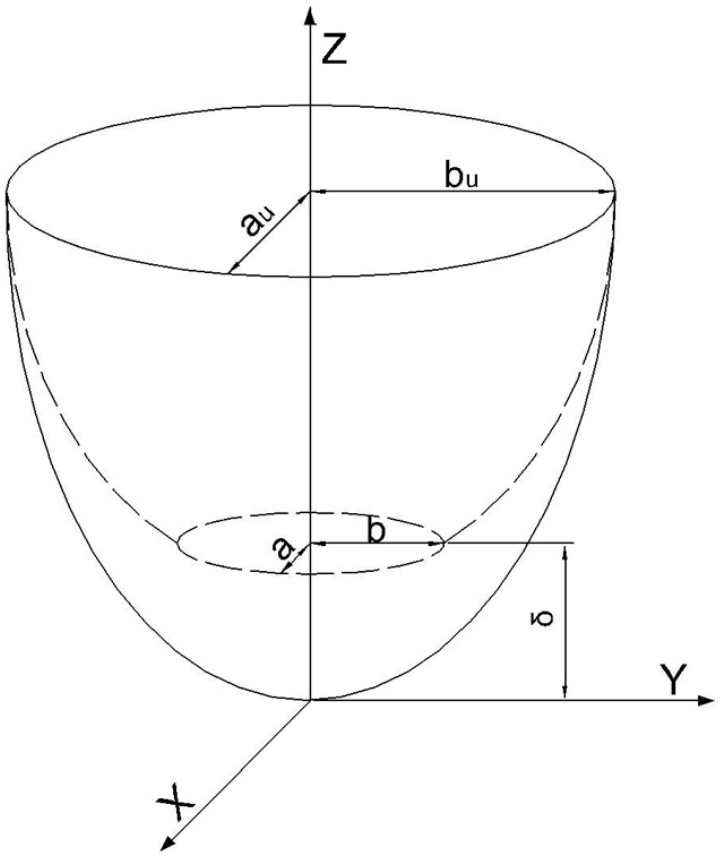

Fig 3.5.1: Schematic of the interference of an deformed asperity.

The contact area in this case is:

$$A = \pi ab \tag{3.5.3}$$

From the theory of elasticity, the contact area of the semimajor contact ellipse radius, can be define by:

$$b = \left[\frac{3E(e)FR_m}{2\pi E^*\left(1-e^2\right)} \right]^{1/3} \tag{3.5.4}$$

The maximum contact pressure:

$$p_0 = \frac{3}{2}\frac{F}{A} \tag{3.5.5}$$

The interference of an asperity:

$$\delta = \frac{2K(e)}{\pi}\left[\frac{\pi\left(1-e^2\right)}{2E(e)R_m} \right]^{1/3} \left(\frac{3F}{4E^*} \right)^{2/3} \tag{3.5.6}$$

where K(e) and F(e) are the complete elliptic integrals of the first and second kinds respectively:

$$K(e) = \int_0^{\pi/2} \left(1-e^2\sin^2\varphi\right)^{-0.5} d\varphi \tag{3.5.7}$$

$$F(e) = \int_0^{\pi/2} \left(1-e^2\sin^2\varphi\right)^{0.5} d\varphi \tag{3.5.8}$$

Combining the equations (3.5.1), (3.5.3), (3.5.4), (3.5.5) and (3.5.6), the real elastic contact area is:

$$A_e(\delta) = \left[\frac{E(e)}{K(e)\left(1-e^2\right)^{0.5}} \right] \pi R_m \delta = f_1(e)\pi R_m \delta \tag{3.5.9}$$

and the load is:

$$F_e(\delta) = \left[\frac{\pi E(e)^{0.5}}{K(e)^{1.5}\left(1-e^2\right)^{0.5}} \right] \frac{4}{3} E^* R_m^{0.5} \delta^{1.5} = f_2(e)\frac{4}{3}E^* R_m^{0.5}\delta^{1.5} \tag{3.5.10}$$

The critical interference can be define according Horng -1998 ([32]):

$$\delta_{c1} = \frac{K(e)E(e)}{(\pi/2)^2} R_m \left(\frac{H}{E^*} \right)^2 \tag{3.5.11}$$

When $\delta < \delta_{c1}$, the contact is elastic, and when $\delta \geq \delta_{c1}$, the contact is either elastoplastic or fully plastic.

Fully plastic contact

Volume conservation is used for the analysis of the fully plastic contact. The fully plastic flow occurs when $\delta \geq \delta_{c2}$:

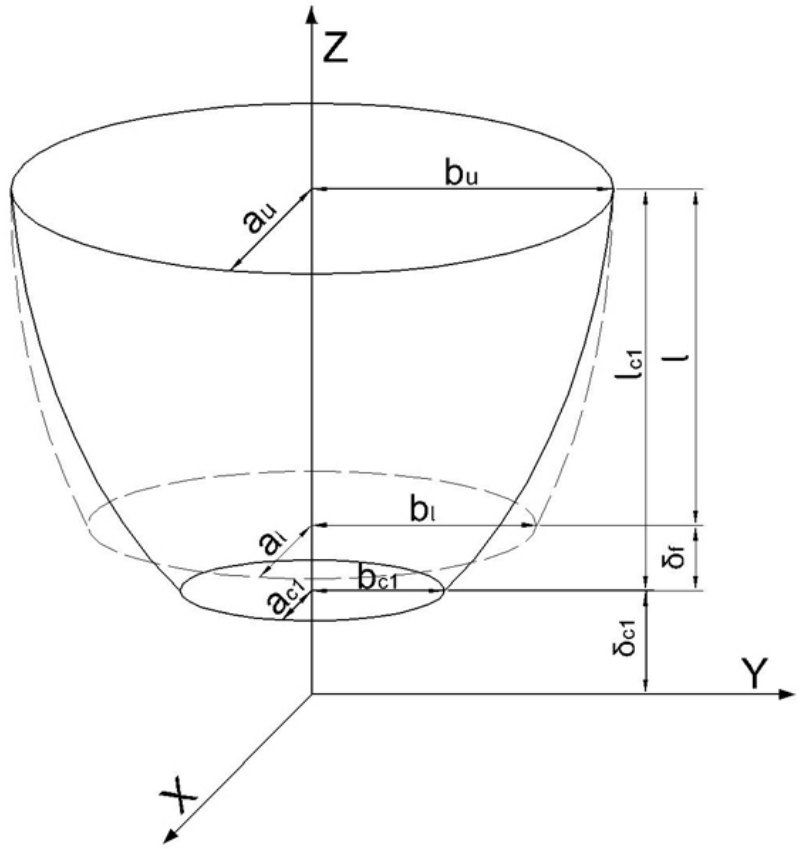

Fig 3.5.2: Schematic of the geometry of an plastically deformed asperity.

Using the equations (3.5.4), (3.5.6) and the equation (3.3.3) from the CEB Model, the radius of the lower boundary of the contact region, can be found. Hence (b_{c1}) can be represented by:

$$b_{c1} = \left[\frac{E(e) R_m \omega_i}{K(e)\left(1-e^2\right)} \right]^{1/2} \tag{3.5.12}$$

and (b_u):

$$b_u = \left[2R_y \left(l_{c1} + \omega_{c1} \right) \right]^{1/2} \tag{3.5.13}$$

the boundary conditions are:

$$x = a_{c1}, \quad y = b_{c1}, \quad z = \omega_{c1} \tag{3.5.14}$$

$$x = a_u, \quad y = b_u, \quad z = \omega_{c1} + l_{c1} \tag{3.5.15}$$

The asperity could be approach by the quadratic function, using the boundary conditions (3.5.14) and (3.5.15), this function is:

$$z = \left(\frac{l}{a_u^2 - a_{c1}^2} \right) x^2 + \left(\frac{l}{b_u^2 + b_{c1}^2} \right) y^2 \tag{3.5.16}$$

Thus, the control volume of this elliptic model is:

$$V = \frac{\pi l_{c1}}{2} \left(b_u^2 + b_{c1}^2 \right) \left(1 - e^2 \right)^{0.5} \tag{3.5.17}$$

Assuming that the eccentricity of the ellipse is uniform during deformation and conservation of volume, the final height l of the deformed portion of the asperity is:

$$l = l_{c1} - \omega_f = l_{c1} - (\delta - \delta_{c1}) \tag{3.5.18}$$

Using the equations (3.5.12), (3.5.13), (3.5.17) and (3.5.18) we can obtain the product of the semiminor and semimajor radius of surface contact:

$$a_l b_l = f_3(e)\, f_4(e) R_m \omega C \tag{3.5.19}$$

where:

$$f_3(e) = \frac{E(e)e^2}{2\left(1-e^2\right)^{0.5}\left[E(e) - K(e)\left(1-e^2\right)\right]} \tag{3.5.20}$$

$$C = \frac{k_l\left[2 - \frac{\delta_{c1}}{\delta}\left(2 - f_4(e)\right)\right] + 2\frac{\delta_{c1}}{\delta}\left(1 - \frac{\delta_{c1}}{\delta}\right)}{\left(k_l - 1\right) + \frac{\delta_{c1}}{\omega}} \tag{3.5.21}$$

$$f_4(e) = \frac{2\left[E(e) - \left(1-e^2\right)K(e)\right]}{K(e)e^2} \tag{3.5.22}$$

and k_l is a constant of proportionality : $l_{c1}=k_l\delta$.

For $\delta>\delta_{c1}$ and provided $k_l>1$, have $2<C<K(e)/E(e)$, assuring that the contact area of a plastically deformed asperity is always larger than that obtained from Hertz solution for the same interference. For purely plastic contact we have:

$$k_l > \frac{2\left[1 - \left(\frac{\delta_{c1}}{\delta}\right)^2\right]}{\left(2 - f_4(e)\right)}\frac{\delta}{\delta_{c1}} \tag{3.5.23}$$

From this equation, when δ_{c1}/δ approaches zero, k_l becomes large, hence, if a sufficiently large value for k_l is selected, the equation (3.5.21) approaches:

$$C = \left[2 - \frac{\delta_{c1}}{\delta}\left(2 - f_4(e)\right)\right] \tag{3.5.24}$$

Using this equation and the equation (3.5.19) are obtains the contact area of a plastically deformed asperity:

$$A_p = \pi R_m \delta f_3(e)\left[2 - \frac{\delta_{c1}}{\delta}\left(2 - f_4(e)\right)\right] \tag{3.5.25}$$

And when the interference δ is much larger than δ_{c1} this equation gives the a fully plastic contact area:

$$A_p = 2\pi R_m \delta f_3(\delta) \tag{3.5.26}$$

These authors assumed that the fully plastic deformed asperities will occur when the mean contact pressure is equal to H. When the maximum pressure approaches to H, and remains constant, the fully plastic contact load is:

$$W_p = 2\pi R_m \delta f_3(\delta) \tag{3.5.27}$$

Elastoplastic contact

The equations to calculate the area of the contact and the elastoplastic load have the same relations which used in Zhao et al. model.

Using the relation between p_m and δ, based in the study of H. A. Francis in 1976:

$$p_m = a_1 + a_2 \ln\left(\frac{\delta}{r}\right) \tag{3.5.28}$$

The relation between δ-r may be established based in the transitional regime from the elastically critical interference and fully critical plastic contact.

The contact area in GW model is: $\pi r^2 = \pi R\delta$ and the contact radius $r = \sqrt{R\delta}$. The elliptic contact area is equal: $A = \pi ab$, simplifying these relations for an elliptic asperity one has:

$$\sqrt{ab} = \left(f_1(e)\delta R_m\right)^{1/2} \quad for \quad \delta \le \delta_{c1} \tag{3.5.29}$$

and

$$\sqrt{ab} = \left(2 f_1(e)\delta R_m\right)^{1/2} \quad for \quad \delta \le \delta_{c2} \tag{3.5.30}$$

Hence, in this case the relation of p_m and δ is:

$$p_m = a_1 + a_2 \ln\left(\frac{\delta}{\sqrt{ab}}\right) \tag{3.5.31}$$

When $\delta=\delta_{c1}$, the equation (3.5.31) can be expressed as:

$$KH = a_1 + a_2 \ln\left[\frac{\delta_{c1}}{\left(f_1(e) R_m \delta_{c1}\right)^{1/2}}\right] \tag{3.5.32}$$

and the inception of fully plastic deformation $\delta=\delta_{c2}$:

$$H = a_1 + a_2 \ln\left[\frac{\delta_{c2}}{\left(2 f_2(e) R_m \delta_{c2}\right)^{1/2}}\right] \tag{3.5.33}$$

Solving these last two equations, the parameters a_1 and a_2 of the function can be determined:

$$a_1 = H - \frac{H(1-k)\times\left[\ln(\delta_{c2}) - \ln\left(2 f_3(e)\right) - \ln(R_m)\right]}{\left[\left(\ln(\delta_{c2}) - \ln(\delta_{c1})\right) - \left(\ln\left(2 f_3(e)\right) - \ln\left(f_1(e)\right)\right)\right]} \tag{3.5.34}$$

and

$$a_2 = \frac{2H(1-k)}{\left[\left(\ln(\delta_{c2}) - \ln(\delta_{c1})\right) - \left(\ln\left(2 f_3(e)\right) - \ln\left(f_1(e)\right)\right)\right]} \tag{3.5.35}$$

Then substituting a_1 and a_2 in equation (3.5.31) are obtains the mean contact pressure in the elastoplastic deformation:

$$p_m = H - H(1-k)\frac{\ln(\delta_{c2}) - \ln(2f_3(e)) - \ln(R_m) - 2\ln(\delta) + \ln(a_l b_l)}{(\ln(\delta_{c2}) - \ln(\delta_{c1})) - (\ln(2f_3(e)) - \ln(f_1(e)))} \tag{3.5.36}$$

When have a=b, $f_3(e) = f_4(e) = 1$, these conditions are admitted in the Zhao model but this equation for p_m is different that the one proposed in the Zhao et al. model (equation (3.4.26)).

Using the relation between the contact area (A_{ep}) and the interference (δ) proposed in Zhao et al. model we have:

$$A_{ep} = A_e + (A_p - A_e) \times \left[-2\left(\frac{\delta - \delta_{c1}}{\delta_{c2} - \delta_{c1}}\right)^3 + 3\left(\frac{\delta - \delta_{c1}}{\delta_{c2} - \delta_{c1}}\right)^2 \right] \tag{3.5.37}$$

$$A_{ep} = f_1(e)\pi R_m \delta + \{2\pi R_m \delta f_3(e) - f_1(e)\pi R_m \delta\} \times \left[-2\left(\frac{\delta - \delta_{c1}}{\delta_f - \delta_{c1}}\right)^3 + 3\left(\frac{\delta - \delta_{c1}}{\delta_f - \delta_{c1}}\right)^2 \right] \tag{3.5.38}$$

or:

$$A_{ep} = \pi R_m \delta \times \left\{ f_1(e) + (2f_3(e) - f_1(e)) \times \left[-2\left(\frac{\delta - \delta_{c1}}{\delta_{c2} - \delta_{c1}}\right)^3 + 3\left(\frac{\delta - \delta_{c1}}{\delta_{c2} - \delta_{c1}}\right)^2 \right] \right\} \tag{3.5.39}$$

and the contact load is:

$$\begin{aligned} W_{ep} = & \left[H - H(1-k)\frac{\ln(\delta_{c2}) - \ln(2f_3(e)) - \ln(R_m) - 2\ln(\delta) + \ln(a_l b_l)}{(\ln(\delta_{c2}) - \ln(\delta_{c1})) - (\ln(2f_3(e)) - \ln(f_1(e)))} \right] \times \\ & \times \pi R_m \delta \times \left\{ f_1(e) + (2f_3(e) - f_1(e)) \times \left[-2\left(\frac{\delta - \delta_{c1}}{\delta_{c2} - \delta_{c1}}\right)^3 + 3\left(\frac{\delta - \delta_{c1}}{\delta_{c2} - \delta_{c1}}\right)^2 \right] \right\} \end{aligned} \tag{3.5.40}$$

The total area for a contact between one rough surface and a smooth plane can be calculated with the amplitude distribution function (Φ(z)):

$$A_t(d) = A_e(d) + A_{ep}(d) + A_p(d) \tag{3.5.41}$$

where:

$$A_e(d) = \eta A_a \pi R_m f_1(e) \int_d^{d+\delta_{c1}} (z-d)\phi(z)\,dz \tag{3.5.42}$$

$$A_{ep}(d) = \eta A_a \pi R_m \int_{d+\delta_{c1}}^{d+\delta_{c2}} \left\{ f_1(e) + (2f_3(e) - f_1(e)) \times \left[-2\left(\frac{\delta - \delta_{c1}}{\delta_{c2} - \delta_{c1}}\right)^3 + 3\left(\frac{\delta - \delta_{c1}}{\delta_{c2} - \delta_{c1}}\right)^2 \right] \right\} (z-d)\phi(z)\,dz \tag{3.5.43}$$

$$A_p(d) = 2\eta A_a \pi R_m f_3(e) \int_{d+\delta_{c2}}^{\infty} (z-d)\phi(z)\,dz \tag{3.5.44}$$

The contact load is:

$$F_t(d) = F_e(d) + F_{ep}(d) + F_p(d) \tag{3.5.45}$$

where:

$$F_e(d) = \frac{4}{3}\eta A_a E^* R_m^{1/2} f_2(e) \int_d^{d+\delta_{c1}} (z-d)^{1.5} \phi(z)\, dz \tag{3.5.46}$$

$$F_{ep} = \eta A_a \pi R_m \int_{d+\delta_{c1}}^{d+\delta_{c2}} \left[H - H(1-k) \frac{\ln(\delta_{c2}) - \ln(2 f_3(e)) - \ln(R_m) - 2\ln(\delta) + \ln(a_l b_l)}{(\ln(\delta_{c2}) - \ln(\delta_{c1})) - (\ln(2 f_3(e)) - \ln(f_1(e)))} \right] \times$$
$$\times \left\{ f_1(e) + (2 f_3(e) - f_1(e)) \times \left[-2\left(\frac{\delta - \delta_{c1}}{\delta_{c2} - \delta_{c1}} \right)^3 + 3\left(\frac{\delta - \delta_{c1}}{\delta_{c2} - \delta_{c1}} \right)^2 \right] \right\} \times \delta\phi(z)\, dz \tag{3.5.47}$$

and

$$F_p = 2\eta A_a \pi R_m H f_3(e) \int_{d+\delta_{c2}}^{\infty} [2(z-d)] \phi(z)\, dz \tag{3.5.48}$$

3.6 Analysis of the asperity contact in FEM

A model of a contact mechanic between an asperity and a smooth plane was done, but it was not possible to obtain results because the model did not converge. Alterations to the used model must be made, changing the element types or the mesh.
In the appendix 3 it has a example of the model used in the software ANSYS and the figure 3.6.1 and 3.6.2 two types of meshes used.

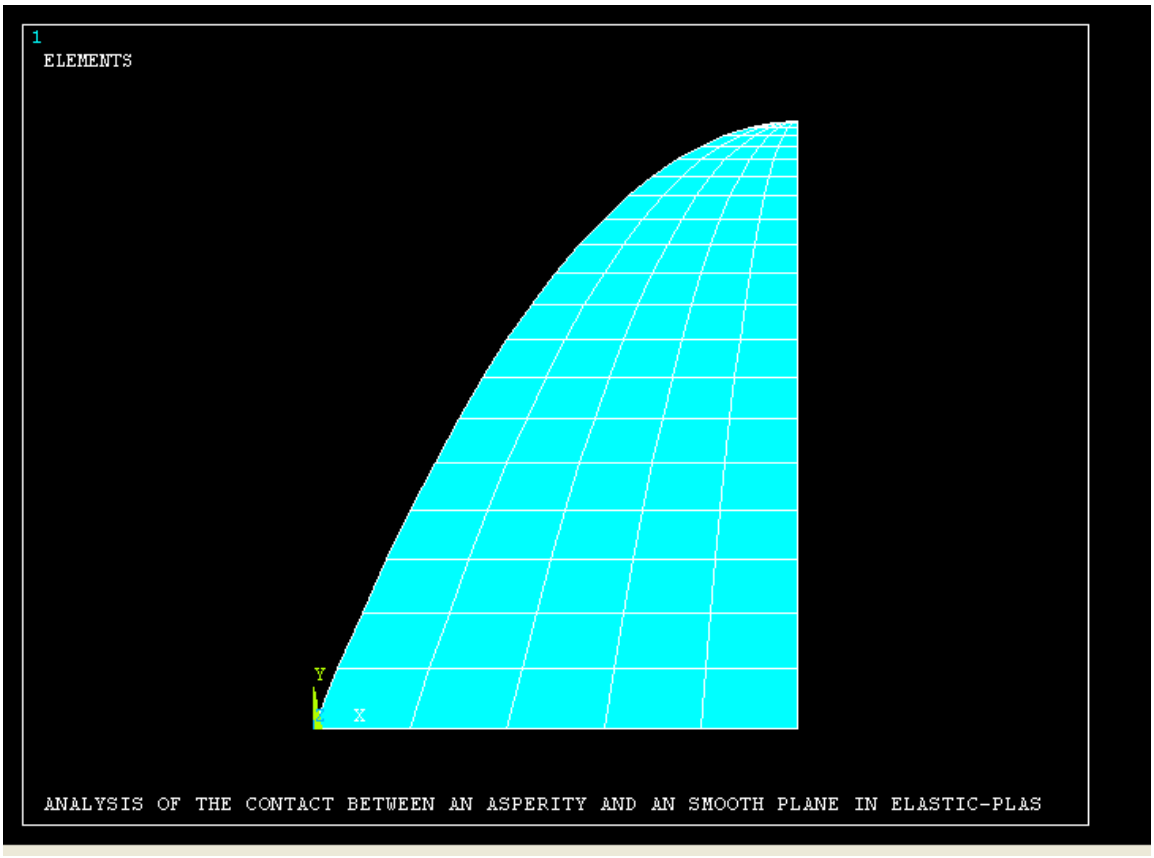

Fig. 3.6.1: Mesh of a parabolic asperity.

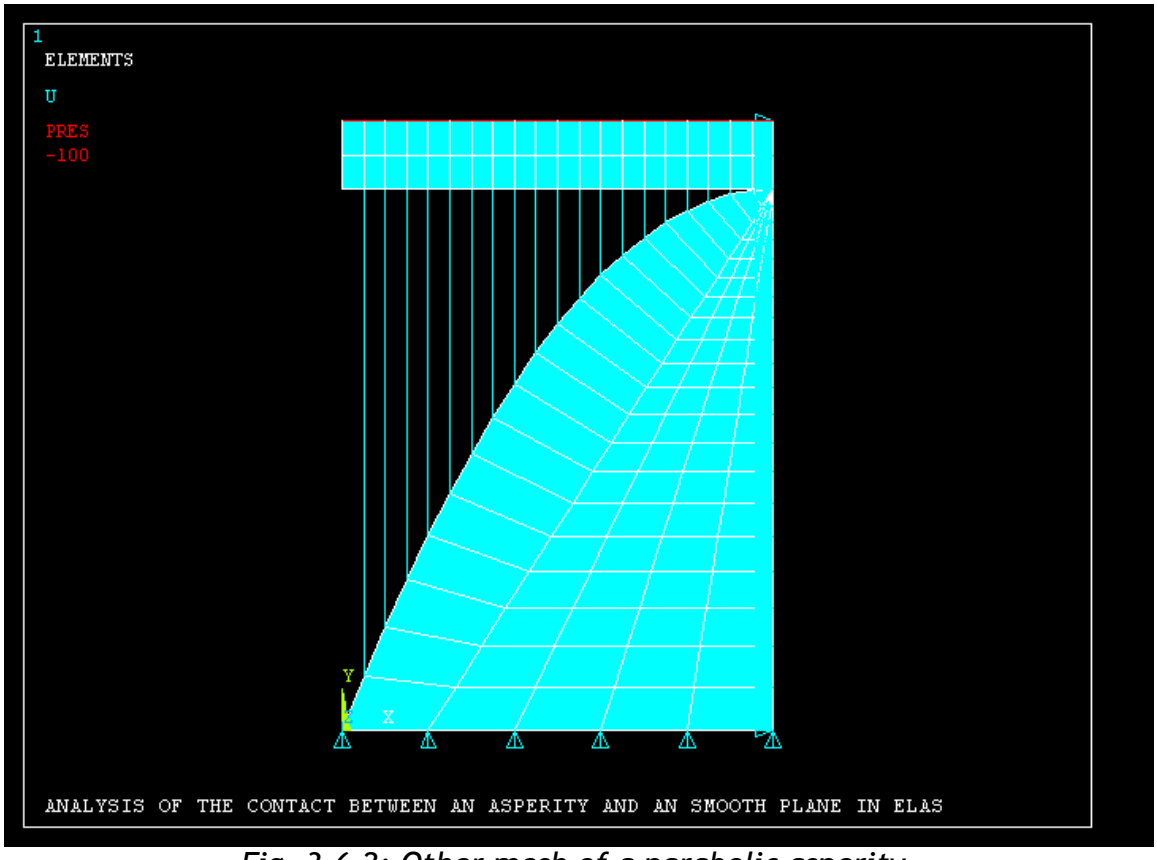

Fig. 3.6.2: Other mesh of a parabolic asperity.

4. Approximation of the roughness profiles by mathematical functions

In order to study the contact mechanics between two rough surfaces the measured profiles, are normally approached by mathematical functions for the application of the existing models. Next, some methods for approximation the 2D roughness profiles by mathematical functions will be displayed.

4.1 Parabola functions using the Aramaki formulation

Aramaki in the paper "The Contact Between Rough Surfaces With Longitudinal Texture – Part I: Average Contact Pressure and Real Contact Area"-[25] propose a form to approach the measured rough profile with quadratic functions in order to calculate the average pressure and the real contact area in a contact between two longitudinally rough surfaces.

First, he define an asperity:

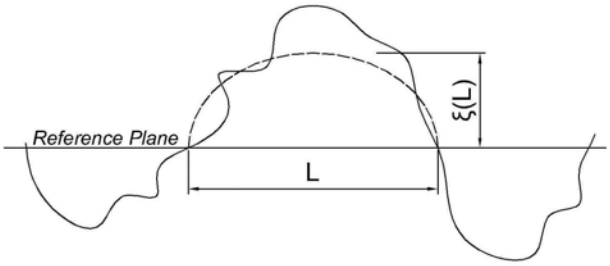

Fig. 4.1.1: Schematic of the definition of an asperity

In this figure L is the asperity width and ξ(L) is the asperity height having with L, this height is defined as the height of the parabola function above the reference plane having the same cross-sectional area as the actual measured asperity.

He admits that the distribution of the asperities widths follow an exponential function:

$$p(L) = \frac{1}{\overline{L}} \exp\left(-\frac{L}{\overline{L}}\right) \tag{4.1.1}$$

The relationship between the asperity width and the asperity height will be found using the autocorrelation function, this relation is:

$$\frac{\overline{\xi}}{\overline{L}} = \sqrt{\frac{2}{\pi}}\alpha\sigma \tag{4.1.2}$$

Where α is a coefficient of autocorrelation function, and defined by:

$$\alpha = \frac{1}{\tau} \tag{4.1.3}$$

and τ is the autocorrelation length: $ACF(\tau) = 0.368$, σ is the standard deviation of the rough profile. The equation (4.1.2) correspond to the equation (8) in the paper [25], where the formulation used to give this equation is described.

The asperity curvature can be given by:

$$K = \frac{\left| f''(x) \right|}{\left[1 + \left(f'(x) \right)^2 \right]^{3/2}} \tag{4.1.4}$$

For an asperity with width L and height ξ the curvature is:

$$K = \frac{8\xi}{L^2} \tag{4.1.5}$$

Using the radius of curvature the quadratic function that describe the asperity is:

$$z = -\frac{4\xi}{L^2} x^2 + \frac{4\xi}{L} x \tag{4.1.6}$$

In the figure 4.1.2 this approximation is represented:

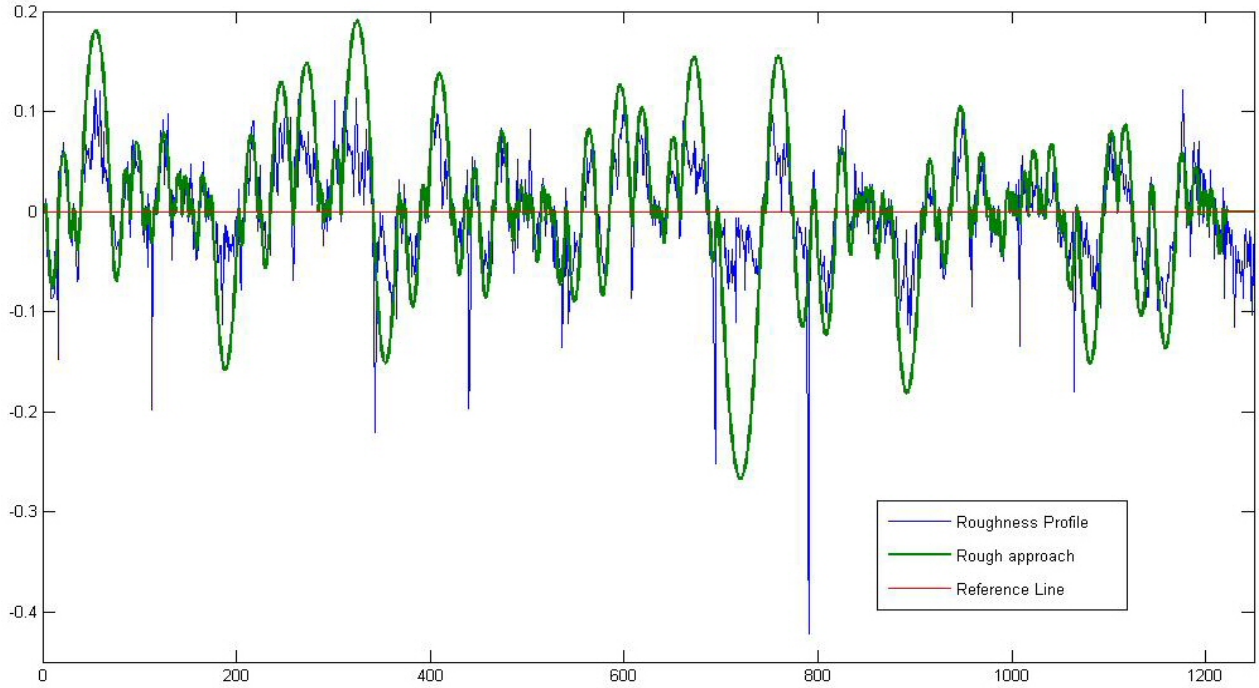

Fig. 4.1.2: Example of the approach the rough profile by parabolas using the method proposed by Aramaki [25] and [26].

The algorithm in Matlab used for calculate this approximation is in appendix 4. This approximation proposed by Aramaki gives good results when the autocorrelation function follows an exponential function. In the case of a small lot of the big asperities this method doesn't give good results.

4.2 Parabola functions using the least mean squares

In this approximation parabolas functions that represent the peaks and the valleys are used. The standard equation used is:

$$z = ax^2 + bx + c \tag{4.2.1}$$

Where, z corresponds to the profile height and x the coordinate of the respective point. A peak or valley is constituted by n points: (x_1,z_1) (x_2,z_2) … (x_i,z_i)… (x_n,z_n). The best fitting function is the function that has the minimum least square error:

$$R = \sum_{i=1}^{n}\left[z_i - f\left(x_i\right)\right]^2 = \sum_{i=1}^{n}\left[z_i - \left(ax_i^2 + bx_i + c\right)\right]^2 = \min. \tag{4.2.2}$$

This function has two points defined, because it must start when the asperity starts ($f(x_0)=0$) and end when the asperity ends ($f(x_1)=0$), then it only has one unknown coefficient (the coefficient *a* was chosen):

$$\begin{cases} 0 = ax_0^2 + bx_0 + c \\ 0 = ax_1^2 + bx_1 + c \end{cases} \Leftrightarrow \begin{cases} b = -a(x_0 + x_1) \\ c = ax_0x_1 \end{cases} \tag{4.2.3}$$

The least square error is:

$$\begin{aligned} R &= \sum_{i=1}^{n}\left(\left(ax_i^2 - a\left(x_0 + x_1\right)x_i + ax_0x_1\right) - z_i\right)^2 = \\ &= a^2\sum_{i=1}^{n}\left(x_i^2 - \left(x_0 + x_1\right)x_i + x_0x_1\right)^2 + \sum_{i=1}^{n} z_i^2 - 2a\sum_{i=1}^{n}\left(x_i^2 - \left(x_0 + x_1\right)x_i + x_0x_1\right)z_i \end{aligned} \tag{4.2.4}$$

In order to obtain the least square error the first derivate in order of *a* must equaled 0:

$$\frac{\partial R}{\partial a} = 0 \tag{4.2.5}$$

Resolving this equation we obtain:

$$a = \frac{\sum_{i=1}^{n}\left(x_i^2 z_i\right) - \left(x_0 + x_1\right)\sum_{i=1}^{n} x_i z_i + x_0x_1\sum_{i=1}^{n} z_i}{\sum_{i=1}^{n} x_i^4 + nx_0^2x_1^2 + \left(x_0 + x_1\right)^2\sum_{i=1}^{n} x_i^2 - 2x_0x_1\left(x_0 + x_1\right)\sum_{i=1}^{n} x_i + 2x_0x_1\sum_{i=1}^{n} x_i^2 - 2\left(x_0 + x_1\right)\sum_{i=1}^{n} x_i^3} \tag{4.2.6}$$

This approximation admitting that the base of the asperity is in x=0, in the figure 4.2.1 is presented a plot with this approximation and the Matlab model used is reported in appendix 5.

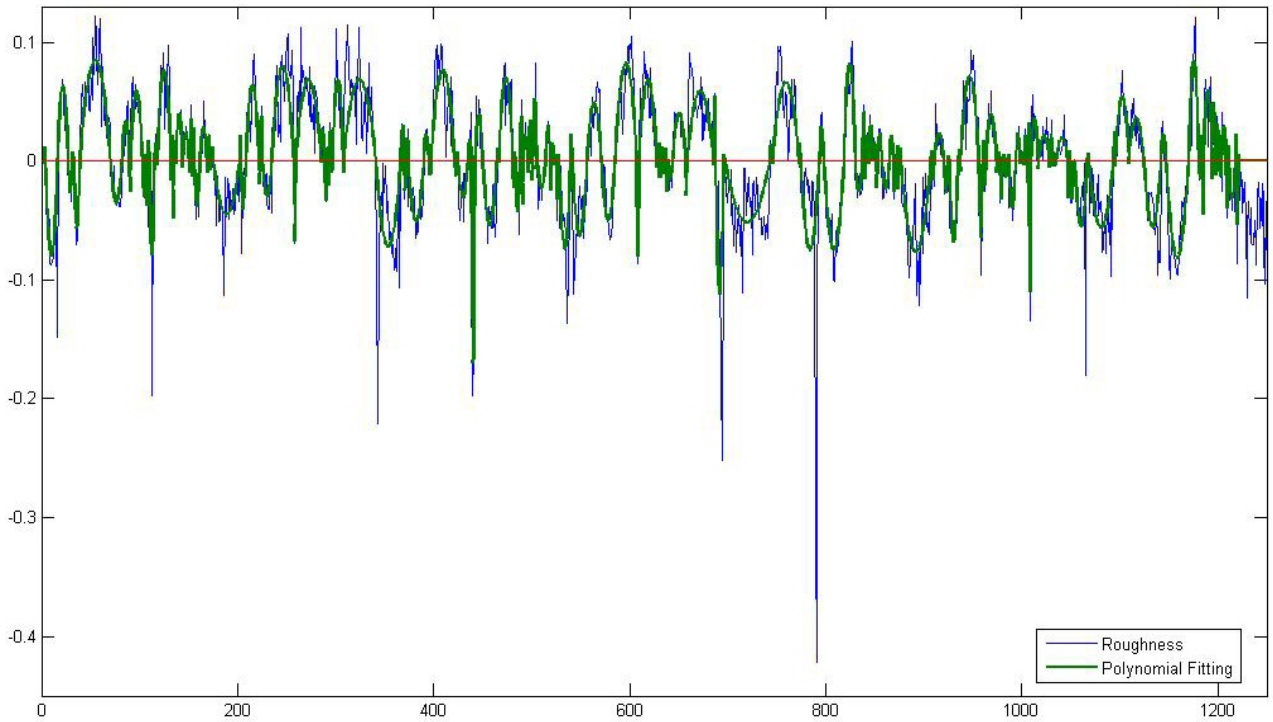

Fig. 4.2.1: Approach with mean squares for c=0

With this approach it is very easy to obtain a profile described by mathematical functions, but it isn't very good for the reason that in order to define one asperity the mean line is used moreover, in this case, the asperity can have one or more 'peaks' or 'valleys' in the same asperity and the asperity has a large size in the base. Alternatively, if we are using for reference lines one distance c1, of the mean line for the peaks and a distance c2, for the valleys we obtain a better approximation because the probability of one parabola describing various peaks or valleys is reduced and the number of the points for the mean squares method is near of the maximum of the asperity. The values of c1 and c2 can be the same used to calculate the peak density (RP_c), but these values don't have a standard. Therefore we will used the amplitude distribution function for estimate these values:

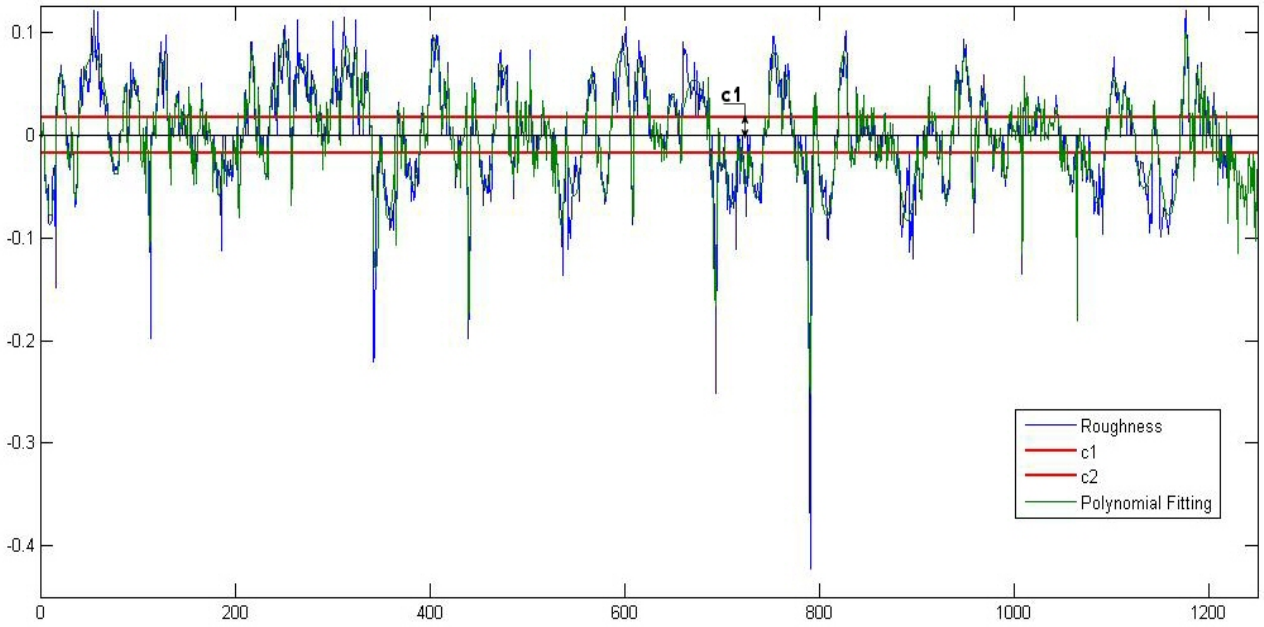

Fig. 4.2.2: Approach with mean squares using reference lines with height c1 and c2 from the mean line.

In this figure the line c1 represents the height for which the amplitude distribution function is equal to 30% ($ADF(c_1)=0.7$), this approach permits to obtain a better approximation and the radius in the peak of the these functions are nearer to the real values. This value must be changed in the function of the approximation objective.

4.3 Parabola functions with the same area

Aramaki in [25] and [26] define asperity height ξ(L) how that height of the parabola function above the reference plane having the same cross-sectional area, but in description of the model, he doesn't use this consideration.

This model, for approaching the rough surfaces uses quadratic functions in order to describe the peaks and the valleys with the condition that the real asperity has the same area that the function used for express the asperity.

The area of an asperity is:

$$A = \Delta x \sum_{i=n_1}^{n_2} z_i \tag{4.3.1}$$

where Δx is the space between two points, and n_1 and n_2 is the initial and finish point of the asperity.

The quadratic function is:

$$z = ax^2 + bx + c \tag{4.3.2}$$

The coefficients a, b and c can be determined using the boundary conditions: for $x=x_0$ and $x=x_1$, z=0 and the area of an asperity described by this quadratic function is the same that the area of an asperity:

$$A = \frac{ax^3}{3} + \frac{bx^2}{2} + cx \Bigg]_{x0}^{x1} \tag{4.3.3}$$

Resolving these equations obtain the quadratic function:

$$z = -\frac{6A}{\left(x_1 - x_0\right)^3} x^2 + \frac{6A\left(x_1 + x_0\right)}{\left(x_1 - x_0\right)^3} x - \frac{6Ax_0x_1}{\left(x_1 - x_0\right)^3} \tag{4.3.4}$$

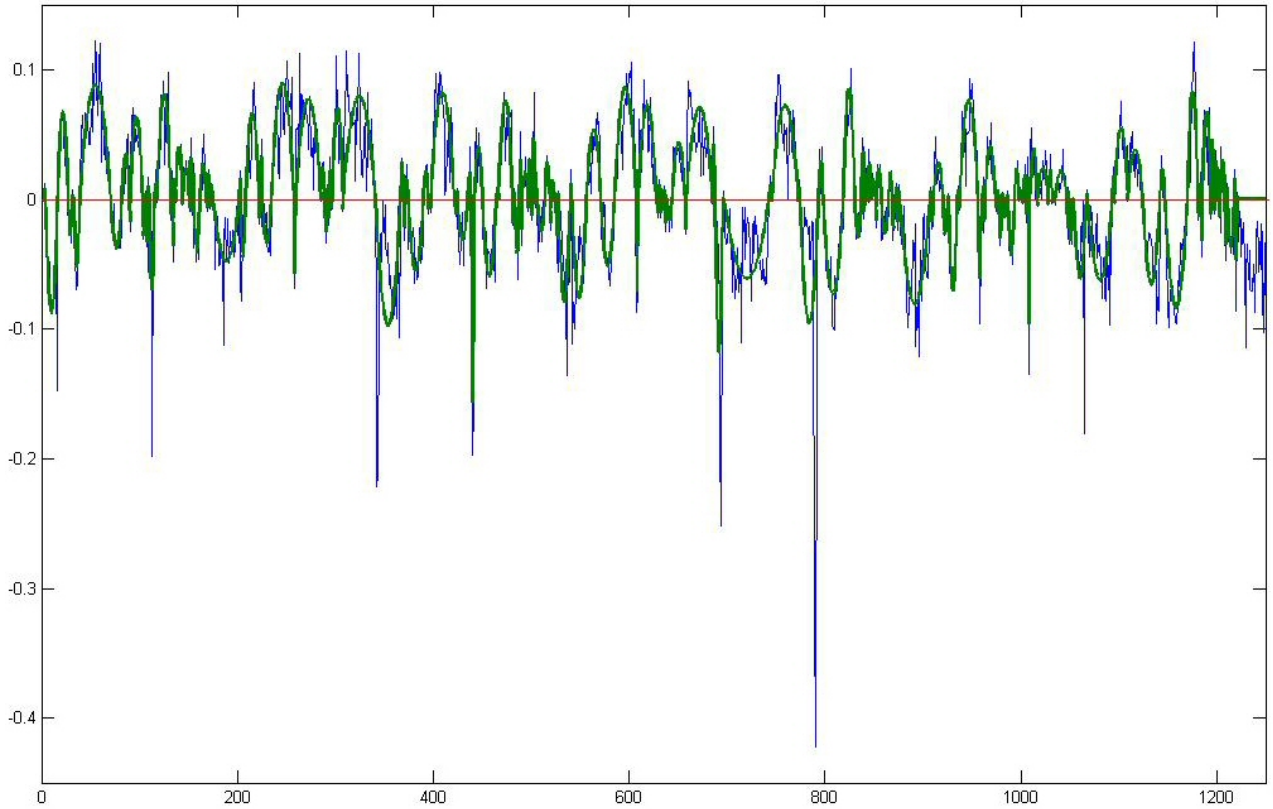

Fig. 4.3.1: Representation of the approach the rough profile by quadratic functions with the same area that the real rough profile.

With this method the approach profile has the same value of Ra but in the cases where big values of Rz exist this approach doesn't follow the highest peaks. Comparing this method with the method proposed for Aramaki this method can be better in the cases that the value Ra/Rz is low.

4.4 Comparison of the approach profiles methods

Others models with quadratic functions can be constructed using the others parameters, for example, a rough surface can be approached with quadratic functions using the condition that the both surfaces have the same Rq, however these approximations has a problem: the radius of curvatures of the asperities. This is a most important value in the mechanical contact analysis and when approach the profile with the means squares method or using the same area the radius of curvature have a big error admitting that the asperity width and the asperity height have the next relation (from [25]):

$$\frac{\xi(L)}{\sigma} = \sqrt{\frac{2\pi}{L^{*^2}+1}} L^* \quad where \; L^* = \frac{\alpha L}{\pi} \tag{4.4.1}$$

and where α is coefficient of autocorrelation. These equation can be simplified by the equation (4.1.2). In figures 4.1.2, 4.1.2, 4.1.2 have a plots with the representation of the asperity width and the asperity height for the three methods and using three different surfaces presented in the figure 4.1.1.

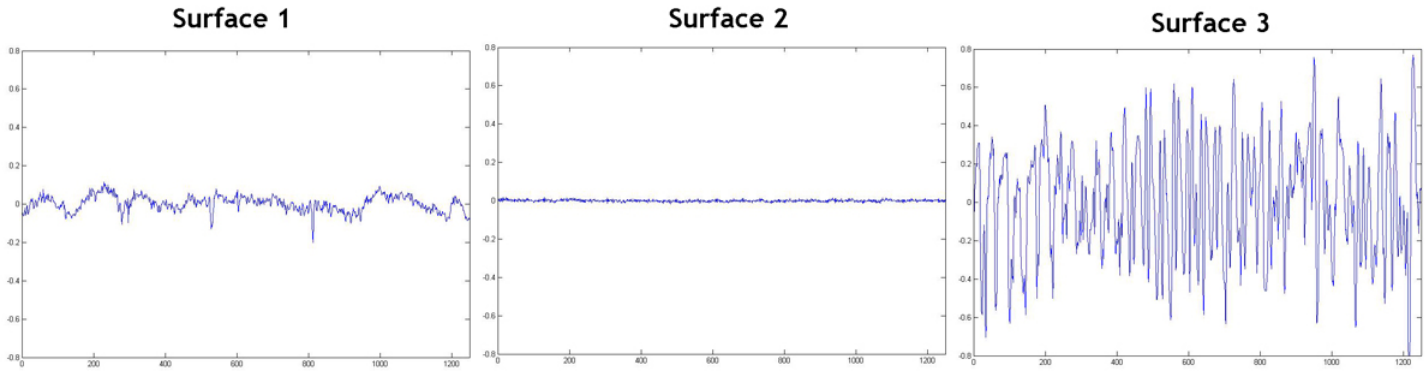

Fig.4.4.1: Roughness profiles of three surfaces.

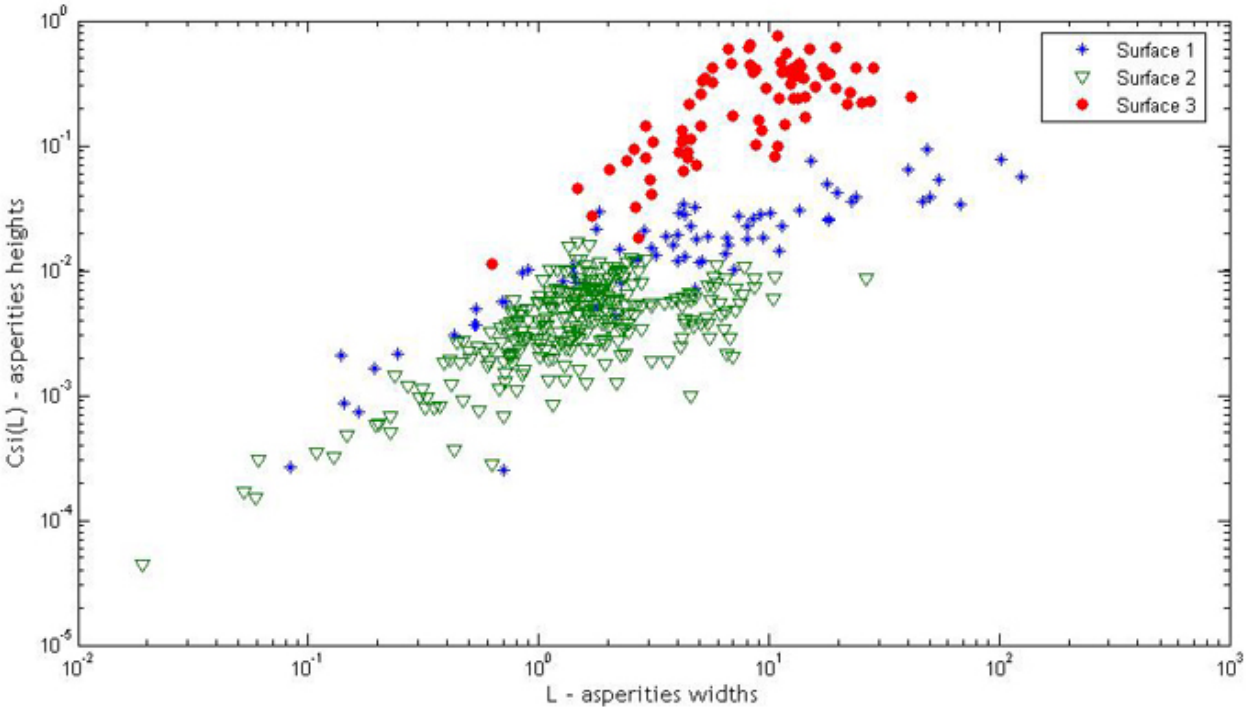

Fig.4.4.2: Asperity height in function of the asperity width for a three approached profiles using the method of the mean squares.

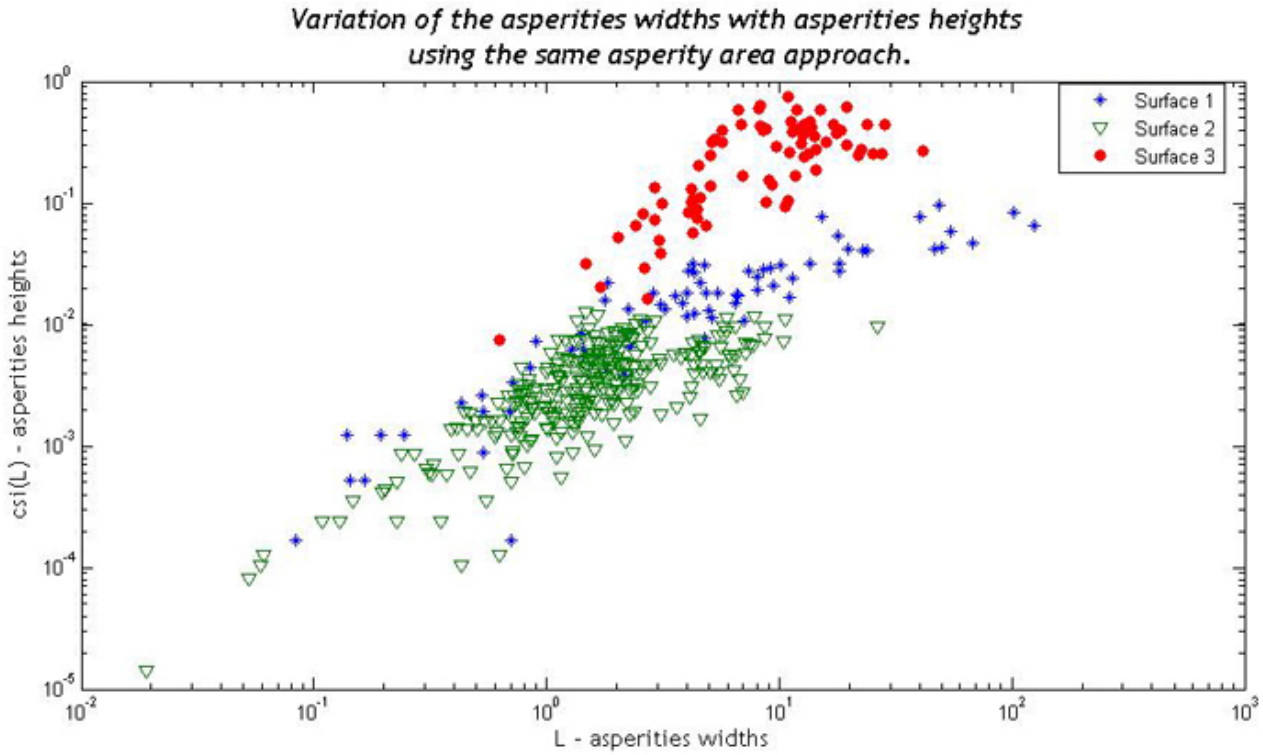

Fig.4.4.3: Asperity height in function of the asperity width for a three approached profiles using the method of the asperity with the same area..

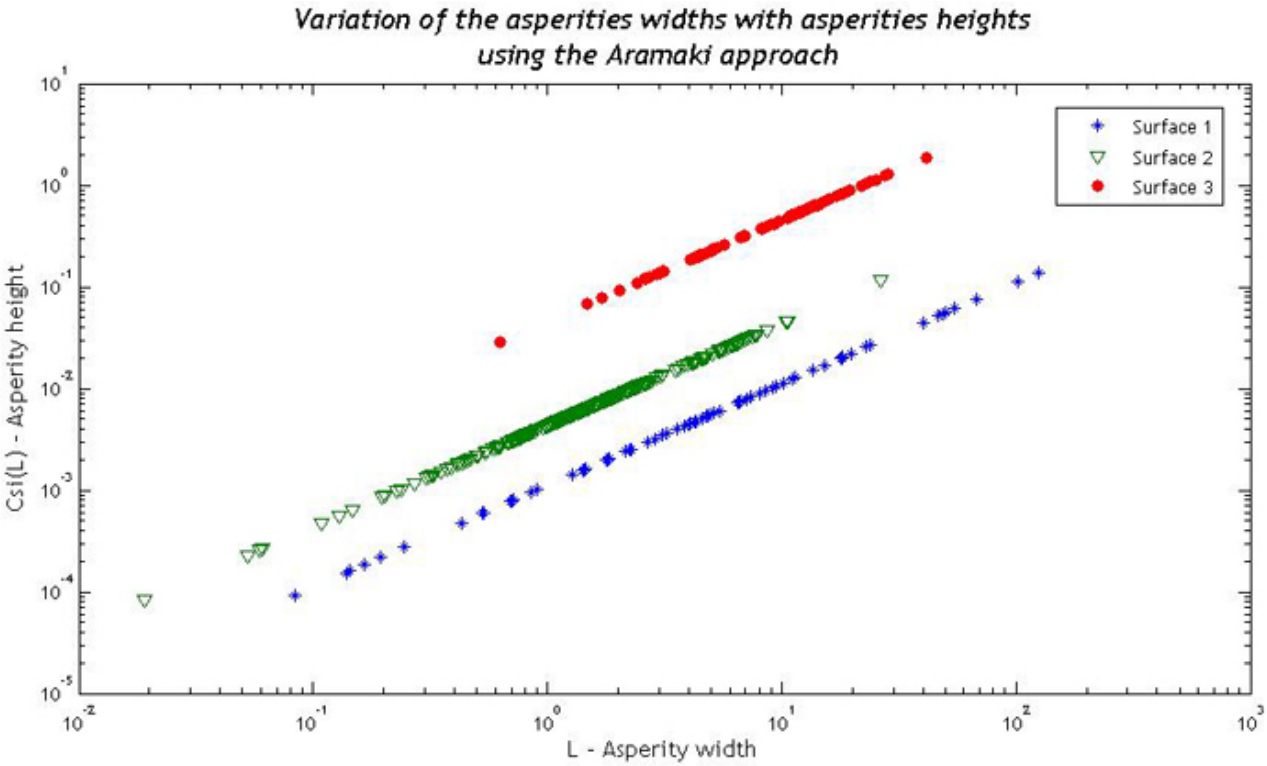

Fig. 4.4.4: Asperity height in function of the asperity width for a three approached profiles using the Aramaki method.

From this plots it is possible to conclude that for high values of asperity widths or heights the relation keep out from the approach used by Aramaki, but this values are most important in mechanical contact studies because are the asperities that to come in contact first.

The asperity radius is an important input data on the contact mechanic models. It is possible to estimate this value from the fourth spectral moment value, this spectral moment is calculated from the second derivate of the rough profile, equation 4.4.2:

$$m_4 = E\left\{\left(\frac{d^2z}{dx^2}\right)^2\right\} \tag{4.4.2}$$

where E{ } denotes a statistical estimator.
The relation between the fourth spectral moment and the asperity radius is given by the equation 4.4.3.

$$\beta = \frac{3\sqrt{\pi}}{8\sqrt{m_4}} \tag{4.4.3}$$

In the article "A simple numerical procedure to calculate the input data of Greenwood-Williamson model of asperity contact for actual engineering surfaces" – [33] three different methods for calculating the second derivate are presented.

Simple derivation:

$$\left(\frac{d^2z}{dx^2}\right)_i = \frac{z_{i+1} - 2z_i + z_{i-1}}{h^2} \tag{4.4.4}$$

Three points derivation:

$$\left(\frac{d^2z}{dx^2}\right)_i = \frac{z_{i+2} - 2z_{i-1} + z_{i-4}}{9h^2} \tag{4.4.5}$$

Finite central differences:

$$\left(\frac{d^2z}{dx^2}\right)_i = \frac{-z_{i+2} + 16z_{i+1} - 30z_i + 16z_{i-1} - z_{i-2}}{12h^2} \tag{4.4.6}$$

Where $h = x_{i+1} - x_i$, in this article h=0.695 μm is used.

Using this method is possible to estimate the asperity radius and approach the profile with a different method proposed by Aramaki [25]. The application of this method was not done in this work. In the future works must be done the confront between the radius of curvature obtained with the various methods.

5. Experimental Results

In this chapter the roughness measures is described in three different surfaces and the analysis of the contact mechanic in these surfaces.

5.1 The measured specimens

Three specimens in steel had been used in order to measure the roughness profile and with these results the variation in the roughness is studied when applied a load in the specimen.

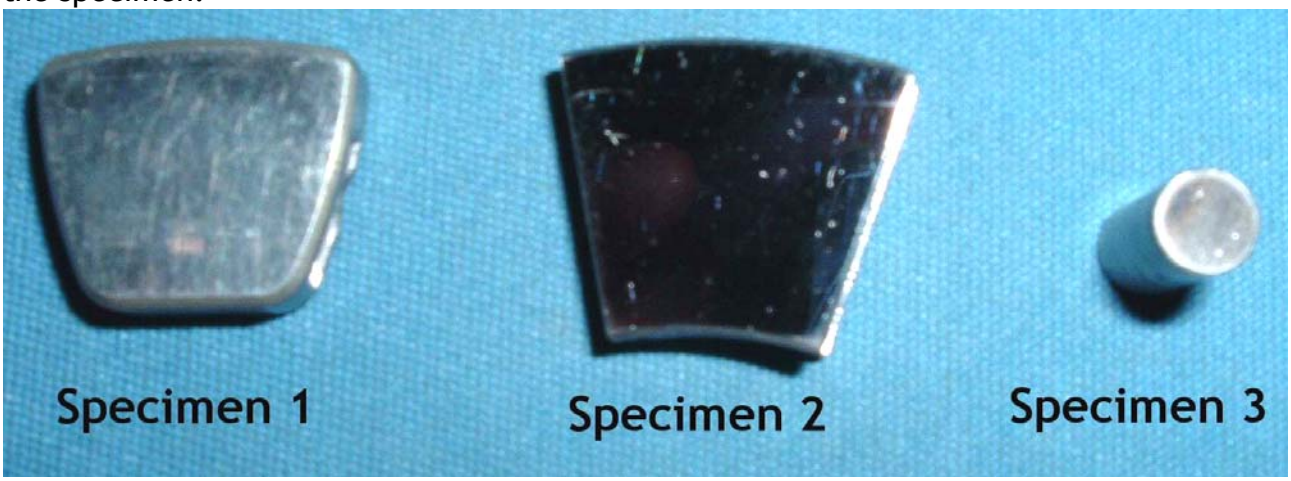

Fig.5.1.1: The three measured specimens.

The specimens 1 and 2 is a bearing pad from the thrust bearings. The specimen 1 is from of the a Glacier Thrust Bearing, these bearings have a small layer in aluminium tin alloy (Al-Sn). The specimen 2 is a bearing pad prepared in the Department of Mechanics, Nuclear and Production Engineering manufactory, the material of this pad is a AISI type 430 stainless steel. The specimen 3 is a cylinder carburized steel specimen (AISI 9310) used in friction and wear experiences in this department. This specimen was cut by a saw, so has a high value of Ra, Rq or Rt in the top. Only the top of this specimen was analysed in stylus and in the microscope.

In the table 5.1.1 has the properties of each used specimen and the glass disc used in the apparatus for a contacts analysis:

Property:	**Specimen 1**	**Specimen 2**	**Specimen 3**	**Glass Disc**
Modulus of Elasticity	≈70 GPa	200 GPa	200 GPa	80 GPa
Poisson Ratio	0.33	0.29	0.29	0.22
Yield Tensile Strength	124 MPa	310 MPa	1238 MPa	-
Ultimate Tensile Strength	165 MPa	517 MPa	993 MPa	-
Hardness Vickers	70	160 (*)	397	403
Hardness (SI Units)	686.5 MPa(**)	1569 MPa (**)	3893 MPa (**)	3952 MPa (**)

Tab.5.1.1 : Mechanical properties of the used specimens.((*) Converted using the web calculator [28] and (**) converted using the web calculator [29]).

5.2 Roughness Measures with stylus method

The topography of the surface was made in the stylus device: Hommel Tester T8000, in the three specimens topography measurements was done, the selected area for these topographies are 2x2 mm. The number of the scanned points in direction 'x' are 2000 and 201 scans in direction 'y' had been made.

The results had been imported for '.asc' files and after converted in the Matlab in matrixes, in the next figures there is the mesh 3d plots of these measures and in appendix 7 the complete analysis of these measures, using the software HommelMap Basic.

The specimen 1, measure 1:

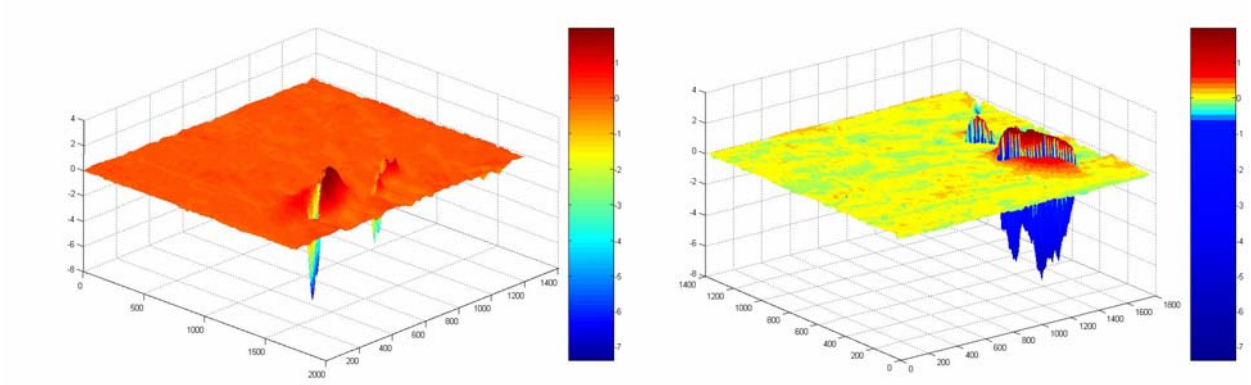

Fig. 5.2.1: Specimen 1 measure 1, three dimension surface representation, dimensions in µm.

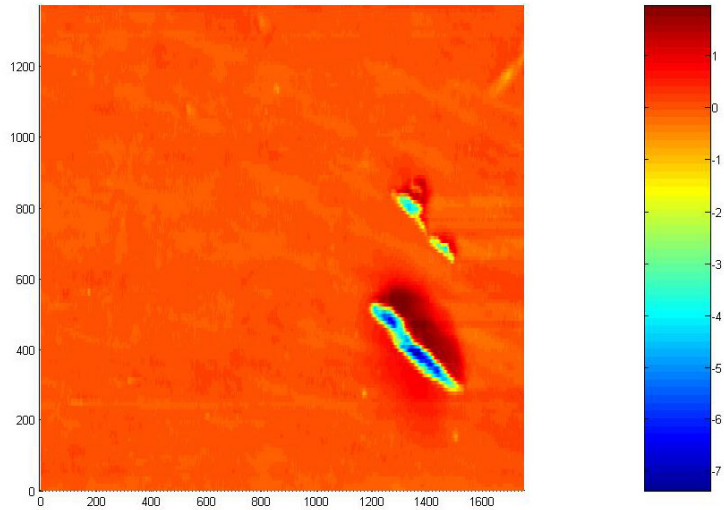

Fig. 5.2.2: Specimen 1 measure 1, two dimensional surface representation, dimensions in µm.

The first measure at the specimen 1 have a problem because in the measure area have a 'micro' defect, this effect induce a false roughness parameters and this measure introduce an error in the contact analysis for the reason that the defect have a big height comparing with the surface. For this reason, this measure was repeated in other zone.

The specimen 1, measure 2:

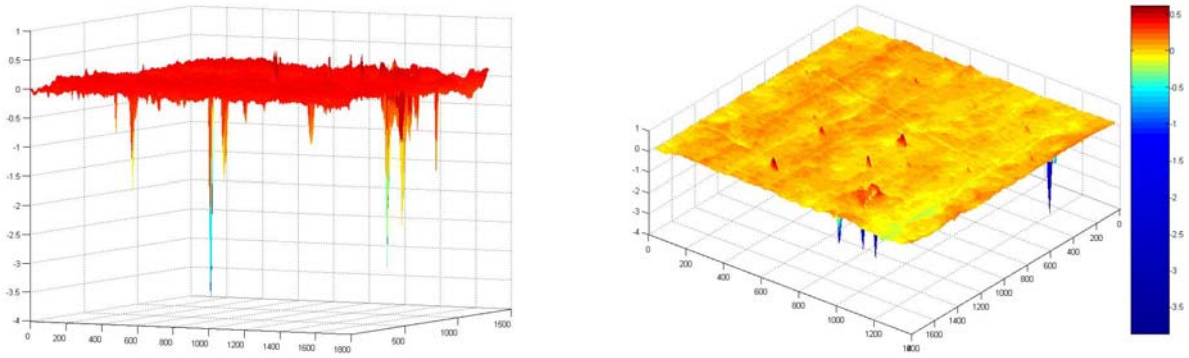

Fig.5.2.3 : Specimen 1 measure 2, three dimension surface representation, dimensions in µm.

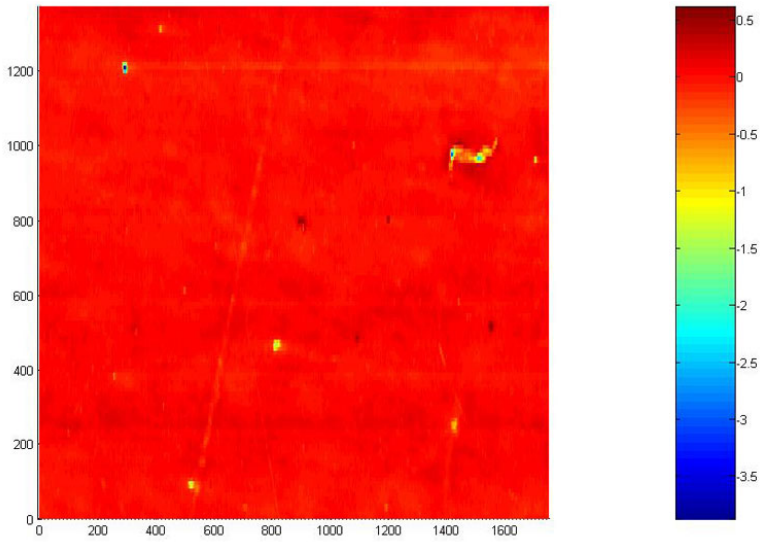

Fig.5.2.4: Specimen 1 measure 2, XY plane representation, dimensions in µm.

The specimen 2:

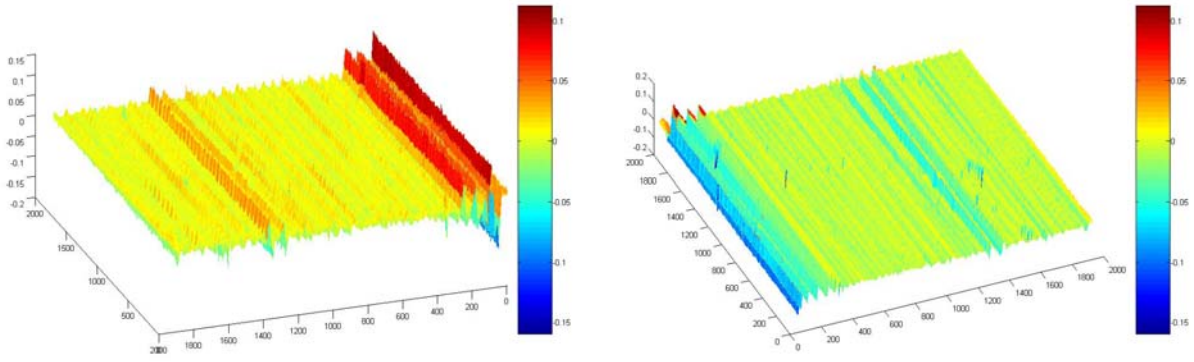

Fig. 5.2.5: Specimen 2, three dimension surface representation, dimensions in µm

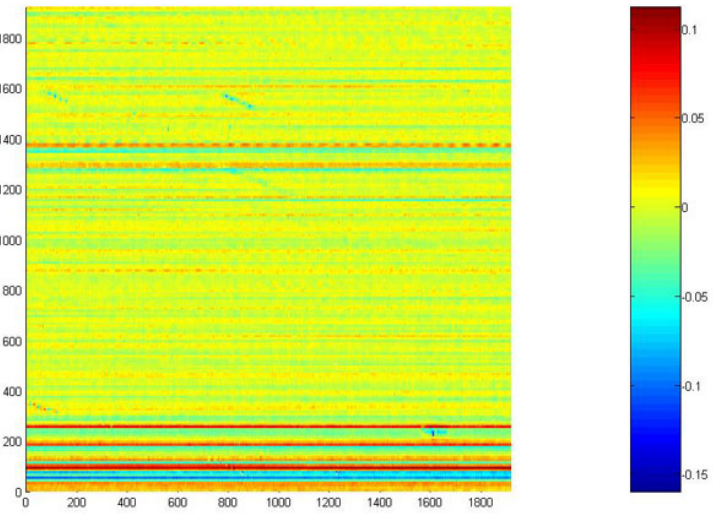

Fig.5.2.6 : Specimen 2, XY plane representation, dimensions in µm

The specimen 3:

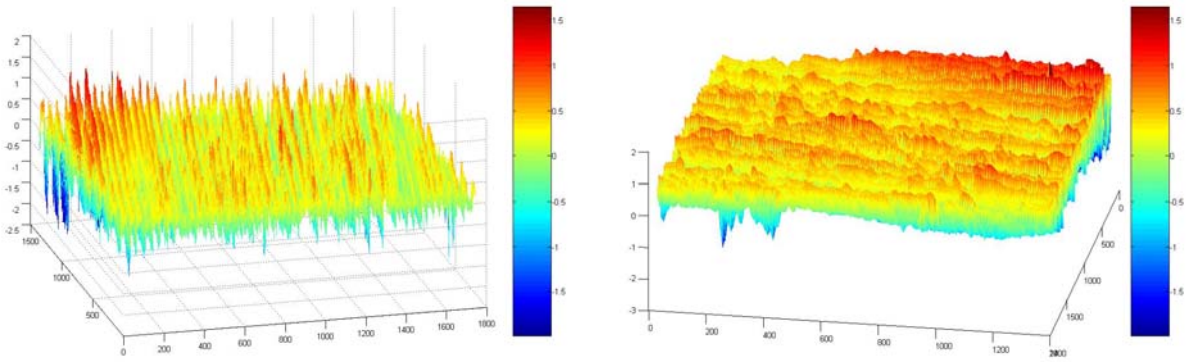

Fig.5.2.7 : Specimen 3, three dimension surface representation, dimensions in µm

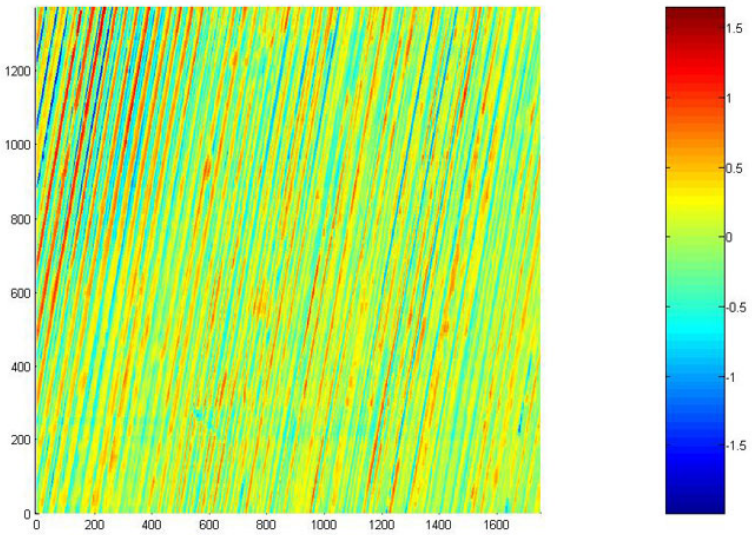

Fig. 5.2.8: Specimen 3, XY plane representation, dimensions in µm

The results in appendix 7 there is an error in the scale, in the measure of the specimen 1, and in 3 there is an error in transversal length (direction y) containing a reduction of 40% caused by a problem in the linear transverse unit in direction 'y', this error influenced the application of the cut off filter. In specimen 2 this error is resolved.

The stylus used for these measures was TKL 100/17, and the specification of this stylus is: tip radius= 5 μm; tip angle= 90º; tip load applied in the surface vertically: 0.8N.

The load applied in the measure is very low but in the specimen 1 is possible to view scratches generated by the tip of the stylus. These impressions are represented in the next image:

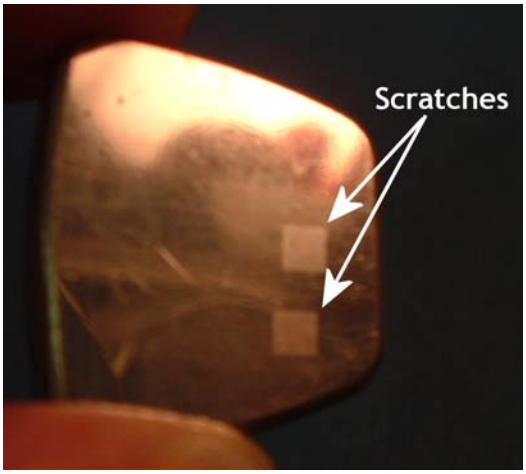

Fig.5.2.9 : "Scratches" generated by the tip of the stylus.

The main cause of these 'scratches' is because the metal of these specimen is ductile.

In the next table there is a summary with the three dimensional parameters and the results of the taker measurements:

	S_a (μm)	S_q (μm)	S_p (μm)	S_v (μm)	S_t (μm)	S_{sk}	S_{ku}	S_z (μm)
Specimen 1-a	0.13	0.349	2.03	7.46	9.49	-7.43	96	8.88
Specimen 1-b	0.0516	0.0872	0.643	3.91	4.56	-9.78	276	3.21
Specimen 2	0.0125	0.0198	0.114	0.162	0.276	0.111	9.48	0.242
Specimen 3	0.304	0.38	1.39	2.06	3.45	-0.278	3.14	3.35

Tab. 5.2.1: Summary of the roughness parameters for the three specimens.

5.3 Analysis of the contact area in the specimens – theoretical values

Using the presented models in the chapters 3.2, 3.3 and 3.4, the interference values and the real contact area was estimated when a load of 40 and 80N are applied to the specimens. These values are approached with the considerations:

- The surface of the specimen is anisotropic;
- The surface of the specimen is plain;
- The apparent pressure is the same on all surface;
- The glass disc is smooth.

The roughness parameters used are one profile of the surface matrix measured and the roughness profile is approached using the Aramaki formulation because a important parameter for these models is the curvature of the asperities, that in the other models this value is sub valuated.

In the next table there are the values of the apparent area of contact in the specimens, the pressure and the equivalent load which is applied in a line of the surface, admitting that this line has a 1.25 mm of length:

	Apparent contact area	Load	Pressure	Equivalent load (in line with 1.25 mm)
Specimen 1	290 mm^2	40 N	0.138 MPa	0.1724 N/mm
		80 N	0.276 MPa	0.3448 N/mm
Specimen 2	290 mm^2	40 N	0.138 MPa	0.1724 N/mm
		80 N	0.276 MPa	0.3448 N/mm
Specimen 3	50.27 mm^2	40 N	0.796 MPa	0.9947 N/mm
		80 N	1.592 MPa	1.9894 N/mm

Tab. 5.3.1: Apparent contact area and the equivalent load in 'line'.

The algorithms used for the determination of the deformation values and the real contact area is in appendix 8.

The results:

Greenwood and Williamson Model:

Load:	40 N		80 N	
	Deformation (μm)	Percentage of the Contact Area (%)	Deformation (μm)	Percentage of the Contact Area (%)
Specimen 1	0.0560	7.55	0.0805	11.08
Specimen 2	0.1041	18.72	0.1142	37.75
Specimen 3	0.3539	1.19	0.6961	2.58

Tab. 5.3.2: Deformation values an real contact area percentage using the Greenwood – Williamson model.

Chang Model:

Load:	40 N		80 N	
	Deformation (μm)	Percentage of the Contact Area (%)	Deformation (μm)	Percentage of the Contact Area (%)
Specimen 1	0.0560	7.55	0.0805	11.08
Specimen 2	0.1041	18.72	0.1142	37.75
Specimen 3	0.8030	3.57	1.0324	7.48

Tab. 5.3.3: Deformation values an real contact area percentage using the Chang model.

Zhao Model:

Load:	40 N		80 N	
	Deformation (μm)	Percentage of the Contact Area (%)	Deformation (μm)	Percentage of the Contact Area (%)
Specimen 1	0.0560	7.55	0.0805	11.08
Specimen 2	0.1041	18.72	0.1142	37.75
Specimen 3	0.8463	4.3	1.0751	8.21

Tab. 5.3.4: Deformation values an real contact area percentage using the Zhao model.

The figures 5.3.1-5.3.3 the variation of the real contact area with the load is presented for a load applied in line with 1.25 mm (N/mm).

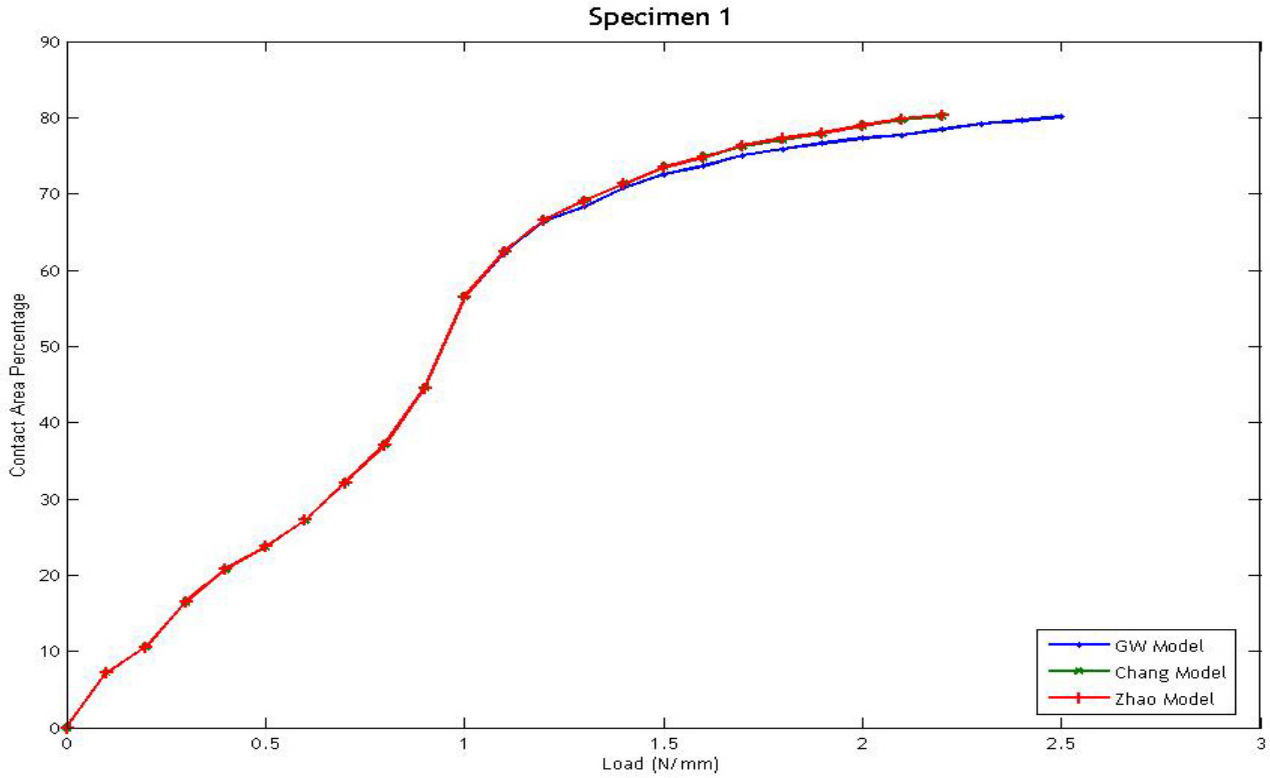

Fig. 5.3.1: Percentage of real contact load of the specimen 1 as a function of load.

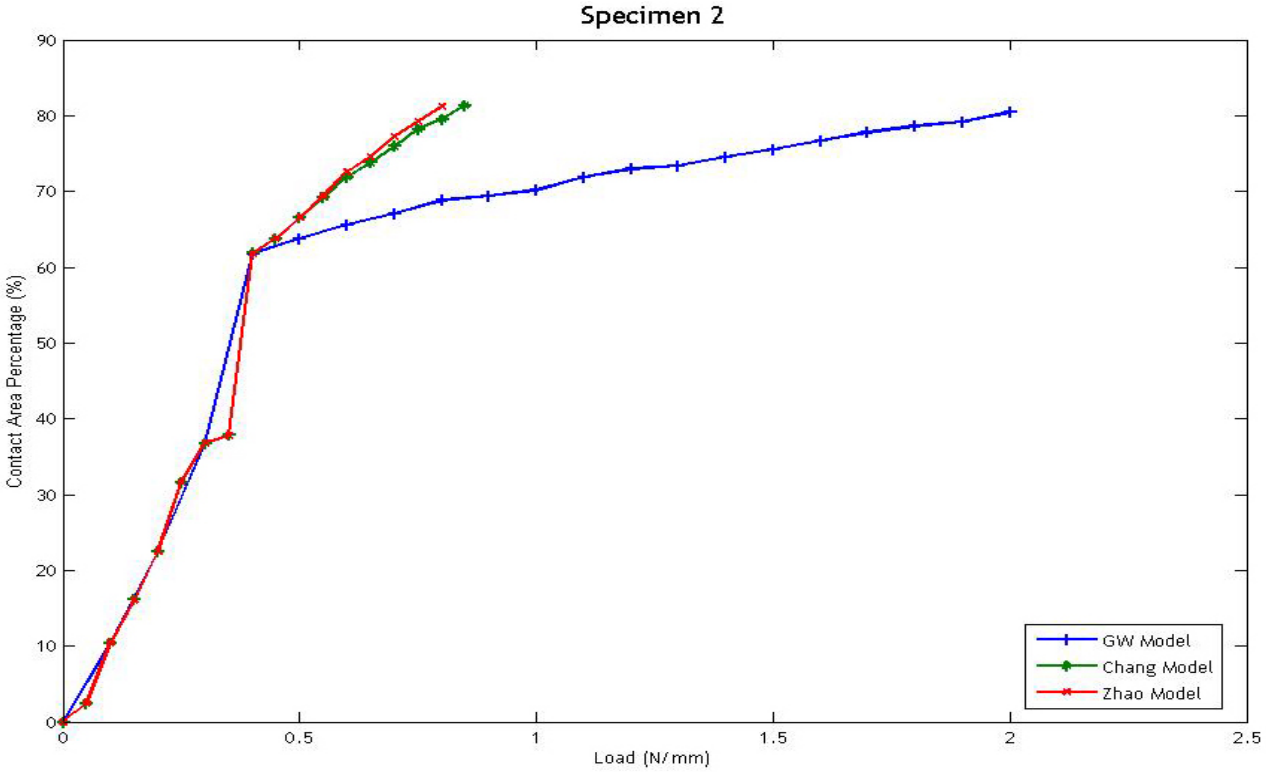

Fig. 5.3.2: Percentage of real contact load of the specimen 2 as a function of load.

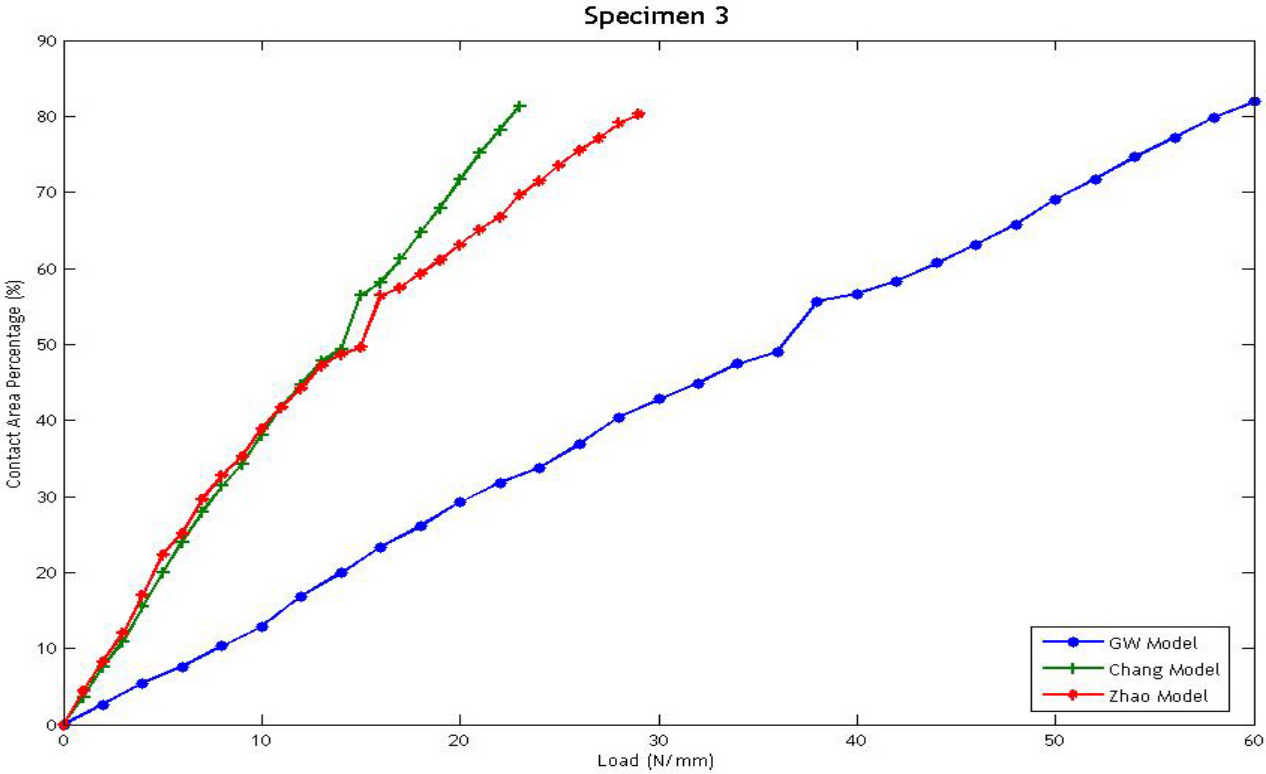

Fig. 5.3.3: Percentage of real contact load of the specimen 3 as a function of load.

The figures 5.3.4-5.3.4 the variation of the interference in μm with the load is presented for a equivalent load applied in line with 1.25 mm.

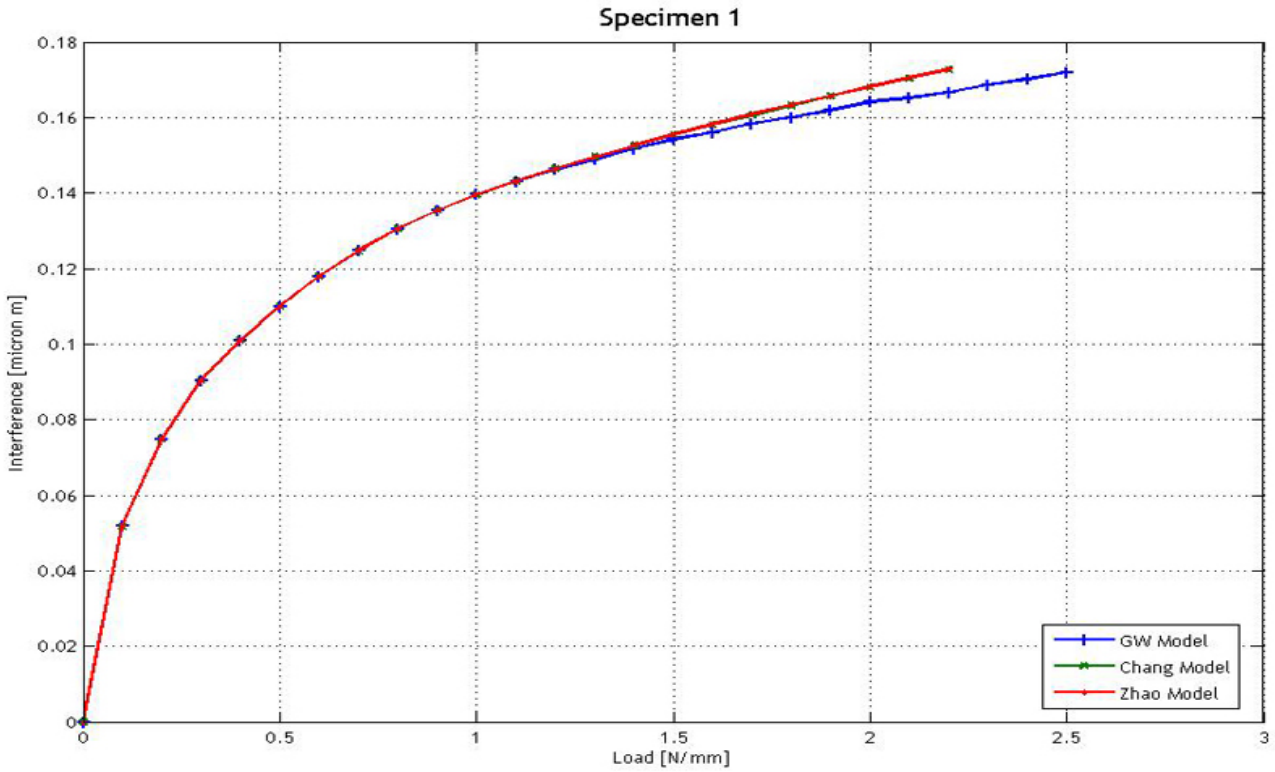

Fig. 5.3.4: Interference of the specimen 1 as a function of load.

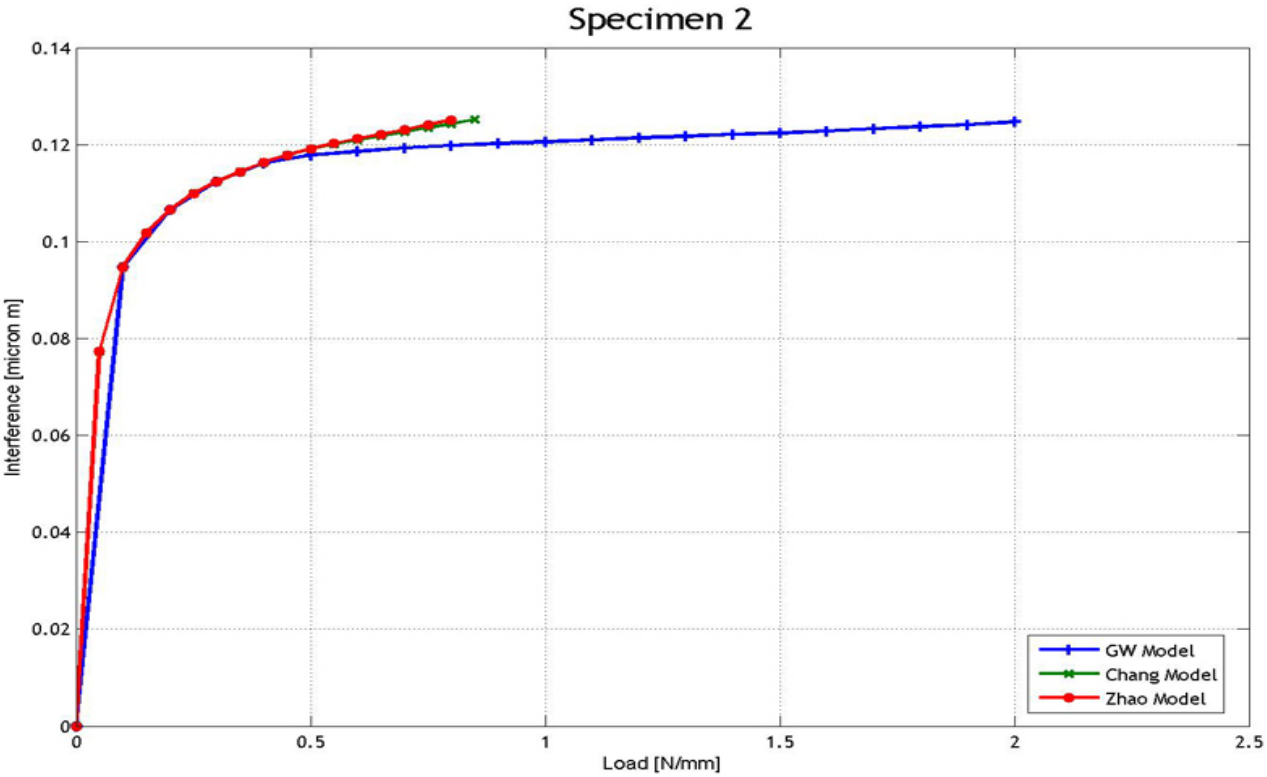

Fig. 5.3.5: Interference of the specimen 2 as a function of load.

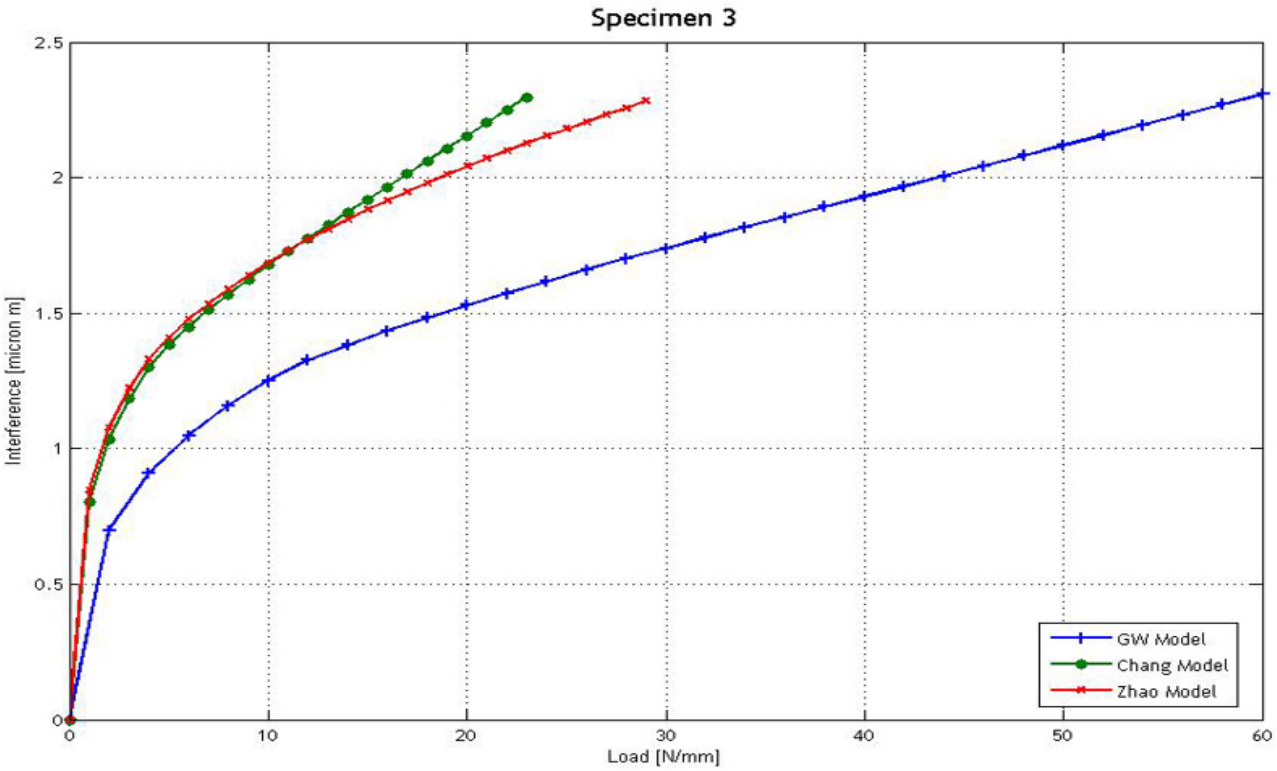

Fig. 5.3.6: Interference of the specimen 3 as a function of load.

5.4 Analysis of the contact area in the specimens using a optical microscope

For the three specimens the variation of the roughness was analyzed in the case of the contact mechanic between the specimen and one smooth plane. In these analyses it the one stereo zoom microscope (Nikon SMZ-10) was used with a maximum magnification (approximately 40x) and the smooth plane is a glass disc. The load was applied using the apparatus represented in the next figure:

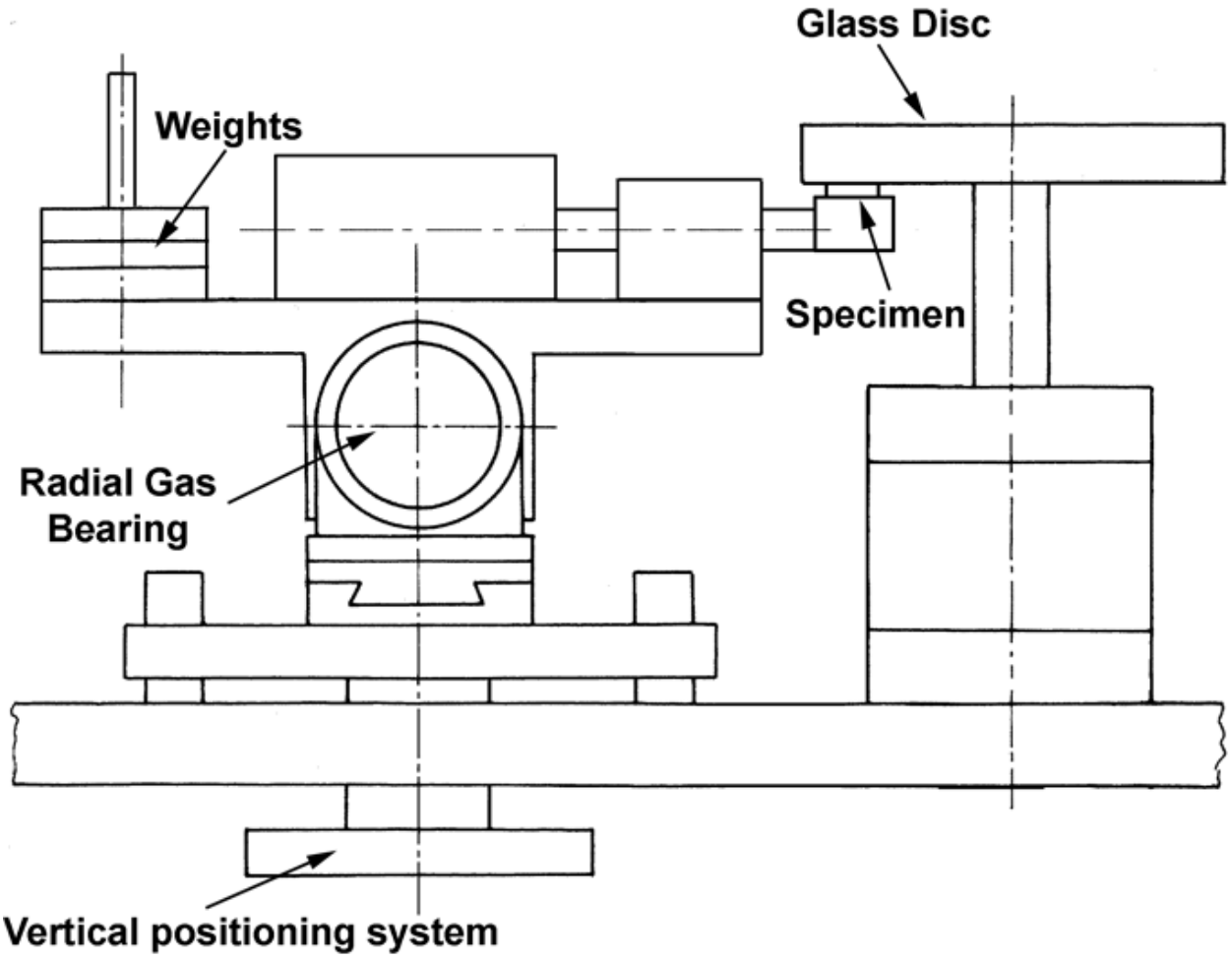

Fig.5.4.1: Apparatus used for applied the load in the specimen.

In the figure 5.4.2 there is a photo of the microscope and the devices used for these analyses:

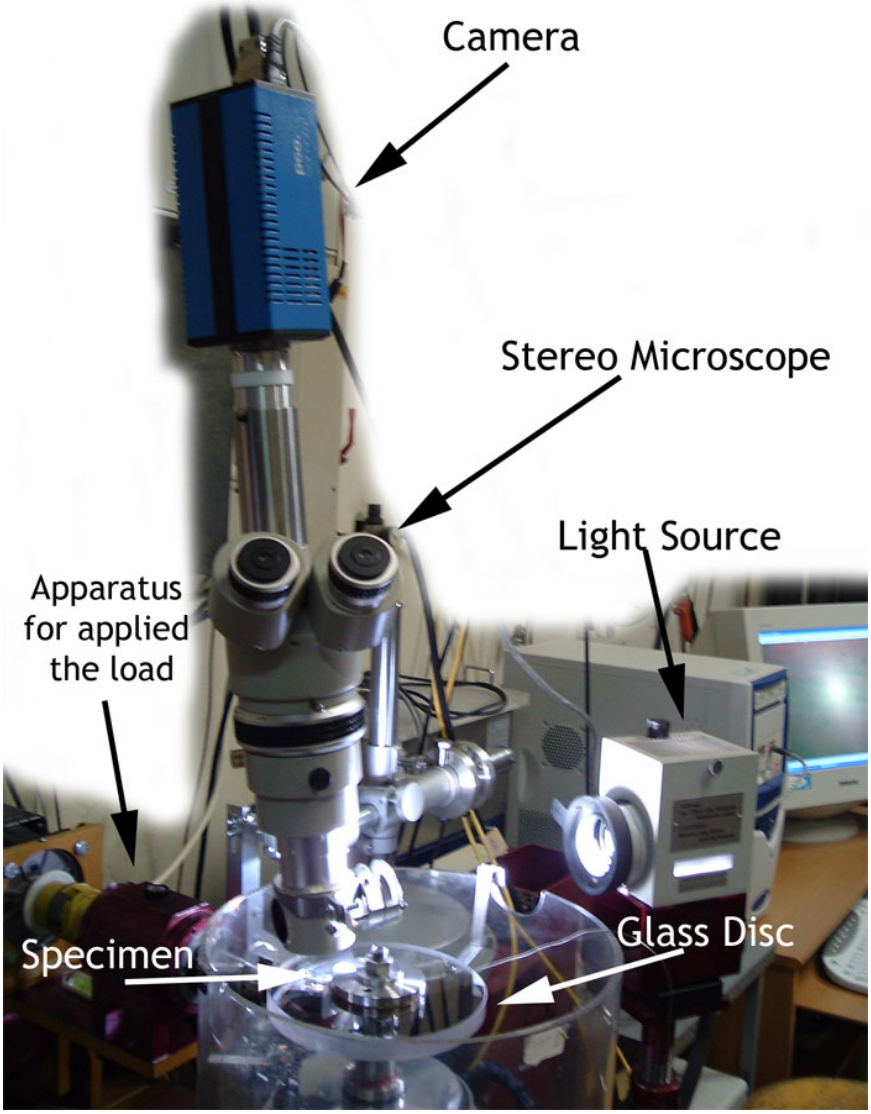

Fig. 5.4.2: Apparatus used for the analysis of the real contact area.

The obtained images

In the appendix 9 have a summary of the obtained images from these analysis. In the next is represented a comparison between the profiles obtained with the stylus and these images.

Specimen 1

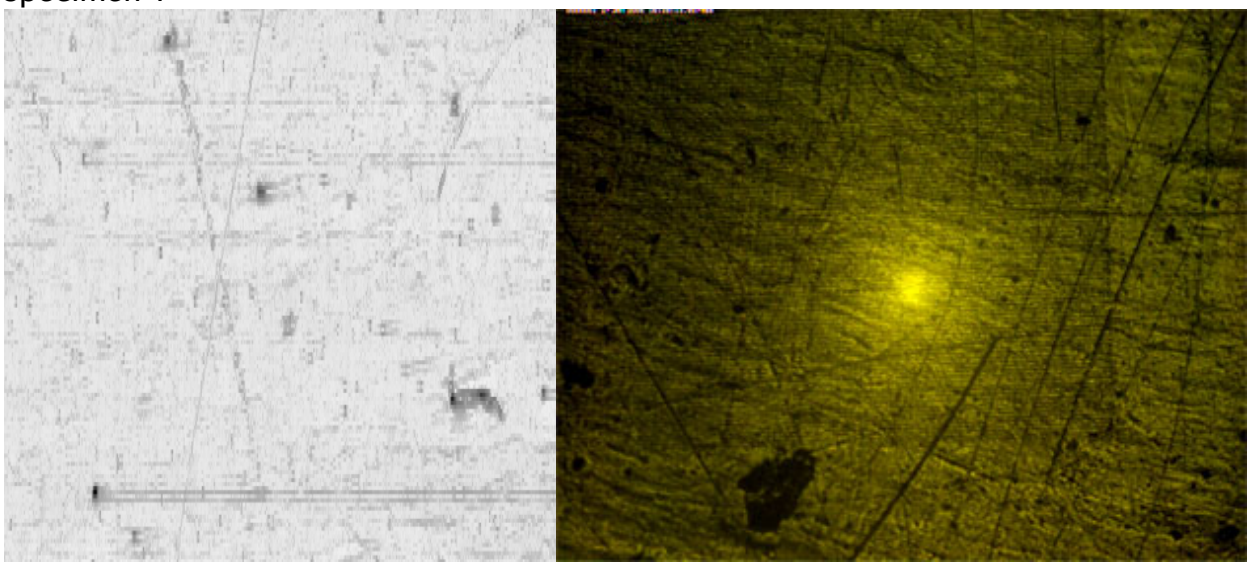

Specimen 2

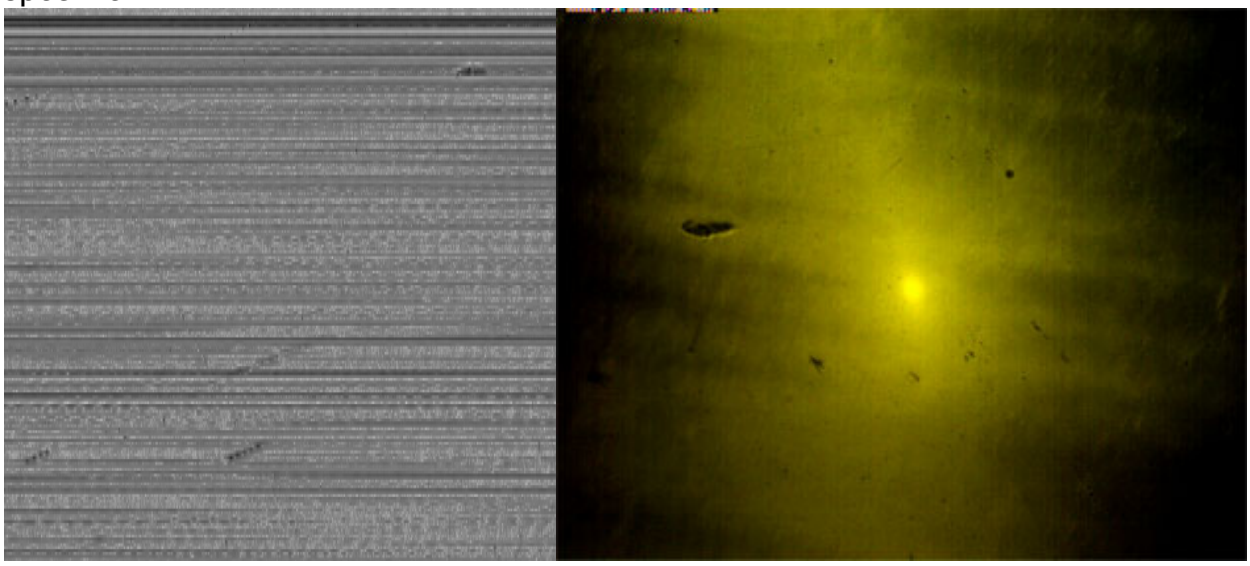

Specimen 3

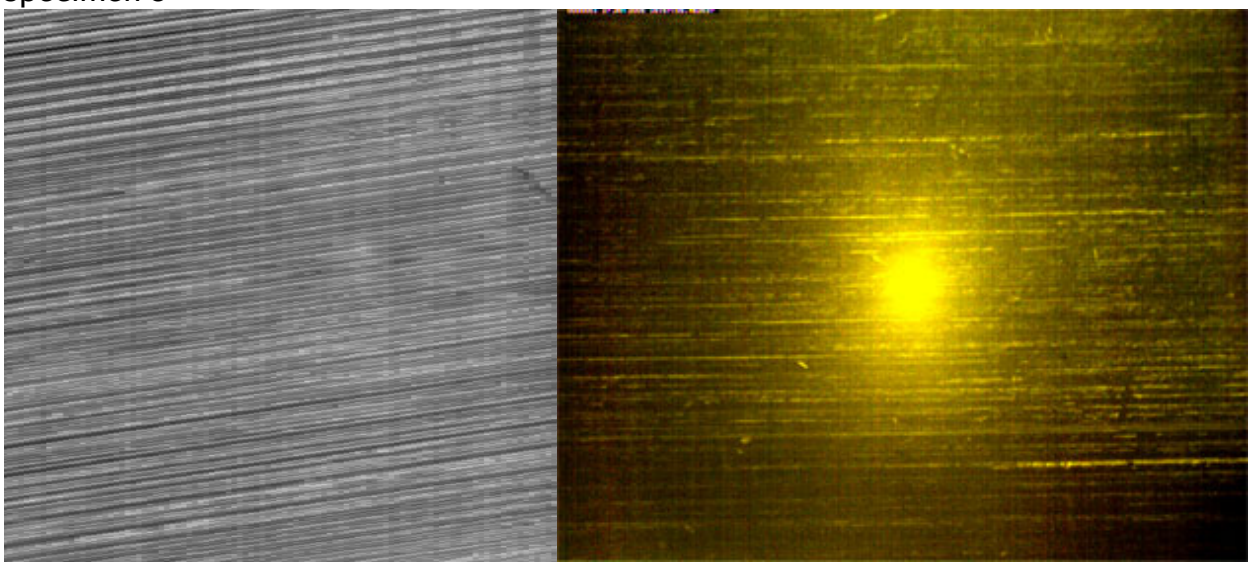

Fig. 5.4.3-8: Comparison between the images obtained with the stylus and the microscope. The images on the left correspond a one real area with 2x2 mm and the right images correspond a one real area with 1.5x1.2 mm.

The specimen 3 have a two sequences of photos, the first sequence is a small indentation executed with a metal pen for the reference of the stylus measure.

The analysis with this method isn't very conclusive because the variation in the images is not significant but contain a small differences if to analyze the variations in small lot of pixels, therefore only do a qualitative analysis.

The total resolution of obtained images is 1280x1024 pixels and with the magnification these images correspond a real area with 1.5x1.2 mm in the specimen (1.17x1.17µm for each pixel).

For a qualitative analysis was crop a lot of pixels in zone approximately with the same intensity of light (200x200 pixels) and convert the images for grayscale. Exporting for Matlab was constructed histograms and images using a diverse color map for a high contrast. The procedure is indicated in fig. 5.4.9.

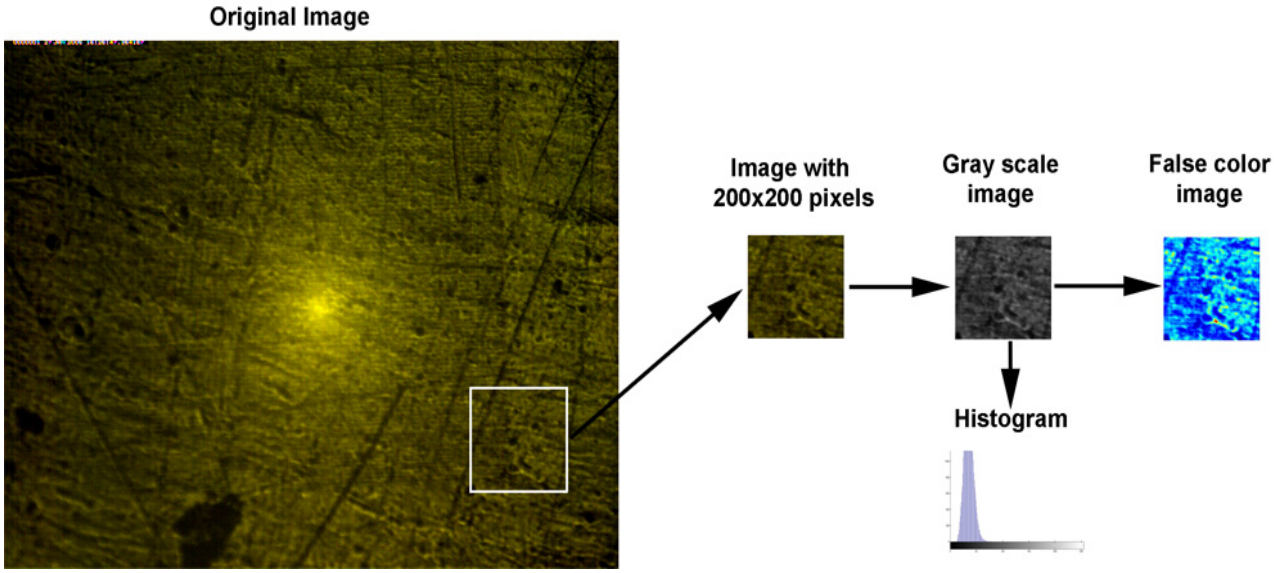

Fig. 5.4.9: Procedure for analysis of obtained images.

The relationship between the colors of the false color image and the gray scale image has represented in the figure 5.4.10.

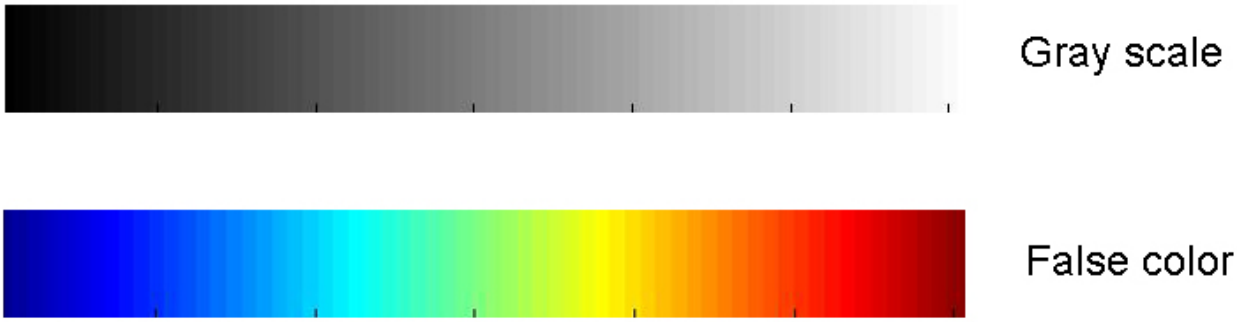

Fig.: 5.4.10: Relationship between the colors of the false color image and the gray scale of the image.

Specimen 1 without filter:

0 N	40 N	80 N
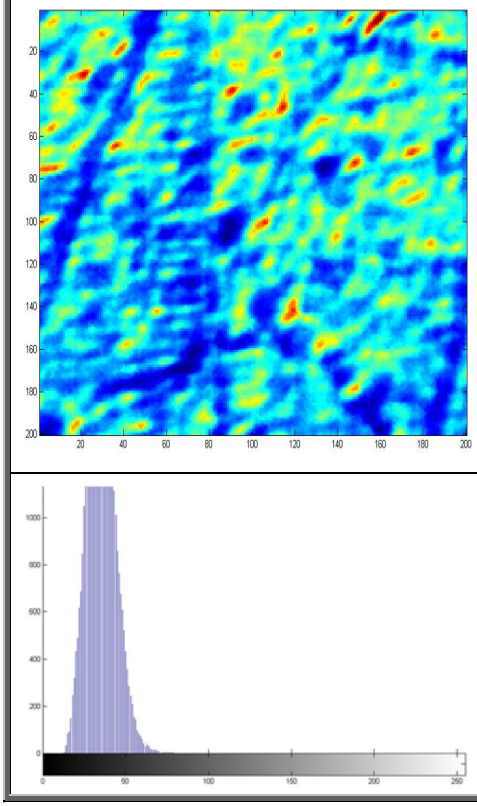	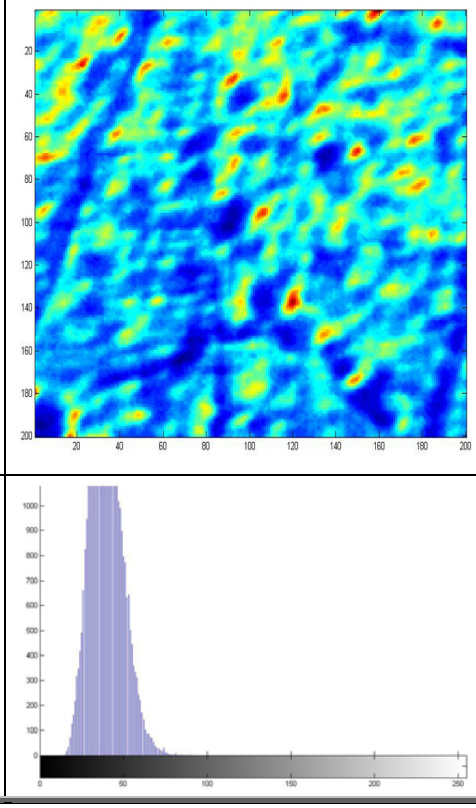	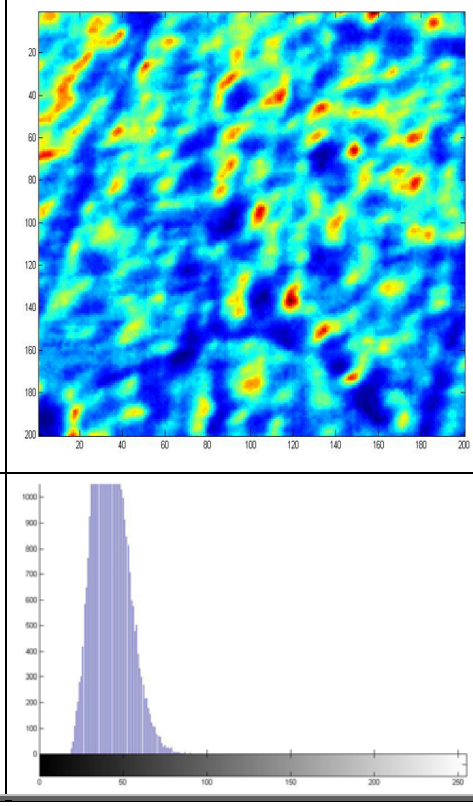

Specimen 1 with yellow filter (λ=577 nm):

0 N	40 N	80 N
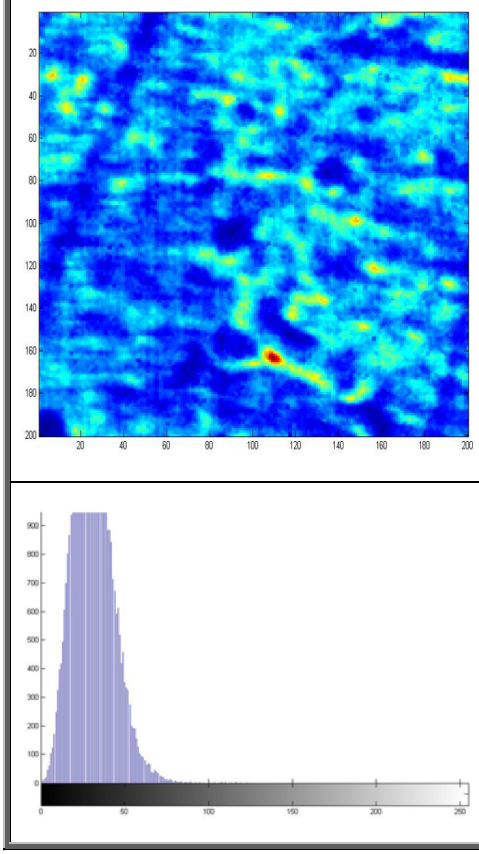	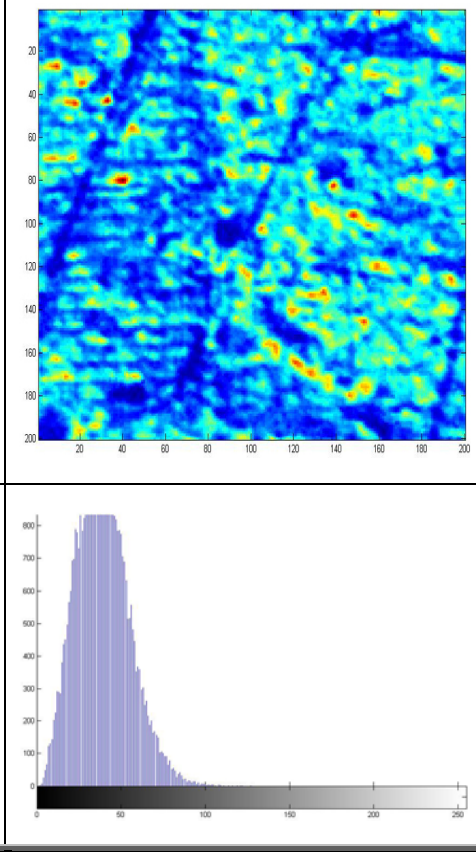	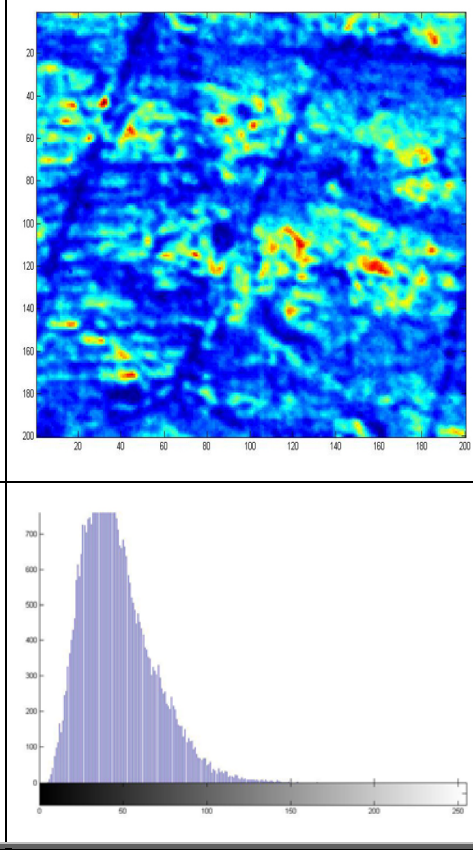

Specimen 2 without filter:

0 N	40 N	80 N
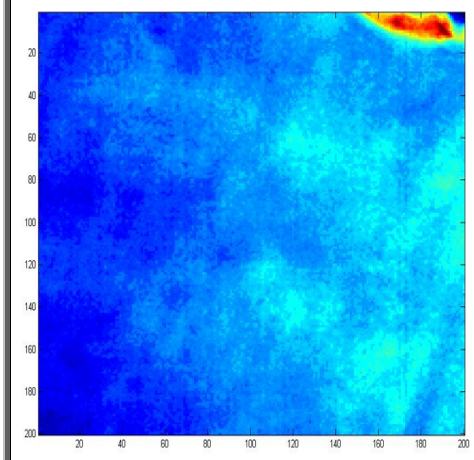	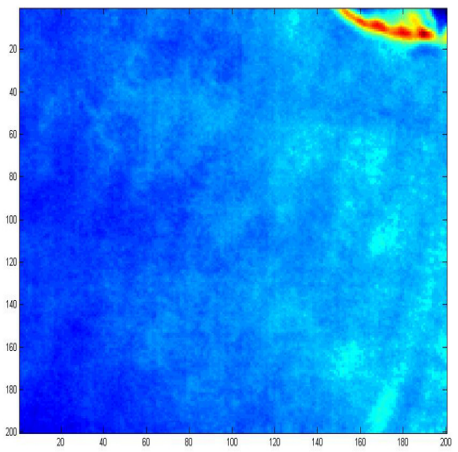	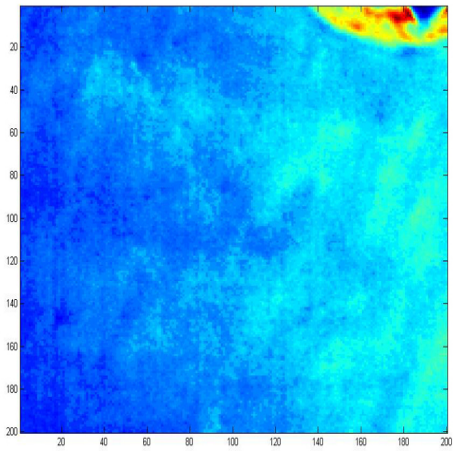
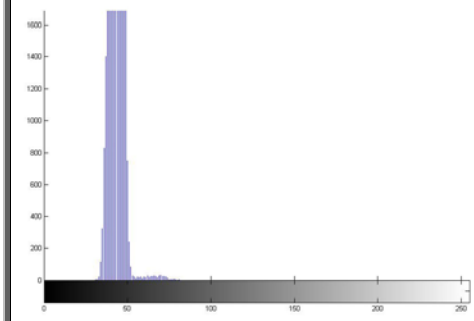	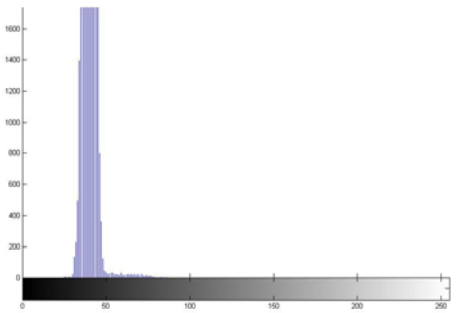	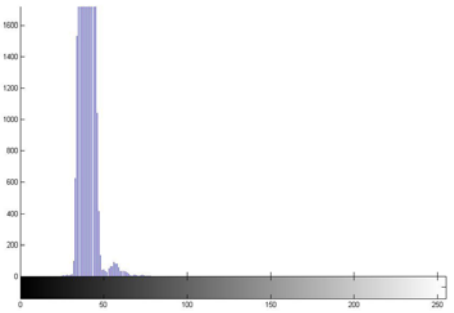

Specimen 2 with yellow filter (λ=577 nm):

0 N	40 N	80 N
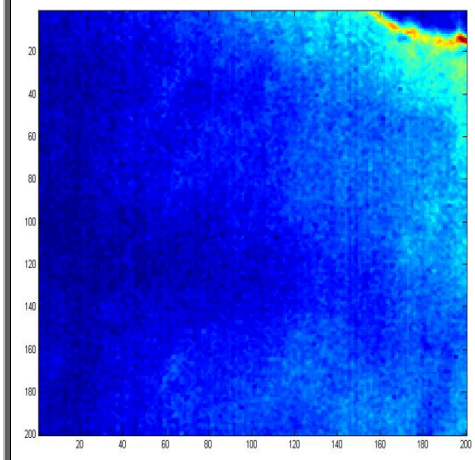	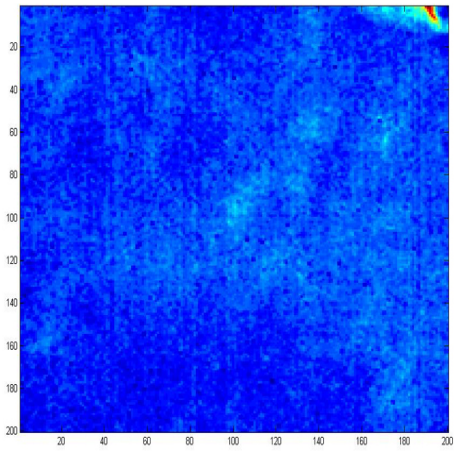	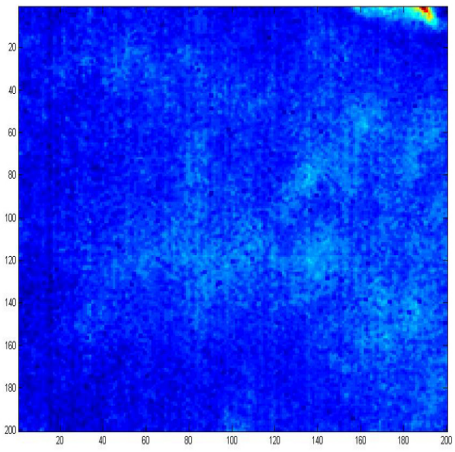
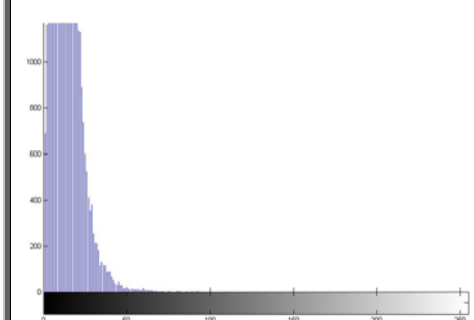	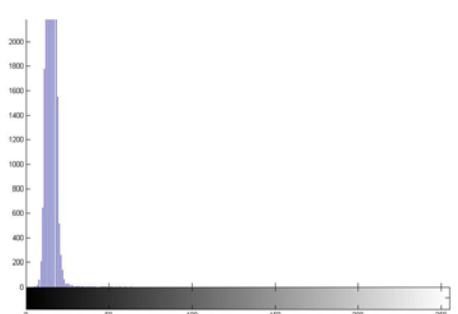	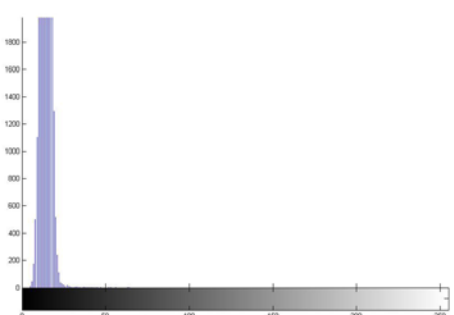

Specimen 3 – zone 1 without filter:

0 N	40 N	80 N
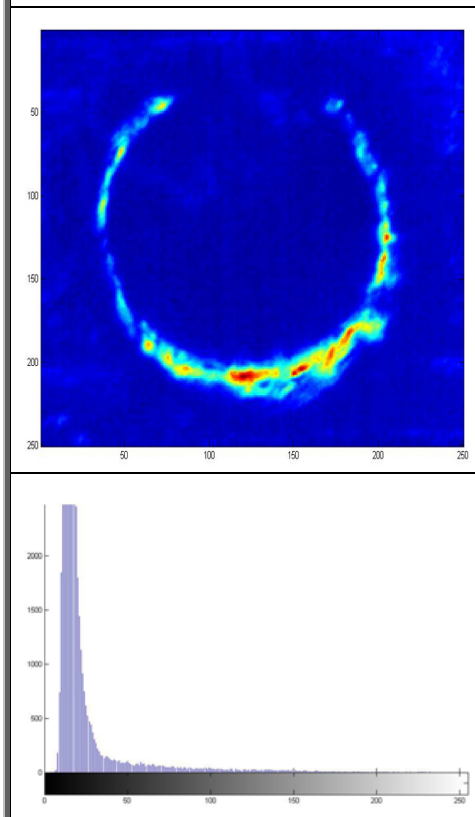	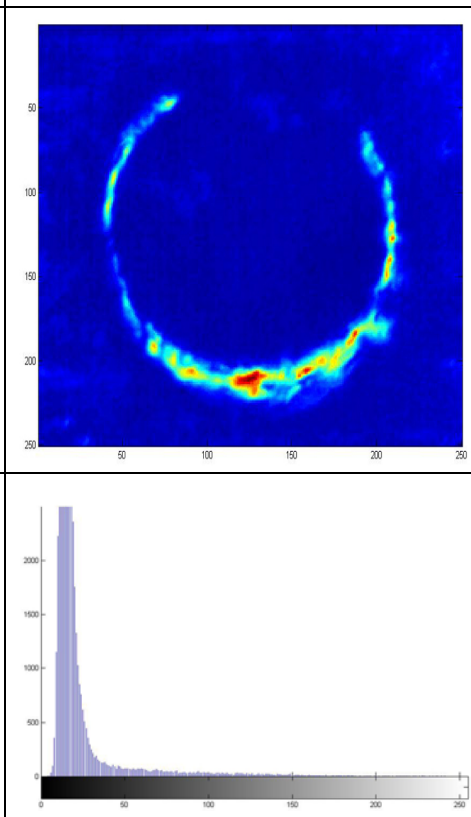	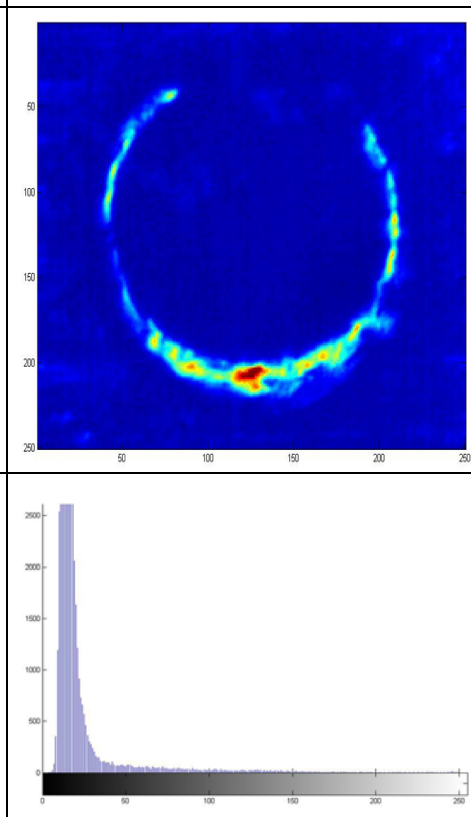

Specimen 3 – zone 1 with yellow filter (λ=577 nm):

0 N	40 N	80 N
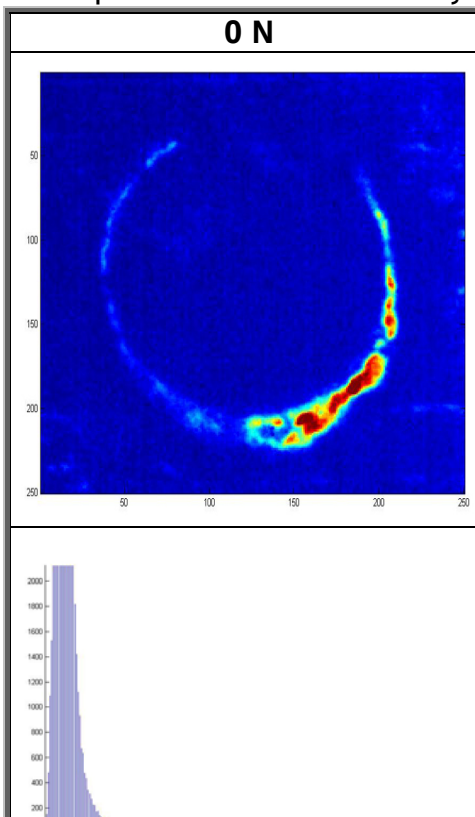	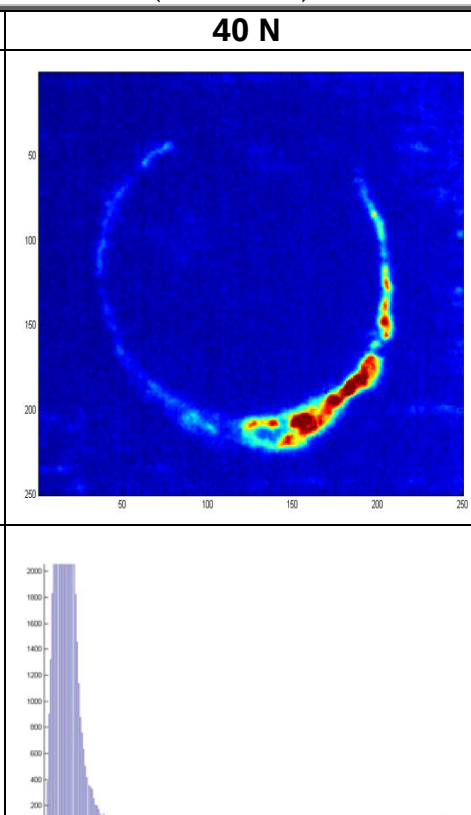	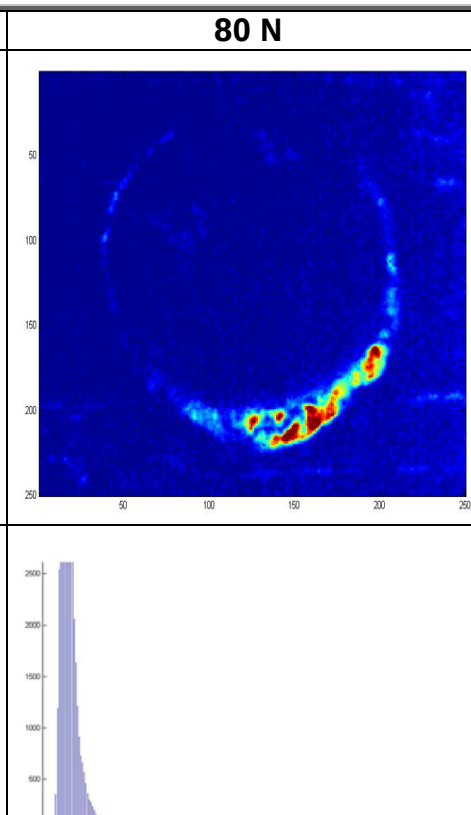

Specimen 3 – zone 2 without filter:

0 N	40 N	80 N
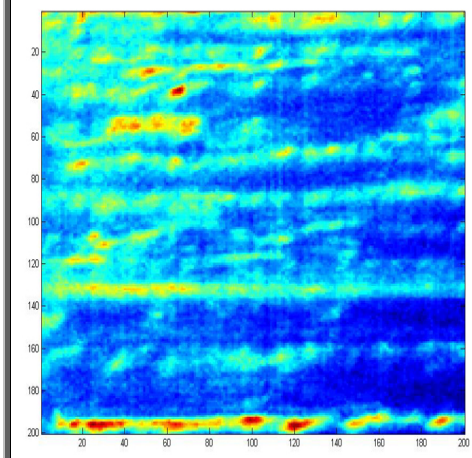	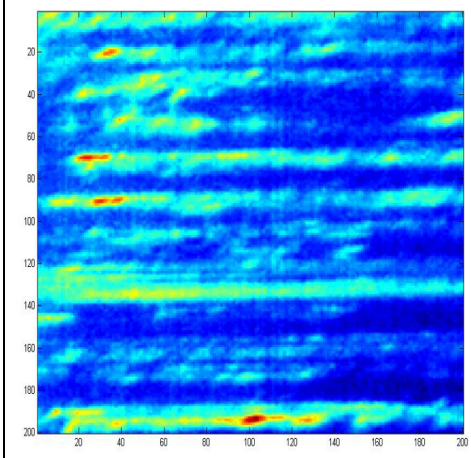	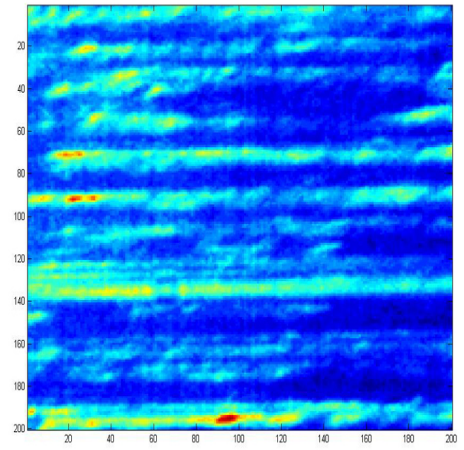
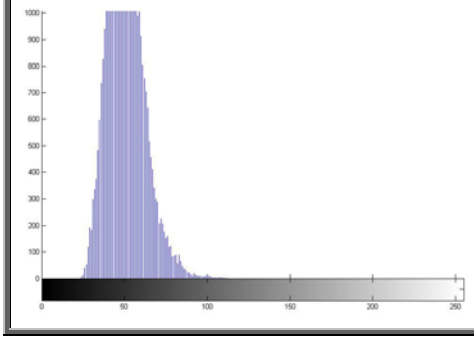	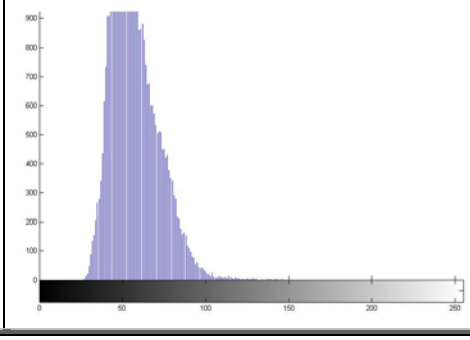	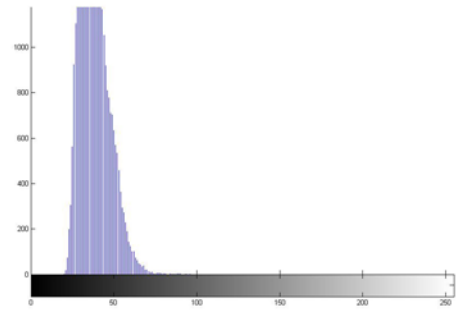

Specimen 3 – zone 2 with yellow filter (λ=577 nm):

0 N	40 N	80 N
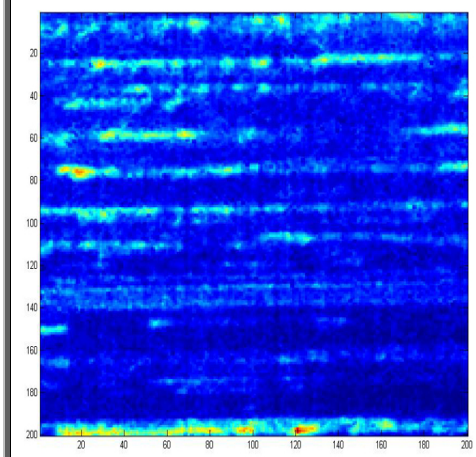	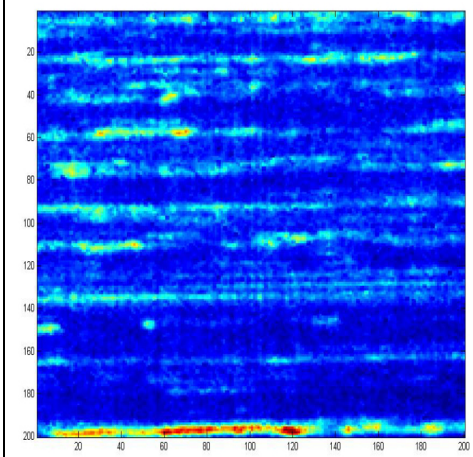	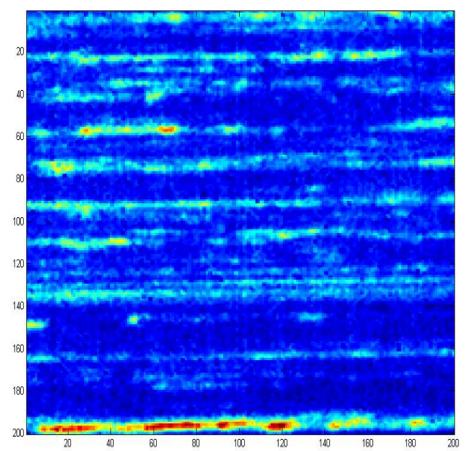
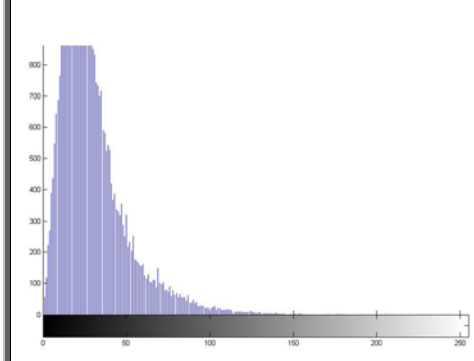	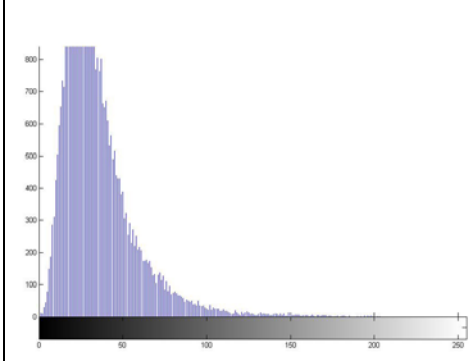	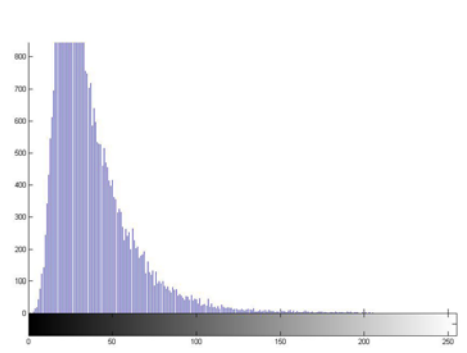

Fig .5.4.11-59: Representation in Matlab® of a part of the microscope images elaborated applying a diverse color map for more contrast (top) and histograms of these images using grayscale(bottom).

From the analysis of these images it can be concluded that the area increase by increasing the load but that from these preliminary experimental investigations is not possible to quantify this increase because there are some error sources using this method:

- The displacements of the glass disc and of the support is significant, this displacement change the image focus and the observable area;
- Humidity or lubricant sediments induce some interference fringes;
- The specimens were not completely flat, for this the apparent area is below the apparent area estimated;
- The microscope magnification isn't very high: for the specimen 2 the roughness isn't detectable in the obtained images;
- The light isn't uniform in the all image; this effect can be reduced using a digital filters but isn't a good solution, other solution is move the light peak to a corner.

Despite these problems, an estimation of the real contact area should be possible using these method by using a more robust apparatus and choosing appropriate specimens.

Conclusions

The main objective of this work has been the study of the roughness changes when mechanical contacts occur between two surfaces.

Some mechanical contact models has been presented in this dissertation. The mechanical contact study between two rough surfaces is not simple because the interactions among asperities. Therefore the contact between two rough surfaces is substituted by a contact between a rough surface (with equivalent roughness) and a smooth plane. In these models the real rough profile needs to be approached by mathematical functions. Some methods are presented, but the main parameter used in mechanical contacts models is the asperity radius of curvature curvatures, with mean squares method and same asperity area method the radius of curvature has high values which influence the results.

A mechanical contact experimental study has been done with an apparatus where a load is applied in the specimen with a glass disc (smooth plane). Three specimens has been tested previously investigated by a stylus device. The changes in the roughness profile have been captured by a computer controlled camera connected to a stereo microscope. From these investigations the results are not completely satisfactory because some error sources, but it is evident that the real contact area increases with the load and that the methodology used is promising.

References

[1] ASME B46.1-1995. "Surface Texture (Surface Roughness, Waviness, and Lay): An American National Standard."; New York: American Society of Mechanical Engineers (1996).

[2] BHUSHAN, Bharat; "Principles and Applications of Tribology"; 1999, Willey – Interscience, USA.

[3] HUGH, Jack; "Engineer On a Disk"; 2001; Grand Valley State University; Michigan; USA (http://claymore.engineer.gvsu.edu/~jackh/eod/manufact/manufact-83.html).

[4] DAVIDSON, Michael W.; Abramowitz, Mortimer; "Differential Interference Contrast"; 2003; Olympus America Inc., and The Florida State University; USA; (http://microscopy.fsu.edu/primer/techniques/dic/dichome.html).

[5] KOMATSU, Hiroshi; Fellers, Thomas J. and Davidson, Michael W.; "Principles and Applications of Two-Beam Interferometry"; National High Magnetic Field Laboratory; The Florida State University; Florida; USA; (http://www.microscopyu.com/articles/interferometry/twobeam.html) .

[6] WYANT, James C.; "White Light Interferometry"; Optical Sciences Center; University of Arizona; Tucson; USA (http://www.optics.arizona.edu/jcwyant).

[7] VERBUNT, J. P. M.; "Simple Optical Interference Method for the Inspection of Solid Surfaces"; Applied Optics; Vol. 12; pp. 1839-1840; August 1973.

[8] MUMMERY, Leigh; "Surface Texture Analysis – The Handbook"; 1992; Hommelwerke GmbH; Germany.

[9] TAYLOR HOBSON Precision; "A guide to Surface Texture Parameters"; Taylor Hobson Limited; 2004; England.

[10] "Development of a basis for 3D Surface Roughness Standards"; 2003; Centre for Ultra Precision Technologies; University of Huddersfield; Queensgate; Huddersfield; UK.
(http://zeus.plmsc.psu.edu/~manias/MatSc597/roughness/definitions.html).

[11] UNI EN ISO 4287-2002; "Specifiche geometriche dei prodotti (GPS) – Stato della superficie: metodo del profilo"; Ente Nazionale Italiano di Unificazione, Milano, Italia.

[12] UNI EN ISO 11562:1996(E); Geometrical Product Specification (GPS)—Surface Texture: Profile Method—Metrological Characteristics of Phase Correct Filters (International Organization for Standardization).

[13] UNI EN ISO 13565-1; "Stato della Superficie: Metodo del profilo; superficie aventi caratteristiche funzionali di pendenti dai livelli (Filtraggio e condizioni generali

di misurazione)"; Maggio 1998; Ente Nazionale Italiano di Unificazione, Milano, Italy.

[14] UNI EN ISO 13565-2:1996(E); "Geometrical Product Specification (GPS)-Surface Texture: Profile Method; Surfaces having stratified functional properties – Part 2: Height characterization using linear material ratio curve."; International Organization for Standardization.

[15] ASME B46.1-1995. "Surface Texture (Surface Roughness, Waviness, and Lay): An American National Standard."; New York: American Society of Mechanical Engineers (1996).

[16] YUAN, Y. B.; Vorburger, T.V.; Song, J. F.; Renegar, T. B.; "A Simplified Realization for the Gaussian Filter in Surface Metrology"; X International Colloquium on Surfaces; Jan. 31 - Feb. 02, 2000; Chemnitz; Germany.

[17] JOHNSON, K. L.; "Contact Mechanics"; 1985; Cambridge University Press; Cambridge; UK.

[18] GREENWOOD, J. A.; Williamson, J. P. B.; "Contact of nominally flat surfaces"; Proc. R. Soc. London, Series A 295, pp. 300-319, 1966; London; UK.

[19] ABRAMOWITZ, Milton; Stegun, Irene A.; "Handbook of mathematical functions : with formulas, graphs, and mathematical tables"; 1972; New York; USA.

[20] CHANG, W. R.; Etsion, I.; Bogy, D. B.; "An Elastic-Plastic Model for the Contact of Rough Surfaces"; Journal of Tribology; Vol. 109, pp. 257-263, April 1987.

[21] ZHAO, Yongwu; Maietta, David M.; Chang, L.; "An Asperity Microcontact Model Incorporating the Transition from Elastic Deformation to Fully Plastic Flow"; Journal of Tribology; Vol. 122, pp. 86-93, January 2000.

[22] POWIERZA, Z. H.; Klimczack, T.; Polijanniuk, A.; "On the Experimental Verification of the Greenwood-Williamson Model for the Contact of Rough Surfaces"; Wear, Vol. 154, pp. 115-124, 1992.

[23] JENG, Yeau-Ren; Wang, Pei-Ying; "An Elliptical Microcontact Model Considering Elastic, Elastoplastic, and Plastic Deformation"; Journal of Tribology; Vol. 125, pp. 232-240, April 2003.

[24] VISSCHER, M; "The Measurement of the Film Thickness and the Roughness Deformation of Lubricated Elastomers"; 1996.

[25] ARAMAKI, Hirotoshi; Cheng, Herbert S.; Chung, Yip-Wah; "The Contact Between Rough Surfaces With Longitudinal Texture – Part I: Average Contact Pressure and Real Contact Area"; Journal of Tribology; Vol. 115, pp. 419-424, July 1993.

[26]ARAMAKI, Hirotoshi; Cheng, Herbert S.; Chung, Yip-Wah; "The Contact Between Rough Surfaces With Longitudinal Texture – Part II: Flash Temperature"; Journal of Tribology; Vol. 115, pp. 425-431, July 1993.

[27]STACHOWIAK, Gwidon W.; Batchelor, Andrew W.; "Engineering Tribology"; 2001; Butterworth Heinemann; ISBN: 0-7506-7304-4.

[28]"Vickers Hardness Converter"; 2005; EFUNDA, Inc.; http://www.efunda.com/units/hardness/convert_hardness.cfm?HD=HV&Cat=Steel#ConvInto .

[29]"Calculator for Conversion between Vickers Hardness Number and SI Units MPa and GPa"; Gordon England; http://www.gordonengland.co.uk/hardness/hvconv.htm .

[30]"Matweb – Material Property data"; http://www.matweb.com/ .

[31]KRAGELSKY, I. V.; ALISIN, V. V.; "Tribology – Lubrification, Friction, and Wear"; Tribology in Practice Series; 2001; Professional Engineering Publishing Limited; London; UK.

[32]HORNG, J. H.; "An elliptic-Plastic Asperity Microcontact Model for Rough Surface" ASME Journal of Tribology; Vol. 120, pp. 82-88; 1998.

[33]TOMANIK, Eduardo; Chacon, Haroldo; Teixeira, Giovanni; "A simple numerical procedure to calculate the input data of Greenwood-Williamson model of asperity contact for actual engineering surfaces"; Tribological Research and Design for Engineering Systems; Elsevier; 2003.

[34]CIULLI, Enrico; Piccigallo, B.; "Elementi di Tribologia"; Notes of the course "Progetto di supporti e dispositivi di lubrificazione"; 2004; Facoltà di Ingegneria della Università di Pisa; Pisa; Italy.

[35]LIU, Geng; Wang, Qian Jane; "A Survey of Current Models for Simulating the Contact between Rough Surfaces"; Tribology Transactions; Vol. 42 – 3; pp. 581-591; 1999.

[36]POLACCO, A.; Pugliese, G.; Ciulli, E.; Bragallini, G. M.; Facchini, M.; "Investigation on Thermal di Stress and Scuffing Failure Under Micro EHL Conditions"; 2004.

[37]BAKOLAS, Vasilios; "Numerical generation of arbitrarily oriented non-Gaussian three-dimensional rough surfaces"; Wear; Vol. 254; pp. 546-554; 2003.

[38]KOGUT, Lior; "A Finite Element Based Elastic-Plastic Model for the Contact of Rough Surfaces"; Tribology Transactions; Vol. 46 – 3; pp. 383-390; 2003.

[39]ABDO, Jamil; Farhang, Kambiz; "Elastic-plastic contact model for rough surfaces based on plastic asperity concept"; International Journal of Non-Linear Mechanics; Vol. 40; pp. 495-506; 2005.

[40]POLONSKY, I. A.; Keer, L. M.; “Fast Methods for Solving Rough Contact Problems: A Comparative Study”; Journal of Tribology; Vol. 122; pp. 36-41; January 2000.

[41]WU, Jiunn-Jong; “The Properties of Asperities of Real Surfaces”; Journal of Tribology; Vol. 123; pp. 872-883; October 2001.

[42]BAI, Mingwu; Kato, Koji; “Analysis of Contact Deformation and Stiction Between Textured Disk and Textured Slider”; Journal of Tribology; Vol. 123; pp. 350-357; April 2001.

[43]ZHAO, Yongwu; Chang, L; “A Model of Asperity Interactions in Elastic-Plastic Contact of Rough Surfaces”; Journal of Tribology; Vol. 123; pp. 857-864; October 2001.

[44]JACQ, C.; Nélias, D.; Lormand, G.; Girodin, D. ; “Development of a Three-Dimensional Semi-Analytical Elastic-Plastic Contact Code”; Journal of Tribology; Vol. 124; pp. 653-667; October 2002.

[45]CHUNG, Jung Ching; Lin, Jen Fin; “Fractal Model Developed for Elliptic Elastic-Plastic Asperity Microcontacts of Rough Surfaces”; Journal of Tribology; Vol. 126; pp. 646-654; October 2004.

Appendix 1 – Abbott-Firestone curve

Model in Matlab (script) for construct the Abbot-Firestone curve, the amplitude distribution function and calculation of the Rk parameters:

```
%Abbott-Firestone Curve and the Probability Distribution Function
%function [abbot,adf]=abbot(data_x,data_z);
x=data_x;
rug=data_z;
resolution=1000;
%===Abbott-Firestone Curve===
maxr=max(rug);
minr=min(rug);
dis=length(rug);
increment=(maxr-minr)/resolution;
abbot=zeros(resolution+1,1);
temp=maxr;
j=1;
while temp>minr
    abbot_y(j)=temp;
    for i=1:dis
        if rug(i)>temp
            abbot(j)=abbot(j)+1;
        end
    end
    j=j+1;
    temp=temp-increment;
end
%normalizing the vector abbot:
for i=1:resolution+1
    abbot(i)=(abbot(i)*100)/max(abbot);
end
subplot(1,2,1)
area(abbot,abbot_y,minr) %plot area
axis([0 100 minr maxr])
xlabel('%')
ylabel('micron m')
title('Abbot-Firestone Curve');
%===Probability Distribution Function===
temp=maxr;
adf=zeros(resolution+1,1);
j=1;
while temp>0
    for i=1:dis
        if rug(i)>temp
            adf(j)=adf(j)+1;
        end
    end
    j=j+1;
    temp=temp-increment;
end;
while temp>minr
    for i=1:dis
        if rug(i)<temp
            adf(j)=adf(j)+1;
        end
    end
    j=j+1;
    temp=temp-increment;
end;
A=sum(adf)*increment; %area of the adf
%normalizing adf
```

```
for i=1:resolution+1
    adf_n(i)=adf(i)/A;
end
subplot(1,2,2)
area(adf_n,abbot_y);
axis([0 max(adf_n)+0.1 minr maxr])
ylabel('micron m')
title('Amplitude Distribution Function (ADF)');

%====Algorithm for calculation of Rk parameters
inte=fix((resolution+1)*0.4);
 for i=1:fix((resolution+1)*0.6)
     m(i)=(abbot_y(i)-abbot_y(i+inte))/(abbot(i)-abbot(i+inte));
 end
 a=find(m==max(m));
c=abbot_y(a(1))-abbot(a(1))*m(a(1)); %y=mx+c
j=1;
for i=1:(resolution+1)
    line(i)=m(a(1))*abbot(i)+c;
end
for i=1:(resolution)
    if or(or(line(i)>abbot_y(i) & line(i+1)<abbot_y(i+1),line(i)<abbot_y(i)
& line(i+1)>abbot_y(i+1)),line(i)==abbot_y(i))
        mr(j)=abbot(i); rk(j)=abbot_y(j);
        j=j+1;
    end
end
Mr1=min(mr)
Mr2=max(mr)
Rk=max(rk)-abs(min(rk))
clear m;
m=find(abbot==Mr1);
A1=0;
for i=1:m(1)
    A1=A1+(abbot(i+1)-abbot(i))*(abbot_y(i)-abbot_y(m(1)));
end
clear m;
m=find(abbot==Mr2);
A2=0;
for i=m(1):resolution
    A2=A2+(abbot(i+1)-abbot(i))*(abs(abbot_y(i))-abs(abbot_y(m(1))));
end
Rpk=2*A1/Mr1
Rvk=2*A2/(100-Mr2)
```

Appendix 2 – Hertz formulas

Table summary with Hertz formulas for elastic contact:

Parameter	Circular Contact (Diameter contact=2a, Load W)	Line Contact (With =2a, Load =W'/unit length along y axis	Elliptical contact (*)
Composite Radius	$\frac{1}{R}=\frac{1}{R_1}\pm\frac{1}{R_2}$	$\frac{1}{R}=\frac{1}{R_1}\pm\frac{1}{R_2}$	$R=\sqrt{R_a R_b}$ $R_a=\frac{1}{(A+B)-(B-A)}$ $R_b=\frac{1}{(A+B)+(B-A)}$
Semi-contact radius	$a=\left(\frac{3WR}{4E^*}\right)^{1/3}$	$a=2\left(\frac{W'R}{\pi E^*}\right)^{1/2}$	$c=\sqrt{ab}=\left(\frac{3WR}{4E^*}\right)^{1/3}F_1$
Normal approach	$\delta=\frac{a^2}{R}$	$\delta=\frac{2W'}{\pi}$ $\left\{\frac{1-\upsilon_1^2}{E_1}\left(\ln\left(\frac{4R_1}{a}\right)-\frac{1}{2}\right)+\right.$ $\left.+\frac{1-\upsilon_2^2}{E_2}\left(\ln\left(\frac{4R_2}{a}\right)-\frac{1}{2}\right)\right\}$	$\delta=\frac{c^2}{R}\frac{F_2}{F_1^2}$
Contact Pressure	$p=p_0\left[1-\left(\frac{r}{a}\right)^2\right]^{1/2}$ $p_0=\frac{3}{2}p_m=\frac{3W}{2\pi a^2}=$ $=\left(\frac{6WE^{*2}}{\pi^3R^2}\right)^{1/3}$	$p=p_0\left[1-\left(\frac{x}{a}\right)^2\right]^{1/2}$ $p_0=\frac{4}{\pi}p_m=$ $=\frac{4W'}{\pi a}=\left(\frac{W'E^*}{\pi R}\right)^{1/2}$	$p_m=\frac{3W}{2\pi c^2}$
Maximum Shear Stresses	$0.31p_0\ at\ z=0.48a$	$0.3p_0\ at\ z=0.78a$	$p\left[0.303+0.0855\frac{b}{a}-0.808\left(\frac{b}{a}\right)^2\right]$ at $z\cong b\left[0.7929-0.3207\frac{b}{a}\right]$

(*)For elliptical contact the parameters:

$$A+B=\frac{1}{2}\left(\frac{1}{R_{1xx}}+\frac{1}{R_{1yy}}+\frac{1}{R_{2xx}}+\frac{1}{R_{2yy}}\right)$$

$$B-A=\frac{1}{2}\left[\left(\frac{1}{R_{1xx}}-\frac{1}{R_{1yy}}\right)^2+\left(\frac{1}{R_{2xx}}-\frac{1}{R_{2yy}}\right)^2+2\left(\frac{1}{R_{1xx}}-\frac{1}{R_{1yy}}\right)\left(\frac{1}{R_{2xx}}-\frac{1}{R_{2yy}}\right)\cos(2\alpha)\right]^{\frac{1}{2}}$$

$$F_1 \cong 1-\left[\left(\frac{R_a}{R_b}\right)^{0.0602}-1\right]^{1.456},\ F_2 \cong 1-\left[\left(\frac{R_a}{R_b}\right)^{0.0684}-1\right]^{1.531}.$$

Appendix 3 – FEM model of mechanical contact between an asperity and a smooth plane, in ANSYS®

```
FINISH
/CLEAR
/PREP7
/TITLE, ANALYSIS OF THE CONTACT BETWEEN AN ASPERITY AND A SMOOTH
PLANE IN ELASTIC-PLASTIC FIELD
C***INTRODUCTION OF THE GEOMETRIC PROPERTIES
R=3 !*ASK,R,THE RADIUS OF ASPERITY,3
L=15 !*ASK,L,THE BASE LENGTH OF THE ASPERITY,10
NX=5 !*ASK,NX,NUMBER OF ELEMENTS IN THE X DIRECTION,5
NY=20 !*ASK,NY,NUMBER OF ELEMENTS IN THE Y DIRECTION,20
PMAX=100 ![MPa]
SPX=2
SPY=4
MYOUNGP1=210E+3 ![MPa]
MYOUNGP2=80E+3 ![MPa]
PO1=0.29
PO2=0.2
YS=360          ! Tensile Strength, Yield [MPa]
MPLAST=5000     ! Tangent modulus Et [N/mm^2]
NSTP=10   !Number of time steps
C***ELEMENT DEFINITION OF THE PARABOLA
ET,1,42,,,1
MP,EX,1,MYOUNGP1
MP,PRXY,1,PO1

C***DEFINITION OF THE PARABOLA
*DO,I,1,NY+1
  N,I,((L/2)/NY)*(I-1),(-(1/8)*(L**2)*((I-
1)**2))/(R*(NY**2))+((1/4)*(L**2)*(I-1))/(R*NY)
*ENDDO
*DO,J,1,NX-1
     M=-(L*NX)/(4*R*(-NX+J))
     B=((L**2)*J)/(8*R*(-NX+J))
     A=SQRT((-(L/2))**2+(-(L**2/(8*R)))**2)
     X=(L/2)-(A/SQRT(1+M**2))
     A0=ABS(SQRT(1+(M**2))*(X-(L/2)))
     A1=SQRT(((L*J)/(2*Nx)-(L/2))**2+(-(L**2)/(8*R))**2)
     F=A1/A0
     *DO,I0,1,NY+1
          M=-(L*NX)/(4*R*(-NX+J))
          B=((L**2)*J)/(8*R*(-NX+J))
          X0=((L/2)/NY)*(I0-1)
          Y0=(-(1/8)*(L**2)*((I0-
1)**2))/(R*(NY**2))+((1/4)*(L**2)*(I0-1))/(R*NY)
          A=SQRT((X0-(L/2))**2+(Y0-(L**2/(8*R)))**2)
          X=((L/2)-(F*A/SQRT(1+M**2)))
          Y=(M*X+B)
          N,(NY+1)*J+I0,X,Y
     *ENDDO
```

```
*ENDDO
J=NX-1
M=-(L*NX)/(4*R*(-NX+J))
B=((L**2)*J)/(8*R*(-NX+J))
A=SQRT((-(L/2))**2+(-(L**2/(8*R)))**2)
X=(L/2)-(A/SQRT(1+M**2))
A0=ABS(SQRT(1+(M**2))*(X-(L/2)))
A1=SQRT(((L*J)/(2*Nx)-(L/2))**2+(-(L**2)/(8*R))**2)
F=A1/A0
*DO,I0,1,NY+1
     M=-(L*NX)/(4*R*(-NX+J))
     B=((L**2)*J)/(8*R*(-NX+J))
     X0=((L/2)/NY)*(I0-1)
     Y0=(-(1/8)*(L**2)*((I0-1)**2))/(R*(NY**2))+((1/4)*(L**2)*(I0-
1))/(R*NY)
     A=SQRT((X0-(L/2))**2+(Y0-(L**2/(8*R)))**2)
     X=((L/2)-(F*A/SQRT(1+M**2)))
     Y=(M*X+B)
     N,(NY+1)*(J+1)+I0,L/2,Y
*ENDDO
E,1,NY+2,NY+3,2
EGEN,NY-1,1,1
E,NY,2*NY+1,NY+1,NY+1
EGEN,NX,NY+1,1,NY
C***ELIMINATION OF KNOTS DUPLICATED IN THE CENTER OF THE SPHERE
NSEL,,LOC,Y,(L**2/(8*R))-0.00001,(L**2/(8*R))+0.00001
NUMMRG,NODE,0.0001
C****DEFINITION oF THE PLANE
*DO,K1,1,3
     *DO,K,1,NY+1
          N,(NX+1)*(NY+1)+K+(K1-1)*(NY+1),((L/2)/NY)*(K-
1),L**2/(8*R)*(1+((K1-1)/16))
     *ENDDO
*ENDDO
C***DEFINITION OF THE ELEMENT TO USE IN THE PLANE AND THEIR
PROPERTIES
ET,2,42,,,1
MP,EX,2,MYOUNGP2
MP,PRXY,2,PO2
MAT,2
C***ELEMENTS OF THE PLANE (GLASS)
E,(NX+1)*(NY+1)+1,(NX+1)*(NY+1)+2,(NX+1)*(NY+1)+2+NY+1,(NX+1)*(NY+
1)+1+NY+1
EGEN,NY,1,(NX*NY)+1
EGEN,2,NY+1,(NX*NY)+1,(NX*NY)+NY
C***INTRODUCTION OF GAP ELEMENTS
ET,3,12,0,0,0,1
R,2,0,1E+10,
TYPE,3
REAL,2
E,2,(NX+1)*(NY+1)+2
EGEN,NY-1,1,NX*NY+2*NY+1
```

```
EPLOT
FINISH
C*** The Solution Processor
/SOLU
C***
C***DOF Constraints
NSEL,,LOC,Y,-0.001,+0.001
D,ALL,UY,0     !DOF constraints at nodes in the base
NSEL,ALL
NSEL,,LOC,X,(L/2)-0.001,(L/2)+0.001
DSYM,SYMM,X   !Symmetry
NSEL,ALL
C***LOADS
NLGEOM,ON !Large-deflection effects are to be included in the
model
TB,BISO,1       !Bilinear isotropic hardening using von Mises
plasticity
TBDATA,1,YS,MPLAST       !Yield stress and Tangent modulus
C***
C*** Options for no-linear analysis
C***
NROPT,FULL          ! Use full Newton-Raphson
NSTP=1
*DO,T,1,NSTP
     TIME,T
     NSEL,,LOC,Y,(L**2/(8*R))*(1+(2/16))-
0.001,(L**2/(8*R))*(1+(2/16))+0.001
     SF,ALL,PRESS,(-PMAX*T)/NSTP     !Load for time step I
     NSEL,ALL
     NSUBST,30               !Number substeps
     AUTOTS,ON               !Use automatic time stepping
     KBC,0                   !Specifies stepped or ramped loading
within a load step
     OUTRES,ALL,ALL      !All solution items except SVAR and LOCI
records for every substep
     NEQIT,50                !Specifies the maximum number of
equilibrium iterations
     LSWRITE,T
     CNVTOL,U,,0.001     ! Sets convergence: displacement-U
     NCNV,0
*ENDDO
LSSOLVE,1,NSTP        ! solve the NSTP load steps.
FINISH
```

Appendix 4 – Matlab® model for approach roughness profiles using the Aramaki formulation

Model to approach the roughness real profile by polynomial functions using the Aramaki formulation [25]:

```
%model for approach the roughness profile by mathematical functions
%function [rug_a]=approach(data_x,data_z)
%the real profile will go approach by one profile with parabolas using the
%========================
%===Aramki formulation===
%========================
%Input data: vector data_z with the roughness points and vector
%data_x with the respective coordinates
%Output data: vector rug_a with the approached roughness and the respective
%vector X with the coordinates
x=data_x;
x=data_x;
rug=data_z;
%determination of ACF length and the coefficient of ACF, ACF length is the
%length where autocorrelation function is 0.368 (=1/e)
[ACF,Lags,Bounds] = autocorr(rug,length(x)-1);
index_ACF_0368=1;
while ACF(index_ACF_0368)>0.368
    index_ACF_0368=index_ACF_0368+1;
end
%plot(x,ACF); %plot whith the fuction of autorrelation
length_ACF=x(index_ACF_0368)-x(1);
alfa=1/length_ACF;
%standard deviation:
sigma=std(rug);
%definition of a vector L_peak (peaks), obtained considering the cross with
the reference line:
n=length(x);
k=1;
for i=1:n-1
    if ((rug(i)<=0)&(rug(i+1)>0));
       j=i+1;
       while ((rug(j)>=0)&(j+1<n))
           if  rug(j+1)<0
               Lpeak(k,1)=x(i)-rug(i)*(x(i+1)-x(i))/(rug(i+1)-rug(i));
               Lpeak(k,2)=x(j)-rug(j)*(x(j+1)-x(j))/(rug(j+1)-rug(j));
               L_peak(k)=Lpeak(k,2)-Lpeak(k,1);
               k=k+1;
           end
           j=j+1;
       end
   end
end
%definition of a vector L_valley (valleys), obtained considering the cross
with the reference line:
k=1;
for i=1:n-1
   if ((rug(i)>=0)&(rug(i+1)<0));
       j=i+1;
       while ((rug(j)<=0)&(j+1<n))
           if  rug(j+1)>0
               Lvalley(k,1)=x(i)-rug(i)*(x(i+1)-x(i))/(rug(i+1)-rug(i));
               Lvalley(k,2)=x(j)-rug(j)*(x(j+1)-x(j))/(rug(j+1)-rug(j));
               L_valley(k)=Lvalley(k,2)-Lvalley(k,1);
               k=k+1;
           end
```

```
            j=j+1;
        end
    end
end
%create one vector whith the x positions of the all crossings whith the
%reference line
for i=1:(length(L_peak))
    Lp(i)=Lpeak(i,1);
    Lp(i+length(L_peak))=Lpeak(i,2);
end
for i=1:(length(L_valley))
    Lv(i)=Lvalley(i,1);
    Lv(i+length(L_valley))=Lvalley(i,2);
end
%vector X that contain all x positions (positions of rough points and the
%crossings)
X=[];
X=[x';Lp';Lv'];
X=unique(X);
X=sort(X);

%create one new vector RUG with the same length that X
RUG=[];
for i=1:length(X)
    for j=1:length(x)
        if X(i)==x(j)
            RUG(i)=rug(j); %the others positions RUG=0
        end
    end
end
%generation of the one profile approach by parabolas
csi_peak=L_peak*sqrt(2/pi)*alfa*sigma; %equation 8 Aramki part I
csi_valley=L_valley*sqrt(2/pi)*alfa*sigma;
mean_L_peak=(mean(L_peak));
mean_L_valley=(mean(L_valley));
mean_L=1/2*(mean(L_peak)+mean(L_valley));
K1_peak=8*(csi_peak)./(L_peak.^2); %equation 9-b Aramki part I
K1_valley=8*(csi_valley)./(L_valley.^2);
%generation of the vector with points that represent parabolas
%start the vectors with zeros and the same length that X
parabola=zeros(1,length(X));
parabola_peak=zeros(1,length(X));
parabola_valley=zeros(1,length(X));
for i=1:length(L_peak)
    j=find(X==(Lpeak(i,1)));
        while (X(j)>=Lpeak(i,1)&X(j)<=Lpeak(i,2))
        parabola(j)=-(4*csi_peak(i)/(L_peak(i)^2))*(X(j)-Lpeak(i,1)-
L_peak(i)/2)^2+csi_peak(i);
        parabola_peak(j)=parabola(j);
        j=j+1;
        end
end
for i=1:length(L_valley)
    j=find(X==(Lvalley(i,1)));
        while (X(j)>=Lvalley(i,1)&X(j)<=Lvalley(i,2))
        parabola(j)=(4*csi_valley(i)/(L_valley(i)^2))*(X(j)-Lvalley(i,1)-
L_valley(i)/2)^2-csi_valley(i);
        parabola_valley(j)=parabola(j);
        j=j+1;
        end
end
rug_a=parabola;
plot(X,RUG,X,parabola)
```

Appendix 5 – Matlab® model for approach roughness profiles using the least mean squares

Model to approach the roughness real profile by polynomial functions using the method of the least mean squares with reference lines at a distance c1 of the mean line for the peaks and c2 for the valleys:

```
%Approach the roughness profile by functions
%using the method of least mean squares
%and using reference lines at c1 for peaks and c2 for valleys
%function [mean_sq]=mean_sq(data_x,data_z)
%Input data: vector data_z with the roughness points and vector
%data_x with the respective coordinates
%Output data: vector rug_a with the approached roughness and the respective
%vector X with the coordinates
x=data_x;
per=30;%percent
x=data_x;
rug=data_z;
%calculate of the ADF function
resolution=500; %number of function points
maxr=max(rug);
minr=min(rug);
temp=maxr;
dis=length(rug);
increment=(maxr-minr)/resolution;
adf=zeros(resolution+1,1);
j=1;
while temp>0
    for i=1:dis
        if rug(i)>temp
            adf(j)=adf(j)+1;
        end
    end
    j=j+1;
    temp=temp-increment;
end;
while temp>minr
    for i=1:dis
        if rug(i)<temp
            adf(j)=adf(j)+1;
        end
    end
    j=j+1;
    temp=temp-increment;
end;
A=sum(adf)*increment; %area of the adf
%normalizing adf
for i=1:resolution+1
    adf_n(i)=adf(i)/A;
end
%calculate the height c1
Ate=per/100;
c1=maxr; ctemp=0;i=1;
while ctemp<Ate
    ctemp=ctemp+adf_n(i)*increment;
    c1=c1-increment;
    i=i+1;
end
%calculate the height c1
```

```
c2=minr; ctemp=0;i=length(adf_n);
while ctemp<Ate
    ctemp=ctemp+adf_n(i)*increment;
    c2=c2+increment;
    i=i-1;
end
%definition of a vector L_peak (peaks), obtained considering the cross
%with the line (z=c1):
n=length(x);
k=1;
for i=1:n-1
    if ((rug(i)<=c1)&(rug(i+1)>c1));
       j=i+1;
       while ((rug(j)>=c1)&(j+1<n))
           if  rug(j+1)<c1
               Lpeak(k,1)=x(i)+(c1-rug(i))*((x(i+1)-x(i))/(rug(i+1)-
rug(i)));
               Lpeak(k,2)=x(j)+(c1-rug(j))*((x(j+1)-x(j))/(rug(j+1)-
rug(j)));
               L_peak(k)=Lpeak(k,2)-Lpeak(k,1);
               k=k+1;
           end
           j=j+1;
       end
   end
end
%definition of a vector L_valley (valleys), obtained considering the cross
%with the line (z=c2):
k=1;
for i=1:n-1
   if ((rug(i)>=c2)&(rug(i+1)<c2));
       j=i+1;
       while ((rug(j)<=c2)&(j+1<n))
           if  rug(j+1)>c2
               Lvalley(k,1)=x(i)+(c2-rug(i))*(x(i+1)-x(i))/(rug(i+1)-
rug(i));
               Lvalley(k,2)=x(j)+(c2-rug(j))*(x(j+1)-x(j))/(rug(j+1)-
rug(j));
               L_valley(k)=Lvalley(k,2)-Lvalley(k,1);
               k=k+1;
           end
           j=j+1;
       end
   end
end
%create one vector with the x positions of the all crossings whith the
%references lines
for i=1:(length(L_peak))
    Lp(i)=Lpeak(i,1);
    Lp(i+length(L_peak))=Lpeak(i,2);
end
for i=1:(length(L_valley))
    Lv(i)=Lvalley(i,1);
    Lv(i+length(L_valley))=Lvalley(i,2);
end
%vector X that contain all x positions (positions of rough points and the
%crossings)
X=[];
X=[x';Lp';Lv'];
X=unique(X);
X=sort(X);
%create one new vector RUG with the same length that X
RUG=[];
```

```
for i=1:length(X)
    for j=1:length(x)
        if X(i)==x(j)
            RUG(i)=rug(j);
        end
    end
end
for i=1:length(Lpeak)
    temp=find(X==Lpeak(i,1));
    RUG(temp)=c1;
end
for i=1:length(Lvalley)
    temp=find(X==Lvalley(i,1));
    RUG(temp)=c2;
end
%determination of an vector with the values of the coefficient 'a' for
%the parabola (z=ax^2+b^2+c), b=f(a) and c=f(a)
%peaks:
a=zeros(length(L_peak),1);
for i=1:length(L_peak)
    x0=Lpeak(i,1);
    x1=Lpeak(i,2);
    k=0;an=0; ad=0;an1=0;
    for j=(find(X==x0)+1):(find(X==x1)-1)
       an=an+(X(j)^2-(x0+x1)*X(j)+x0*x1)*RUG(j);
       an1=an1+(X(j)^2-(x0+x1)*X(j)+x0*x1)*c1;
       ad=ad+((X(j))^2-(x0+x1)*X(j)+x0*x1)^2;
   end
   a(i)=(an-an1)/ad;
end
%function parabola for approach the peaks
parabola_fit=zeros(1,length(X));
parabola_peak_fit=zeros(1,length(X));
for i=1:length(L_peak)
    j=find(X==(Lpeak(i,1)));
        while X(j)<=Lpeak(i,2)
        parabola_fit(j)=a(i)*(X(j))^2-
(Lpeak(i,1)+Lpeak(i,2))*a(i)*X(j)+c1+a(i)*(Lpeak(i,1)*Lpeak(i,2));
        parabola_peak_fit(j)=parabola_fit(j);
        j=j+1;
        end
end
%valleys:
parabola_valley_fit=zeros(1,length(X));
av=zeros(length(L_valley),1);
for i=1:length(L_valley)
    x0=Lvalley(i,1);
    x1=Lvalley(i,2);
    k=0;an=0; ad=0;an1=0;
    for j=(find(X==x0)+1):(find(X==x1)-1)
       an=an+(X(j)^2-(x0+x1)*X(j)+x0*x1)*RUG(j);
       an1=an1+(X(j)^2-(x0+x1)*X(j)+x0*x1)*c2;
       ad=ad+((X(j))^2-(x0+x1)*X(j)+x0*x1)^2;
   end
   av(i)=(an-an1)/ad; %coefficient 'a' for the valleys parabolas fitting
end
for i=1:length(L_valley)
    j=find(X==(Lvalley(i,1)));
        while X(j)<=Lvalley(i,2)
        parabola_fit(j)=av(i)*(X(j))^2-
(Lvalley(i,1)+Lvalley(i,2))*av(i)*X(j)+c2+av(i)*(Lvalley(i,1)*Lvalley(i,2));
        parabola_valley_fit(j)=parabola_fit(j);
        j=j+1;
```

```
        end
end
for i=1:length(parabola_fit)
    if parabola_fit(i)==0
        parabola_fit(i)=RUG(i);
    end
end
mean_sq=parabola_fit;
```

Appendix 6 – Matlab® model for approach roughness profiles using the same asperity area

Function in Matlab to approach the real rough profile by quadratic functions with the same asperity area:

```
%model for approach the roughness profile by mathematical functions
%function [rug_a]=approach(data_x,data_z)
%the real profile will go approach by one profile with parabolas using the
%================================
%=======Same Asperity Area========
%================================
%Input data: vector data_z with the roughness points and vector
%data_x with the respective coordinates
%Output data: vector rug_a with the approached roughness and the respective
%vector X with the coordinates
x=data_x;
rug=data_z;
%definition of a vector L_peak (peaks), obtained considering the cross with
the reference line:
n=length(x);
k=1;
for i=1:n-1
    if ((rug(i)<=0)&(rug(i+1)>0));
       j=i+1;
       while ((rug(j)>=0)&(j+1<n))
           if  rug(j+1)<0
               Lpeak(k,1)=x(i)-rug(i)*(x(i+1)-x(i))/(rug(i+1)-rug(i));
               Lpeak(k,2)=x(j)-rug(j)*(x(j+1)-x(j))/(rug(j+1)-rug(j));
               L_peak(k)=Lpeak(k,2)-Lpeak(k,1);
               k=k+1;
           end
           j=j+1;
       end
   end
end
%definition of a vector L_valley (valleys), obtained considering the cross
with the reference line:
k=1;
for i=1:n-1
   if ((rug(i)>=0)&(rug(i+1)<0));
       j=i+1;
       while ((rug(j)<=0)&(j+1<n))
           if  rug(j+1)>0
               Lvalley(k,1)=x(i)-rug(i)*(x(i+1)-x(i))/(rug(i+1)-rug(i));
               Lvalley(k,2)=x(j)-rug(j)*(x(j+1)-x(j))/(rug(j+1)-rug(j));
               L_valley(k)=Lvalley(k,2)-Lvalley(k,1);
               k=k+1;
           end
           j=j+1;
       end
   end
end
%create one vector with the x positions of the all crossings whith the
%reference line
for i=1:(length(L_peak))
    Lp(i)=Lpeak(i,1);
    Lp(i+length(L_peak))=Lpeak(i,2);
end
```

```
for i=1:(length(L_valley))
    Lv(i)=Lvalley(i,1);
    Lv(i+length(L_valley))=Lvalley(i,2);
end
%vector X that contain all x positions (positions of rough points and the
%crossings)
X=[];
X=[x';Lp';Lv'];
X=unique(X);
X=sort(X);
%create one new vector RUG with the same length that X
RUG=[];
for i=1:length(X)
    for j=1:length(x)
        if X(i)==x(j)
            RUG(i)=rug(j); %the others positions RUG=0
        end
    end
end
%vector with the area of the peaks and valleys
na=length(L_peak)+length(L_valley);
A=zeros(na,1);
rug_0=find(RUG==0);
for i=1:(length(rug_0)-1)
    for j=rug_0(i):(rug_0(i+1)-1)
        A(i)=A(i)+((RUG(j)+RUG(j+1))/2)*(X(j+1)-X(j));
    end
end
j=1; k=1;
for i=1:length(A)
    if A(i)>0
        A_peak(j)=A(i);
        j=j+1;
    else
        A_valley(k)=A(i);
        k=k+1;
    end
end
%generation of the vector with points that represent parabolas
parabola=zeros(1,length(X));
parabola_peak=zeros(1,length(X));
parabola_valley=zeros(1,length(X));
%peaks:
for i=1:length(L_peak)
    j=find(X==(Lpeak(i,1)));
        while (X(j)>=Lpeak(i,1)&X(j)<=Lpeak(i,2))
        parabola(j)=(-6*A_peak(i)/L_peak(i)^3)*(X(j)-
Lpeak(i,1))^2+(6*A_peak(i)/L_peak(i)^2)*(X(j)-Lpeak(i,1));
        parabola_peak(j)=parabola(j);
        j=j+1;
        end
        csi_peak(i)=(-
6*A_peak(i)/L_peak(i)^3)*(L_peak(i)/2)^2+(6*A_peak(i)/L_peak(i)^2)*(L_peak(i
)/2);
end
%valleys:
for i=1:length(L_valley)
    j=find(X==(Lvalley(i,1)));
        while (X(j)>=Lvalley(i,1)&X(j)<=Lvalley(i,2))
        parabola(j)=(-6*A_valley(i)/L_valley(i)^3)*(X(j)-
Lvalley(i,1))^2+(6*A_valley(i)/L_valley(i)^2)*(X(j)-Lvalley(i,1));
        parabola_valley(j)=parabola(j);
        j=j+1;
```

```
        end
end
%Curvature of the asperities (k(x)=2*a) and the cordinate point of the
maximum
for i=1:length(L_peak)
    K1_peak(i)=abs(-6*A_peak(i)/L_peak(i)^3);
end
rug_a=parabola;
plot(X,RUG,X,parabola);
```

Appendix 7 – Results of stylus device measures

Results of the stylus measures using the software Hommel Map Basic:

Specimen 1 - Prove 1

Without Cut-off Filter

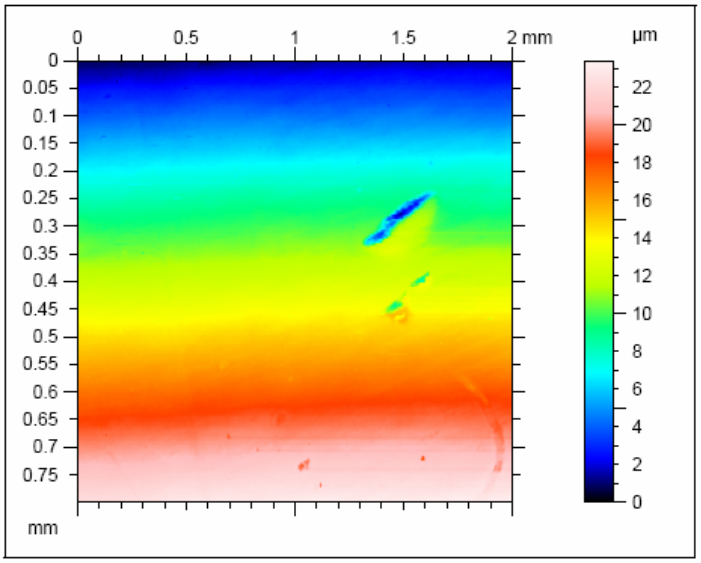

Pseudo-colour Image

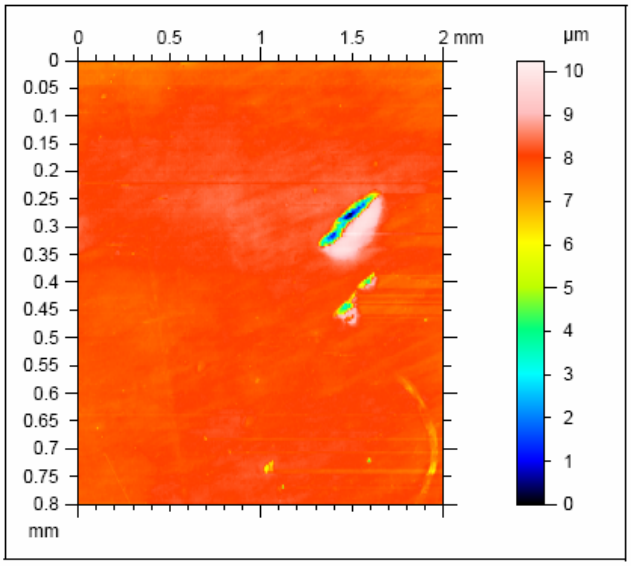

Aligned pseudo-colour Image

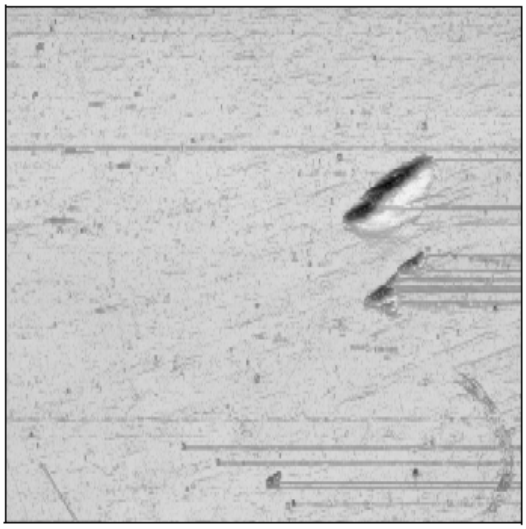

Photo Simulation

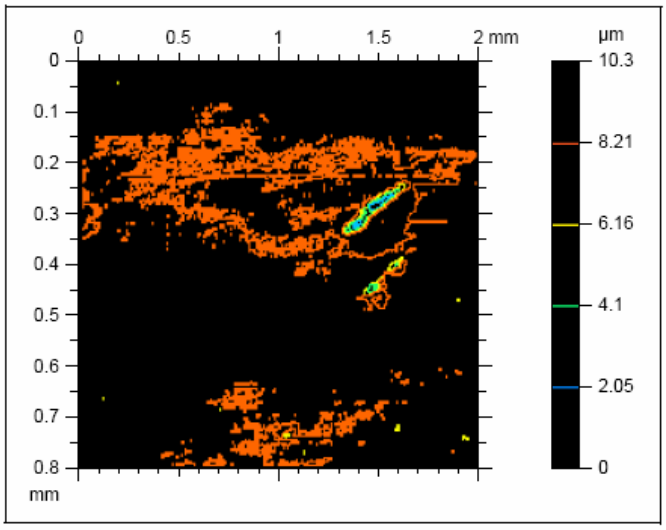

Countor Diagram

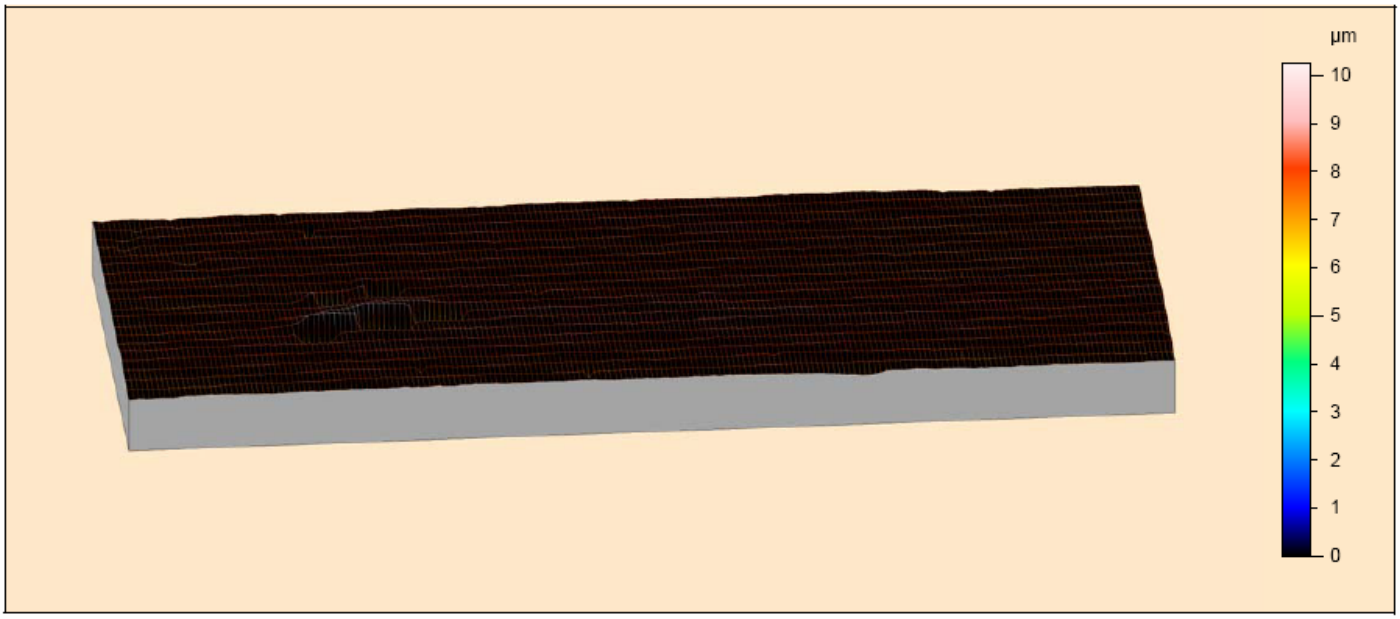

Meshed Axonometric

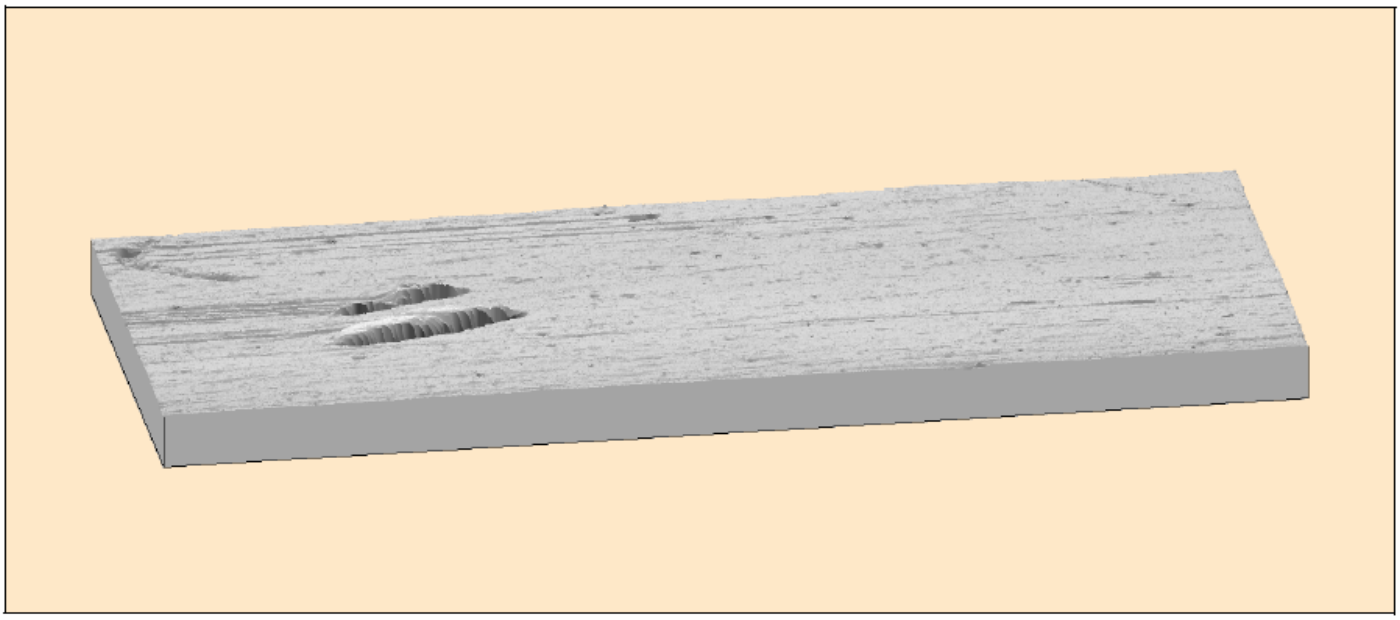

Continuous Axonometric

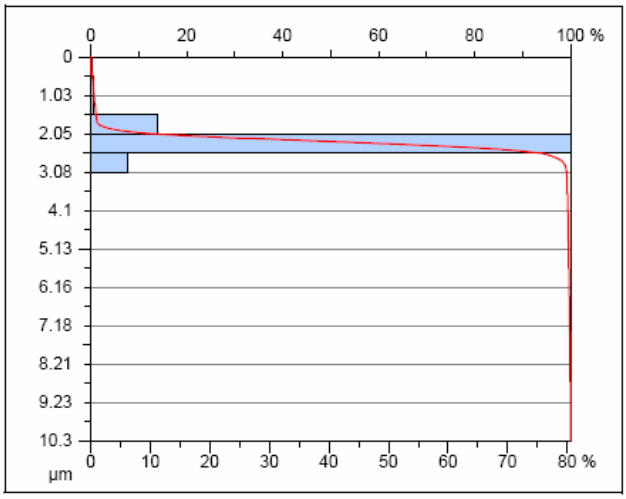

Abbott - Firestone

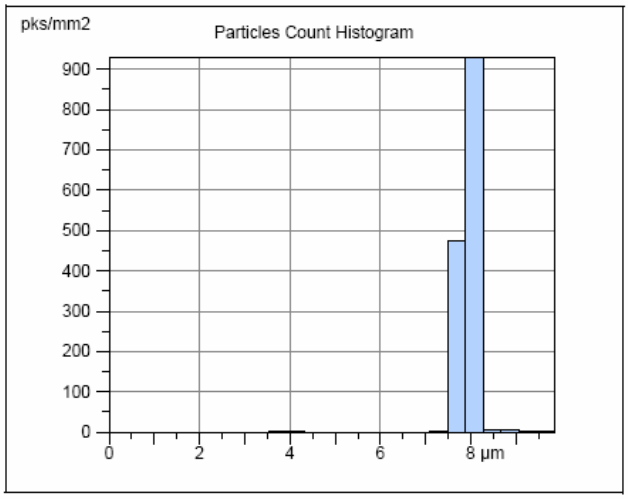

Peak Count Distributrion

Parameters calculated on the surface
Specimen 1 - Prove 1
Levelled (MZ) (0 µm)

```
Amplitude Parameters

   Sa     = 0.192 µm
   Sq     = 0.415 µm
   Sp     = 2.28 µm
   Sv     = 7.98 µm
   St     = 10.3 µm
   Ssk    = -7.21
   Sku    = 106
   Sz     = 9.54 µm

Area & volume Parameters

   STp    = 0.7 %      (1 µm under the highest peak)
   SHTp   = 0.322 µm   (20%-80%)
   Smmr   = 0.00798 mm3/mm2
   Smvr   = 0.00228 mm3/mm2
   Smr    = 0.7 %      (1 µm under the highest peak)
```

With Cut-off Filter 0.25 mm

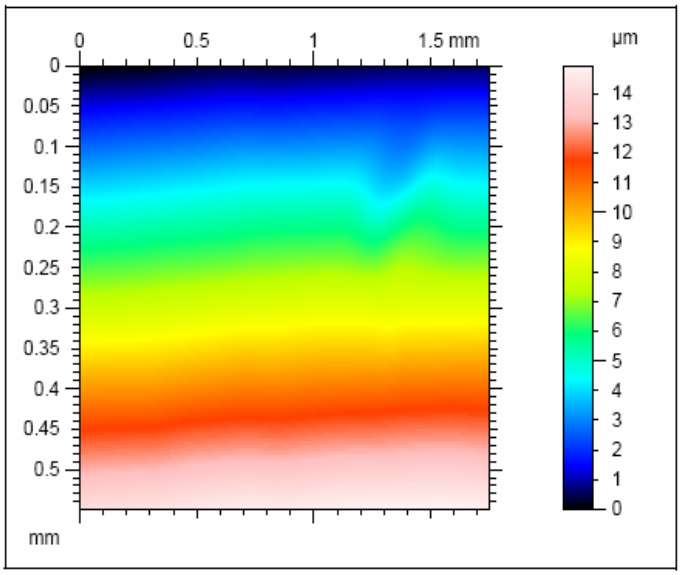

Pseudo-colour Image

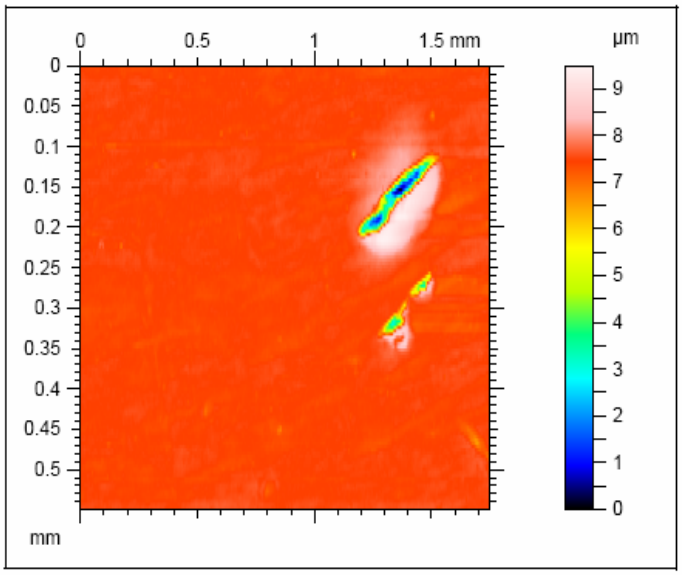

Aligned pseudo-colour Image

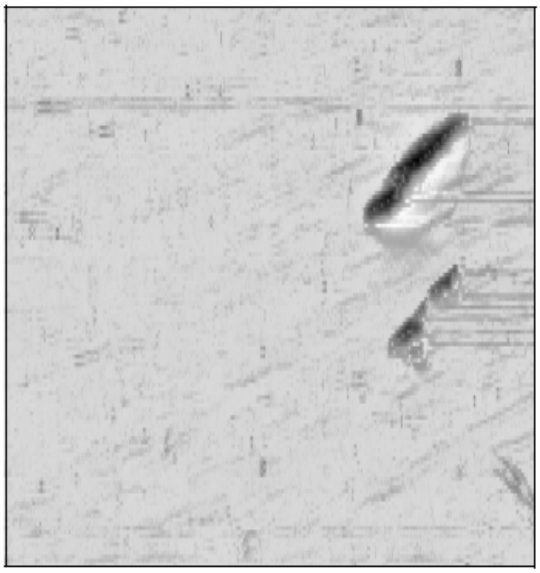

Photo Simulation

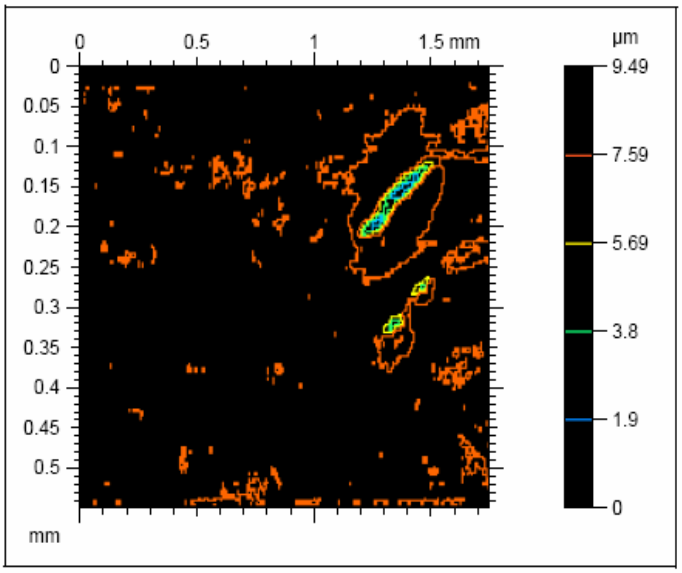

Countor Diagram

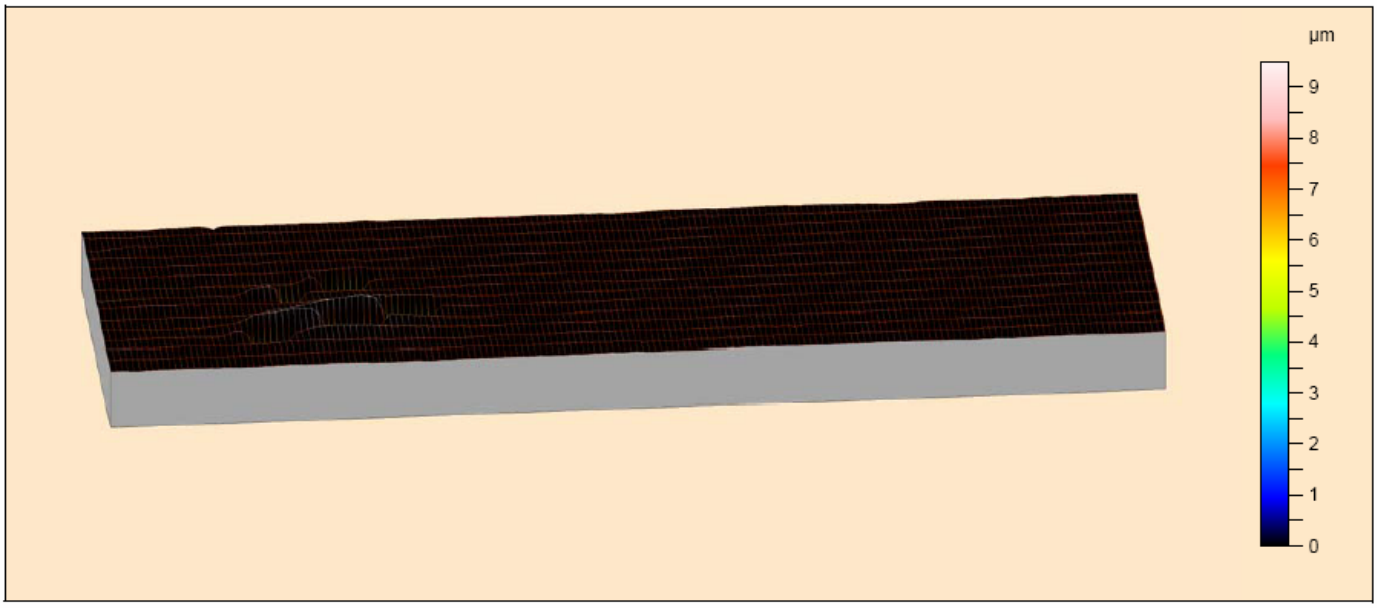

Meshed Axonometric

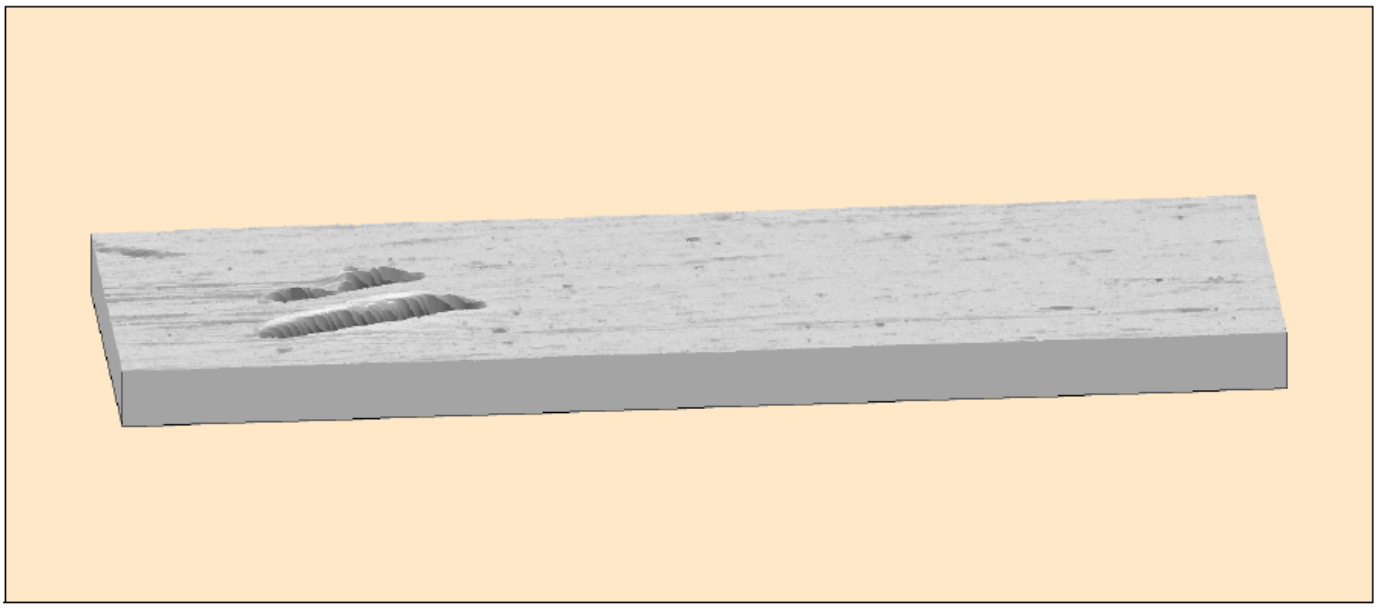

Continuous Axonometric

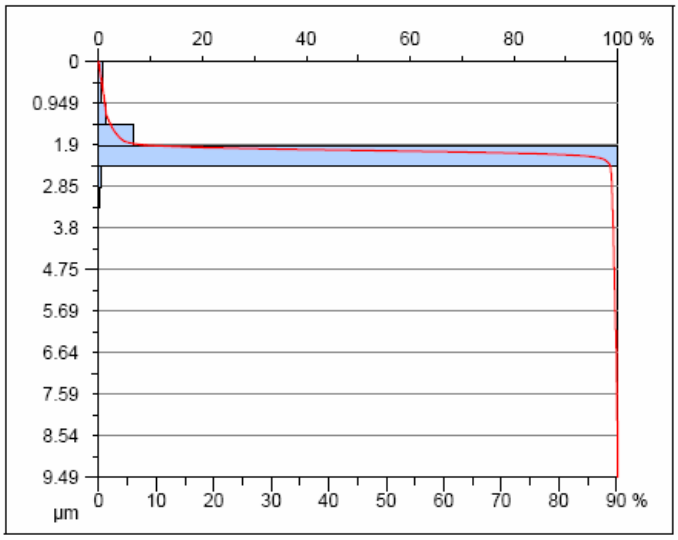

Abbott - Firestone

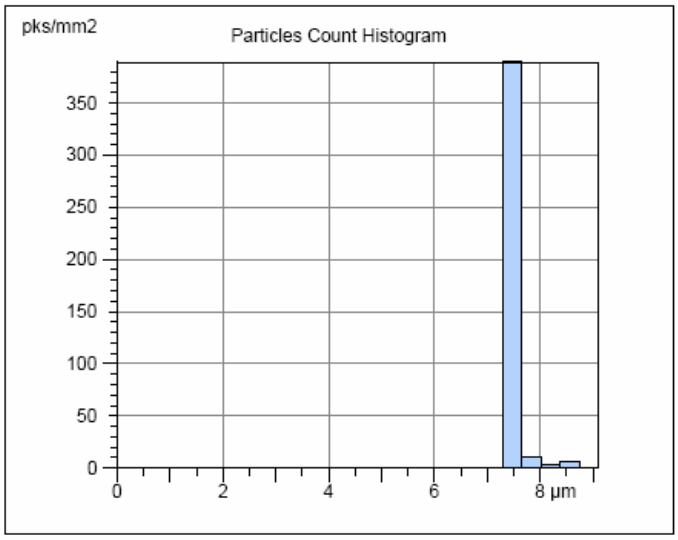

Peak Count Distributrion

Parameters calculated on the surface
Specimen 1 Prove 1
Waviness, gaussian filter, 0.25 mm

```
Amplitude Parameters

   Sa     = 0.13 µm
   Sq     = 0.439 µm
   Sp     = 2.03 µm
   Sv     = 7.46 µm
   St     = 9.49 µm
   Ssk    = -7.43
   Sku    = 96
   Sz     = 8.88 µm

Area & volume Parameters

   STp    = 1.2 %      (1 µm under the highest peak)
   SHTp   = 0.13 µm    (20%-80%)
   Smmr   = 0.00746 mm3/mm2
   Smvr   = 0.00203 mm3/mm2
   Smr    = 1.2 %      (1 µm under the highest peak)
```

Specimen 1 - Prove 2

Without Cut-off Filter

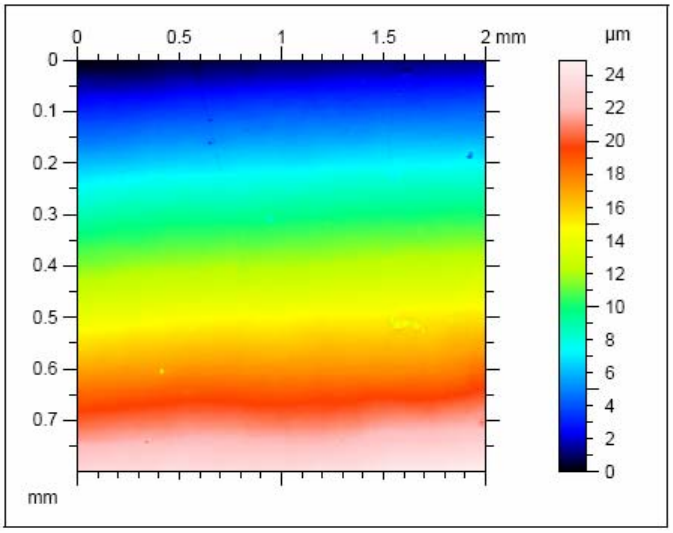

Pseudo-colour Image

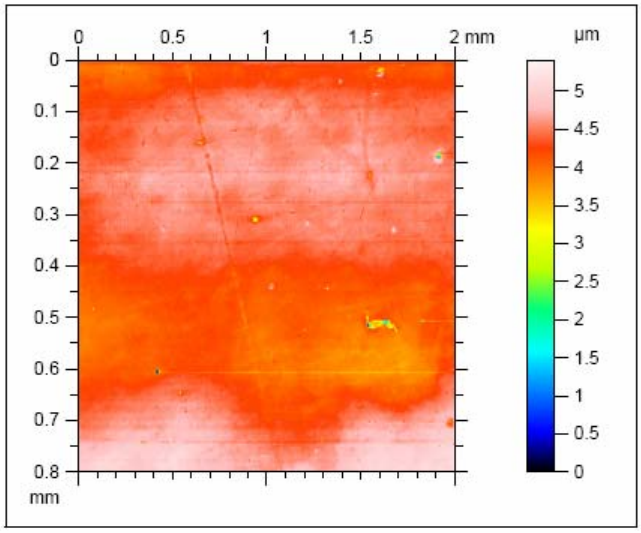

Aligned pseudo-colour Image

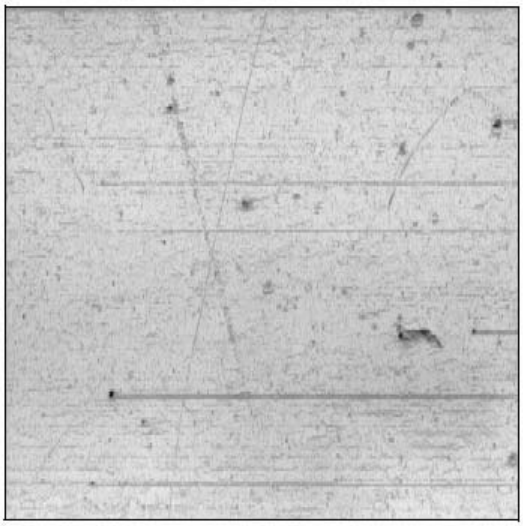

Photo Simulation

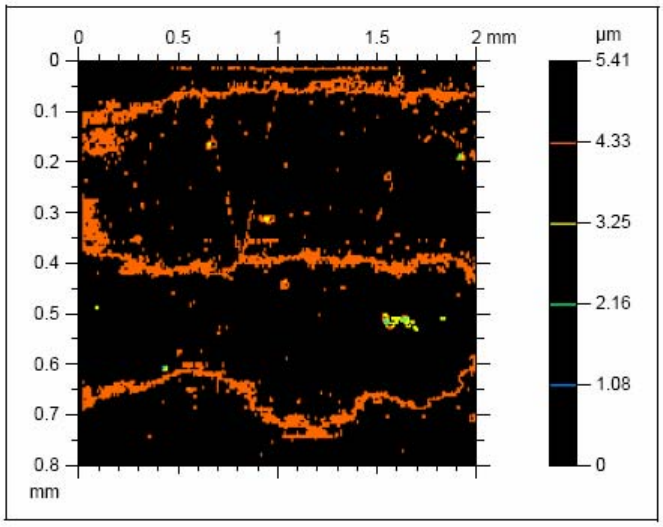

Countor Diagram

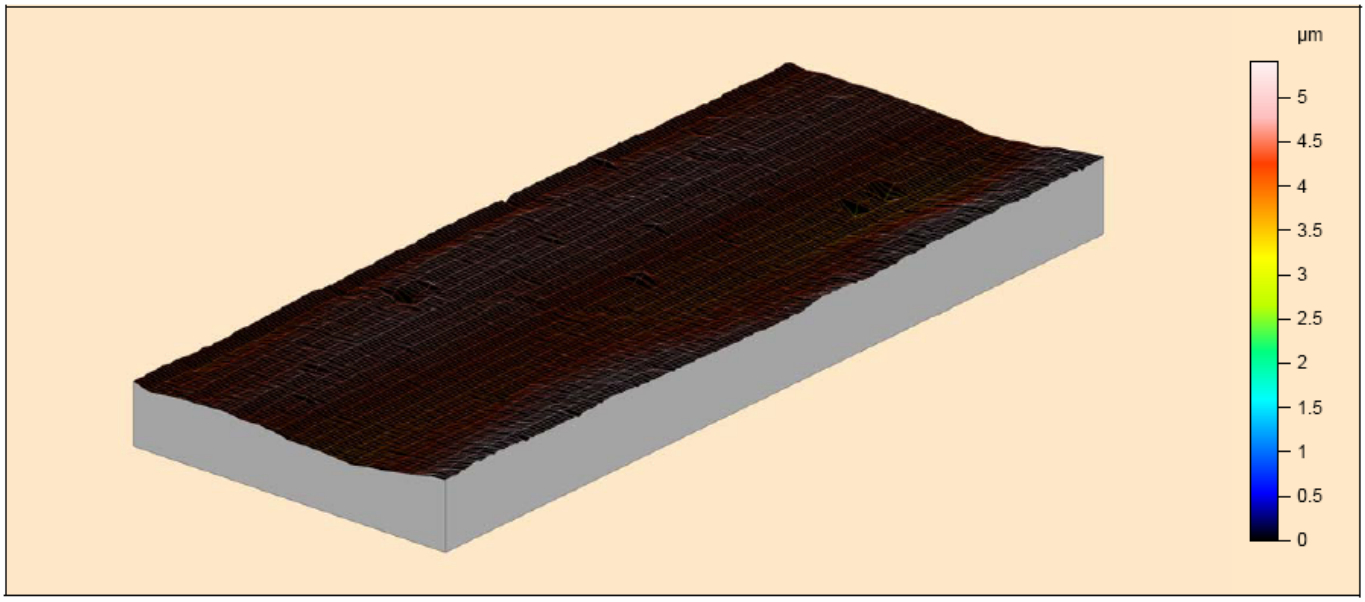

Meshed Axonometric

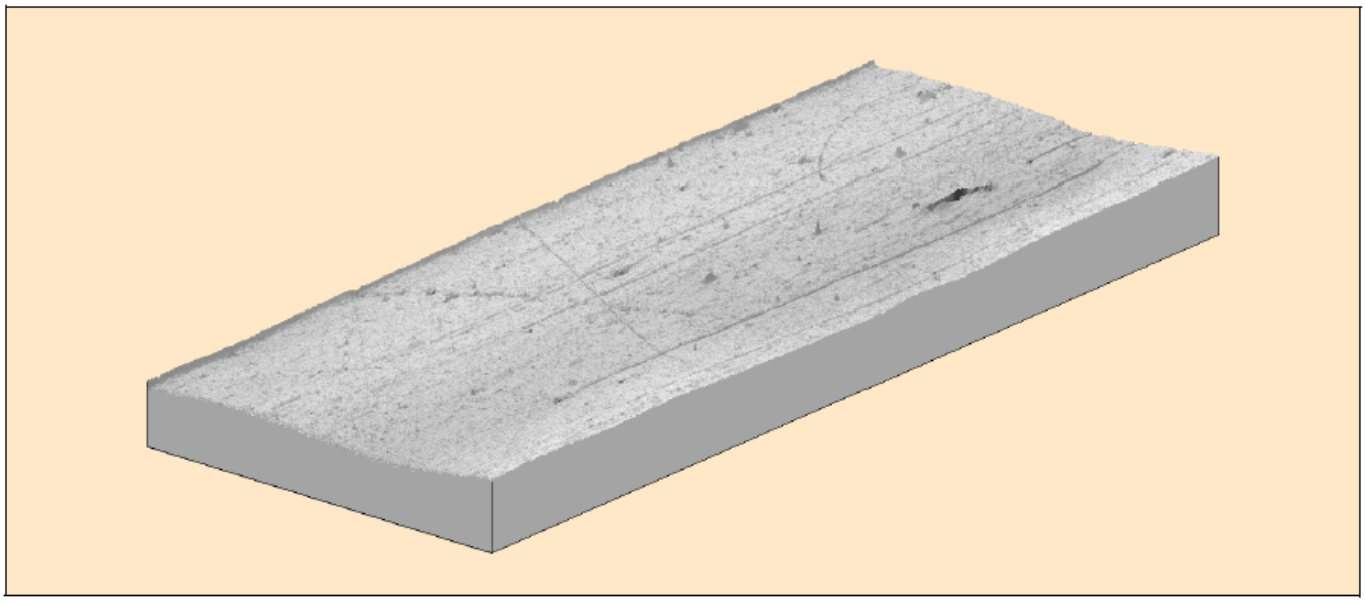

Continuous Axonometric

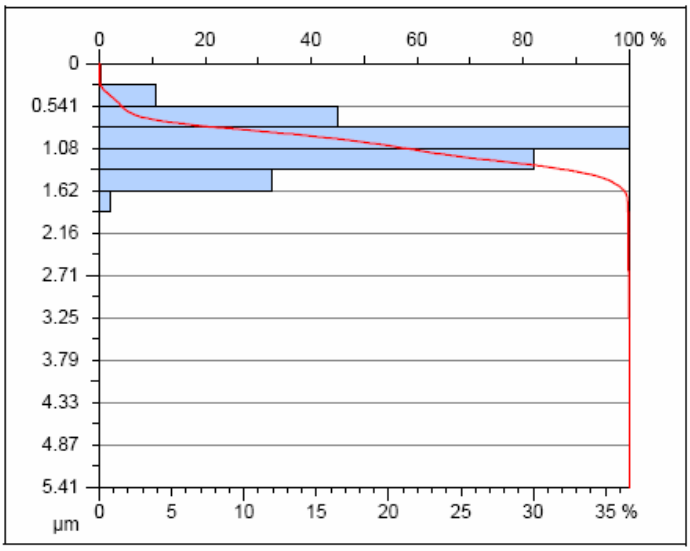

Abbott - Firestone Curve

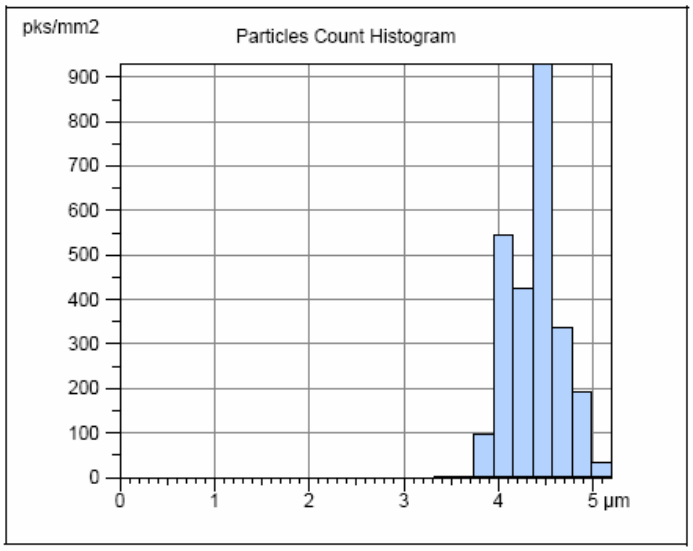

Peak Count Distributrion

Parameters calculated on the surface
prova041207_5 > Levelled (MZ) (0 µm)

```
Amplitude Parameters

   Sa     = 0.229 µm
   Sq     = 0.282 µm
   Sp     = 1.03 µm
   Sv     = 4.38 µm
   St     = 5.41 µm
   Ssk    = -0.443
   Sku    = 8.14
   Sz     = 4.41 µm

Area & volume Parameters

   STp    = 49.7 %     (1 µm under the highest peak)
   SHTp   = 0.481 µm   (20%-80%)
   Smmr   = 0.00438 mm3/mm2
   Smvr   = 0.00103 mm3/mm2
   Smr    = 49.7 %     (1 µm under the highest peak)
```

With Cut-Off Filter 0.25 mm

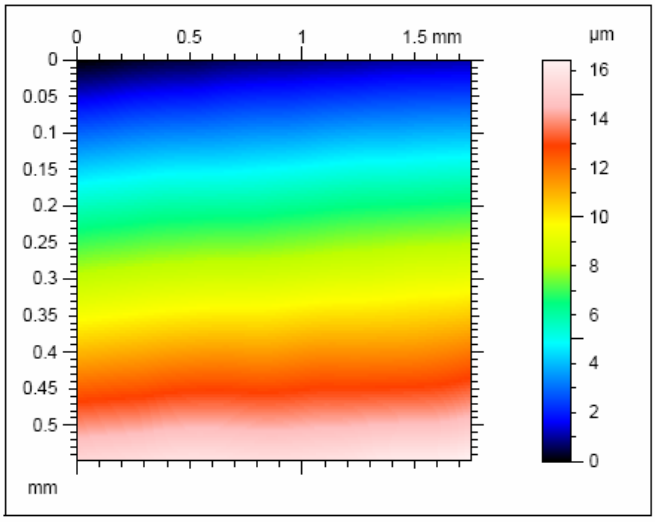

Pseudo-colour Image

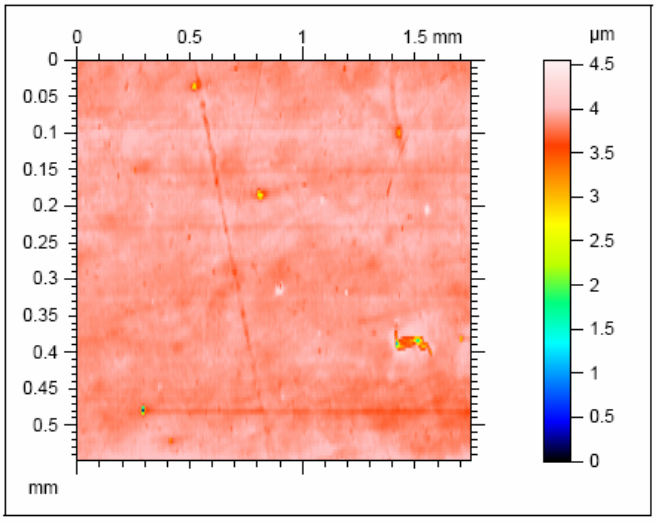

Aligned pseudo-colour Image

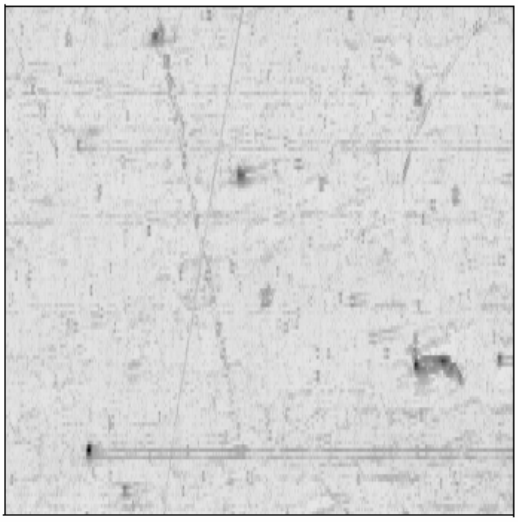

Photo Simulation

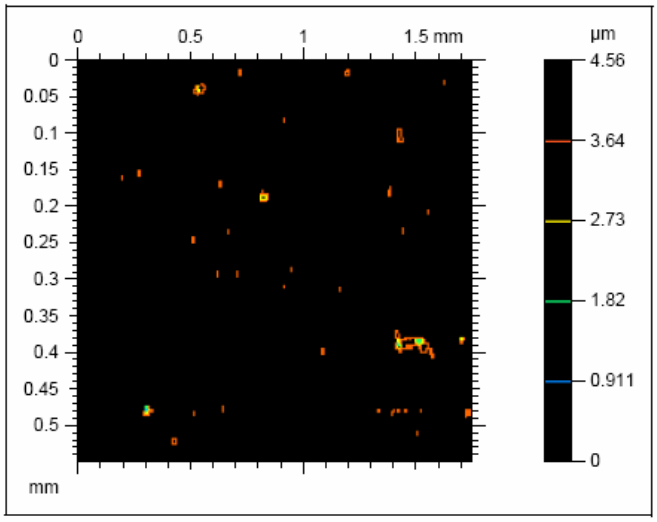

Countor Diagram

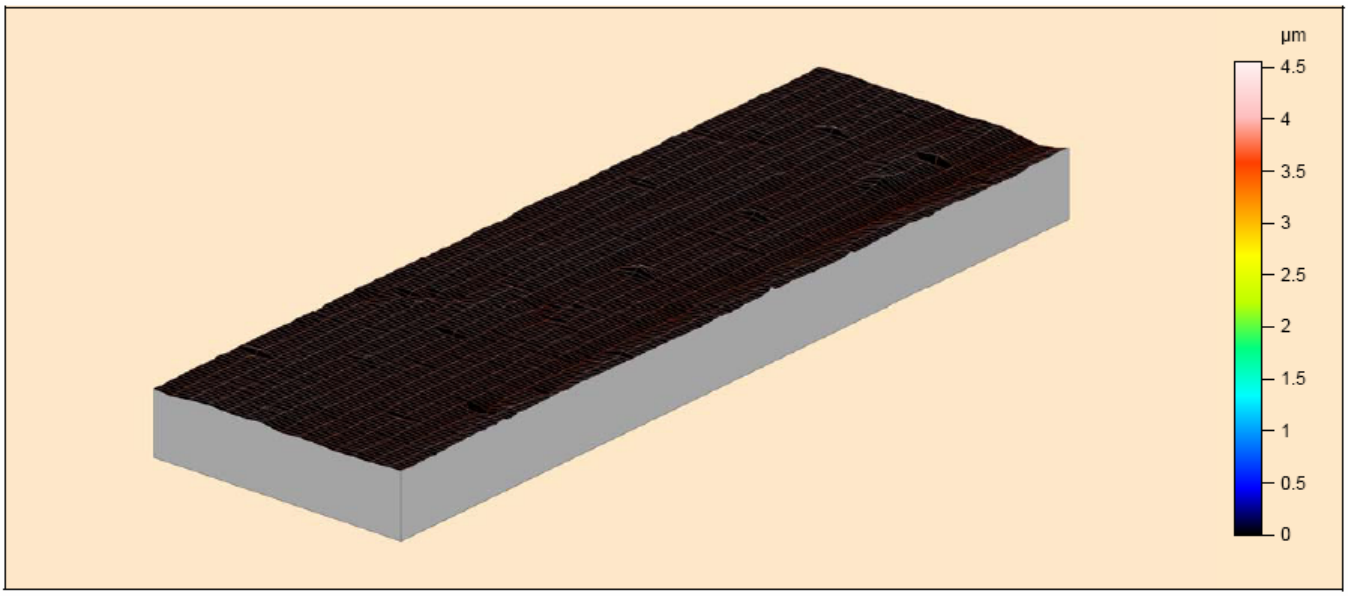

Meshed Axonometric

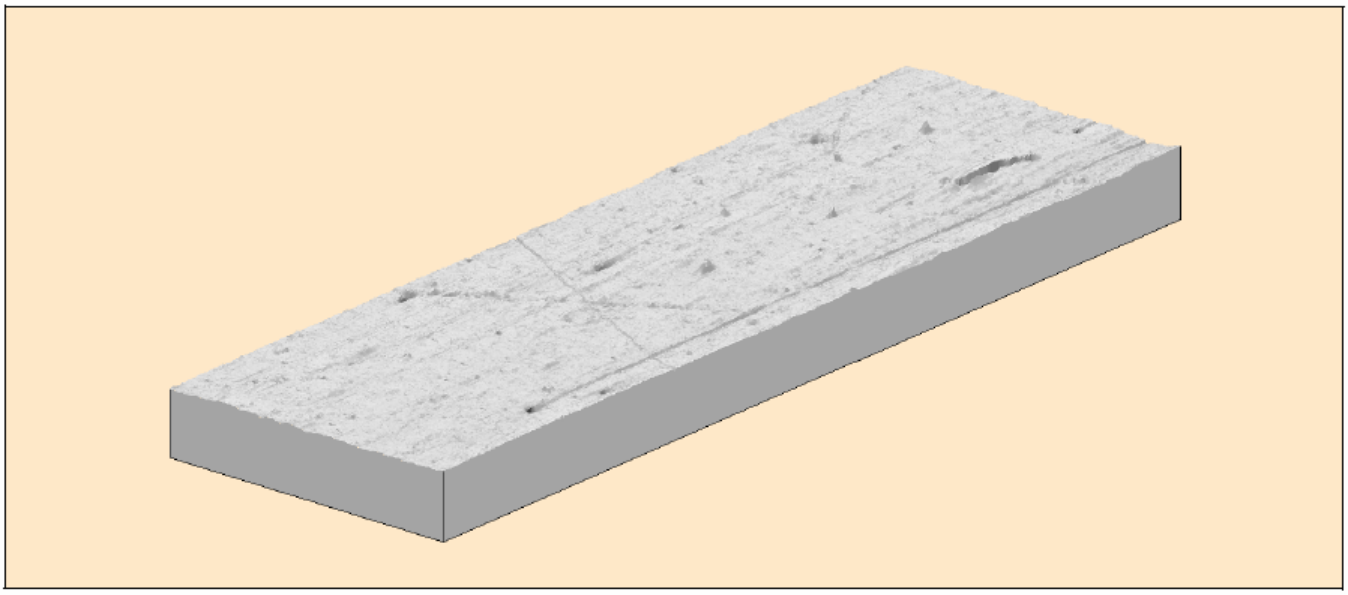

Continuous Axonometric

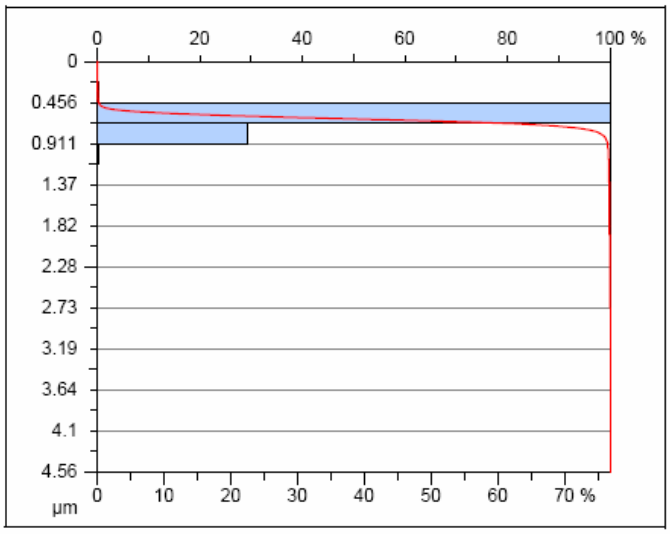

Abbott - Firestone Curve

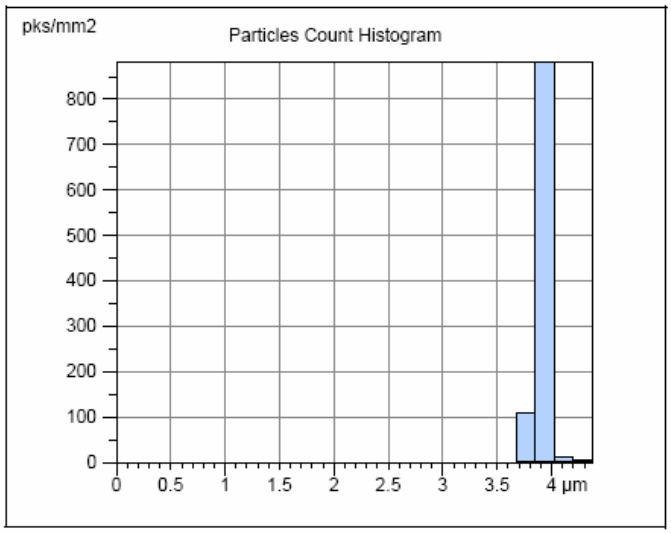

Peak Count Distributrion

Parameters calculated on the surface prova041207_5 > Waviness, gaussian filter, 0.25 mm

```
Amplitude Parameters

   Sa     = 0.0516 µm
   Sq     = 0.0872 µm
   Sp     = 0.643 µm
   Sv     = 3.91 µm
   St     = 4.56 µm
   Ssk    = -9.78
   Sku    = 276
   Sz     = 3.21 µm

Area & volume Parameters

   STp    = 99.7 %     (1 µm under the highest peak)
   SHTp   = 0.0984 µm (20%-80%)
   Smmr   = 0.00391 mm3/mm2
   Smvr   = 0.000643 mm3/mm2
   Smr    = 99.7 %     (1 µm under the highest peak)
```

Specimen 2

Without Cut-off Filter

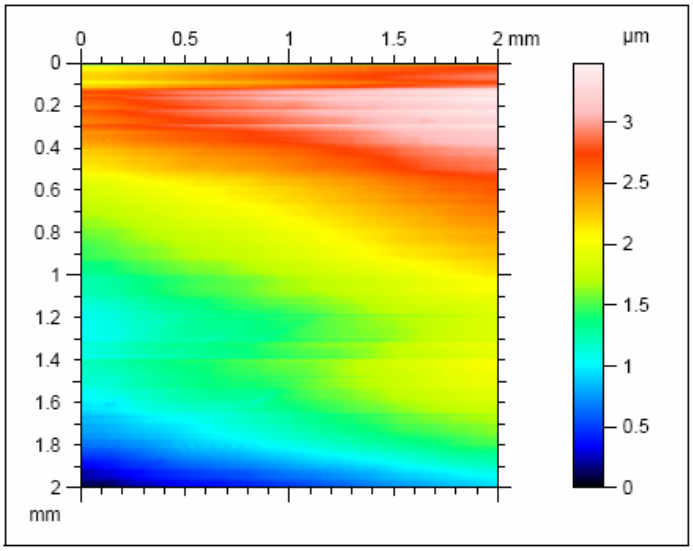

Pseudo Colour Image

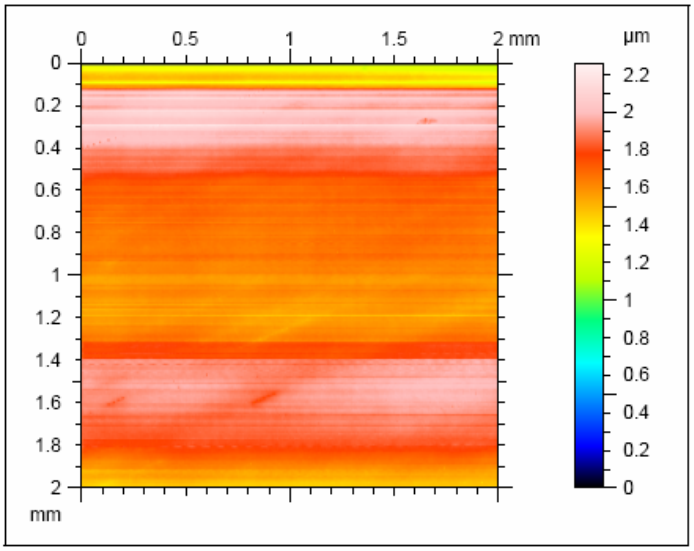

Aligned Pseudo Colour Image

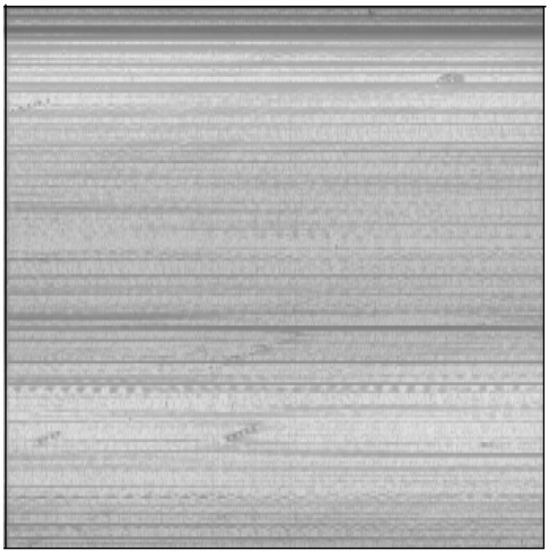

Photo Simulation

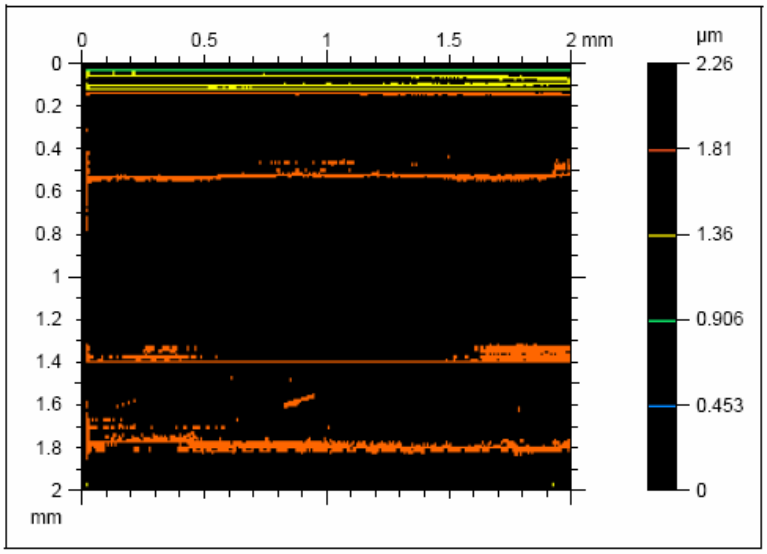

Contour Diagram

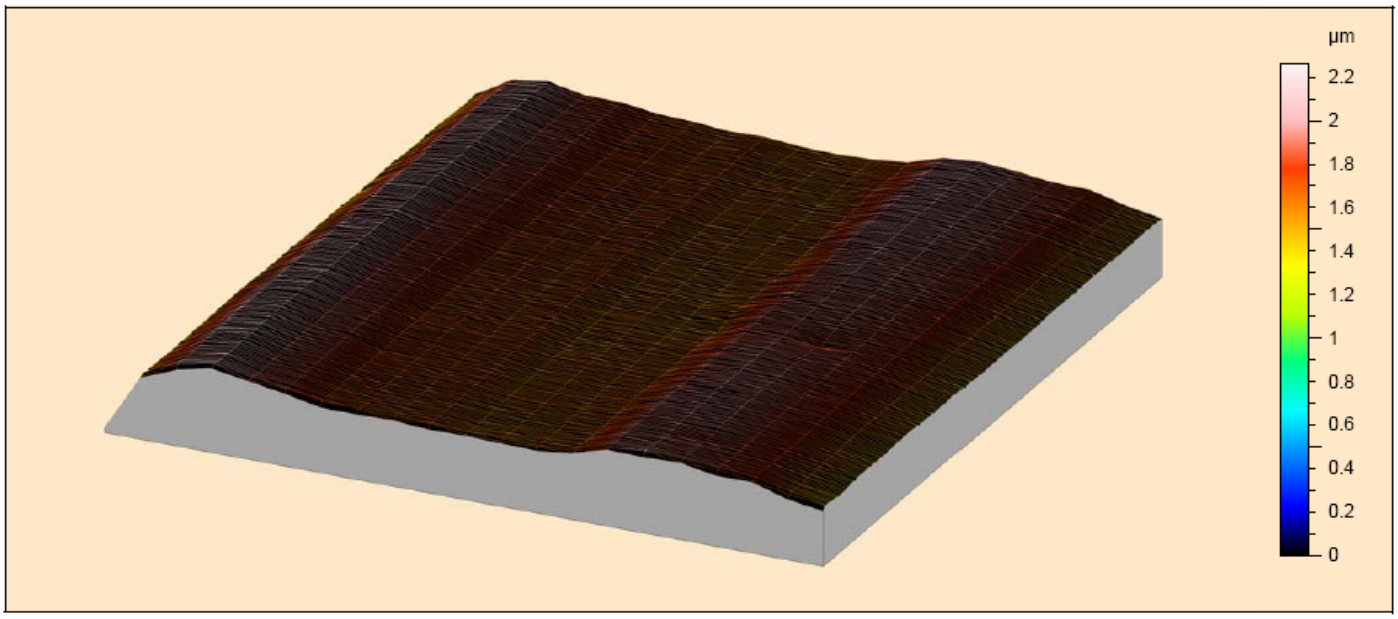

Meshed Axonometric

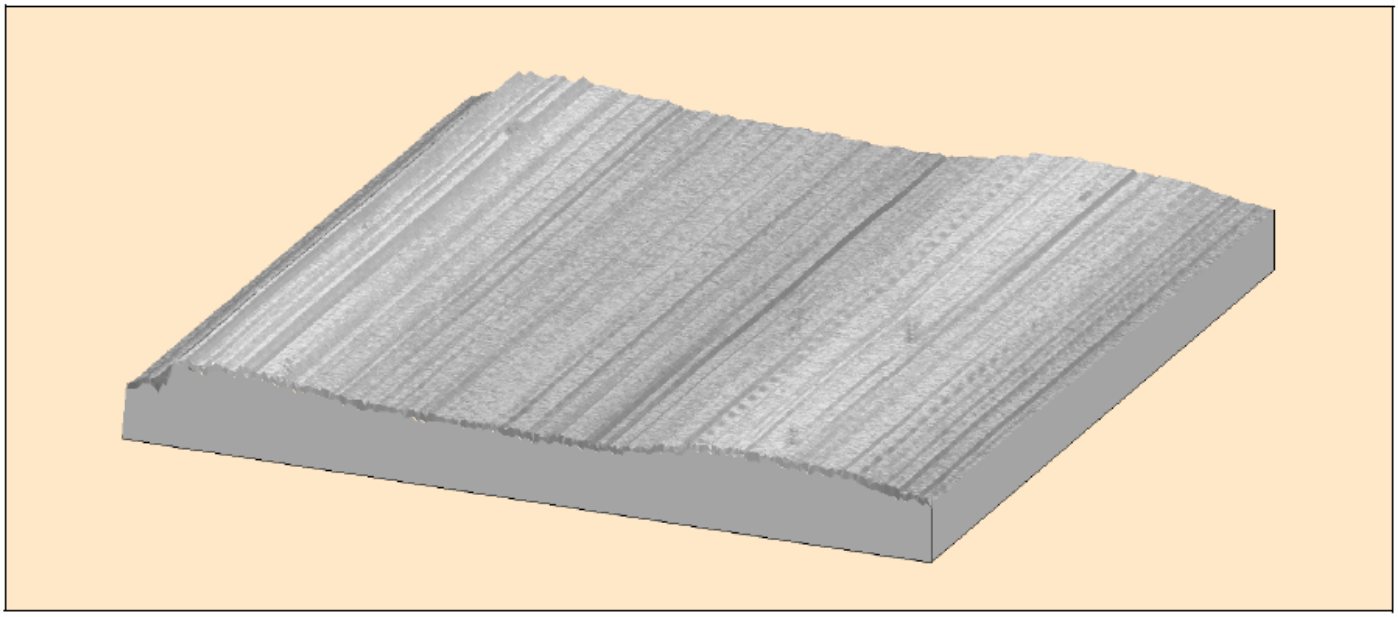

Continuous

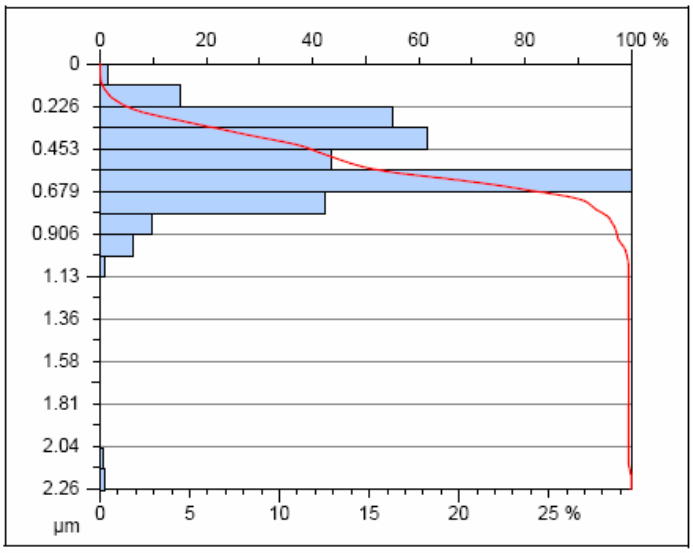

Abbott-Firestone Curve

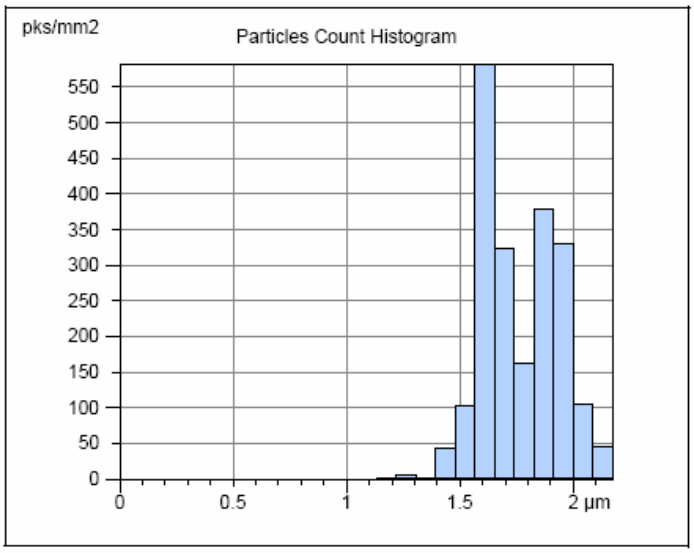

Peak Count Distribution

Parameters calculated on the surface
Specimen 2
Levelled (MZ) (0 µm)

Amplitude Parameters

Sa	= 0.163 µm	
Sq	= 0.217 µm	
Sp	= 0.523 µm	
Sv	= 1.74 µm	
St	= 2.26 µm	
Ssk	= -2.09	
Sku	= 17.5	
Sz	= 1.08 µm	

Area & volume Parameters

STp	= 99 %	(1 µm under the highest peak)
SHTp	= 0.338 µm	(20%-80%)
Smmr	= 0.00174 mm3/mm2	
Smvr	= 0.000523 mm3/mm2	
Smr	= 99 %	(1 µm under the highest peak)

With Cut-off Filter 0.08 mm

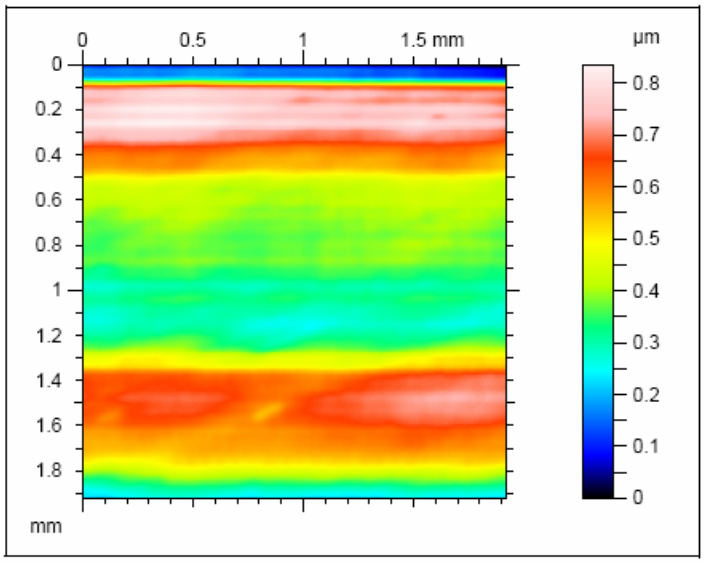

Pseudo Colour Image

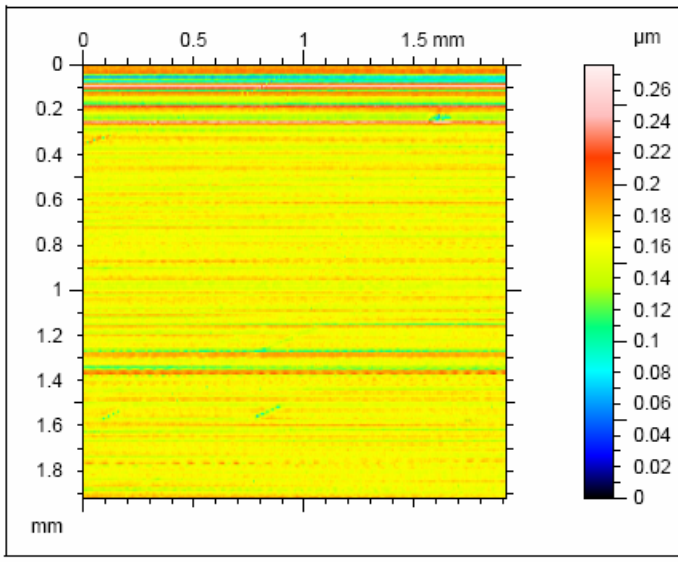

Aligned Pseudo Colour Image

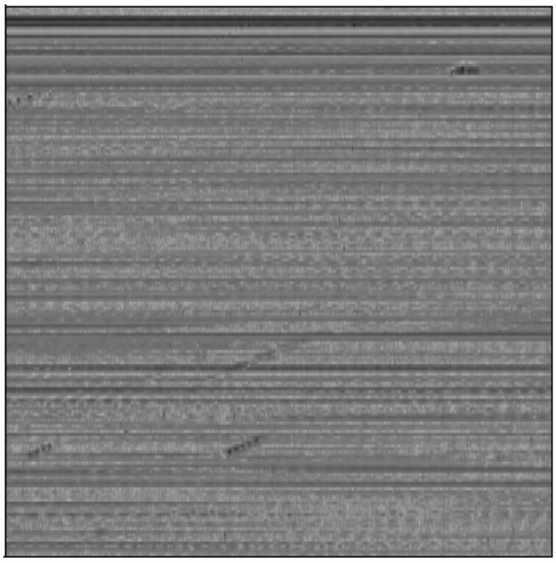

Photo Simulation

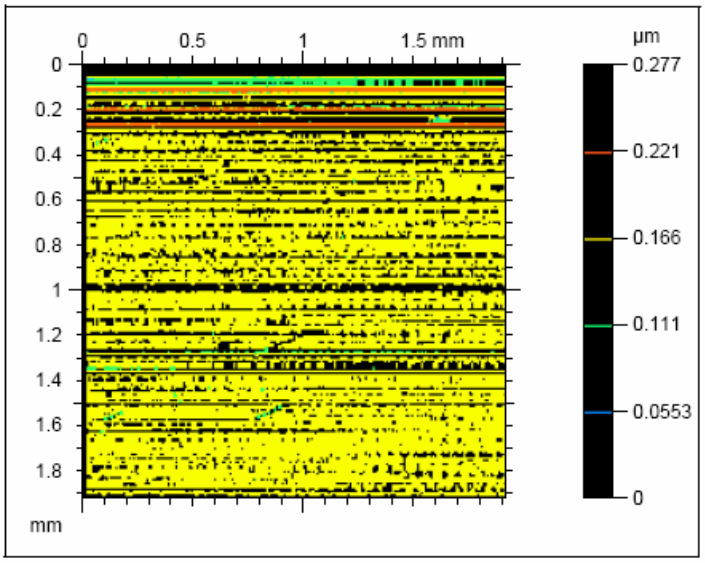

Contour Diagram

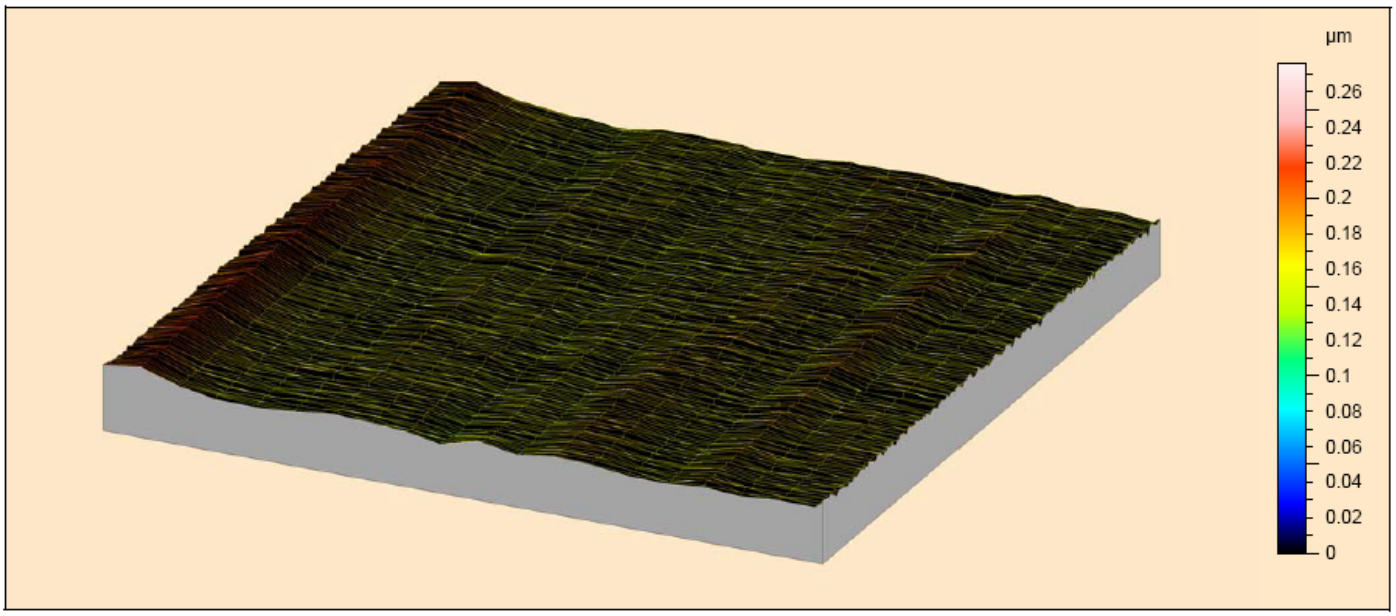

Meshed Axonometric

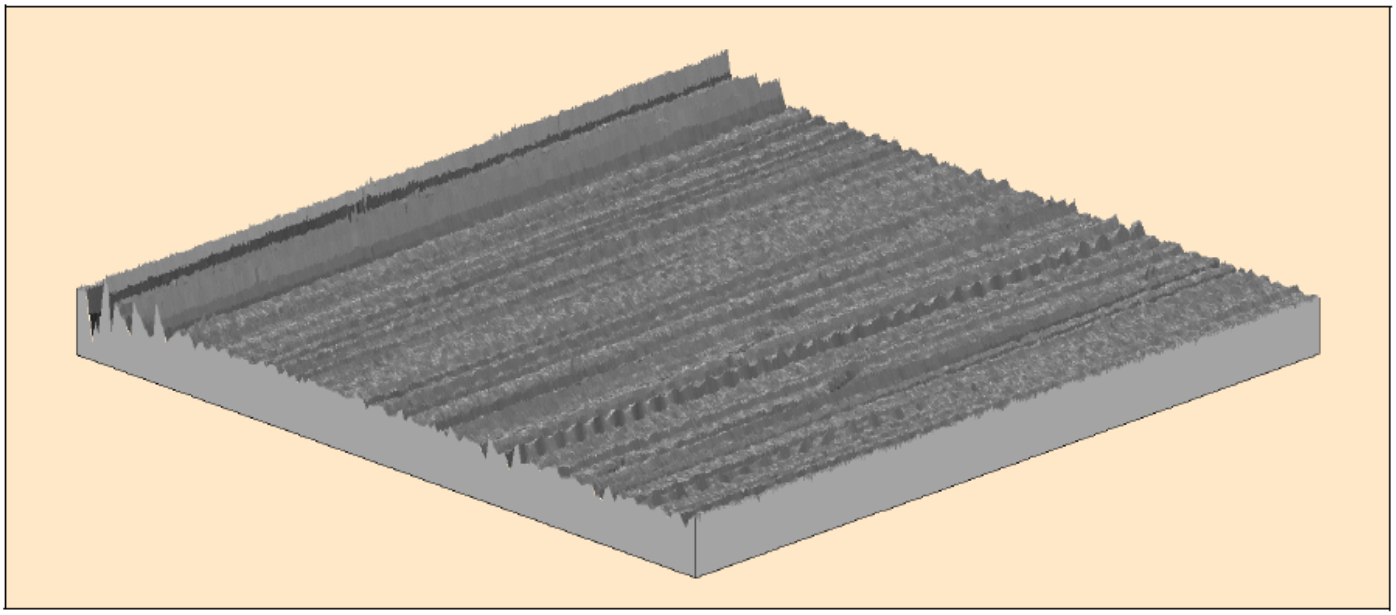

Continuous

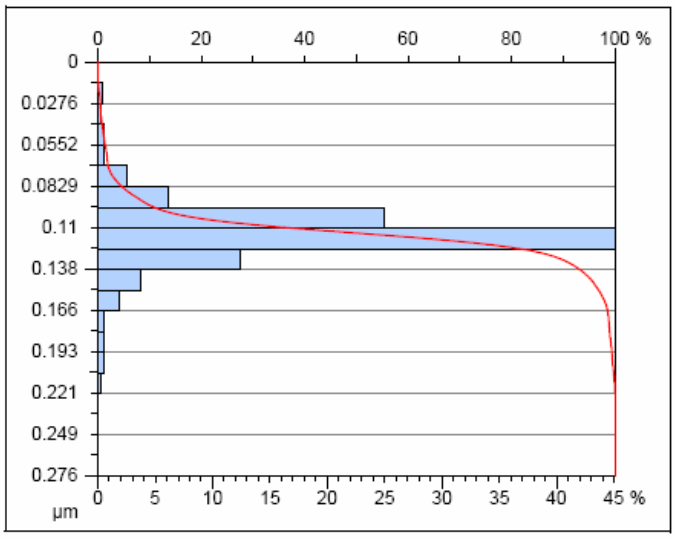

Abbott-Firestone Curve

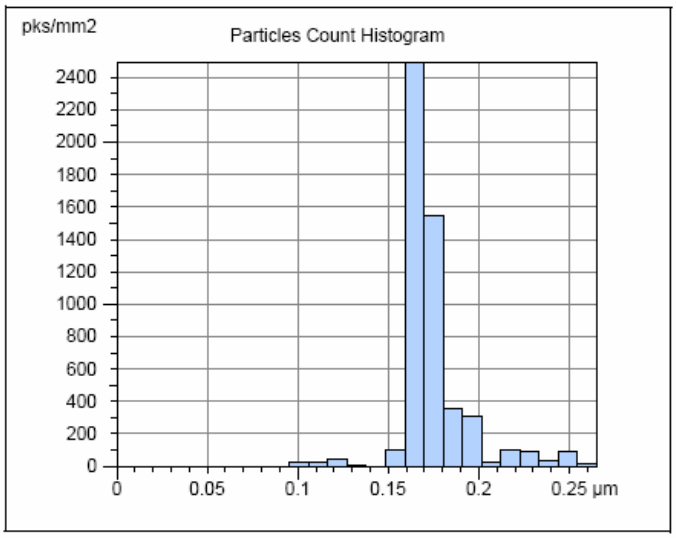

Peak Count Distribution

Parameters calculated on the surface
Specimen 2
Waviness, gaussian filter, 0.08 mm

```
Amplitude Parameters

   Sa     = 0.0125 µm
   Sq     = 0.0198 µm
   Sp     = 0.114 µm
   Sv     = 0.162 µm
   St     = 0.276 µm
   Ssk    = 0.111
   Sku    = 9.48
   Sz     = 0.242 µm

Area & volume Parameters

   STp    = *****      (1 µm under the highest peak)
   SHTp   = 0.0193 µm (20%-80%)
   Smmr   = 0.000162 mm3/mm2
   Smvr   = 0.000114 mm3/mm2
   Smr    = *****      (1 µm under the highest peak)
```

Specimen 3

Without Cut-off Filter

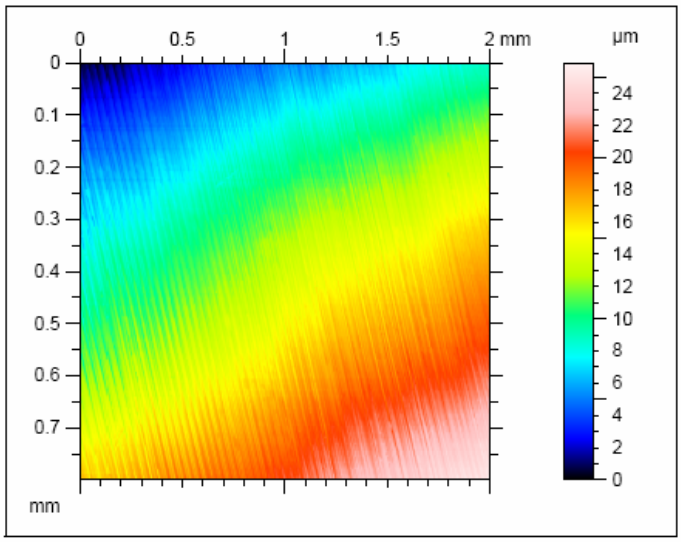

Pseudo-colour Image

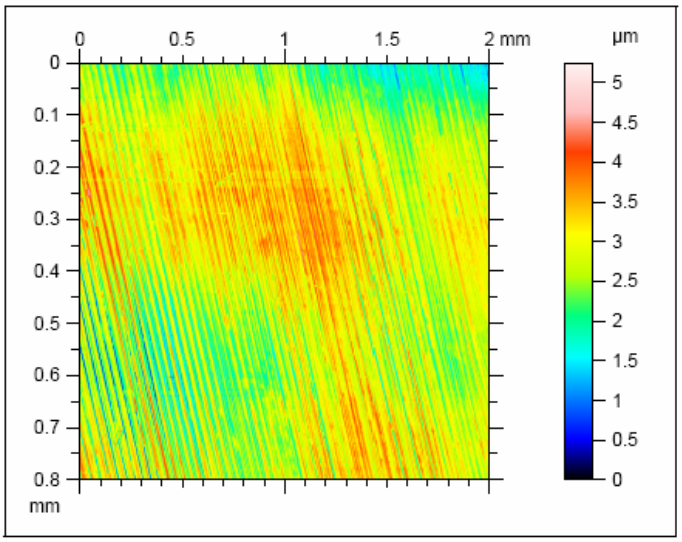

Aligned pseudo-colour Image

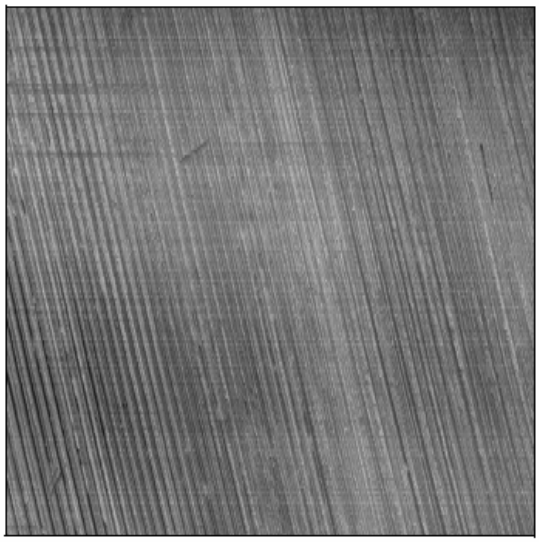

Photo Simulation

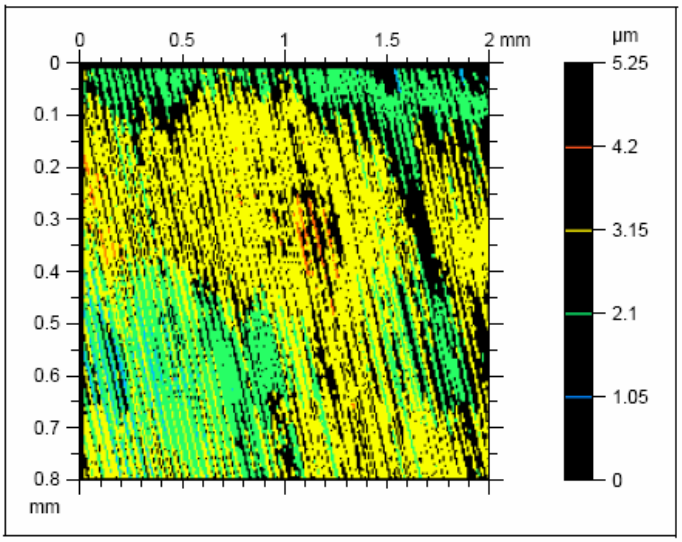

Countor Diagram

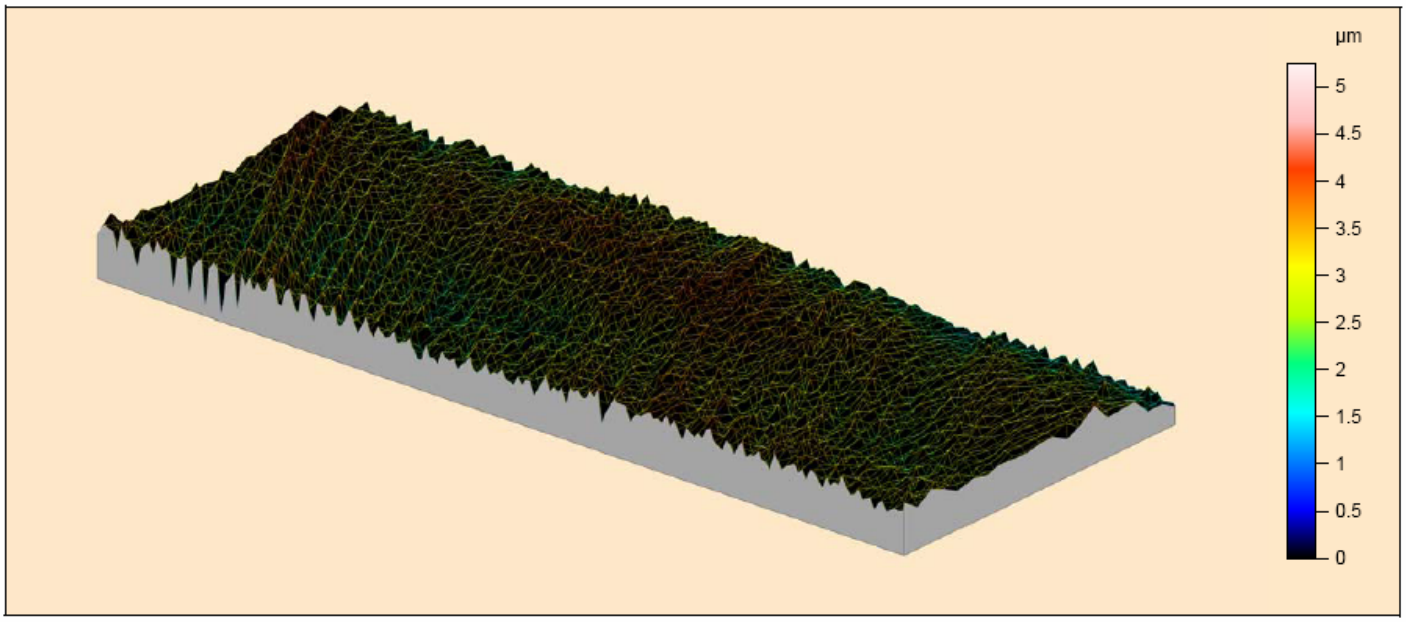

Meshed Axonometric

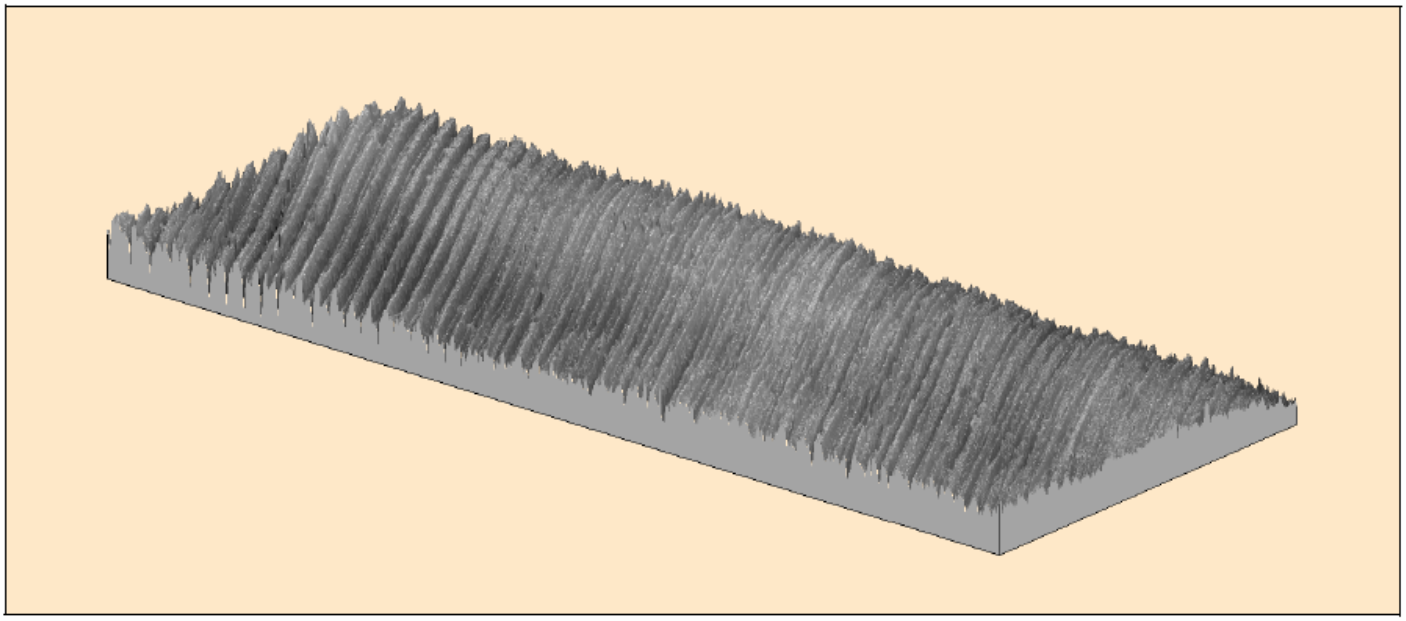

Continuous Axonometric

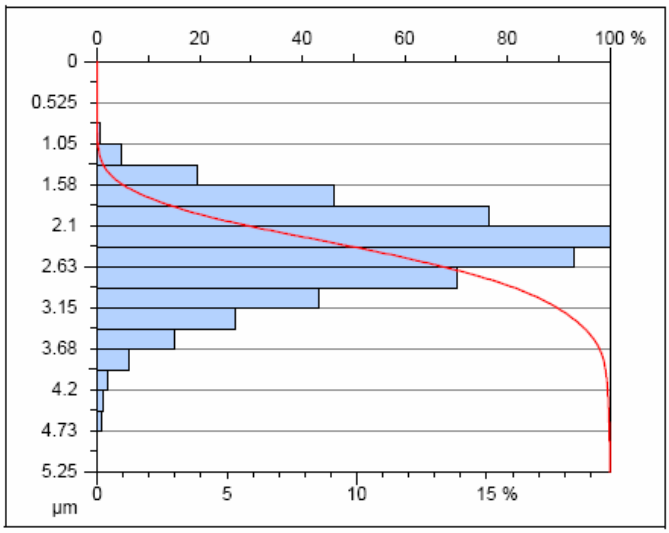

Abbott - Firestone Curve

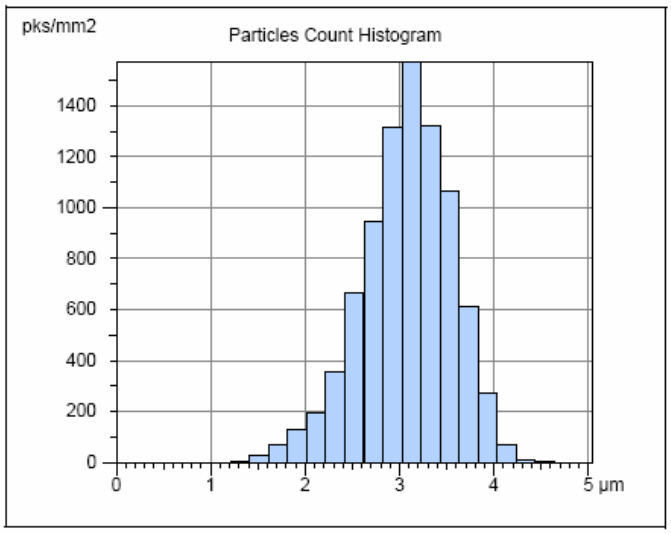

Peak Count Distributrion

Parameters calculated on the surface
Specimen 3
Levelled (MZ) (0 µm)

```
Amplitude Parameters

   Sa     = 0.44 µm
   Sq     = 0.559 µm
   Sp     = 2.42 µm
   Sv     = 2.83 µm
   St     = 5.25 µm
   Ssk    = -0.485
   Sku    = 3.54
   Sz     = 4.72 µm

Area & volume Parameters

   STp    = 0.1 %      (1 µm under the highest peak)
   SHTp   = 0.906 µm   (20%-80%)
   Smmr   = 0.00283 mm3/mm2
   Smvr   = 0.00242 mm3/mm2
   Smr    = 0.1 %      (1 µm under the highest peak)
```

With Cut-off Filter 0.8 mm

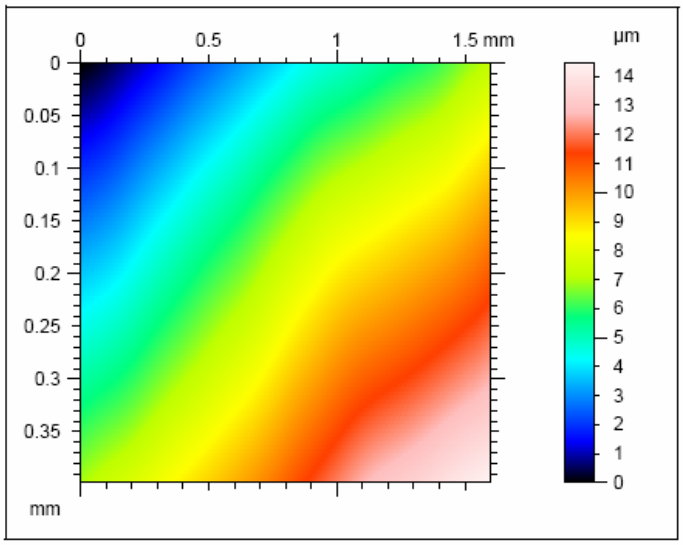

Pseudo-colour Image

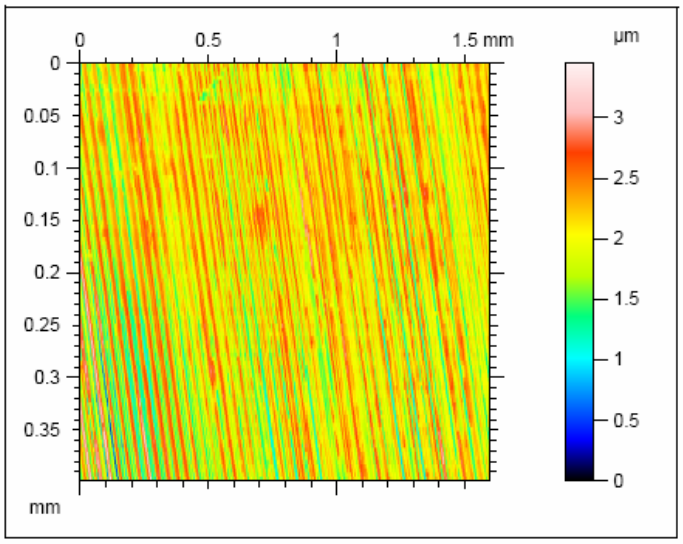

Aligned pseudo-colour Image

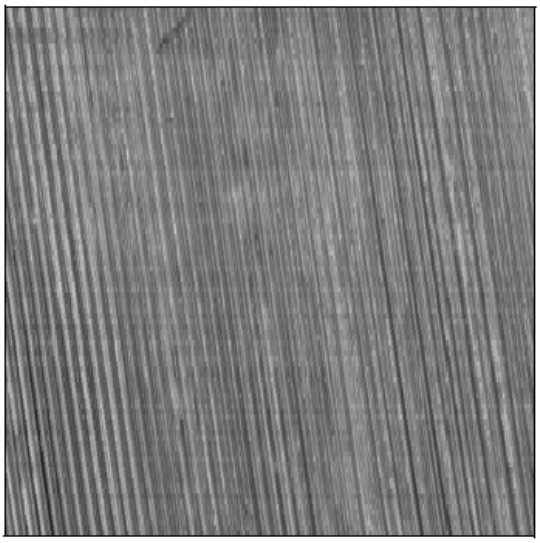

Photo Simulation

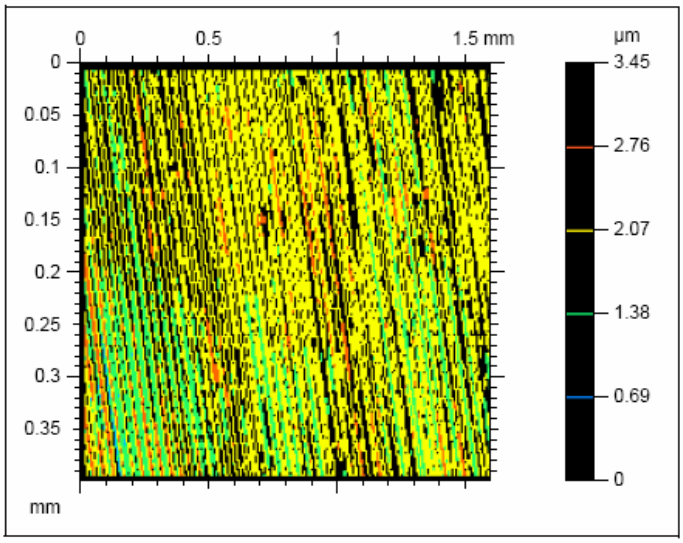

Countor Diagram

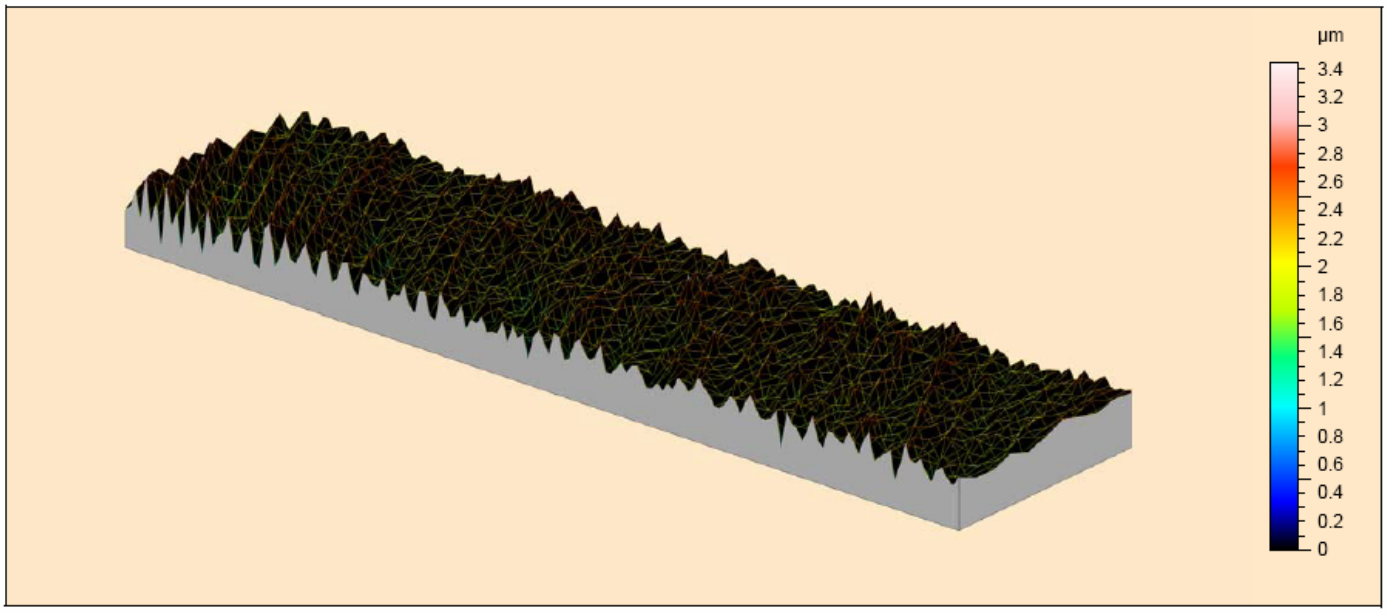

Meshed Axonometric

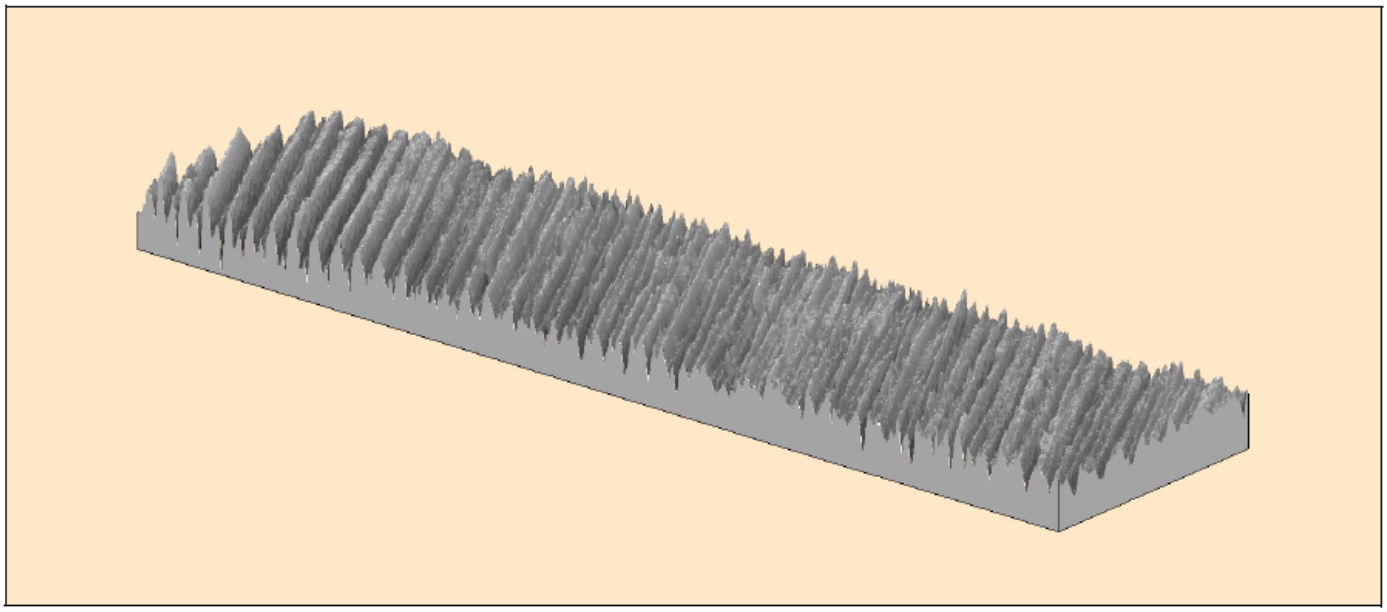

Continuous Axonometric

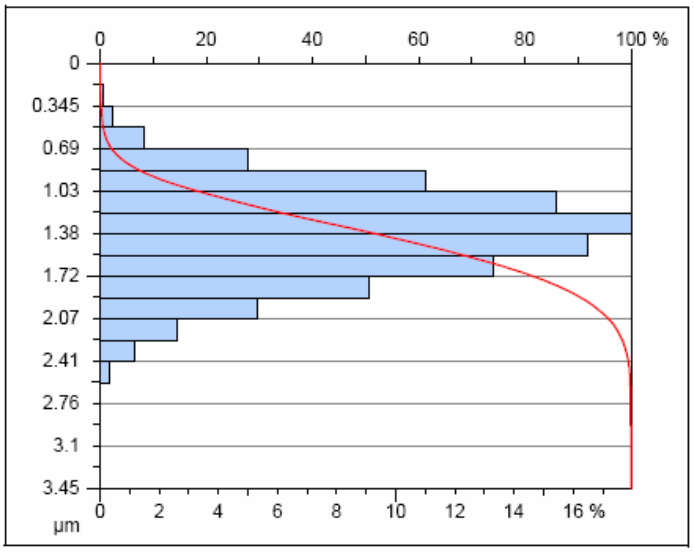

Abbott - Firestone Curve

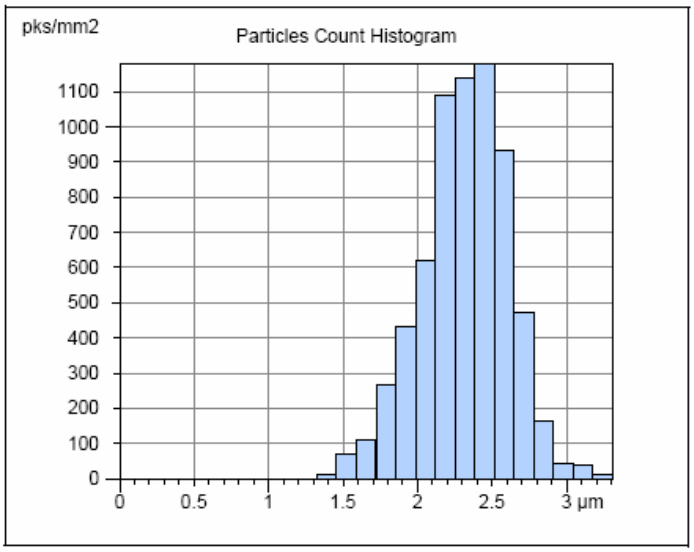

Peak Count Distributrion

Parameters calculated on the surface
Specimen 3
Waviness, gaussian filter, 0.8 mm

```
Amplitude Parameters

   Sa     = 0.304 µm
   Sq     = 0.38 µm
   Sp     = 1.39 µm
   Sv     = 2.06 µm
   St     = 3.45 µm
   Ssk    = -0.278
   Sku    = 3.14
   Sz     = 3.35 µm

Area & volume Parameters

   STp    = 15.6 %     (1 µm under the highest peak)
   SHTp   = 0.648 µm   (20%-80%)
   Smmr   = 0.00206 mm3/mm2
   Smvr   = 0.00139 mm3/mm2
   Smr    = 15.6 %     (1 µm under the highest peak)
```

Appendix 8 – Models in Matlab® for contacts mechanics analysis

Greenwood and Williamson Model:

```
%model Greenwood and Williamson (GW)
%function [p_g]=greenwood
%==================================
%===Greenwood and Williamson Model===
%==================================
%Input data: vector data_z with the roughness points and vector
%data_x with the respective coordinates
%Output data: percentage of contact real area, deformation, plot with the
%original profile and deformed profile
x=data_x;
rug=data_z;
%load aplied
load=1.9894; %N/mm
%properties of the material
H=2785; %MPa
E1=205000; %MPa
E2=62750; %MPa (%Glass)
niu1=0.29;
niu2=0.2;
Ecom=1/((1-niu1^2)/E1+(1-niu2^2)/E2); %[MPa]
%rug is the vector with one profile of the roughness topography
%the profile will be approached by polynomial functions using the
%Aramki formulation
%determination of ACF length and the coefficient of ACF, ACF length is the
%length where autocorrelation function is 0.368 (=1/e)
[ACF,Lags,Bounds] = autocorr(rug,length(x)-1);
index_ACF_0368=1;
while ACF(index_ACF_0368)>0.368
    index_ACF_0368=index_ACF_0368+1;
end
%plot(x,ACF); %plot whith the fuction of autorrelation
length_ACF=x(index_ACF_0368)-x(1);
alfa=1/length_ACF;
%standard deviation:
sigma=std(rug);
%definition of a vector L_peak (peaks), obtained considering the cross with
the reference line:
n=length(x);
k=1;
for i=1:n-1
    if ((rug(i)<=0)&(rug(i+1)>0));
       j=i+1;
       while ((rug(j)>=0)&(j+1<n))
           if  rug(j+1)<0
               Lpeak(k,1)=x(i)-rug(i)*(x(i+1)-x(i))/(rug(i+1)-rug(i));
               Lpeak(k,2)=x(j)-rug(j)*(x(j+1)-x(j))/(rug(j+1)-rug(j));
               L_peak(k)=Lpeak(k,2)-Lpeak(k,1);
               k=k+1;
           end
           j=j+1;
       end
   end
end
%definition of a vector L_valley (valleys), obtained considering the cross
with the reference line:
k=1;
for i=1:n-1
   if ((rug(i)>=0)&(rug(i+1)<0));
       j=i+1;
```

```
        while ((rug(j)<=0)&(j+1<n))
            if  rug(j+1)>0
                Lvalley(k,1)=x(i)-rug(i)*(x(i+1)-x(i))/(rug(i+1)-rug(i));
                Lvalley(k,2)=x(j)-rug(j)*(x(j+1)-x(j))/(rug(j+1)-rug(j));
                L_valley(k)=Lvalley(k,2)-Lvalley(k,1);
                k=k+1;
            end
            j=j+1;
        end
    end
end
%create one vector whith the x positions of the all crossings whith the
%reference line
for i=1:(length(L_peak))
    Lp(i)=Lpeak(i,1);
    Lp(i+length(L_peak))=Lpeak(i,2);
end
for i=1:(length(L_valley))
    Lv(i)=Lvalley(i,1);
    Lv(i+length(L_valley))=Lvalley(i,2);
end
%vector X that contain all x positions (positions of rough points and the
%crossings)
X=[];
X=[x';Lp';Lv'];
X=unique(X);
X=sort(X);

%create one new vector RUG with the same length that X
RUG=[];
for i=1:length(X)
    for j=1:length(x)
        if X(i)==x(j)
            RUG(i)=rug(j); %the others positions RUG=0
        end
    end
end
%generation of the one profile approach by parabolas
csi_peak=L_peak*sqrt(2/pi)*alfa*sigma; %equation 8 Aramki part I
csi_valley=L_valley*sqrt(2/pi)*alfa*sigma;
mean_L_peak=(mean(L_peak));
mean_L_valley=(mean(L_valley));
mean_L=1/2*(mean(L_peak)+mean(L_valley));
K1_peak=8*(csi_peak)./(L_peak.^2); %equation 9-b Aramki part I
K1_valley=8*(csi_valley)./(L_valley.^2);
%generation of the vector with points that represent parabolas
%start the vectors with zeros and the same length that X
parabola=zeros(1,length(X));
parabola_peak=zeros(1,length(X));
parabola_valley=zeros(1,length(X));
for i=1:length(L_peak)
    j=find(X==(Lpeak(i,1)));
        while (X(j)>=Lpeak(i,1)&X(j)<=Lpeak(i,2))
        parabola(j)=-(4*csi_peak(i)/(L_peak(i)^2))*(X(j)-Lpeak(i,1)-
L_peak(i)/2)^2+csi_peak(i);
        parabola_peak(j)=parabola(j);
        j=j+1;
        end
end
for i=1:length(L_valley)
    j=find(X==(Lvalley(i,1)));
        while (X(j)>=Lvalley(i,1)&X(j)<=Lvalley(i,2))
```

```
        parabola(j)=(4*csi_valley(i)/(L_valley(i)^2))*(X(j)-Lvalley(i,1)-
L_valley(i)/2)^2-csi_valley(i);
        parabola_valley(j)=parabola(j);
        j=j+1;
        end
end
temp_rq=0;
for i=1:length(rug)
    temp_rq=temp_rq+(rug(i))^2;
end

increment=0.0001; %increment of the displacement delta [micron]
%critic interference for each peak
for i=1:length(L_peak)
    delta_c(i)=(pi*k*H/(2*Ecom))^2*(1/K1_peak(i));%micron
end
y=max(parabola);
lt=zeros(length(L_peak),1); %vector that indicate if the deformation is
elastic (0) or plastic (1)
ltemp=0;
f=zeros(length(L_peak),1); %load applied in each asperity
n_steps=0;
while sum(f)<load
    y=y-increment;
    n_steps=n_steps+1;
    for i=1:length(L_peak)
        %elastic
        if lt(i,1)==0 & (csi_peak(i)-y)>0
            f(i)=(4/3)*Ecom*((1e-3/K1_peak(i))^(0.5))*((csi_peak(i)-y)*1e-
3)^(3/2);
            if (csi_peak(i)-y)>delta_c(i)
                lt(i,1)=1;
            end
        end
        %plastic
        if lt(i,1)==1 & (csi_peak(i)-y)>0
            f(i)=2*pi*(1e-3/K1_peak(i))*(csi_peak(i)-y)*1e-3*H;
        end
    end
end
%contact area
A_cont=0;
for i=2:length(RUG)
    if parabola(i)>=y
        A_cont=A_cont+(X(i)-X(i-1));
    end
end
%percentage of contact area
A_cont_a=A_cont/X(length(X))
%plot deformed profile
for i=1:length(RUG)
    if parabola(i)>y
        parabola_de(i)=y;
    else
        parabola_de(i)=RUG(i);
    end
end
plot(X,parabola,'k');
hold on;
plot(X,parabola_de,'LineWidth',1.4);
hold off;
%deformation
deformation=max(parabola)-abs(y)
```

Chang Model

Only a part of the algorithm changes, the changes are in the last part are of the model:

```
increment=0.001; %increment of the displacement delta [micron]
%critic interference for each peak
for i=1:length(L_peak)
    delta_c(i)=(pi*k*H/(2*Ecom))^2*(1/K1_peak(i));%[micron] %Equation 14
end
y=max(RUG);
lt=zeros(length(L_peak),1); %vector that indicate if the deformation is elastic
(0) or plastic (1)
ltemp=0;
f=zeros(length(L_peak),1); %load applied in each asperity
n_steps=0;
while sum(f)<load
    y=y-increment;
    n_steps=n_steps+1;
    for i=1:length(L_peak)
        %elastic
        if lt(i,1)==0 & (csi_peak(i)-y)>0
            f(i)=(4/3)*Ecom*((1e-3/K1_peak(i))^(0.5))*((csi_peak(i)-y)*1e-
3)^(3/2);%Equation 9
            if (csi_peak(i)-y)>delta_c(i)
                lt(i,1)=1;
            end
        end
        %plastic
        if lt(i,1)==1 & (csi_peak(i)-y)>0
            f(i)=pi*(1e-3/K1_peak(i))*((csi_peak(i)-y)*1e-3)*(2-
(delta_c(i)/(csi_peak(i)-y)))*k*H; %Equation 27
        end
    end
end
```

Zhao Model

The changes to the algorithm of Greenwood and Williamson model in final part are:

```
    increment=0.001; %increment of the displacement delta [micron]
    %critic interference c1 for each peak
    for i=1:length(L_peak)
        delta_c1(i)=(pi*k*H/(2*Ecom))^2*(1/K1_peak(i));%[micron] %Equation 8
        delta_c2(i)=54*delta_c1(i); %[micron] %Equation 20
    end
    y=max(RUG);
    lt=zeros(length(L_peak),1); %vector that indicate if the deformation is
    elastic (0) or elastoplastic (1) or fully plastix (2)
    ltemp=0;
    f=zeros(length(L_peak),1); %load applied in each asperity
    n_steps=0;
    while sum(f)<load
        y=y-increment;
        n_steps=n_steps+1;
        for i=1:length(L_peak)
            %fully elastic
            if lt(i,1)==0 & (csi_peak(i)-y)>0
                f(i)=(4/3)*Ecom*((1e-3/K1_peak(i))^(0.5))*((csi_peak(i)-y)*1e-
    3)^(3/2);%Equation 3
                if (csi_peak(i)-y)>delta_c1(i)
                    lt(i,1)=1;
                end
            end
            %elasto-plastic
```

```
        if lt(i,1)==1 & (csi_peak(i)-y)>0
            f(i)=(H-H*(1-k)*((log(delta_c2(i))-log(csi_peak(i)-
y))/(log(delta_c2(i))-log(delta_c1(i)))))*(1-2*(((csi_peak(i)-y)-
delta_c1(i))/(delta_c2(i)-delta_c1(i)))^3+3*(((csi_peak(i)-y)-
delta_c1(i))/(delta_c2(i)-delta_c1(i)))^2)*pi*(1e-
3/K1_peak(i))*(csi_peak(i)-y); %Equation 36
            if (csi_peak(i)-y)>delta_c2(i)
                lt(i,1)=1;
            end
        end
        %fully plastic
        if lt(i,1)==2 & (csi_peak(i)-y)>0
            f(i)=2*pi*(1e-3/K1_peak(i))*((csi_peak(i)-y)*1e-3)*H;  %Equation
11
        end
    end
end
```

Appendix 9 – Results from the mechanical contact apparatus

Images from the contact analysis on the stereo microscope and high resolution CCD camera, the real area of the these image is 1.5x1.2 mm.

Specimen 1 without filter:

0 N	40 N	80 N
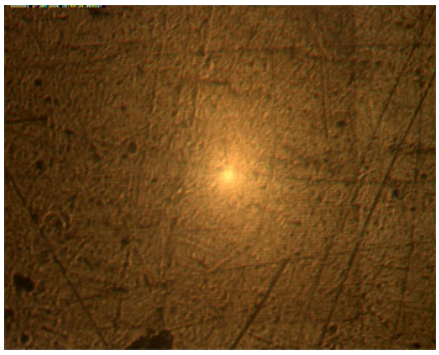	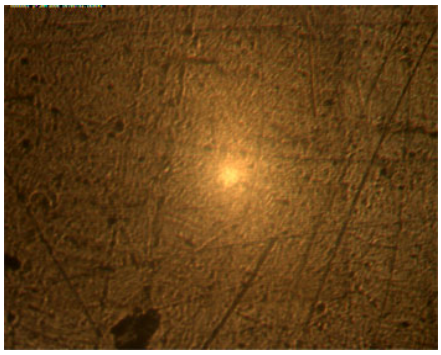	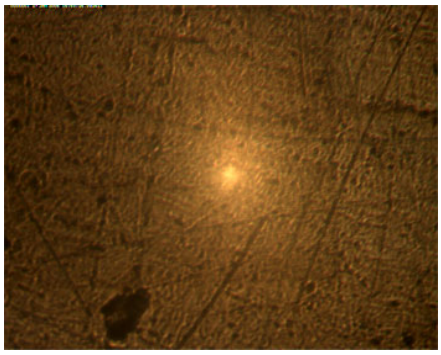

Specimen 1 with yellow filter (λ=577 nm):

0 N	40 N	80 N
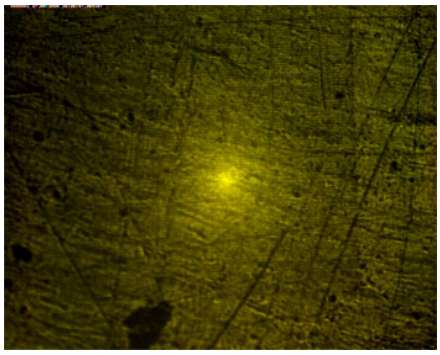	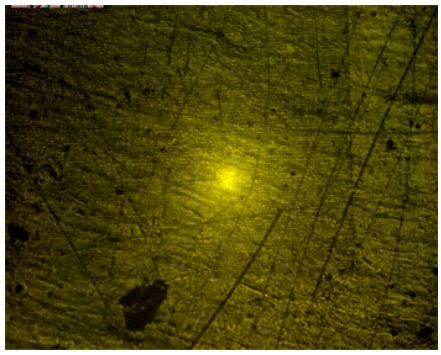	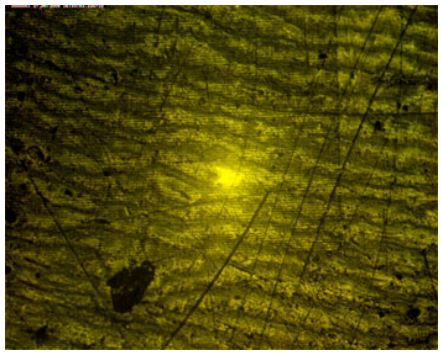

Specimen 2 without filter:

0 N	40 N	80 N
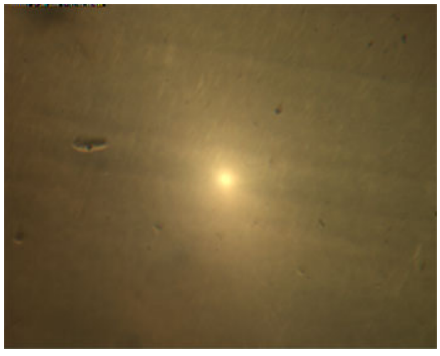	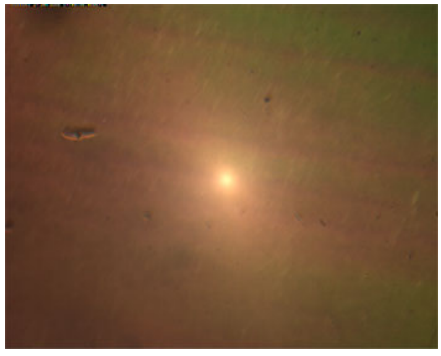	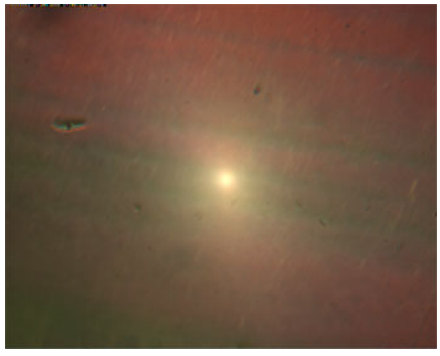

Specimen 2 with yellow filter (λ=577 nm):

0 N	40 N	80 N
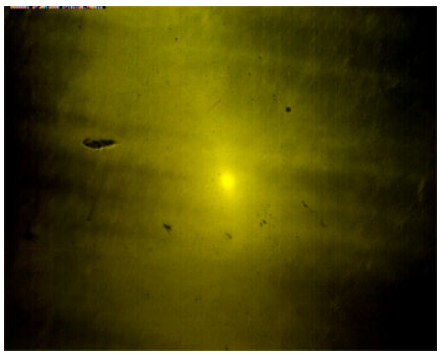	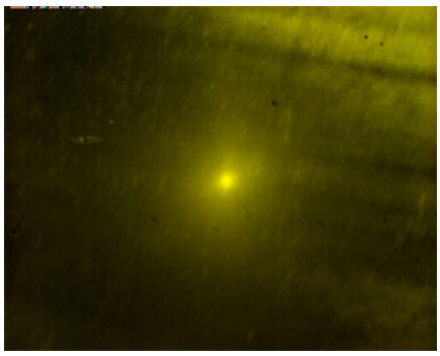	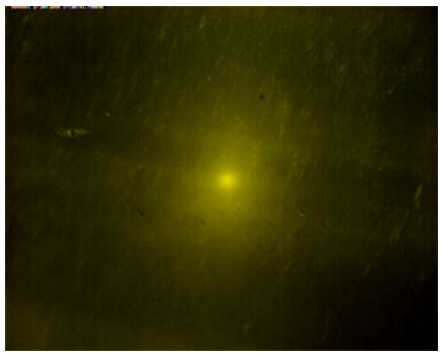

Specimen 3 without filter, zone 1:

0 N	40 N	80 N
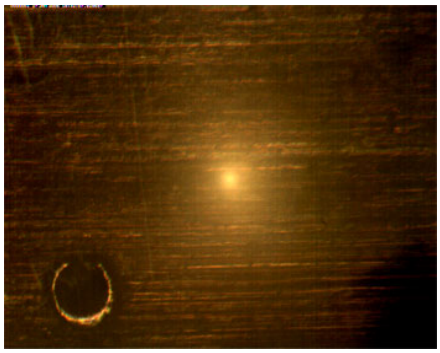	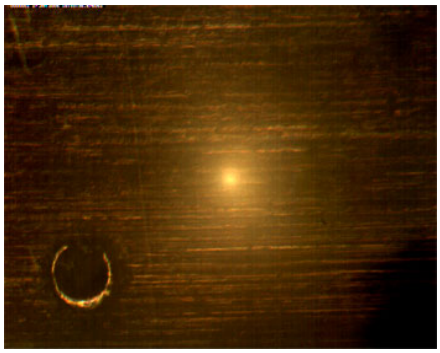	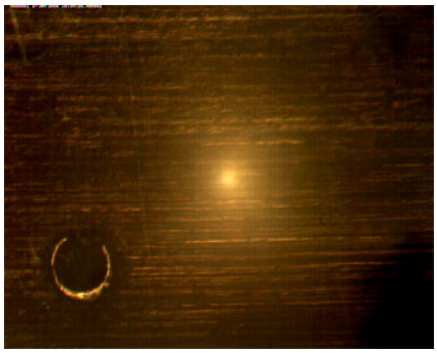

Specimen 3 with yellow filter (λ=577 nm), zone 1:

0 N	40 N	80 N
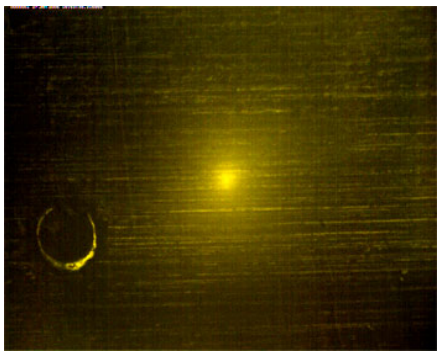	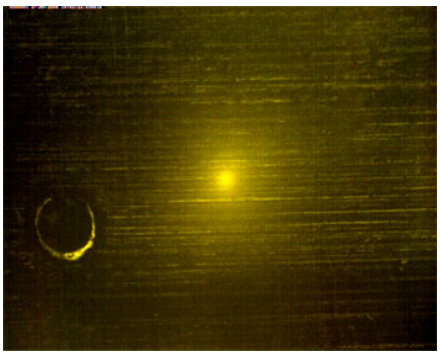	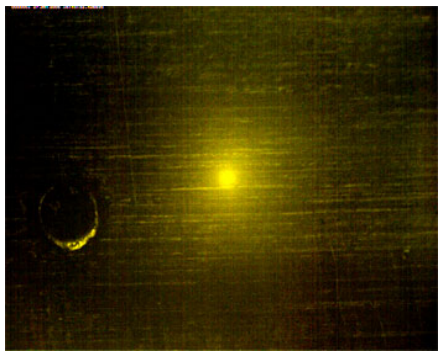

Specimen 3 without filter, zone 2:

0 N	40 N	80 N
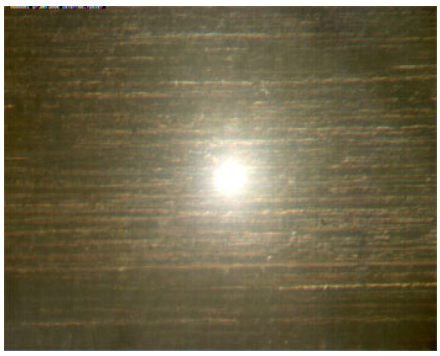	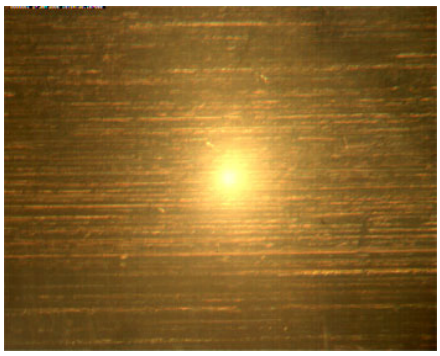	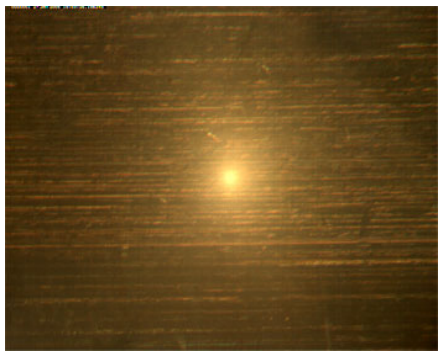

Specimen 3 with yellow filter (λ=577 nm), zone 2:

0 N	40 N	80 N